The analysis of fuel spray penetration and distribution in a medium-speed diesel engine using optical techniques

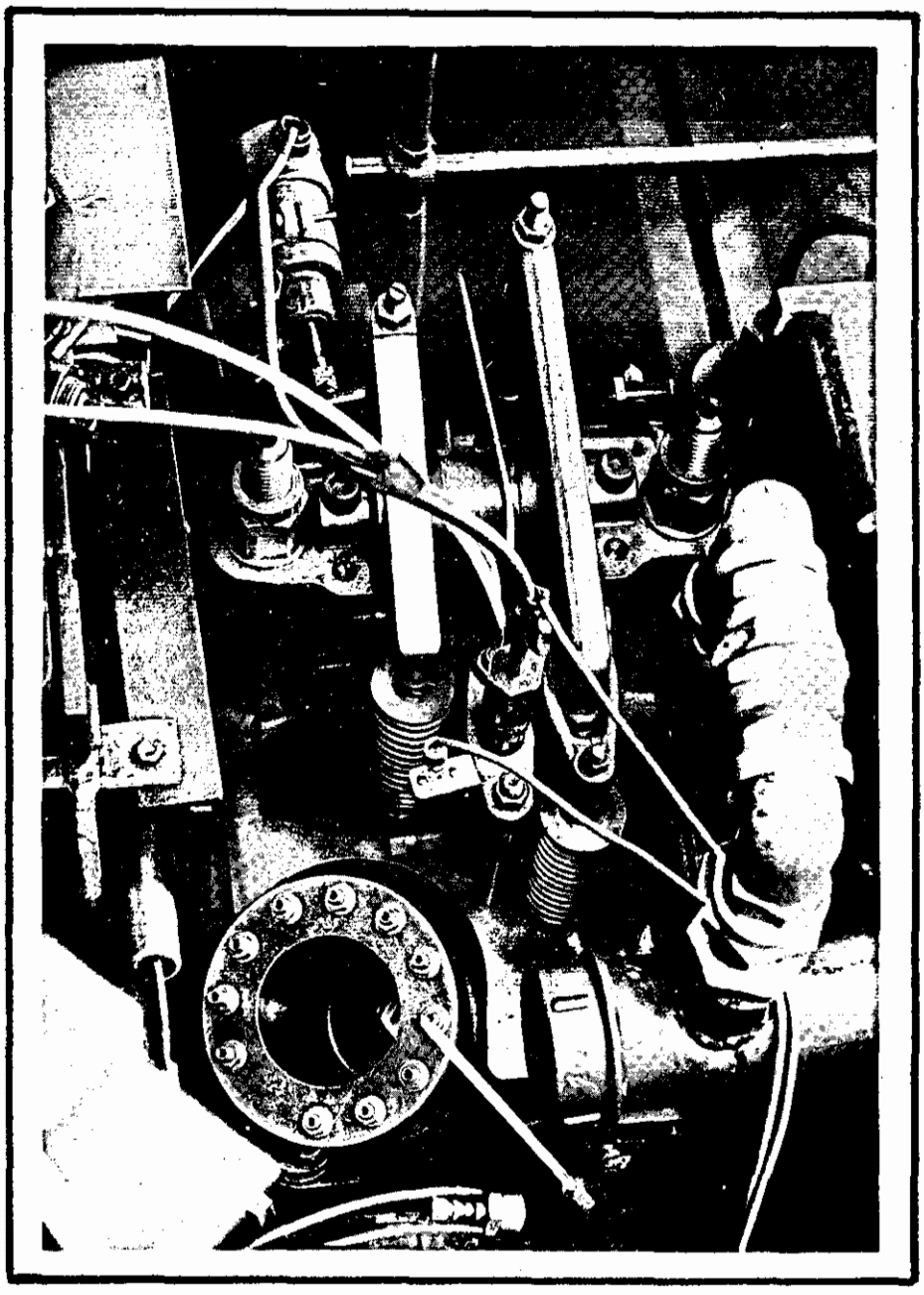

THE ANALYSIS OF FUEL SPRAY PENETRATION AND DISTRIBUTION IN A MEDIUM SPEED DIESEL ENGINE USING OPTICAL TECHNIQUES

by

D. H. C. TAYLOR

THESIS Submitted in partial fulfilment of the requirements for the award of Doctor of Philosophy of Loughborough University of Technology.

SUPERVISORS P. H. Broadhurst, B.Sc., Ph.D., M.I.Mech.E.,
A. J. Glasspoole, M.A., B.Sc.(Eng. Hons).,
C.Eng., M.I.Mech.E.

SYNOPSIS

The investigations described were initiated in order to provide information and understanding on the mechanism of combustion in a medium speed diesel engine. In this way more economic engine development could be achieved by prediction of the fuel injection and combustion system performance.

Work carried out at Loughborough University of Technology comprised a literature survey, indicating the areas of knowledge that required elucidation and a study of diesel nozzle spray characteristics. The penetration and distribution of a fuel spray in a cold bomb at engine densities and atmospheric temperatures was measured, using high speed photography. The work differed from previous investigations by using an actual injection system.

The feasability of using a double pass schlieren technique in a working engine was tested on a small three-inch bore high speed diesel engine, with a mirror on top of the piston and a window in the cylinder head. This optical system allows the different phases of the cylinder charge (i.e., the air and the liquid, vapour and burning fuel) to be identified, and greatly facilitates study of the total penetration of the fuel spray, air swirl, combustion and scavenging processes.

The knowledge and experience obtained in the prosecution of this work showed that it was feasible to apply this system to a large medium speed engine. Although difficulties with piston tilt and oil passing up the bore and obscuring the piston mirror were encountered, methods to overcome these were found, as also was a method of mounting the sensitive schlieren mirror, so that the engine vibrations were minimized.

Application to the large engine meant major design modifications to allow a quartz window to be fitted into the cylinder head. Experiments were carried out using various optical arrangements, to change the range and sensitivity of the schlieren system in order to distinguish all the phases of fuel distribution. Electronic instrumentation was developed which allowed measurement of transient cylinder and injection system conditions during direct and schlieren high speed photography tests.

From the cold bomb work an equation is proposed:-

$$\frac{s}{d} = 4.13 \left(\frac{t}{d} \sqrt{\frac{\Delta p}{\rho g}} \right)^{.64} \left(\frac{L}{d} \right)^{.18}$$

This allows the prediction of unevaporated spray penetration from an actual injection system taking into account nozzle upstream conditions and changes in length to diameter ratio.

The large engine work shows that no appreciable air movement exists. Fuel spray penetration is radically affected by evaporation in hot gas but the vapour continues to penetrate as a spray. The penetration of the vapour is identical to that of a spray without evaporation, thus the proposed equation also predicts the total penetration of a hot gas. Using this equation, a concept of combustion is proposed in which the fuel spray is deliberately allowed to impinge upon the piston, as opposed to the accepted theory of non-impingement. A 12½-inch bore engine using this form of combustion has demonstrated that an improvement in efficiency can be obtained at the same time as substantial reductions in mechanical loading of the injection system.

LIST OF CONTENTS

Section.

NOMENCLATURE

General

A_o	=	Surface Area of Droplet
C	=	Coefficient of discharge of optic
C_o	=	Drag coefficient
D	=	Tobal Ignition Delay
D_p	=	Physical Ignition Delay
D_c	=	Chemical Ignition Delay
d	=	Droplet diameter or orifice diameter
d_o	=	reference orifice diameter
f_c	=	Function of chamber and nozzle configuration
h	=	New transfer coefficient
k_g	=	Mass transfer coefficient
L	=	Length of orifice
L_{th}	=	Theoretical Air Quantity
M	=	Mass of Droplet
N	=	Engine speed in r.p.m.
n	=	Number of molecules
P_c	=	Pressure in Combustion Chamber
P_{fl}	=	Partial pressure of fuel vapour of surface of Droplet
ΔP	=	Pressure drop across orifice
Q	=	Heat transferred to liquid surface of Droplet
q_j	=	Mass of fuel injected
R	=	Air Resistance
R_{HR}	=	Rate of heat release
R_I	=	Rate of fuel injected
R_o	=	Initial rate of heat release
S	=	Penetration of droplet or tip of spray

ST	=	Standard Deviation
T	=	Temperature
T_B	=	Temperature of air surrounding Droplet
TL	=	Temperature of Liquid Droplet
TM	=	Mean Gas Temperature
t	=	Time
t_i	=	Time of injection of fuel element after first element
t_o	=	Time of timing of first element
V	=	Velocity of tip of spray
V_o	=	Velocity of oil at orifice
v	=	Velocity of Droplet
v_o	=	Velocity of Droplet at orifice
W	=	Rate of Evaporation
X_J	=	Set of Errors
$\overline{X}$	=	Arithmetic Mean of Set of Errors
Z	=	Dimensionless Correction factor used in mass transfer
α	=	Dimensionless Correction factor used in heat transfer
γ_a	=	Specific weight of fuel
γ_f	=	Specific weight of air
2θ	=	Cone Angle of Spray
$2\theta_{eff}$	=	Effective Cone Angle of Spray
λ	=	Excess Air Coefficient
μ_a	=	Viscosity of Air
μ_f	=	Viscosity of fuel
ρ_a	=	Density of Air
ρ_f	=	Density of Fuel
$\Delta\rho_a$	=	Gas Density Relative to Atmospheric Density
$\Delta\rho_f$	=	Fuel density relative to density of Water
σ	=	Surface tension
Ω_b	=	Brake Thermal Efficiency
Ω_{comb}	=	Combustion Efficiency

Ω_{cycle} = Cycle Efficiency

Ω_{HL} = Heat Loss Efficiency

Ω_{mech} = Mechanical Efficiency

Optics

F = Focal length of First Minor

H = Height of Source

R = Range of Schlieren System

S = Sensitivity of Schlieren System

INTRODUCTION

In the past, much time and effort has been devoted to understanding combustion in the diesel engine. However, the emphasis has been on the smaller high speed engines rather than the medium or low speed types. This could be due to two factors; first, the relative ease of experimental investigations on small engines and second, that only in recent years have the medium and low speed engines warranted closer investigation, either on technical or economic grounds.

The increase in interest on the larger type of engine has been prompted by two inter-related problems. With the increasing awareness of economics in engineering the ability to predict at the design stage the correct fuel injection and combustion chamber, particularly with the rapid increase in horse power, is essential if development cost and time are to be kept at a reasonable level.

With this increase in power per unit the mechanical loadings on the engine are increasing in an effort to keep the unit efficient. Fuel line pressures of the order of .16-18000 lb/in^2 and cylinder firing pressures of 1800 lb/in^2 are not uncommon.

There is a limit above which the complexity of a unit makes it uneconomical to produce. Therefore an understanding of the mechanism of combustion and the major parameters affecting it could be used to reduce unnecessary complexity.

At the end of 1962 when the author became involved with fuel injection development, effort was being turned towards being able to predict the injection system characteristics before the engine was tested.

Up to this date trial and error had been employed. An attempt was made by Cockburn [1] * to evolve a rational explanation of the resulting changes in engine performance with changes in injection equipment. The relationship gained was useful over a limited range.

The next stage was a more basic approach. This thesis[4] describes the work carried out in this stage between January, 1963 and January, 1967.

Chapters I and II report the survey carried out on previous work. Chapter I deals with the mechanism of fuel atomization and spray penetrations, whilst Chapter II considers the broader aspect of combustion.

Chapter III attempts to outline the areas in which information is required.

Chapter IV describes work carried out on a cold bomb reproducing engine densities at room temperature, whilst Chapter V analyses the results of spray penetration measurements taken.

Chapter VI details the problems encountered when applying double pass schlieren system to a small three-inch bore diesel engine, and Chapter VII continues with the application of the same system to an 8-inch bore engine.

Chapter VIII considers results of spray penetration using both direct and schlieren photographs, and describes the application of the work to a 12½-inch bore engine.

Conclusions are drawn in Chapter IX and recommendations for future work detailed in Chapter X.

*see References

CHAPTER I

SPRAY SURVEY

1.1. INTRODUCTION

This chapter surveys the work carried out on the atomization and penetration of fuel sprays, with special emphasis on the type of spray found in the medium speed direct injection engine.

A basic understanding of atomization is sought. Methods of calculating spray cone angle and penetration are looked at, together with the effects of evaporation, air motion, air swirl and combustion.

1.2. ATOMIZATION

A wealth of information is in existence [2, 3, 4, 5, 6, 7, 8, 9, 10, 11, 12, 13, 14] on the basic mechanisms of atomization and distribution of fuel from orifices and it is not intended to repeat this but attention is drawn to the bibliography.

It is sufficient at this point to summarize only the major conclusions. Considering plain orifices, through which the fuel is injected by a pressure drop across the orifice (as in the multi-hole injector), the four main factors to consider about the spray development are:- (a) penetration; (b) cone angle; (c) spray dispersion and (d) droplet size and distribution. The effect on these of the cylinder gas properties, fuel properties, injection pressure and nozzle configuration should be looked at, and these will be considered in turn.

1.2.1. Cylinder Gas Properties

Before delving into the effects of gas properties, it

is possibly helpful to look at the motion of a single droplet from a nozzle.

The equation describing this motion is:-

$$M \frac{dv}{dt} + R = 0 \quad \ldots\ldots\ldots\ldots\ldots\ldots\ldots\ldots (1)$$

Where M = mass of the droplet

v = velocity

R = air resistance

t = time

The value of R changes depending on the type of flow around the droplet.

It can be shown that:-

for Laminar flow $R = 3\pi\mu_a v d$ ..... (2)

for turbulent flow $R = 0.055\pi\rho_a v^2 d^2$ ..... (3)

From equation (1) and using (2), (3) ~~and (4)~~

i.e., laminar flow $$\frac{dv}{dt} = - \frac{18\mu_a v}{d^2 \rho f} \quad \ldots\ldots\ldots\ldots (4)$$

turbulent flow $$\frac{dv}{dt} = - \frac{0.33\rho_a}{d\rho_f} v^2 \quad \ldots\ldots\ldots (5)$$

From these it can be shown that for:-

laminar flow $$S = \frac{d^2 \rho f v_a}{18\mu_a} \left(1 - e^{\frac{18\ \mu a}{d^2 \rho_f} t}\right) \ldots (6)$$

turbulent flow $$S = - \frac{d\rho_f}{0.33\ \rho_a} \log e \left[1 + \frac{0.33\ \rho_a v_{ot}}{d\rho_f}\right] .. (7)$$

Where d = droplet diameter

ρ_f = density of fuel

μ_a = viscosity of air (absolute)

v_o = initial velocity of droplet

ρ_a = density of air

S = penetration

However, it is as well at this point to note the

penetration of a droplet calculated by using these equations. Figure 1 shows for an initial velocity equivalent to a drop leaving an engine nozzle that after five milliseconds the penetration is about 7 cm (2.7 inches) while at a gas density of 30 atmospheres it is less than 1 cm (.4 inches). Compare this with results taken from Schweitzer's work [3], and shown in Figure 2. With similar initial velocities (8000 lb/in^2 injection pressure) and a gas density of 15 times atmospheric the penetration is of the order of 5½ inches in 5 milliseconds, i.e. greater than the droplet at atmospheric.

This difference in penetration can be ascribed to the leading droplets giving up their energy to the air, giving it a forward motion. This reduces the air resistance for the following droplets and they, in their turn, give up energy. The tip penetratinn is thus greater than that of a single drop.

Considering equations (6) and (7), we can draw some conclusions on the effect of the gas property. The increase in air density will cause a decrease in penetration. An increase in air viscosity will also reduce penetration.

The first effect has been noted by many workers [3, 4 and 5], and Figure 3 is an example.

Not much information exists on changing the viscosity; this may be due to the fact that to increase the viscosity of air, its temperature must be increased and then evaporation may mask any effect.

Joachim [6] used nitrogen, carbon dioxide and helium to vary the viscosity. His results are plotted in Figure 4.

From this it would appear that the penetration is independent of gas viscosity. The injection pressure of 8000 lb/in^2 may explain this as the Reynolds number of the flow around the drops is in the region covered by equation (7), where there is no viscosity effect.

The cone of spray is formed mainly by turbulence in the orifice giving rise to a radial velocity. From Figure 5 $\frac{v_r}{v_a} = \tan \frac{\alpha}{2}$ where v_a is much bigger than v_r. As the density is increased, its effect on v_a will be greater and thus α will increase. Sass [7] showed this, as is seen in Figure 6.

Using this approach viscosity will not have much effect because, as mentioned above, at the high injection pressures it does not affect the velocity of the droplet.

Figure 7 shows the effect of the gas density on spray dispersion. The radius referred to is the radius of cross-section of the spray cone at a point in front of the nozzle. A larger radius denotes a better dispersed spray. It is interesting to note that this improvement reaches an optimum above which increasing the air density has no effect.

For future reference it is also important to observe that a larger cone angle and dispersion usually involves more air entrained in the spray.

The effect of density on droplet size is shown in Figure 8. This indicates that as the gas density increases the droplet size decreases. Again from the literature a minimum is reached beyond which no further decrease is affected. In fact Giffen and Muraszew [8] suggest that further increase in density can increase droplet size due

to the decrease in effective pressure drop across the orifice, which is not compensated for by the increased air resistance. Under pressures obtained in a medium speed engine, 8000 to 18000 lb/in^2 injection pressure, and 800 to 1500 lb/in^2 cylinder pressure, this may be a negligible effect.

1.2.2. Fuel Properties

Three properties of the injected fuel can be considered; surface tension, viscosity and density.

In the mechanisms of atomization there are the three stages to consider. In the orifice the viscosity determines the Reynolds number and thus the amount of turbulence. This in turn controls the radial and tangential components which play an important part in the disintegration of the spray.

Once the fuel emerges from the orifice then surface tension is important in the break-up into droplets.

In the final stage, subdivision of the droplets in flight is a property of surface tension and viscosity (and of course air resistance which has been covered earlier).

It would be expected that for a denser fuel the penetration would increase and the cone angle decrease, but over the range of diesel fuels used the density varies so little that its effect can be neglected. Schweitzer [9] showed that when testing fuels of different densities and the same viscosity, the results were inconclusive but indicated that, particularly at high air density, the effect of fuel density could be neglected.

Again surface tension varies so little for the range of fuels used (heavy fuel oil 30 dynes/cm at 20°C to Kerozine 23.9 dynes/cm at 20°C) that its effect can be ignored.

However, the viscosity changes radically over the range of fuels used, and it can have a large effect on spray characteristics.

As has been noted, the viscosity affects the tangential and radial component velocities in the nozzle. The higher the viscosity the more compact the spray and the greater the penetration. Schweitzer [9] showed the overall effect (Figure 9), where the spray velocity decreases more rapidly the less viscous the fuel. At the high air densities, similar to engine conditions, the effect is smaller than at atmospheric density. The viscosity also has an effect on the process of atomization. This is shown in Figure 10 where the higher viscosity fuel No. 2 (.102 poise) has a lower percentage of small droplets than the fuel No. 1 with .022 poise viscosity.

1.2.3. Injection Pressure

Considering equations (6) and (7), if the injection pressure is increased (and therefore the initial velocity v_o) it would appear that the penetration should increase. It has been shown by Thiemann [10] that with an increase in initial velocity there is a decrease in droplet size, and this, according to the equations, tends to decrease the penetration. These two effects may cancel each other out.

Schweitzer [3] supports Riehm [11] in suggesting that final penetration is independent of injection pressure.

Sass [12] using a jerk pump system showed an increase in penetration with injection pressures. The difference lies in that Sass was considering the penetration of the spray during a relatively short time, while Schweitzer considered the final penetration.

Figure 11 shows results produced by Holfelder [13] and shows the effect of injection pressure on cone angle. This effect is not appreciable as for an increase of pressure from 800 to 4500 lb/in^2 the cone angle only changes by 1^o.

This small increase is probably due to the increase in turbulence in the orifice and hence the radial and tangential velocities.

The effect of atomizer opening pressure on atomization is shown well in Figure 12 from Sass' [7] work on a jerk pump system. It can be seen that as the pressures are increased so the frequency curve is moved towards the small droplets. It is as well to note that with Sass' work the injection pressure is varying over the injection period and with it the instantaneous droplet size, thus care must be taken when comparing his results with workers who have used constant injection pressures.

1.2.4. Nozzle Configuration

Considering the nozzle orifice, two factors affect penetration; the diameter of the orifice and its length to diameter ratio $\frac{L}{d}$.

The effect of increasing the orifice diameter is to increase the penetration of the spray for a given injection pressure. It has been suggested [Mehlig 14] that this is due to the momentum of the discharging fuel being

proportional to the square of the orifice diameter while the area of jet exposed to air resistance is proportional directly to the diameter. Figure 13 from Schweitzer's [9] work demonstrates this result.

The effect of $\frac{L}{d}$ ratio is slightly more complex. Figure 14 shows the effect of $\frac{L}{d}$ on penetration. The reason for the shape of this curve may be explained by the flow patterns occurring in the nozzle.

As the $\frac{L}{d}$ ratio increases, at very small values (≈ 1) the orifice length is too short to control the fuel, but there is a slight increase in friction losses. This reaches a minimum and thereafter the increasing length of the orifice gives an increasing control over the fuel resulting in an increase in the coefficient of discharge. Maximum penetration is reached at an $\frac{L}{d}$ value of about 5 and thence the penetration decreases due to a continual increase in friction but no more effective control.

It should be noted that the curve can be more or less pronounced and be displaced one way or the other, depending on the type of nozzle.

The effect of orifice size on spray atomization is summed up by Figure 15 from Sass [7]. It shows that as the orifice diameter is increased the frequency curve moves toward the region of coarse atomization. It has been suggested that this is due to the fact that the increase in contact surface between the fuel and air increases less than the volume of fuel discharged.

When the $\frac{L}{d}$ of the orifice is varied a curve similar to Figure 16 Thiemann[10] is obtained. This supports

the conclusion set down before, that, with the increase in coefficient of discharge of the orifice, the initial velocity increases and hence better atomization.

In any consideration of the nozzle there must be included the effects of the fuel flow up stream and the condition (i.e., finish) of the orifice. If the conclusions drawn about the effect of coefficient of discharge and turbulence in the orifice are correct, then these must have an appreciable effect which must be borne in mind when comparing experimental results.

1.3. METHODS OF CALCULATING PENETRATION AND CONE ANGLE

1.3.1. Survey of Methods

In the foregoing discussion, although an understanding of the underlying principles of penetration and atomization have been gained, only qualitative results have been shown. Further survey is needed to indicate quantitative approaches.

Sass [7] put forward fairly simple relationships that could be used to predict the penetration and cone angle of a spray, if a datum condition was already known. This was unsatisfactory from the point of view of actual predictions on engines unless, as in Cockburn's [1] work, an assumption is made about the spray path.

The first notable attempt to form a theory for prediction of diesel fuel spray penetration was Schweitzer [9]. He developed the equations shown below from test results, using a dimensional approach.

$$\frac{s}{d}\left(\frac{\Delta\rho_a}{\Delta\rho_f}\right)^{\frac{1}{4}} = 2265 \ln\left(\frac{1}{115.5}\frac{t\Delta\rho a}{d\Delta\rho_f}\sqrt{\frac{\Delta p}{\Delta\rho_f}} + 1\right) \quad \ldots\ (8)$$

For oil of viscosity 6 centistokes

$$\frac{s}{d}\left(\frac{\Delta\rho_a}{\Delta\rho_f}\right)^{\frac{1}{4}} = 2490 \ln\left(\frac{1}{115.5}\frac{t\Delta\rho_a}{d\Delta\rho_f}\sqrt{\frac{\Delta p}{\Delta\rho_f}} + 1\right) \quad \ldots\ldots (9)$$

For oil of viscosity 13.5 centistokes

Where t in seconds

Δp in lb/in^2

s in inches

$\Delta\rho_a$ = air density relative to atmosphere

$\Delta\rho_f$ = fuel density relative to water

Further work was published in 1960 by Wakuri et al [15] and Lyshevskii [16].

Wakuri developed an equation based on a momentum theory with allowance for air being induced into the spray.

The complicated equation arrived at can be simplified somewhat and re-written:-

$$s = \left(\frac{2c\Delta p}{\rho_a}\right)^{0.25} x \left(\frac{td}{\tan\theta}\right)^{0.5} \quad \ldots\ldots\ldots\ldots (10)$$

Where c = coefficient of discharge of nozzle

ρ_a = density of air

t = time

d = diameter of fuel nozzle

s = penetration at time t

2θ = cone angle of spray

The spray cone angle θ was shown to be dependent only on a function of the ratio of density of fuel oil and air.

By using dimensional analysis Wakuri also showed that

$$\frac{s}{\sqrt{t}} = \sqrt{V_o}\, d\, f\left(\frac{\rho_a}{\rho_f}\ \frac{V_o d\rho_f}{\mu_a}\right) \quad \ldots\ldots\ldots\ldots\ldots\ldots (11)$$

Where the letters are as in equation (10) but include:-

V_o = velocity of oil at nozzle

ρ_f = density of fuel

μ_a = viscosity of air

It was shown that the effect of air viscosity was small and that the term $\left(\frac{V_o d \rho_f}{\mu_a}\right)$ could be ignored.

$\therefore$ if $\frac{s}{\sqrt{t}} = k$

then $\frac{k}{\sqrt{V_o d}} = f\left(\frac{\rho_a}{\rho_f}\right)$ ..... (12)

Results were plotted in graphical form based on equation (12).

From equation (10) it was then established that:-

$$2\theta = 2 \tan^{-1} \sqrt{\frac{C \frac{\rho_f}{\rho_a}}{\left(\frac{k}{\sqrt{V_o d}}\right)^2}} \quad \text{..... (13)}$$

and from dimensional analysis, bearing in mind the negligible effect of air viscosity

$$2\theta = f\left(\frac{\rho_f}{\rho_a}\right) \quad \text{..... (14)}$$

Wakuri found that equation (13) gave good correlation with experimental results plotted as per equation (14).

Lyshevskii's work [16] was, in some ways, unfortunately aimed at the change in cone angle with time and the factors affecting it, and not with penetration.

Experiments show that the cone angle decreased with time for a portion of the development and then became constant.

He suggested that, if 2θ was the cone angle of spray then:-

$$\tan \theta = f(\rho_f, \mu_f, \sigma, V_o, \rho_a, d\ t) \quad \text{..... (15)}$$

Where the symbols are as before except:-

μ_f = viscosity of fuel

σ = surface tension

Then using, again, dimensional analysis

$$\tan \theta = f(M, W, \rho, \varepsilon) \quad \ldots\ldots\ldots\ldots\ldots\ldots\ldots\ldots \quad (16)$$

Where $M = \frac{\mu f^2}{\rho_f d \sigma}$

$$W = \frac{V_o^2 \rho_f d}{\sigma}$$

$$\rho = \frac{\rho_a}{\rho_f}$$

$$\varepsilon = \frac{t^3 \sigma}{\rho_f d^3}$$

By analysing the results the following relationship were gained.

For the section where the cone angle was decreasing:-

$$\tan \theta = 6.77 \times 10^{-3} \frac{W^{0.35} \sqrt{\rho}}{M^{0.07} \times \varepsilon^{0.12}} \quad \ldots\ldots\ldots \quad (17)$$

For the section where the cone angle was constant

$$\tan \theta = 3.64 \times 10^{-3} \frac{W^{0.32} \times \rho^{0.26}}{M^{0.07}} \quad \ldots\ldots\ldots \quad (18)$$

It was considered that the constant would change with nozzle design.

Lyshevskii applied equation (21) to Sass' results and found that the constant was affected by not only the nozzle but also the back pressure.

For low back pressures the equation became

$$\log \tan \theta \frac{M^{0.07}}{W^{0.32}} = 3.2 \times 10^{-3} \log \rho \quad \ldots\ldots\ldots \quad (19)$$

and for high back pressures

$$\log \tan \theta \frac{M^{0.07}}{W^{0.32}} = 10.2 \times 10^{-3} \log \rho \quad \ldots\ldots\ldots \quad (20)$$

With these expressions Sass' results correlated reasonably well.

Later Rusinov [17] published work based on the assumption that the kinetic energy was partially imparted to the gas and that the velocities of the fuel and gaseous medium in contact were equal:

He showed that

$$V = V_o e^{-\left(\frac{\pi \gamma_a \tan^2 \theta}{n^2 \, 6 q_f} \right)} \quad \ldots\ldots\ldots\ldots\ldots\ldots\ldots\ldots (21)$$

$$V_o = c \sqrt{\frac{2g\Delta p}{\gamma f}} \quad \ldots\ldots\ldots\ldots\ldots\ldots\ldots\ldots (22)$$

$$q_f = \gamma_f f_n V_o t \quad \ldots\ldots\ldots\ldots\ldots\ldots\ldots\ldots (23)$$

Where V = velocity at any instant in time t

γ_f = specific weight of fuel

γ_a = specific weight of gas

q_f = amount of fuel injected

Δp = pressure drop across orifice.

c = coefficient of discharge

f_n = area of nozzle orifice

Ω was a correction factor which took into account the actual conditions in the transfer of energy, namely the loss of part of the available energy due to its conversion into heat energy during the process of friction between fuel and air and the non-uniformity of velocity distribution of fuel in the cross-section of the spray.

By making the assumption that the penetration power of a spray was determined by the cone of the jet, then an effective cone angle can be admitted.

i.e., $\tan \theta_{eff} = \frac{\tan \theta}{\Omega}$ ..... (24)

By analysing other data with the expression (21) the variation of Ω with injection pressure was found.

Although the results calculated by this method gave

good correlation Rusinov considered that it was unsuitable for practical calculation. He derived from the same base, another form of the equation

$$t = \frac{Ml^3}{3V_o \log\left(\frac{Ml^2}{\xi} + 1\right)} \qquad \ldots\ldots\ldots\ldots\ldots\ldots (25)$$

Where

$$M = \frac{2\gamma_a \tan^2 \theta eff}{\gamma_f d^2}$$

d = diameter of nozzle
ξ = Correction Factor

From analysis of experimental results for injection pressures between 100 and 400 kg/cm^2 ξ varied between 2.45 and 3.0. Correlation was reasonable when comparing the penetration of fuel injection nozzle with the calculated value.

1.3.2. Comparison of Methods

The next step is obviously to compare the various methods of calculation.

To make the results more meaningful it was decided to consider the injection conditions prevailing in a 12½-inch bore engine (Appendix I), on which fairly adequate information was available.

Figure 17 shows the cylinder pressure with crankangle diagram, taken from the engine running at 500 r.p.m. 176 lb/in^2. b.m.e.p. Figure 18 shows the fuel injection pressures together with the needle lift diagram. The rate of fuel injected was calculated by a simple approach shown in Appendix II. The correlation between the total calculated and measured mass injected is fairly accurate. Then, knowing the running conditions, i.e., boost pressure and temperature, mean combustion chamber wall temperature, etc., the gas density was calculated using a program which was available

and the basis of which is explained in Appendix III.

This program analysed the pressure diagram between inlet valve closing and exhaust valve opening. The limitations of this method of analysis are fully realised, particularly in respect of assumption on trapping conditions and heat lost to the wall. Indications of heat pick up in the induction period and heat lost to the walls were taken from work done by Whitehouse et al [21].

The resulting cylinder density plot is shown in Figure 19. The nozzle diameter was taken as that used in the engine, namely .018 inches, and the coefficient of discharge chosen as .7 [18]. The oil viscosity and density were taken as 6 centistokes and .0308 lb/in^3 respectively.

All the workers reviewed, used a constant initial oil velocity and air density in their experiments and correlated their results by using mean initial velocities and air densities where these parameters were varying. Schweitzer [9], however, did show a valid method by which, varying injection pressures and air densities could be taken into account.

Taking the conditions already stated, and shown in Table I, the penetration was calculated by using this method and compared with Schweitzer's original equation (8) but using a time mean injection pressure and air density. The result is plotted in Figure 20. The comparison was so close that, for the further calculations, mean injection pressure and air density were used.

The results of using Schweitzer, Wakuri and Rusinov's equations are shown in Figure 21. Curve 1 shows the effect of Schweitzer's equation, while curve 2 gives the penetration according to the analysis of Wakuri's results.

There is a discrepancy after .008 seconds. If his second method, the purely theoretical approach, is used then curve 3 is obtained. The correlation with Schweitzer is worse. In equation (10) the cone angle of the spray appears as a parameter and in curve 3 the angle was taken as 17^{o}, as suggested from Sass' results quoted by Wakuri. If the cone angle measured by Wakuri is used in the theoretical equation then close agreement is obtained between his two approaches. This is shown by Curve 4. In his paper Wakuri did not try to explain this discrepancy in cone angle between his and Sass' results.

One possible discrepancy between Wakuri and Schweitzer lies in the calculation of V_o. The coefficient of velocity C_v was taken as 1 by Wakuri and in the above calculations, i.e.,

$$V_o = C_v \sqrt{\frac{2g\Delta p}{\rho_p}} \qquad \ldots\ldots\ldots\ldots\ldots\ldots\ldots (26)$$

Schweitzer suggested a value of .95. Figure 22 shows Wakuri's analytical method, using .95, compared with Schweitzer's result. The correlation is improved.

Curve 5 in Figure 21 demonstrates Rusinov's equation using the values of cone angle suggested by Sass. Curve 6 is the same equation (25) but using θ as suggested by Wakuri's work.

There is no agreement between Rusinov's and the two workers, Schweitzer and Wakuri, at this condition.

However, before pursuing this any further, let two points be considered that have been brought out by the above simple comparison.

Firstly, the equations obviously depend on the cone angle θ for their comparison and there seems to be a disagreement as to its value. For the conditions being

considered, Sass' work would indicate a cone angle of about 17°.

If Wakuri's equation (13) is re-written, i.e.,

$$2\theta = 2 \tan^{-1} \sqrt{\frac{2c\Delta p}{\rho_a}} \times \frac{d}{s^2} \times t \quad \ldots\ldots\ldots\ldots (27)$$

then, using the stated conditions, the cone angle remains essentially constant with time at 12°.

Work done by Meckel with an apparatus, injecting the fuel into a liquid media to represent air density, showed that the cone angle varied with the type of fuel used. For diesel fuel the 2θ was of the order of 15°. Considering Lyshevskii's work he developed the equation for the cone angle in the second or constant θ period (18). If this equation is used then the cone angle is 17.8°. Rusinov does not show any results from his experimental work, but from data used in his calculations, the cone angle at the test conditions would be about 10°.

The discrepancy between the various workers as to the cone angle, could be due to at least two reasons. Firstly, the accuracy of measurement. Films of the sprays show a very ragged edge and it would seem difficult to define accurately the cone angle. The second reason is probably more important, and that is, the difference in test apparatus.

Referring back to previous discussion, the three major factors affecting cone angle were gas density, fuel viscosity and nozzle configuration. All the work considered was carried out in a bomb where gas density was constant with time, and thus easily measured. Little error should occur from this source. Lyshevskii and Schweitzer both state that they used diesel fuel of similar viscosity. Rusinov

used diesel, as did Wakuri, but no viscosity is given. Sass again states only that he used diesel fuel. Therefore this is a possible source of error.

The nozzle configuration is important, as has been stated previously, not only from the orifice itself, but the upstream conditions. Schweitzer's nozzle is shown in Figure 23 and compared with a normal diesel injector. The L/d of the orifice was kept constant at 2:1. No drawings were available from Lyshevskii's paper, but he described his nozzles as "an open nozzle where atomizing portion had a cylindrical orifice. All atomizers were made of brass and their holes drilled with steel drills". His L/d ratio varied from 2.0 to 4.5:1. Wakuri gives no information on the nozzles other than the diameters, but from the description of the apparatus, the nozzle assembly would seem to be similar to Schweitzer's apparatus. Rusinov again gives no information on the shape of the upstream portion of the nozzle, but he states that the L/d ratio of the nozzles were about 6:1. No information was available on the nozzles used by Sass.

Considering the above information on the nozzles, the 6:1 L/d ratio used by Rusinov explains the high rates of penetration that his equation predicts when compared with the other workers. In the datum chosen for this comparison, the nozzle used in the AT engines has an L/d ratio of about 3.3:1. This is more in line with the L/d ratios used by Schweitzer and Lyshevskii. From the correlation in Figure 22 it would appear that Wakuri used a similar L/d ratio to Schweitzer. However the upstream conditions

affect the penetration, such as passage ways, needle shape and fluctuating pressures, as well as L/d ratio and thus the above equation may be misleading if used.

Schweitzer's equation does not take account of L/d effects which vary on engines; Wakuri does, in the form of a coefficient of discharge, but it is an important factor in the equation and it is difficult to set a value.

Rusinov's constants were gained using the long nozzle and, as such, they would have to be re-calculated from different experimental results.

At this point it is worth stopping and considering the overall picture that this analysis gives. Considering the AT engine, the injection period is 10 milliseconds in duration and the spray path, from nozzle to piston bowl, is $4\frac{1}{4}$ inches. Considering Figure 21 this would suggest that the spray has reached the piston after about 2.5 milliseconds and considerable impingement of the fuel on this piston would ensue. As is discussed in Chapter II, literature considers that impingement does not occur in a well matched engine. Therefore two possibilities exist. Firstly, the spray does impinge on the piston.

Figure 24 shows the marking of an AT piston with an injector nozzle having .020 holes, indicating that fuel hits the piston. Consideration of Figures 21 and 18 would suggest that more than $\frac{2}{3}$ of the fuel hits the piston. This would put the onus of mixing of fuel and air, not on the fuel jet itself, but on the impingement mechanism at the piston. This would be a completely different mechanism than the accepted 'spray just licking the piston'.

The second possibility is that the equations surveyed do not apply to a normal injection nozzle and engine cylinder conditions. The possible effect of L/d ratio and upstream conditions has already been considered. The effect of flow paths as shown in Figure 23 and variation in L/d and fluctuation in injection pressure, may all contribute to a discrepancy between the actual and calculated penetrations. Giffen and Muraszew [8], point out, that the distribution and atomization will be affected particularly at the beginning and end of injection on an actual system. Although this may not be directly important to the present discussion, nevertheless, in actual injection matching this effect could mask correct penetration and distribution of the spray.

However, there are other factors which could influence penetration that have not been taken into account when comparing the work surveyed with an engine. These are the conditions prevailing inside the cylinder and may be listed as:-

(a) evaporation of fuel due to high gas temperatures

(b) air motion

(c) combustion effects.

These points are worthy of individual discussion.

1.3.3. Effect of Evaporation on Fuel Spray Penetration

Although at this point, interest is directed to the effect of evaporation on the overall penetration, it is worthwhile considering from first principles the mechanism of evaporation.

Considerable work has been carried out to investigate

the evaporation and combustion of a single droplet of fuel [23 and 24] . It is considered that combustion occurs in the vapour phase. The fuel enters the cylinder and is atomized into small droplets. At this point a layer of air and vapour mixture is formed around the drop. Heat is transferred across this layer into the liquid and vapour diffuses out. At a point in the air vapour layer there is a stoichiometric mixture. When this point reaches self-ignition temperature, ignition occurs. This temperature is dependent on the fuel vapour partial pressure, chemical composition and the gas pressure.

E. L. Wakil et al [25] have been able to compute the vapourization histories of the fuel drops from aerodynamic forces, heat and mass transfer. Unfortunately, although the single droplet theory may fit the conditions at the outside of the spray, at the centre, considerable influence must be exercised by its neighbours. E. L. Wakil and Priem conducted tests [26 and 27] and considered that as well as the first condition, a second existed at the centre of the spray where adiabatic saturation was approached very closely in the cone.

However, these calculations only allow the prediction of mass evaporated, and although helpful in later considerations, do not indicate the effect on penetration. Direct calculated evidence seems lacking on this point.

In the late twenties and thirties, Bird [28], Rothrock and Waldron [29, 30 and 31] , Gelalles [32] and Holfelder [33] looked at the evaporation and combustion of fuel sprays. From these, an attempt has been made to elucidate the effect of evaporation. Results from Gelalles are plotted in Figures 25 and 26. These show that there was a large

difference in evaporation for room temperature and air at 1100°F. Rothrock [31] considered that the results obtained by Gelalles were misleading and that the decrease in penetration in hot air could be attributed to the fact that the fuel was heated before injection. His results from a running engine are shown in Figure 27, and show the effect of increasing the air temperature.

The theory of atomization and evaporation should be considered. It has been said that in the case of a single drop, a vapour air mixture is formed around it and mass transfer from, and heat transfer to, the drop takes place. Considering more deeply E. L. Wakil's work [25] and the case of the single drop the three equations governing evaporation are:-

The slowing down of the droplet by aerodynamic drag forces

$$\frac{dV}{dt} = -\frac{3}{8} C_o \frac{\rho_m}{\rho_f} \frac{V^2}{r_o} \quad \ldots\ldots\ldots\ldots\ldots\ldots (28)$$

Where C_o = drag coefficient

ρ_m = average density of air vapour mixture in the film

r_o = radius of droplet

The others as before.

The transfer of mass from the droplet

$$W = A_o K_g P_{fl} \alpha \quad \ldots\ldots\ldots\ldots\ldots\ldots (29)$$

Where W = rate of evaporation of droplet

A_o = surface area of droplet

K_g = mass transfer coefficient

P_{fl} = partial pressure of the fuel vapour at the surface of the droplet

α = dimensionless correction factor for the fact that the film is semi-permeable.

The transfer of heat to the drop

$$Q = h A_o (T_B - T_L) Z \quad \ldots\ldots\ldots\ldots\ldots\ldots \quad (30)$$

Where Q = heat transferred to the liquid surface of the drop

h = heat transfer coefficient

T_B = temperature of air surrounding the droplet

T_L = temperature of liquid drop

Z = dimensionless correction factor for the effect of mass transfer in heat transfer.

From these equations it can be seen that if the surface area of a drop is increased or the gas temperature T_B is increased, then both mass and heat transfer are increased, i.e., the greater is the evaporization rate. This type of analysis fits the single drop but the second condition mentinned above should be considered, that of adiabatic saturation. That is the temperature of the air surrounding the droplet, and not the initial gas temperature due to the cooling effect of other droplets in close proximity. E. L. Wakil [25] considered that this condition existed at the centre of the spray. Then, for fuel sprays with a dense formation, i.e., low air/fuel ratios at the centre this cooling effect will have a large effect in spray evaporation.

From this it can be deduced that for a given mass of fuel if the atomization is finer, i.e droplet size smaller, and the distribution of these droplets better, the evaporation rate would be higher and thus the penetration of the liquid spray is important and must be borne in mind for future discussion.

Reconsidering section 1.2.1. in this chapter, it can be seen that the gas density will affect both droplet size and distribution, but at the range of engine densities this could be small (see Figures 7 and 8). Again, at normal engine injection pressures it would seem that the effect of these pressures would be small (Figure 12). However, this would not be so for changes in viscosity of the fuel or for changes in hole diameter or L/d ratio, both of which affect droplet size and distribution. As the hole size is decreased, so the droplet size decreases. The effect of increasing the L/d ratio above 1.5:1 is to decrease the distribution. Viscosity increases, resulting in both larger droplets and worse distribution.

Summarizing the above discussion, it would appear that not only will gas temperature affect evaporation, but if the nozzle diameter is reduced, evaporation will be increased and hence penetration decreased, as is the case if the fuel viscosity is decreased.

Immediately there can be deduced a reason for the difference between Rothrock and Gelalles' work. Rothrock used an .018 inch diameter nozzle and Gelalles a .004 inch nozzle. Thus a difference would be expected. Re-plotting the results shown in Figures 25 and 26 as the difference in penetration from cold to hot conditions Figure 28 shows this as suggested injection pressure has little effect.

On investigation of Holfelder's [33] work, all the nozzles were of the pintle variety and further analysis was rejected, in view of the fact that the analysis was

to cover plain multi-holed orifices as used in the direct injection diesel engine.

1.3.4. Air Motion

In considering the effect of air motion on spray penetration, it is important to bear in mind the type of engine which fostered the investigation, that of a medium speed direct injection engine. There are then two standpoints. One is the air flow in this type of engine and the other is past work on the effects of air flow on the spray.

Taking the last point first. Considerable work was done by N.A.C.A. between 1930 and 1940. Rothrock and Beardsley [34] tested various nozzles at ambient temperature and 200 lb/in^2 pressure and injection pressures of 6000 lb/in^2 with air velocities of 59 ft/sec perpendicular and head onto the spray. They concluded that this air velocity had little effect on the penetration for nozzle sizes of .012 and .022 inches. However, the penetration from a .001 inch diameter orifice was considerably reduced. They considered that the effect of air flow increased as the orifice diameter decreased. The principal effect of the air motion was to increase the distribution of the fuel from the outside of the spray cone and after the end of injection, to distribute the fuel throughout the spray chamber. Figure 29 shows the results for the .006 inch diameter orifice and it is interesting to note that the wind direction directly opposite to the spray motion has the greatest effect, whilst the side wind only effects penetration after 2½ inches travel.

Further work was carried out by Rothrock [35] at much higher air velocities but atmospheric temperature and air pressure. He concluded that from this, with a .020 inch diameter orifice, air velocities in the region of 400 ft/sec were needed to affect the centre cone and that lower velocities had little effect. He also pointed out that air velocities directed counter to the spray had more effect on spray dispersion than velocities directed normal to it. His conclusion was tempered by the fact that, with increased density and temperature, the above factors could be magnified.

The effect of air swirl at engine conditions was later considered by Rothrock [31] with a .020 inch orifice and 6000 lb/in^2 injection pressure. The air velocity required to have a decided effect on penetration was about 300 ft/sec. This observation bears out his previous remarks on effect of increased gas density and temperature. Also, it is suggested by Fledderman [36] that air motion can increase the evaporation rate by affecting the flow around the droplets.

In more up to date work, Alcock [37] using a small direct injection engine, showed that the spray tip from a .010 inch diameter nozzle was just deflected by air motion computed to be around 300 to 350 ft/sec at the periphery of the piston. Fitzgeorge [38] found slightly less swirl in a static rig, but still using a small engine of 5 inches diameter bore. At the edge of the piston bowl his air speed was compiled to be of the order of 200 ft/sec. Methods of calculating the droplet motion have been put forward for instance in Borman's work [39] , but these are only applicable to the droplets

at the outside edge of a spray, or the spray from a high dispersion nozzle such as a pintle or swirl type.

At this point it is worth surveying information on the motion of air inside a four-stroke direct injection engine between 8 and 17 inches cylinder diameters. Published work on this size of engine giving quantitative results could not be found apart from work carried out by B.I.C.E.R.I. for member Companies. Thornycroft [40] concluded that for engines of this size, a four-valve head gave more satisfactory air swirl than the two-valve head, but no figures for either were given nor did he describe whether the swirl created at valve open period was continued to injection. Tull [41] attempted to measure swirl in the valve open period by using a static rig and vane anemometers. His results from a 9¾ inch bore, four-valve head, showed that the swirl speed was controlled by valve lift, mass flow and pressure drop across the valve.

The 12½inch bore engine, already considered from the fuel spray aspect, had a four-valve head and for its valve lift at dwell Figure 30 is extrapolated from Tull's work. The calculated mean inlet velocity for the engine at full lift is of the order of 113 ft/sec, which would indicate a swirl speed of 1360 r.p.m. If solid rotation of air is assumed then the velocity at the edge of the piston bowl would be 53 ft/sec. Tull does point out that the static rig tests are likely to be different to those in a running engine, and again the question arises, does the swirl created at port opening continue up to

fuel injection?

On small engine work such as Alcocks [37] it has been found that in some cases, swirl can increase as the piston moves towards T.D.C. Thus, it would seem from available information that the swirl on the medium speed four-stroke engine is of a low order, possibly 40 to 60 ft/sec at the outer edge of the piston bowl. This would indicate that no effect could be expected on penetration. At the most, some movement of the outer portion of the spray would occur.

1.3.5. Combustion Effects

In the previous discussion, although evaporation has been considered, no account has been taken of ignition and combustion of the spray and its effect on penetration. In most of the references considered so far, ignition and combustion did take place but usually after injection had finished. In the larger engines the injection period is of the order of 30° of crank, while the ignition delay is some 4 to 6° of crank. Hence combustion must start while the spray is still developing.

Little evidence is available, but Broeze [42] suggests that the spray is affected by ignition due to an impulse of hot gas that disrupts the spray cone. If the ignition takes place on the tip then this may have the effect of decreasing penetration, but if ignition occurred some way down the spray then increased penetration would result. Blume [43] showed that ignition occurred at the periphery of the spray, (Figure 31). Holfelder [33] plotted the tip velocity with this type of ignition (Figure 32) and this shows that the velocity in the ignition case is

increased due to the sudden local pressure rise, then remains constant during combustion. After this, it falls off very rapidly to a value below that of a non-burning spray.

This consideration of combustion leads naturally onto the effect of spray penetration on the course of combustion inside the cylinder. The next chapter considers this, together with the parameters affecting ignition delay.

CHAPTER II

COMBUSTION SURVEY

2.1. INTRODUCTION

The previous chapter dealt with physical mechanics of the fuel spray. However, this cannot be considered in isolation and the interdependance of combustion and the fuel spray must be understood if the equations, as already stated, are to be used in predicting the correct injection system match.

Already two different extreme types of combustion have been considered possible in the 12½ inch bore engine, one of spray just reaching the wall, and one on the spray hitting it. The dependence of these types of mechanisms on chemical parameters must also be investigated.

2.2. Chemical and General Consideration of Combustion

Combustion in a diesel engine is a complex process in which the course of reaction in one stage depends on the path taken in the previous stage. It is difficult to divide into separate parts both in time and in the nature of the process. A rough time division is as follows: the first part is the reaction in the cylinder before injection. This is followed by injection, atomization and evaporation in the ignition delay period. After ignition the fuel evaporated during the delay burns rapidly, giving a sharp pressure rise. The next stage is the period in which the fuel is burnt at a fairly controlled rate. The final stage is the combustion which takes place very late in the cycle, although it is an extension of the previous stage. This is basically

Ricardo's original concept of combustion.

2.3. Ignition Delay Period

The delay period in itself can cause the next stage of combustion to change either chemically or physically. Long ignition delays give rise to high rates of pressure rise in the cylinder and short delays can lengthen the heat release period. Broeze [42] showed this latter effect of a short ignition delay on the subsequent heat release. Figure 33 is taken from his work on a small engine. The injection period is constant but the delay period is varied. He suggests that the disproportionate change in length of heat release was due to the delay being too short in the one case. The fuel is then injected into a flame, evaporates rapidly and looses its penetration powers, giving a bad air fuel mixture.

Earlier, Blume [43] had observed this effect and given the same reason for its occurrence, but suggested that the mechanism could be tied to chemical kinetics, which caused the fuel to decompose through lack of oxygen and thus take longer to burn. It is thus pertinent to consider the mechanism of the delay period in itself.

It is usually considered to be the time from fuel first entering the cylinder until ignition takes place. This can be further broken down into the time required for spray break up, the time for spray atomization, and for the chemical process to get under way. Hurn [44] showed that the first part is not an important part of the delay period. The second part, that of atomization, has been considered in the previous chapter, together with

the concept of a vapour-air layer around each droplet. Ignition will occur only between fairly narrow limits of air fuel ratio, the value depending on the pressure and temperature. E. L. Wakil [45] considered that if one value of air fuel ratio is picked, say stoichiometric, then this mixture will be formed first at the surface of the drop and then, with time, move out through the vapour film to regions of higher temperature. At some point, this mixture will reach its self ignition temperature and the chemical reaction will begin. This first part can be considered to be the physical part of the delay period, the next part is the chemical part which is the delay between the mixture reaching its self-ignition temperature and the reaction becoming explosive.

The major factors affecting the physical, or fuel vaporization part, of the delay have been investigated. Once the spray begins to break up, then the greatest factor is the droplet size and distribution. De Juhusz [46] has shown how the oil viscosity and hole size controls the distribution for a given gas condition. Wakil [45] considers that both these factors, when used to give a better distribution and droplet size, i.e., low viscosity fuel and small orifice (and, of course, high injection pressures), cause the adiabatic saturation to be approached more rapidly. This also suggests that this gives a better possibility of self-ignition occurring because there is a more gradual change in temperature and air fuel ratio with distance across the spray. Both Holfelder [33] and Blume [43] observed the ignition at the edge of the spray.

With the physical delay having established the correct mixture and temperature, there is the time required before the reaction becomes explosive. It has been shown by Yu et al [47] that difference in this time varies widely with fuels. E. L. Wakil [45] suggests that the difference in ignition delay between fuels is largely due to differences in chemical delay. He also concludes that the physical and chemical delay are of the same order of time. Experimental work done by Herele [48] agreed with E. L. Wakil's observations on the components of the ignition lag and also measured ignition occuring on the 'outside layers' of the spray. He also noted that a single locally constant centre of ignition could not be discovered, rather simultaneously ignition at a number of isolated points.

At least two methods of calculating ignition delay are available, one by Tsao [49] and the other by E. L. Wakil [50] . Tsao's produced an equation which considers the delay period with variation in compression temperature, compression pressure and engine speed, while acknowledging that the octane number of the fuel and the chamber configuration affected it. He did demonstrate that, knowing one ignition delay time for a given fuel and injection system, the trend of delay could be calculated as follows:-

$$D = \left(\frac{123}{P} + 0.415\right)\left[\left(\frac{-36.3}{T} + 0.0222\right) N + \left(\frac{47.45 \times 10^3}{T} - 26.66\right) + \left(\frac{T}{1000} - 1.45\right)\left(\frac{1000-N}{60}\right)\right] \quad \ldots\ldots (31)$$

Where D = ignition delay mins

T = temperature at injection point ^{o}R

P_c = pressure at injection point lb/in^2

N = engine speed r.p.m.

Figure 34 shows the results of his equation together with an experimental point. The trend has then been reproduced for this point.

E. L. Wakil furthers his previous work in which he studied the two periods comprising the ignition delay and proposes two equations.

For the physical delay:

$$D_p = 1.10\, d_o^{0.5} \left(0.025 + \frac{1}{T_B - 1850} \right) N^{0.465} \quad \ldots\ldots (32)$$

and the chemical delay

$$D_c = 10.3\, d_o^{0.85}\, e^{A} + Bn \quad \ldots\ldots\ldots\ldots\ldots\ldots\ldots (33)$$

Where D_p = physical delay sec.

D_c = chemical delay sec.

d_o = initial droplet diameter in.

T_B = free-stream air temperature ^{o}R

n = number of carbon mols.

and $$A = 20.5 - 35.9\left(\frac{T_B}{1850}\right)^2 + 13.2\left(\frac{T_B}{1850}\right)^4$$

$$B = 0.364\,(7.775 - \log_e T_B)$$

2.4 Main Combustion Period

The previous section touched upon the possible influence of chemical decomposition and oxidation. Although the chemical reactions, as applied to heat release such as this, were known and referred to from time to time, Meurer[52] finally proposed the full mechanism and used it to prove the principle of the M.A.N. 'M' type engine.

There are two chemical processes which take place simultaneously. There is the oxidation of the fuel and there is the thermal decomposition or cracking. Thermal decomposition is the stripping of hydrogen atoms from the hydrocarbon chain. After further decomposition, polymersation and dehydrogenation, smoke is formed.

Thus, the interest lies around the conditions which assist thermal decomposition. It takes place at relatively low temperatures (lower limit of decomposition temperature is thought to be about 750 to 1000°F, Schweitzer [53]) and occurs whether in the presence or absence of oxygen. However, when oxygen molecules are present the oxidation reaction interacts and competes with the cracking. High pressures and temperatures accelerate decomposition, but it can still predominate at low temperatures, depending on the primary products.

All diesel fuels will have this low temperature cracking predominance and, such is the speed of cracking, that carbon may be formed at an intermediate stage before oxidation takes place. In the engine cylinder the fuel is injected in an atomized state and it has been estimated that a 50 micron drop has 10 molecules [43] of which only a few are on the surface. The rest must rely on evaporation and diffusion processes to come into contact with oxygen. The rate of these processes are slow compared with the rate of decomposition. Meurer emphasised the radical effect of temperature on decomposition and said that in the diesel engine, balance of the two mechanisms characterises the first stage, for which the necessary conditions of oxygen concentration and fuel evaporation are prepared during the ignition delay. However, once the temperature rapidly increases, it becomes impossible to feed enough oxygen to the fuel, and decomposition predominates. Using the normal mixing process, described in the previous chapter, Neurer suggests that as the distribution is improved, although the oxygen has easier access to the drops, the cracking rate increases proportionally greater and thus,

carbon and longer heat release period results.

In short, Meurer suggests that chemical kinetics have a strong influence on the course of heat release inside the cylinder. The M.A.N. system was designed to counter the above objections by laying the fuel onto the combustion chamber wall, and thus minimising the portion of fuel involved in the auto ignition, allowing the fuel to gradually vapourize at a temperature below decomposition level and then mixing the vapour and hot gases quickly by means of effective air swirl.

The Pischinger brothers' work [54] supported Meurer's theory, but objections have been raised. Doubt is expressed as to the ability to form a film on the piston, the mechanism upon which Meurer's theory revolves. Chemists claim that at gas temperatures involved, decomposition only takes place at a significant rate in the vapour phase and would not be predominant in the liquid phases. Meurer counters this by pointing out that the local flame temperatures are much higher than general gas temperatures, and are largely independent of overall air/fuel ratio.

Evidence of the effect of 'chemical kinetics' has been furnished by other workers. Garner et al [55, 56, 57 and 58] established the importance of free radicals in the ignition delay and combustion processes. This principle used by Schweitzer and Alperstien [59] in fumigation of a small engine which reduced ignition delay and smoke in the exhaust. Lyn [60] studied the combustion with a spectroscope and detected the production of carbon early on in the cycle and in work [61 and 62] on another small high speed engine, analysed pressure diagrams and fuel injected rates and

studied the overall effects on heat release. He found that the rate diagrams were similar for all conditions and could be divided into three parts. At first the rate of burning is generally high and lasts about 3° crank. Then there is a gradual decrease in heat release. These first two stages amount to 80% of the total. The last portion or tail was burning at a very slow rate. The effect of delay period on the maximum rate of heat release is to increase it in the first part, and like Blume [43] and Broese [42] he found that the heat release period was shortened. But when the ignition delay was added there was no significant difference in overall period. He also found that the absolute rate of heat release increased in proportion to the engine speed so that in terms of crank degrees the burning time remained constant. The period of burning was long in comparison to the injection period.

In general Lyn found that gas temperatures, fuel viscosity and volitility did not have much effect on heat release and that chemical kinetics did not play a part in controlling combustion. However, he accepted that he was considering the length of heat release and thermal efficiency and did not consider smoke conditions which could be controlled by chemical phenomena.

2.5 Combustion Principles

To restate the interest in combustion in a simple way would be more helpful. It is to obtain a stated brake thermal efficiency at a stated speed and load with acceptable exhaust conditions and given constraints on thermal and mechanical loading at design stage. It may over simplify the situation but the following equation may be used:-

$$\Omega_b = \Omega_{comb}\ \Omega_{HL}\ \Omega_{cycle}\ \Omega_{mech} \quad \ldots\ldots\ldots\ldots (34)$$

Where

Ω_b = brake thermal efficiency

Ω_{comb} = combustion efficiency

Ω_{HL} = heat loss efficiency

Ω_{cycle} = cycle efficiency

Ω_{mech} = mechanical efficiency

The important aspect to the present discussion is Ω_{cycle}. Mention has been made of the 'shape' of the heat release curve, or when and at what rate the fuel releases its energy. This controls Ω_{cycle}. In a simpler form, the cycle efficiency is a function of rate of heat release

$$\Omega_{cycle} = f\,(R_{HR}) \quad \ldots\ldots\ldots\ldots\ldots\ldots (35)$$

Where R_{HR} is the rate of heat release.

Now the following form can be proposed

$$R_{HR} = R_I \times f_c \quad \ldots\ldots\ldots\ldots\ldots\ldots (36)$$

Where R_I = rate of fuel injected

f_c = some function of the chamber and nozzle conditions which allow the fuel to release its heat energy.

That is to say, that the rate of heat release is a function of injection period and f_c.

From Lyn's work the indications are the rate of heat release is controlled by R_I and f_c where f_c is based on purely physical factors such as engine speed combustion chamber shape and direction of nozzle. Chemical kinetics do not play any part.

By measuring pressure-crank angle diagrams from

engines and bomb rigs, and making certain assumptions about heat losses the shape of the heat release curve can be calculated, and it is worth considering Lyn and other workers' results. Figure 35 shows the types of heat release diagrams for various engines as considered by Lyn [62] . Three basic mechanisms are proposed; Type (A), as in the direct injection engine, in which the 'fuel crosses the chamber with considerable momentum - mixing proceeds immediately as it enters the chamber and is little affected by ignition'. Type (B), seen in both the DI with fuel on the wall and the indirect swirl chamber where 'fuel deposition on wall - negligible mixing during delay period due to limited evaporation. After ignition evaporation becomes rapid and rate is controlled by access of hot gases to the surface, radial mixing being induced by differential centrifugal forces. Burning is therefore delayed by ignition lag'.. The third, Type (C), which appears in the latter two types of engine, is 'fuel distributed near the wall - mixing proceeds during delay but at rate smaller than (A). After ignition, mixing is accelerated by same mechanism as (B)'.

Lyn suggested a method of predicting the rate of heat release . It is based on a triangular rate of burning with the triangle being at right angle with the maximum rate at the start. Increasing burning time for each successive element of fuel was considered. The burning rate was defined as:-

$$R = R_o \left(1 - \frac{t}{t_b} \right) \quad \ldots\ldots\ldots\ldots\ldots\ldots\ldots\ldots \quad (37)$$

Where R_o is the initial rate (determined by the size of

the element).

$t_b = t_o + a\, t_i$

t_o = burning time of first element

t_i = time of injection after first element

a = constant.

He suggested values for a and t_o which gave a reasonable fit with his experimental results. Thus, given the ignition delay period, the rate of heat release and hence the cycle efficiency can be calculated.

All three systems have high air swirl which tends towards high physical mixing rates, but some work has been carried out using constant volume bombs. Figure 36 shows the results calculated by Blume [43] using a constant volume bomb. He also found that the ignition delay had a decided effect on the course of combustion, not only from the maximum rate, but the duration. As the ignition delay decreased so the duration increased (he decreased ignition delay by increasing air temperature). Blume explained this phenomena by evaporation and decomposition of the fuel. With the shorter ignition delays, the fuel injected after ignition must pass through a mantle of burning fuel while still lacking oxygen. The fuel is more quickly evaporated and its penetration is reduced, which lowers the speed at which the fuel and air mix. Further, the fuel, in passing through the flame zone without oxygen, is subjected to decomposition.

The amount of information on combustion in the relatively larger direct injection diesel engine is small. Whitehouse et al [21] measured the cylinder pressure diagram from what is thought to be a 10-inch bore engine, and

analysed it. Although they admitted difficulty in gaining an accurate diagram, Figure 37 shows their 'probable pattern'. The program described in Appendix III also became available and is very similar to that used by Whitehouse. It was used to analyse some cylinder pressure diagrams from the 12½-inch bore engine described in Chapter I, and the result is shown in Figure 38. It is very similar in shape to that obtained by Whitehouse, and except for the reduced peaks due to ignition delay, to that of Lyn's direct injection engine shape. Also plotted in Figure 38 is the pattern for the 12½-inch bore engine based on the injection rate shown in Figure 18, and calculated as per Lyn's method. The fit is not very effective but to attain this the constants suggested by Lyn were radically changed. Lyn recognised this and suggested that if the constants were fitted for one type of engine then various speeds and loads can be studied. This can lead to misinterpretation. If the constants are used for one engine then it is implied that the major factor other than delay period is the rate and duration of injection of fuel into the cylinder. However, it has been observed on the larger direct injection diesel engines that if the injector nozzle area is kept constant (i.e., same rate and duration) but the hole configuration is changed, then the engine can react by a change in B.S.F.C. and exhaust condition. Thus it would seem that in the larger direct injection engine a further correlation between the above and how far the spray penetrates is necessary.

It is suggested by Borman and Deluca [63] that the air is relatively quiescent so that the efficient injection

system is required to properly distribute the fuel through the air for complete combustion. The nozzle is usually positioned at the centre of the piston and the nozzle orifice diameter and number are such that the penetration and distribution is satisfactory, i.e., that over and under penetration are not obtained. There is little time for mixing, some 25 to 30 crank degrees for four-stroke engines and the atomization must be fine with injection pressures in the range 5000 to 12000 lb/in^2. The allowable penetration up to the chamber wall is dependent on the injection pressure, but primarily on orifice diameter.

Borman and Deluca are suggesting then that the allowable penetration is to the wall of the combustion chamber and implied the fact that over-penetration and under-penetration are undesirable, the latter not utilizing the air at the outside of the chamber, and the former giving bad combustion and heavy carbon build up on the piston wall. Therefore, the ability to calculate the penetration to the wall coupled with an equation similar to Lyn's, based purely on physical factors, should give the ability to predict the injection match and heat release pattern required.

Beyond this, however, must be borne in mind Blume's work, which indicates that chemical kinetics do play a part in combustion and it is just possible that his rig, with no air motion, could bear a closer resemblance to the large engine than does Lyn's work.

A second point is that of the assumption that the spray just reaches the edge of the combustion chamber. If the 12½-inch engine is reconsidered and the calculations of penetration carried out in Chapter 1, it was suggested that

the spray would reach the piston wall after 2.5 milliseconds if no evaporation took place. Figure 39 replots curve 1 (Figure 21) and the possible maximum reduction in penetration due to evaporation is plotted as a broken line, estimated from Gelalles and Rothrock's work [31 and 32] and Figures 25 and 27. Bearing in mind the errors that may be induced by using Schweitzer's equation the spray would seem to impinge on the crown after about only 40% of the injection period is over. This with the photographic evidence in Figure 24 indicates that piston impingement is possible and may affect the rate of heat release. If in fact evaporation is more pronounced than has been indicated then the spray may penetrate as a vapour air mixture and not a liquid-vapour-air mixture. The effect of changes in combustion shape and air motion could more radically affect this type of spray.

Evidence is thus required which can elucidate the mechanism controlling the heat release inside the cylinder of a medium speed diesel engine.

Conclusions on the work surveyed in this, and the preceding chapter, can be drawn.

CHAPTER III

CONCLUSIONS FROM SURVEY

In the previous chapter the concept of f_c, the ability of the combustion chamber and injection nozzle to control the heat release was introduced. It has been suggested that the mechanism involved in f_c, at least on medium speed engines, is that of little air motion and the fuel spray just 'licking' the edge of the piston bowl. The nozzle is usually located at the centre of the piston and the number of sprays is such that full coverage of the chamber is obtained. The onus of mixing the air and the fuel lies with the injection system, the air being induced into the spray in which the fuel has been atomized into small droplets. Thus to predict a match of nozzle and combustion chamber a knowledge of the course of spray and combustion is necessary.

The survey has shown that information available is incomplete on the parameters affecting spray penetration. There are equations available for calculating spray penetration and cone angle but their application to an actual jerk system is in doubt. This is due to difference in upstream conditions and L/d ratios found in the engine system ~~and~~ compared with those used by researchers to establish the equations. These equations are further limited in that no account is taken of the conditions around the spray in an engine cylinder such as high gas temperatures (leading to evaporation), air motion and combustion. There is evidence to suggest that evaporation effects penetration with orifice diameters below about .020 inches but available information does not allow predictions.

Air motion would have tobe of a high order to effect penetration of any but the smallest diameter orifice,

but again there is some doubt as to the type and magnitude of air motion in a medium speed diesel engine. It is suggested that it is of a low order.

Ignition can effect penetration depending on the position in the spray that it occurs. If it occurs between the nozzle and the tip of the spray it has been shown that the penetration will be greater.

The work surveyed has essentially concentrated on the penetration of the tip of the fuel spray. That is to say the liquid:air spray. As the spray develops it entrains air which is then moving with the fuel droplets. If no disruption takes place, such as high air swirl, then fuel that evaporates will still continue to move away from the nozzle. If evaporation is considerable then it could be that the penetration and cone angle of the vaporized spray is much more important than the liquid part of the spray as far as correct matching is concerned.

Work carried out up to the present time suggests that in the large bore engine chemical kinetics could play a part, particularly in relation to the delay period, although work on smaller engines is conflicting with regard to the predominance of physical or chemical factors.

Impingement of the fuel onto the combustion chamber wall is a possible mechanism that may be occurring in large engines at high brake mean effective pressures.

The survey thus points out the main avenues of further investigation. These are to correlate penetration of a fuel spray from an actual jerk system with rig work already carried out. To investigate the effect of evaporation on penetration and incorporate the finding into any prediction

equation. To find the magnitude and pattern of air flow in a medium speed diesel engine, and consider the conditions prevailing inside this type of engine with a view to applying the prediction equation to combustion problems.

The following chapters describe work carried out by the author in an attempt to fill some of the gaps brought to light by the survey.

CHAPTER IV

EXPERIMENTAL WORK ON COLD BOMB

4.1. INTRODUCTION

This chapter describes the experimental work carried out on the development of fuel sprays in still gas at high densities and atmospheric temperatures between January, 1963 and February, 1964 at Loughborough University. The objective was to correlate the actual injection system results with those in previous work.

It is divided into five main sections, the first covers the basic design and intention of the rig, the second covers the development of the rig with a back pressure cylinder and cold pressure chamber together with all the instrumentation. The third section deals with the photographic techniques used. The method of measuring the results obtained is detailed in the fourth section, followed by a discussion section.

4.2. Basis for Building Rig

From the revision of other work on this topic, the basic objectives of an experimental rig were laid down. The fuel spray was to be injected into gas. A chamber was to be built which could contain the gas at pressures up to 400 lb/in^2 giving equivalent engine cylinder densities at room temperature. The gas pressure was to remain static during the injection cycle. Heating of the gas was to be considered later.

The form of injection was to be a normal jerk fuel injection system. The nozzle was to be the standard multi-hole type as used on the engine, as it has been indicated previously that the flow in the nozzle sac could have a great influence on the spray formation.

The size of the injection equipment was determined by the fact that an 8-inch bore engine would be available for any future work. The injection equipment is designated C size pump and T size injector by international standards.

The size of the chamber was dictated by the possible penetrations that would occur. As future interest could centre on engines having cylinder bore sizes of 14 to 15 inches observation of the spray penetration should be of the order of 12 inches.

Residual as well as Class A fuel was to be handled by the rig so that difference in fuel could be seen. Temperature control of the fuel was important so that viscosity would be controlled.

The following properties of the spray were to be measured:-

(a) tip penetration with time

(b) cone angle

(c) spray angle

(d) droplet size

(e) droplet distributions

(f) effect of air movement.

These would be measured against different gas densities, fuel viscosity and injection pressures. The range of fuel line pressures would be that supplied in the normal system, giving up to 10,000 lb/in^2 peak line pressures.

The method of measuring cone angle, tip penetration and spray angle was to be such that no interference to the spray was introduced. Photography was chosen and divided into

two types. One was the single flash spark source method. The second was to use a High Speed Camera with continuous light source photographing the whole of one injection. The first method was to be used for developing the rig as it was considered to be inexpensive.

One further piece of apparatus was considered. It was thought that the total fuel output per injection would be needed. The difficulty of measuring this under high pressure conditions in the cold chamber led to the design of a simple apparatus to apply back pressure to the nozzle. In this way, the effect of back pressure could also be investigated.

4.3. Development of the Cold Bomb Rig

4.3.1. Basic Rig

As has been stated above, the C size injection system was chosen because of the availability of the 8-inch bore engine. The basic rig reproduced the camshaft, cam follower and pump of the jerk injection system. A diagrammatic layout is shown in Figure 40. It consisted of a 2-foot, 6-inch long camshaft, which was mounted in a cambox. This cambox provided a sump for lubricating oil. A small belt driven pump supplied this at 15 lb/in^2 to the shaft bearings and cam follower. At each end of the shaft were mounted flywheels. These helped to keep the rig at a constant speed. The shaft and assembly were driven by a 30 H.P. D.C. motor. This drive was via a vee belt system onto one of the flywheels. The speed of rotation of the camshaft could be varied from 0 to 350 r.p.m. by adjusting the supply voltage to the D.C. motor. This speed range could be extended by fitting a larger pulley to the motor shaft.

Bolted on top of the cambox was the cam follower assembly and jerk pump. Allowance was made for adjustment of the pump tappet. From the jerk pump, the injector and pipe could be fitted in the normal manner, the injector coming in front of the cambox and being bolted to the cold chamber or back pressure cylinder, discussed later. Fuel for the pump was supplied from a header tank. This tank was 2 foot above the pump and the fuel fed from this via a control valve and filter. At a later date, a second tank was added together with another filter. This tank carried an immersion heater and was lagged to retain heat. It could handle heavy fuel or Class A fuel which was to be heated before entry to the pump. The output of fuel from the cold chamber or pressure cylinder was collected in a reservoir beneath the cambox and returned by a small electric pump to the header tank.

4.3.2. Back Pressure Cylinder

At first it was thought useful to measure the mean quantity of fuel injected in each cycle. It is known that the injection system works against a back pressure, both in the engine and the bomb. Thus to investigate the effect of back pressure on fuel flow, a short experiment was carried out to apply a back pressure from atmospheric to at least engine compression pressures, i.e., 900 lb/in^2.

By allowing the fuel to inject into a cylinder filled with fuel a pressure can be created. If the flow out of the cylinder is controlled by a valve and the pressure inside kept constant, then the fuel injected can be measured under these back pressure conditions. The first design of apparatus to apply back pressure to the nozzle was a small

flanged cylinder with Bosch peak pressure indicator valve. This proved unsatisfactory due to an increase in back pressure during one cycle. The cause of this was the compressing of the fuel in the valve cylinder during injection owing to the small cylinder volume.

The second design incorporated a much larger volume. Figure 41 shows this cylinder with a Stein-Atkinson-Vickers variable relieve valve in place at the bottom. This valve allowed a high degree of control over the pressure in the cylinder, the pressure being created by the injected fuel. The range of back pressure was 0 to 1000 lb/in^2. The continuous flow from this cylinder could be measured accurately over a period while the back pressure remained constant. The cylinder pressure was measured by means of a capacitive type transducer located in the side of this cylinder. The associated equipment of this transducer will be covered later.

It was found that back pressures even to the order of 1000 lb/in^2 did not seem to have an effect on the flow output, as measured in this way. This will be discussed later.

4.3.3. Cold Pressure Chamber

The pressure chamber (Figure 42) consisted of a rectangular steel box measuring 18 by 6 inches. To one pair of opposite sides were clamped $\frac{7}{8}$ inch armour-plate glass, 12 inches by 4 inches in size. An inspection cover at one end gave full width access to the chamber. The injector was fitted into a round flange mounted on top of the chamber, rested on an 'O' ring. It was held by four clamps which allowed the flange and injector to be rotated

when locating the direction of a nozzle orifice. The injector itself was held onto the flange by two studs and a cross strap. The nozzle tip protruded through the bottom of the flange and was so positioned that when the flange was in place on the chamber, the tip appeared in the top inside corner of the field of view when looked at through the armoured windows.

The floor of the chamber was slightly sloped to the back so that fuel was drained down to an outlet plug. This outlet was controlled by a high pressure needle valve which had a fine adjustment. Pressures of up to 400 lb/in^2 could be safely contained, although during tests the maximum used was 300 lb/in^2.

The gas used in the cylinder throughout the tests was nitrogen. This was supplied from a bottle at 1500 lb/in^2, through a regulating/safety valve, to an inlet at the back of the chamber. With this regulator and the outlet needle valve a steady flow of nitrogen through the chamber could be maintained while the pressure in the chamber remained constant. It was thought that this would help cut down fuel mist in the chamber.

4.4. General Instrumentation

4.4.1. Temperature Measurements

The temperature of the nitrogen gas was measured in four places by thermocouples; Figure 43 shows the positions. During a run these temperatures were continuously monitored on an ultra violet recorder and calibrated on a potentiometer. The temperature of the fuel in the nozzle was important from the point of view of viscosity. In Figure 44, position of

the thermocouple can be seen on the injector, the thermocouple wire passing down into the nozzle feed ring. The thermocouple was a Cu/con and,as in the case of previously mentioned thermocouples, continuous monitoring was done on the U/V recorder.

Dial gauges were used in conjunction with copper/con thermocouples for measuring the temperature of the fuel at the tank and at the inlet to the pump. As the dials were remote from the thermocouples care was taken to use compensated leads.

In all cases, the cold junction for the thermocouples was supplied by ice enclosed in a thermos flask.

4.4.2. Pressure Transducer

Two types of transducer were available at the time. One was the standard R & H strain gauge, the other was the CAV/Rotax strain gauge type. The Rotax transducer was chosen at first because its physical size allowed it to be placed near the nozzle as is shown in Figure 44. However, during initial test runs the line pressures were found to vary cyclically when the rack was locked in one position. The pump and injector were checked for correct operation as was the speed variation of the camshaft. Both these proved to be satisfactory. The Rotax transducer was placed at the centre of the injection pipe and then the results were compared with the larger R & H transducer in the same place. The pressure variations still persisted, but the mean pressure readings on the R & H pick-up were higher than those from the Rotax. The difference depended on the rack setting, but at pressures equivalent to engine operation, this was as much as 1500 lb/in^2. The calibration

of the transducers were checked on the same dead weight tests and proved to be correct. After a further short inspection, the only significant difference to be found was that the R & H transducer strain tube was part of the pipe and was an inch long, whereas the Rotax strain tube was 3/16" long and was at right angles to the main injector pipe. On looking at results from engine tests at R & H, it was found that these pressure fluctuations were present and could be a function of the filling of the pump. Further study on this subject was discontinued and the Rotax transducer chosen as being the most accurate pressure measuring device for the rig.

Both transducers were strain gauge type and so the same auxiliary equipment was used. A standard type decade box was used to complete the bridge circuit, together with a fine graduated potentiometer for measuring change of resistance. The output of the decade box was coupled to a D.C. chopper amplifier and this to a two beamed oscilloscope. The Rotax transducer was temperature compensated.

4.4.3. Needle Movement Transducer

The transducer to measure the needle movement was an inductance type. This was placed on the top of the injector, Figure 44. It formed part of an oscillating circuit where output frequency varied with change in inductance. This output was fed to an F.M. amplifier and thence to the oscilloscope. The delay caused by the compression of the long rod had to be allowed for when studying needle lift diagrams as were the vibrations encountered on these diagrams at the end of opening and closing due to this same rod.

4.4.4. The Sweep Unit

A standard Southern Instruments Sweep Unit was used to trigger the scope beams to supply crank degrees marking on the F.M. output beam. This unit was driven from the camshaft by a 1:1 power grip belt assembly.

4.4.5. Oscilloscope and Camera

The fuel line pressures and needle lift movement traces obtained on the oscilloscope had to be photographed. Therefore a standard Southern Instruments Engine Indicator was used. This incorporated the scope and camera which could be modified to use continuous paper film or single shot films on a drum. There was also a device which allowed the traces on the scope, initially switched off, to be switched on for one cycle.

4.4.6. Chamber Pressure Measurement

The pressure in the chamber remained constant throughout a test and therefore a Bourdon type gauge of 0 to 400 lb/in^2 was used for measurement. This was accurately calibrated against a dead weight test. The position is shown in Figure 42.

4.4.7 Cam Rotation Measurement

The speed of rotation of the camshaft was measured by using a Farnell digital tachometer and a proximity probe. The probe was placed at right angle to and a short distance from a brass wheel carrying 4 steel studs. Figure 45 shows the arrangement. In this way, rotational speeds could be measured to about 1% accuracy.

4.4.8 Rack Setting

The pump rack movement was limited and measured by a micrometer stop. Once the rack was in the desired

position, it could be locked by means of the lock nut on the end of the rack.

4.4.9. Back Pressure Measurement

In section 3.2 the back pressure cylinder was described and the fact mentioned that a capacative transducer was used to measure the cylinder pressure. This transducer was coupled up with the oscillator and F.M. equipment already mentioned and used in conjunction with the engine indicator scope.

4.5. The Nozzle Hood

As the actual injection system was to be used, this meant dealing with nozzles which had from 4 to 10 orifices. If all the orifices were left uncovered, they would interfere directly (getting in the line of sight) and indirectly (misting up the chamber) with the one hole under investigation. Thus some form of hood had to be made. If only one hole was allowed to spray into the chamber, the rest had to be prevented from developing, but blocking the other orifices would change the flow conditions in the sac.

The hood that was successful is shown in Figure 46, and the section in Figure 47. The outer case was made of brass while the tube to the orifice under investigation was stainless steel. Great care had to be taken when fitting this tube and the bore was reamed by hand to make sure that it did not in any way interfere with the developing spray. The other end of the tube was carefully shaped to the contour of the nozzle tip so that no fuel from the other orifices could enter the tube. To make sure that the tube fitted exactly on to the tip, a light was directed up the drain tube and the orifice viewed

through the steel tube, and vice-versa. The hood outer section bolted onto the bottom of the chamber flange, thus allowing it to be fitted onto the injector external to the chamber. Final adjustment of the height of the nozzle in the hood when testing the fit of the steel tube on the nozzle tip was achieved by tightening the stud and cross strap on top of the injector. Before actual test runs, the nozzle was photographed close up, spraying under gas pressure, with the still camera and in some cases the high speed camera (to be discussed later). This was a final check that no interference took place.

The fuel from the other orifices was collected in the drain tube and ran down a polythene pipe. At the end of this pipe was located a loose wire wool plug which helped kill any fuel mist before the fuel passed out into the main chamber to be drained out through the needle valve.

At one stage, a shutter was placed over the test orifice tube to stop misting before the photographs were taken. This shutter was actuated by a fast response solenoid placed below the hood. Figure 48 shows the shutter in place in the bomb. The fast response solenoid is also located inside the chamber and applied a direct pull on the shutter which slides on the brass tube of the hood. The solenoid and its associate trigger circuitry were made available by R & H from work done by Kimpton [64]. However, the shutter was discarded. Firstly, the solenoid was unreliable. Secondly, while the shutter was up over the steel tube, fuel built up in the tube and interfered with the spray development after the shutter had been moved. Lastly, it was found that the chamber did not mist up over about 20 cycles due to only one hole being allowed to

develop,and the large internal size of the chamber.

During preliminary tests, it was found that after seven or so cycles, the injection equipment had reached a steady state condition. Therefore the method used to actuate the spray was to push the rack in by hand, to hold for ten or so cycles and then start the camera. This method proved most satisfactory.

4.6. Method of Measuring Fuel Output

At first it was considered necessary to know the total output of fuel from each nozzle. A very simple method was chosen. Due to the reasons found in 3.2 that the back pressure on the nozzle has little effect on the fuel output, all outputs were measured with atmospheric back pressure which consisted of draining the fuel ejected from the nozzle into a weighing can via a short length of plastic tube. The rig would be set running to the required speed. Then the rack would be sharply put in until it rested on the micrometer stop. In doing this, a circuit was closed starting a Farnell digital counter. When the rack was moved back again, the counter stopped. The fuel collected was weighed on a set of scales weighing .1 gram.

4.7 Single Flash Photography

The reason for developing this method was mainly one of economics. It was limited to being used for the development of the rig and no results were recorded because of the cyclic fluctuations described in section 3.4.2.

The basic equipment was a 35mm single lens reflex Zenitz camera and a Lunartron Ultra High Speed single flash unit (H.S.I.). This flash unit had a flash duration of 0.4 microseconds to 25% peak, and a peak intensity of

50 million beam C.P. It could be triggered by a voltage source and had a re-cycle time of 10 seconds. The injection rig was enclosed in a light tight booth and thus the camera could be set with shutter open and the film exposed by the flash. This simplified the control of the system so that a camshaft operated switch could be used. This switch is shown in Figure 49, and consisted of a slip ring with the outer edges of brass and the centre of tufnol. At one point, spanning the tufnol centre, there was a steel insert. Bolted to the cambox was a steel spring whose point could be moved in an arc relative to the camshaft. The tip was spring loaded on the centre and if a voltage was supplied across the slip rings and pointer, then a circuit was made when the steel insert contacted the pointer. The position relative to the camshaft at which the insert did this was controlled by moving the pointer in an arc around the shaft. A clamp and scale were provided to facilitate this. This switch was incorporated in the camera set up, and Figure 50 shows this arrangement.

The Southern Engine Indicator Camera was modified to drum trace recording. On the drive to the drum was a cam and micro switch. This could be set at any desired position and would be switched on for one revolution. It triggered a relay which in turn switched the scope/beam on and made it possible for the flash circuit to trigger. When the slip ring made with the pointer, the flash triggered. Thus with the correct setting of the cam a film of the pressure trace and needle lift was obtained at the exact time as the film of the spray. As the positioning of the slip ring trigger was not very accurate, a Selenium photoelectric cell was placed in front of the flash point. The output from this

was shaped to a square pulse and superimposed on the needle lift trace. Thus the exact time of film exposure was recorded on the traces.

Three methods of illumination were tried. The flash source was placed directly opposite one window (Figure 51a) and the camera opposite the other. No diffuser was used, only a graduated transparent plastic panel, which will be discussed later. This method proved most unsatisfactory as the illumination on the film was localised, so an opal glass diffuser was inserted on the light source side. This was an improvement, but again illumination of the spray was not even. With the source angled across the results were better, but finally another method was tried. This method is demonstrated in Figure 51b. The flash source was placed under the chamber angled up at 45°. The light was then reflected into the chamber by a wooden hood painted matt white inside. The opal glass remained in the same position; this gave good results.

With the open shutter method, a range of both aperture settings and films were tried. The aperture range was from F.2 to F.16. The best results were obtained with F.2.8. The films were tried as follows:-

Ilford HP 3	ASA 400
Ilford HPS	ASA 800
Kodak TRI-X	ASA 400
Ilford FP 3	ASA 125
Kodak Panatomic X	ASA 40

Ilford FP 3 and Kodak Panatomic-X were far too slow. Kodak TRI-X and Ilford H.P.S. gave too much grain under contrast development. Ilford HP 3 proved to be most suitable.

Great care had to be exercised in the developing of the film. Over development gave increased grain and led to an overestimation of cone angle and penetration, while under development gave smaller cone angles and penetrations than the actual spray. To help in this matter of correct development and as an aid in the earlier development of the rig, the flash unit was replaced by a Dawer Stroboscope unit which would trigger every revolution. Then, with the camshaft trigger working continuously, actual observation of the spray could be carried out.

The camera was placed about 3 feet from the chamber giving enough depth of field to focus the spray and a graduated panel. The centre point on the plastic had to be in the same position as the nozzle tip. This was ensured by using Vernier height and depth gauges on the inside and outside of the chamber. Once this has been achieved, then the camera could be lined up on the nozzle tip and centre point. This gave a slight parallax effect on the film which amounted to about $\frac{1}{4}$ inch in 5 inches. Therefore the camera was moved horizontally and parallel to the spray axis, the error being halved. In Figure 52 the camera, chamber and flasher unit can be seen in place. Figure 53 shows the type of results gained. Each photograph is from a different injection cycle with the rack, fuel temperature and chamber pressure held constant. Due to the cyclic fluctuations already mentioned they must only represent, at best, the mean spray development. With this technique, the development of the nozzle hood was carried out quickly and cheaply, which would not have been the case with the high speed technique described below.

4.8 High Speed Photographic Technique

4.8.1. Camera and Illumination

The high speed (H/S) photographic technique was chosen as the method giving the most accurate results without interfering in any way with the spray itself. The basic apparatus was a Fastax High Speed camera with its speed control equipment. Three types of continuous light sources were tried, and further control equipment had to be manufactured.

The camera was a Fastax W.F.I. running up to 16000 frames/second, (see Appendix IV). The film used was Kodak Plus-X 16 mm movie with 8mm perforations. The speed the camera attained during a test run was set by a standard 'goose' control unit. Except for one run, this unit set the camera to reach about 16000 fps during the tests. This gave film coverage of three injection cycles. Because of this and the cyclic variations mentioned in section 3.4.2, the camera on the oscilloscope was changed from drum to continuous feed to give equal coverage of the pressure and needle lift traces.

The H/S camera was placed six feet from the chamber with the continuous light source directly opposite. Figure 54 shows the general set up with the projection lamp light source. The foreshortening mentioned in 4.7 was therefore cut down to 1/16" in 4" of penetration. The three light sources tried are listed below (see Appendix V for details).

1. 8 tungsten lamps (750 watts each)
2. One Xenon lamp plus 4 tungsten lamps
3. One 1200 watt episcope projection lamp with concave backing mirror.

Using the first method a strong diffuser was necessary to give even illumination hence the need for eight tungsten lamps. The second method was better, but still a strong diffuser was used and the Xenon lamp had to be backed up with 4 tungsten lamps. These lamps were used to illuminate the chamber corners more evenly. The last method with the projection lamp proved the best. With the concave mirror a strong beam of light could be focused onto the chamber and very little diffusion was necessary. When the close up shots of the nozzle were taken the diffuser was removed completely.

The illumination provided by this method was sufficient at an aperture of F.11 and a 5 microsecond exposure.

4.8.2 Control Equipment

When using the higher speed camera and equipment, it became impossible to control all the operations by hand. Therefore some method of sequence control was needed.

There were seven operations:-

(i) Trigger H/S camera (via Goose control)

(ii) Trigger oscilloscope trace camera

(iii) Trigger pulse marker on H/S film

(iv) Trigger pulse marker on trace film

(v) Switch camer lights to full power

(vi) Switch in fuel pump rack

(vii) Switch on ultra violet recorder

(viii) Switching off operations 1, 2, 5, 6 and 7.

To keep the control unit as simple as possible, three of the above were not included in the sequence of operations. As has been stated in 3.4, the ultra violet recorder was measuring nozzle and chamber temperature.

These were fairly steady and the recorder could be set on a low paper speed. It could be switched on manually before a test run and left to monitor the temperature throughout the run. The fuel rack had not been fitted with a solenoid and this was left to manual operation. The third operation, manually controlled, was the changeover of the continuous light source. All three types of lighting used were set at low power for focusing and setting up of the camera and equipment simply to lengthen their useful life. They were left at this setting until just before the camera started. At this point they were switched to full power. At the completion of the run, the lights were switched off. The control box was then constructed using high speed relays and R-C delay circuits.

The sequence can be described as follows. On depression of the start switch, the trace camera started. After a set delay, the H/S camera automatically switched on. After a further delay, which could be varied, a pulse marker was superimposed simultaneously on the trace and H/S films using a R.A.R.D.E. SPARKTIMER (Appendix VI). The duration of this pulse could be controlled. The pulse marker made it possible to tie up the exact line pressure and needle lift traces on the trace film with the spray it caused on the H/S film. At the end of the run, the H/S camera cut off automatically when all the film had passed through. The trace camera was switched off by releasing the start switch.

The time of one run from depression to release of the control switch was approximately 3 seconds, the H/S camera running for about one second. The relays were

driven by an external 24 volt power supply. No control of the oscilloscope beams was necessary, as they were left on continuously. This was made possible by the continuous feed film on the oscilloscope camera.

It was essential, from the point of view of delays, to develop the film from a test run immediately. The H/S film was processed on a Hadland Processor, it taking about 20 minutes to complete 100 feet of film. The paper film from the trace camera was developed using Kodak 163 developer and Kodak-Kodafix fixer. The film was slowly unrolled and re-rolled while immersed in either the fixer or developer under dark-room conditions. Thus both sets of films could be checked within half an hour of the run.

4.9 Methods of Measuring Results

Figure 55 shows an example of the type of result obtained and the first four films' sequences, in the films appended to the thesis, demonstrate actual results. They show the effect of change in hole size and gas density.

To analyse the results the H/S film was projected onto a screen. On this screen was drawn a radial and diametral network of lines marked in half-inches and degrees respectively. The image of the graduated lines on the film were lined up with the radial markings. The centre of the network was made coincidental with the nozzle and the image adjusted so that the horizontal line on the film graduations was horizontal on the screen. Then by projecting a frame at a time onto the screen (the projector was a single frame machine), penetration and cone angle could be measured. The time ordinate was gained from the film on the H/S camera by the R.A.R.D.E. spark timer. This placed on the film a mark at milsecond intervals.

These can just be seen on Figure 55 on the right hand side of the film.

The paper trace yielded the pressures and needle lift with time; Figure 56 shows an example. As has been said in 4.2.2, the pulse markers allowed the trace and H/S film to be correlated. The time ordinate on the trace film was originally supplied by the sweep unit in the usual way. This gave it in crank degrees. However, quite by accident, the R.A.R.D.E. unit superimposed fine 1000 c/s pulses. These did not interfere with the main trace so that they were left and made it unnecessary to convert cam degrees to absolute time. The pressure traces and needle lift were accurately measured on a horizontal and vertical travelling microscope.

4.10 Discussion

The original idea of using an actual injection system proved attainable with the use of the hood. When using close-up photography on the hood there was no evidence of interference and it can therefore be reasonably assumed that the results obtained are of the development of a spray from an injection nozzle working under normal hydraulic conditions.

The method of measuring speed rotation within 1% needs no comment, but the measurement of line pressure, although done by a travelling microscope (measuring to 1/10 of a mm) were taken from small traces. One inch represented about 6000 lb/in^2. However, the reading error was less than 2%.

If both needle lift and pressure traces are to be carried on the film, then this is near the maximum amplification. Possibly an improvement would be to let both traces have the same baseline as long as the needle

trace did not interfere with the pressure trace too much. A further inaccuracy in the traces was the delay in the needle trace due to the long rod in the injector. This could be allowed for to some extent by lining the start of the needle lift with the momentary drop in pressure shown on the pressure trace and due to the needle moving up.

The positioning of the transducer 3 inches from the nozzle does lead to some difference in pressure and in trace displacement owing to the pressure waves having finite velocities. However, the pressure wave velocity is the speed of sound in oil which in this case is the region of 4000 ft/sec. Thus the delay due to the pressure travelling 3 inches is negligible. The difference in pressure in the pipe and the nozzle is also small.

The temperatures measured on the ultra violet recorder are accurate to 2% by use of the potentiometer and the fact that they were steady. The chamber pressure could be read to an accuracy of 2%.

The method of measuring mass of fuel injected per cycle was covered in section 3.6. With this method the readings were accurate to 2% but this was an average reading and did not give the amount of fuel injected for an actual cycle. This could differ greatly.

The accuracy of the method of measuring penetration mentioned in 5 is limited by the inaccuracy caused by the camera angles shown in 4.1 and 4.2. This was about 3%. Unfortunately the quality of reproduction of some of the film made it difficult to exactly pin point the tip of the spray. In bad cases the test was discarded. Another factor that occurred was that of the spray tip becoming erratic towards the end of injection due to the rapid and uneven fall of

line pressure. The method used to overcome spurious results was to ignore the results after spill on the pressure trace.

As for general performance, these points may be noted. Firstly, a more substantial spring could be used on the cam switch as this was prone to fatigue. Secondly, the power grip belt method of driving the sweep units lead to some picture instability and it would be better if the unit were driven off the end of the camshaft. Third, it would make operation easier were the fuel pump rack U/V recorder and camera light made fully automatic. Lastly, the method used to control the fuel rack, that of intermittent injecting, made it impossible to control the fuel temperature. At the nozzle, even when Class A fuel was heated in the tank, the fuel temperature changed by only 3^{o} to 4^{o}C making negligible difference in viscosity. If viscosity effects are to be looked at with the same fuel or if more running was carried out on residual fuel, heating of the injector pipe will be essential.

With reference to residual fuel, although only a few runs were carried out with this, it proved difficult to handle after injection and modification was needed here. No test results were taken.

On the photographic techniques both provided quite good results from a clarity point of view. It must be noted that if higher definition of the spray was wanted then the graduated plate could be omitted and the camera focused on the centre of the spray. An advantage with the flash method would be to use a plate camera. Unfortunately this was not available at the time.

It was stated in 4.2 of this chapter that droplet

distribution, velocity and size together with air swirl should be looked at. At this stage this had not been carried out. It was considered that the results already obtained should be analysed first and the next chapter describes the methods used.

CHAPTER V

ANALYSIS OF COLD BOMB RESULTS

5.1 INTRODUCTION

This chapter sets out to analyse the results obtained with the rig described in the last chapter, and to compare them with previous work.

5.2 Test Conditions

If a theory is to be generally applicable to any size of injection system, the objective is to reduce the parameters that effect spray development to these in the immediate vicinity of the nozzle and in doing so, remove from the final relationship any dependancy on such things as pump speed, system volume, etc. Therefore as far as the system is concerned, it is the pressure drop across the nozzle, time of injection, orifice dimensions and properties of the gas surrounding the nozzle that must be used. From the work surveyed in Chapter I, the following parameters would effect the spray penetration and cone angle.

Nozzle hole roughness

Nozzle orifice diameter

Nozzle orifice length

Pressure drop across orifice

Gas density

Oil density

Oil viscosity

Surface tension of oil

Mean droplet size of oil

Cone angle of spray

Time of injection

Mass of fuel injected

The parameters measured on the bomb were limited to:-

Fuel line pressure

Fuel line temperature

Nozzle orifice size

Nozzle orifice length

Nitrogen pressure

Nitrogen temperature

Spray penetration

Spray cone angle

Time

Fuel properties

Mean mass of fuel injected.

However, as has been discussed previously, only one fuel (Class A diesel oil) was used and its temperature kept constant at 50°C and thus the oil viscosity held constant. The camera and apparatus were not designed to measure the droplet diameter, velocity or its distribution. Thus the oil density and surface tension were constant while any analysis attempted must not rely on a knowledge of droplet velocity, size or distribution. After the experimental work had been concluded the test orifice in each nozzle was inspected under a microscope and the surface finish and up stream conditions were the same.

Consideration was then given to the results. The first important observation was that although the chamber conditions could be held constant the fluctuation in fuel line pressure made the analysis difficult when looking at the effect of any parameter other than this. Figure 57 shows a typical set of results plotted from the High Speed film.

To allow ease of comparison and formulation, the mean effective pressure during the needle opening period was taken as a function of the total upstream energy. All the pressure diagrams were analysed between needle opening and closing, in one degree steps. A simple computer program was written to calculate the mean effective pressure and this allowed time for some 200 diagrams to be analysed.

The range used with each parameter was as follows:-

Mean effective pressure drop 2000-7000 lb/in^2

($12\frac{1}{2}$ inch bore engine mean injection pressure 6900 lb/in^2)

Nozzle orifice diameter .00985-.0236 ins

Nozzle L/d 3.5:1 - 4.18:1

Gas density $.5 \times 10^{-3}$ - $.8 \times 10^{-3}$ lb/in^3

($12\frac{1}{2}$ inch bore engine mean cylinder density $.72 \times 10^{-3}$ lb/in^3)

Figures 58 to 61 show some of the results plotted and compared. Figure 58 shows the effect of increasing the density from $.573 \times 10^{-3}$ to $.800 \times 10^{-3}$ lb/in^3. The effect of hole size can be seen in Figure 59 while that of pressure in Figure 60. Figure 61 shows three sets of results with density and hole diameter constant and the injection pressure within 250 lb/in^2. This gives an indication of the inaccuracies involved in these results. It was also noted that the development of a spray was not smooth but had fluctuations possibly due to the pressure fluctuations upstream of the nozzle. This fluctuation also made the cone angle difficult to measure throughout one injection and it would appear to vary by at least 2^o when the spray was fully developed.

5.3. Analysis of Results

The nature of the experiment and its results dictated that the simplest and most effective approach would be to use Dimensional Analysis to obtain the form of a prediction equation, to curve fit, and then to statistically analyse the results. The accuracy of this method depends on the number of results analysed.

Some 200 test conditions were available with 10 penetration versus time points to each condition - in all, about 2000 were available for analysis. With this amount of data available a preliminary approach was tried. In Chapter I, Figure 14 had shown that for a change in L/d ratio from 3 to 4 the change in penetration was less than half an inch in $4\frac{1}{2}$ inches. Also, as the nozzle diameter changed as well as the L/d ratio for each series of tests it was decided that for the first approach the L/d change would be ignored. Because of the fluctuation in fuel line pressure covered in the previous chapter, and the way it was measured, the mass of fuel injected per cycle was eliminated, it being noted that it is a function of mean effective pressure and time.

Bearing in mind the discussion above on the parameters that were held or found constant, this leaves the following

Nozzle orifice	d
Mean effective pressure drop across orifice	ΔP
Gas density	ρ_g
Time of injection	t

and their effect on penetration of the spray S.

Dimensionalizing these

Parameter	ρ_g	d	ΔP	t	S
Units	$\frac{M}{L^3}$	L	$\frac{M}{LT^2}$	T	L

Five quantities 3 dimensions $\therefore$ 2π quantities

i.e.,

$$\pi 1 = \rho_g^{a^1} \times d^{b^1} \times P^{c^1} \times t$$

$$\pi 2 = \rho_g^{a^2} \times d^{b^2} \times P^{c^2} \times S$$

This gives

$$\pi 1 = \frac{t}{d}\sqrt{\frac{\Delta P}{\rho_g}}$$

$$\pi 2 = \frac{S}{d}$$

$$\therefore \quad \frac{S}{d} = f\left(\frac{t}{d}\sqrt{\frac{\Delta P}{\rho_g}}\right) \quad \ldots\ldots\ldots\ldots\ldots\ldots\ldots\ldots \quad (38)$$

or $$\frac{S}{d} = K\left(\frac{t}{d}\sqrt{\frac{\Delta P}{\rho_g}}\right)^x \quad \ldots\ldots\ldots\ldots\ldots\ldots\ldots\ldots \quad (39)$$

The results were plotted in this form and are shown in Figure 62 and a log plot in Figure 63. A considerable scatter resulted. Results from each hole size were taken and plotted separately. The scatter was reduced. This is shown for the .0118 inch orifice in Figure 64.

Using equation (39) the constant K and power x were calculated for each hole size for a number of results. Figure 65 shows these plotted against L/d ratio. The discrepancy may therefore be due to the change in L/d ratio. Thus the analysis was widened and the parameters are as follows:-

ρ_g	d	ΔP	L	t	S
$\frac{M}{L^3}$	L	$\frac{M}{LT^2}$	L	T	L

Six quantities 3 dimensions $\therefore$ 3π quantities

i.e.,

$$\pi 1 = \rho_g^{a^1} \times d^{b^1} \times P^{c^1} \times L$$

$$\pi 2 = \rho_g^{a^2} \times d^{b^2} \times P^{c^2} \times t$$

$$\pi 3 = \rho_g^{a^3} \times d^{b^3} \times P^{c^3} \times S$$

From these

$$\pi 1 = \frac{L}{d}$$

$$\pi 2 = \frac{t}{d}\sqrt{\frac{\Delta P}{\rho_g}}$$

$$\pi 3 = \frac{S}{d}$$

It is reasonable to assume that:

$$\frac{S}{d} = f\left(\frac{t}{d}\sqrt{\frac{\Delta P}{\rho_g}}\ \frac{L}{d}\right) \quad \ldots\ldots\ldots\ldots\ldots\ldots\ (40)$$

If the results are now re-plotted, Figures 66 and 67, the scatter is reduced for all hole sizes. The dimensional groups seem to fit fairly closely with the data. Thus the equation could be written:-

$$\frac{S}{d} = K\left(\frac{t}{d}\sqrt{\frac{\Delta P}{\rho_g}}\right)^x \left(\frac{L}{d}\right)^y \quad \ldots\ldots\ldots\ldots\ (41)$$

In the simpler analysis, no attempt had been made to use all the results. It was now considered that the major parameters affecting penetration had been included and a more stringent approach was necessary. A curve fitting technique should be used.

The experimental results were listed and curve fitted to the above equation. Two methods of fitting were tried as a check. First a log fit was tried.

Equation (41) can be written:-

$$\text{Log}\ \frac{S}{d} = \log K + X \log \frac{t}{d}\sqrt{\frac{\Delta P}{\rho_g}} + y \log \frac{L}{d} \quad \ldots\ldots\ldots\ (42)$$

$$\text{or } C = Z + ax + by \quad \ldots\ldots\ldots\ldots\ldots\ldots\ (43)$$

$$\text{where } a = \log\left(\frac{t}{d}\sqrt{\frac{\Delta P}{\rho_g}}\right)$$

$$b = \log\left(\frac{L}{d}\right)$$

$$c = \log\left(\frac{S}{d}\right)$$

$$z = \log\ K$$

Then following Legendre's principles of least squares:-

$$E_o = C_o - [Z.1 + a_o x + b_o y]$$

and $E_1 = C_1 - [Z.1 + a_1 x + b_i y]$ etc

to $E_n = C_n - [Z.1 + a_n x + b_n y]$ etc ..... (44)

Now $\sum E_n^2$ should be a minimum

i.e., $\sum (C_n - [Z.1 + a_n x + b_n y])^2$ should be a minimum

$$\therefore \sum C_n^2 - 2Z \sum C_n.1 - 2x \sum C_n a_n - 2y \sum C_n b_n$$

$$+ Z^2 \sum 1 + 2xZ \sum a_n 1 + 2yZ \sum b_n 1$$

$$+ x^2 \sum a_n^2 + 2xy \sum a_n b_n + y^2 \sum b_n^2 = \sum E_n^2 = S \ldots (45)$$

Now let $\sum E_n^2 = S$ and if $\sum E_n^2$ is a minimum

$$\therefore \frac{\partial s}{\partial x} = 0$$

$$\frac{\partial s}{\partial y} = 0$$

$$\frac{\partial s}{\partial z} = 0$$

in the limit

$$\frac{ds}{dx} = 0$$

$$\frac{ds}{dy} = 0$$

$$\frac{ds}{dz} = 0$$

Now if equation (45) is differential with respect to x, y and z, three equations are obtained,

i.e., $x \sum a_n^2 + Z \sum a_n 1 + y \sum a_n b_n = \sum C_n a_n \ldots (46)$

$x \sum a_n.1 + Z \sum 1 + y \sum b^a 1 = \sum C_a^1$ ..... (47)

$x \sum a_n b_n + Z \sum b_n 1 + y \sum b_n^2 = \sum C_n b_n$ ..... (48)

A computer programme was written which summated the constants of equations (46), (47) and (48) from the experimental rig and by use of simple determinate methods calculated x, y and Z and hence x, y and K in the original equation.

Because the above fit was essentially a log fit a second method was tried, that of a direct power law fit. Re-writing equation (41)

$$Q = K P^x L^y \quad \ldots\ldots\ldots\ldots\ldots\ldots\ldots\ldots \quad (49)$$

Now as before

$$E_n = Q_n - K P_n^x L_n^y \quad \ldots\ldots\ldots\ldots\ldots\ldots \quad (50)$$

$\therefore \sum \left[Q_n - K P_n^x L_n^y\right]^2$ should be a minimum

$\therefore \sum Q_n^2 - 2K \sum Q_n P_n^x L_n^y + K^2 \sum P_n^{2x} L_n^{2y}$ should be a minimum, now differentiating with respect to K, x and y, we get

$$- \sum Q_n P_n^x L_n^y + K \sum P_n^{2x} L_n^{2y} = 0 \quad \ldots\ldots\ldots\ldots \quad (51)$$

$$- \sum Q_n P_n^x \log_e P_n L_n^y + K \sum P_n^{2x} \log_e P_n L_n^{2y} = 0 \quad \ldots \quad (52)$$

$$- \sum Q_n P_n^x L_n^y \log_e L_n + K \sum P_n^{2x} L_n^y \log_e L_n = 0 \quad \ldots\ldots \quad (53)$$

The method of solving equations (51), (52) and (53) was by using Newton's method.

Now for a one variable function

$$f(x_1) = f(x_o) + (x_1 - x_o) f'(x_o) = 0$$

$$\therefore (x_1 - x_o) = \frac{f(x_o)}{f'(x_o)}$$

$$\therefore x_1 = x_o - \frac{f(x_o)}{f'(x_o)}$$

Where x_1 is the value of x on the present iteration and x_o the value of x on the preceding iteration.

Now for two variables

$$f_1(x_1 y_1) = f_1(x_o y_o) + (x_1 - x_o) \frac{\partial f_1}{\partial x}(x_o) + (y_1 - y_o) \frac{\partial f_1(y_o)}{\partial y} = 0 \quad \ldots\ldots\ldots \quad (54)$$

and

$$f_2(x_1y_1) = f_2(x_oy_o) + (x_1-x_o)\frac{\partial f_2(x_o)}{\partial x}$$

$$+ (y_1-y_o)\frac{\partial f_1(y_o)}{\partial y} = 0 \quad \ldots\ldots\ldots\ldots (55)$$

By equating equations (54) and (55) and in the limit

$$x_1 = x_o - \left[\frac{f_1\frac{df_2}{dy} - f_2\frac{df_1}{dy}}{\frac{df_1}{dx}\frac{df_2}{dy} - \frac{df_2}{dx}\frac{df_1}{dy}}\right] \quad \ldots\ldots\ldots\ldots\ldots (56)$$

$$y_1 = y_o - \left[\frac{f_1\frac{df_2}{dx} - \frac{f_2\,df_1}{dx}}{\frac{df_1}{dy}\frac{df_2}{dx} - \frac{df_2}{dy}\frac{df_1}{dx}}\right] \quad \ldots\ldots\ldots\ldots\ldots (57)$$

From equations (51), (52) and (53)

$$f_1,\ f_2,\ \frac{df_1}{dx},\ \frac{df_1}{dy},\ \frac{df_2}{dx},\ \frac{df_2}{dy}$$

can be found.

For example

from equation (51)

$$K = \frac{\sum Q_n P_n^{\,x} L_n^{\,y}}{\sum P_n^{\,2x} L_n^{\,2y}} \quad \ldots\ldots\ldots\ldots\ldots\ldots\ldots\ldots (58)$$

i.e., $$f_1 = (\Sigma Q_n P_n^{\,x} \log_e P_n L_n^{\,y}) + \frac{\Sigma Q_n P_n^{\,x} L_n^{\,y}}{\Sigma P_n^{\,2x} L_n^{\,2y}}(\Sigma P_n^{\,2x} \log_e P_n L_n^{\,2y})$$

$$\ldots\ldots (59)$$

$$f_2 = (\Sigma Q_n P_n^{\,x} \log_e L_n L_n^{\,y}) + \frac{\Sigma Q_n P_n^{\,x} L_n^{\,y}}{\Sigma P_n^{\,2x} L_n^{\,2y}}(\Sigma P_n^{\,2x} L_n^{\,2y} \log_e L_n) \quad \ldots(60)$$

and hence the rest.

This second fit was added to the computer programme. The data was applied and the following results obtained

	K	x	y
Log fit	4.1327	.6397	.1844
Power fit	4.2223	.6397	.1844

The predicted and measured results were then statistically analysed. The two equations were taken and re-arranged:-

$$\text{ERROR} = S/d - K\left(\frac{t}{d}\sqrt{\frac{\Delta P}{\rho_g}}\right)^x \left(\frac{L}{d}\right)^y \quad \ldots\ldots\ldots\ldots\ldots\ldots (61)$$

The value of S/d could thus be compared from prediction and measurement for each point and the error noted. The number of points considered was 350 for each of the five nozzles used. These points were picked by using random tables and the error calculated. The arithmetic mean of these errors was calculated for both equations and gave:

	Log fit	Power fit
Arithmetic mean of ERRORS	.05 in	.03 in

This indicates no significant parameter has been omitted from the equation.

The error results were then plotted on probability graph paper and the results are shown in Figures 68 and 69. The degree to which the plotted results lie on a straight line determines the closeness of fit to the given normal distribution. Both figures show that there is a normal distribution. This having been determined, the simple standard deviation could be calculated.

$$ST = \sqrt{\frac{\sum_{j=1}^{N} (X_j - \overline{X})^2}{N}} \quad \ldots\ldots\ldots\ldots\ldots\ldots\ldots\ldots\ldots\ldots (62)$$

Where S = standard deviation

X_j = a set of ERRORS N in number

$\overline{X}$ = the arithmetic mean of the set of ERRORS

The standard deviations calculated in this way gave

Log fit	Power fit
.2 in	.25 in

Thus log fit equation gives results whose errors have the least dispersion.

From the properties of a normally distributed set of data 68.27% of the computed results will lie within a band $\pm$ .2 inches and 95.45% will be within $\pm$ .4 inches. The dispersion is fairly large but this is in part due to the uneven development of a single spray. If a smooth curve is drawn through all the points of each spray penetration with time graph then the dispersion is considerably reduced such that 95.45% of the results lie within $\pm$ .2 inches.

The equation that gives the best correlation with measured results can be written:

$$\frac{S}{d} = 4.13\left(\frac{t}{d}\sqrt{\frac{\Delta P}{\rho_g}}\right)^{.6}\left(\frac{L}{d}\right)^{.18} \quad \ldots\ldots\ldots\ldots\ldots\ldots (63)$$

Compare this with Schweitzer and Wakuri's equations

$$\frac{S}{d}\left(\frac{\Delta\rho_a}{\Delta\rho_o}\right)^{\frac{1}{4}} = .2265\ \ln\left(\frac{1}{1155}\ \frac{t}{d}\ \frac{\rho_a}{\rho_o}\sqrt{\frac{\Delta P}{\rho_o}} + 1\right) \quad \ldots (8)$$

$$S = \left(\frac{2c\Delta P}{\rho_a}\right)^{.25} x \left(\frac{t\ \ d}{\tan\ \theta}\right)^{.5} \quad \ldots\ldots\ldots\ldots\ldots\ldots (10)$$

By inspection of the equations it can be seen that the shape of the curves derived will be different and that the importance of each parameter is different. Figures 70 to 77 show measured results compared with Schweitzer, Wakuri and derived formula.

The value of θ in Wakuri's equation was gained from the present measured results shown in Figure 78. This shows Wakuri, Sass and the measured values of cone angle plotted against a base of the ratio of fuel to gas density. There is a large scatter in the measured results but a line

has been drawn through them, the slope being in agreement with those of Sass and Wakuri. Wakuri's equation in all cases underestimates the fuel spray penetration.

At the small hole sizes (Figures 70, 71, 72 and 73) there is close agreement between the measured, predicted and Schweitzer curves. If anything, Schweitzer's equations fit better at the lower penetrations but begin to deviate at the large penetrations. In the middle range of holes, Figures 74 and 75, the agreement is close all the way up the curve. However, Figures 76 and 77, showing results from the largest hole, indicates that although the derived curve is still in fair agreement, as it should be, Schweitzer's equation is overestimating the penetration.

Figures 79 to 81 show Schweitzer and the derived equation compared with change in various parameters. Figure 79 compares the two equations with varying hole size, Figure 80 with varying gas density and Figure 81 varying injection pressure. The effect of L/d ratio found in the analysis of results is shown in Figure 82 and is compared with Gelalles' work [65]. The effect is less with the multi hole nozzle used in the present tests.

5.4 Discussion

The above analysis complete, it has shown the following points. The first is the justification in using the dimensional approach coupled with a curve fitting technique. This gives a reasonable method of predicting the overall behaviour of a spray given the pressure and density conditions up and down stream of an orifice whose dimensions are known.

Although using the concept of a mean pressure drop across the orifice over the injection period has proved

valid, the pressure fluctuation does affect the spray penetration over the first half, or in some cases, one millisecond. Figure 83 shows the type of variation from the calculated mean. The variation depended on hole size and mean injection pressure, but not on needle opening pressure. Due to limitations with the injector needle spring, the injection opening pressure was a variable from 2500 to 3200 lb/in^2. Rothrock and Marsh [66] using an actual jerk pump system found that the injection opening pressure could affect the beginning of penetration by delaying it. They pointed out that as the pump speed increased, (i.e., maximum fuel line pressure) so the effect decreased. That is to say, as the maximum pressure to opening pressures ratio increased, the effect of opening pressure on penetration decreased. Their opening pressures varied from 500 to 2500 lb/in^2, and the pump speed from 180 to 750 r.p.m. They showed no effect at the latter speed. The computed maximum line pressure at this speed was 5000 lb/in^2. In the present tests the lowest peak line pressures encountered were between 6000 and 10,000 lb/in^2. Thus not being able to detect any effect due to opening pressure, is in agreement with Rothrock's observations.

Of the work surveyed in Chapter I, Wakuri and Schweitzer have been compared with the test results. Wakuri's equations always underestimate the penetration even with a coefficient of discharge of .7. From Berwerk [18] the value would seem high for a multi-hole nozzle, so it would seem that the discrepancy lies in Wakuri's original cone angle measurements which produced much smaller figures than those measured on the present rig. The test results show that Schweitzer's equation fits reasonably

well at the smaller orifice size and penetration, but results at the higher penetrations and hole sizes are in error.

The major difference is the dependance of penetration on L/d ratio found with the present work and upstream conditions. Figures 79, 80 and 81 show that, for the conditions calculated, the importance of orifice diameter is overestimated by Schweitzer, that his equation underestimates the importance of gas density, and that for injection pressures, he overestimates up to about 4 milliseconds, and then underestimates its effect. Returning to Chapter I, Figure 5, with the multi-holed nozzle and the change in direction of the fuel in the sack it is probable that the radial and tangential velocity components become greater for the same injection pressure. Thus the gas density will effect the cone angle and penetration much more markedly. The fluctuating pressures may in some way contribute to this by giving rise to rapid changes in flow around and in the nozzle. A further effect of fluctuating pressure is the fact that in the spray from a jerk system the volume of fuel injected is small compared with that of Schweitzer's system and thus a corresponding smaller amount of energy, with time is transmitted to the air, hence less air movement and more air resistance, then the penetration is less. Another possible cause is the difference in finish of the orifices between Schweitzer and the present tests.

No measurement of cone angle was carried out by Schweitzer but Figure 78 shows that, although a large scatter was encountered, the cone angle of the sprays was about 2° greater than those measured by Sass. Again this

would seem to confirm the effects mentioned above and suggested in Chapter I.

One important factor that must not be forgotten in an investigation of the overall spray pattern is the effect on droplet size. The difference in penetration rates due to the jerk system can be plotted from the present work but no information was gained on droplet size. Figure 84 from work carried out by Giffen and Muraszew [8] shows the variation of Sauter Mean Diameter throughout the injection period. The larger droplets formed at the end of the injection, due probably to the rapidly falling injection pressure and could affect combustion considerably from the point of view of smoke production.

5.5. Application and Conclusion of Analysis

Given then that Schweitzer's equation is in some error when applied to a jerk pump system and given that the equation derived from the present work allows more accurate prediction. How has this part of the work helped?

The engine conditions chosen for Chapter I can be used to plot Figure 85. The spray path length is $4\frac{1}{2}$ inches and this is reached in about $7\frac{1}{2}$ degrees of crank in a 30 degree injection period. This is compared with the original predicted spray path shown in Figure 39, as calculated by Schweitzer's equation. The present equation shows that the penetration is less but not to a significant degree.

The present work has thus produced an equation which predicts more accurately the penetration of a spray from an actual engine system taking into account changes in L/d ratio and the effect of upstream conditions found in

an actual system. For the conditions under consideration in the 12½ bore engine it also shows that if the spray does not impinge on the wall then the effect of using an actual system does not account for the apparent reduction in penetration.

The next step is to investigate the effects of evaporation and consider the conditions prevailing in the combustion chamber of a medium speed diesel engine.

CHAPTER VI

SMALL ENGINE EXPERIMENTAL WORK

6.1 INTRODUCTION

The work up to this point had clarified the effect of using an actual injector system on spray penetration, results had broadly agreed with Schweitzer's earlier work. The next step was obviously to modify the rig so that evaporation effects and air motion could be studied.

However, the lack of direct information on combustion process in the larger diesel engines made the obvious step a dubious one. More information was required on such points as, what air motion existed in a large 4-stroke engine; whether the sprays were affected by it; what effect if any did the proximity of other sprays have; does piston impingement occur; and if the concept of vapour penetration was correct, what governs the mixing process?

Summing up, it was concluded that insufficient evidence was available about the conditions in the cylinder of a large engine, and that study of actual combustion might not only provide the required information on evaporation and combustion effects on sprays, but also on the entire mixing and combustion process itself.

Therefore this line of investigation was undertaken. This chapter describes work involved in photographing combustion inside a small diesel engine with a prototype schlieren system, it being more economical to test the principle and develop the system on a small engine rather than the large 8-inch bore engine. The work was carried out between March, 1964 and April, 1965.

It is divided into two major parts. The first considers the various methods of investigating actual

combustion and the outline of the best method chosen from these. The second part describes the experimental work carried out.

6.2. Method of Investigation

6.2.1 Survey of Methods

Considerable information is available on methods used by other workers to investigate combustion. If distribution of the fuels, air motion and combustion are to be investigated then many of them have severe limitations. The use of pressure transducers will only help in seeing the effect of changes [21, 61] as with the hot motored technique [44, 45]. The use of an ionizing gap [48 and 67] is limited in that the coverage of the whole of one spray is difficult and no measurement of air movement can be gained. Sonic apparatus [68] would only give temperature history inside the cylinder, and then only in a limited area. Thermocouples in the chamber [6] have been considered but suffer as all the above do in being too specific, and it is very difficult to analyse the results. Some most useful work has been covered by using the gas sampling valve technique [55, 56, 57 and 58] and shock tube apparatus [69]. This has indicated the effects of chemical kinetics on the combustion process especially in the delay period. However, where an overall picture is required of the combustion mechanism, the viewing of the combustion process by the eye must be the first step. This gives the general concept of a particular process from which the more specific measurement mentioned above can follow.

It has already been shown in the fields of small diesel and petrol engines and gas engines [37, 70, 71 and 72] that photographing combustion has much to offer

in forming the initial concepts of combustion and when used in conjunction with pressure and Spectroscopic Analysis [60], can form a powerful tool. Applying it to a large engine seemed difficult but would be the most rewarding.

6.2.2. Method of Photography

If the physical factors controlling combustion such as the movement of air, liquid fuel, evaporated fuel, together with preflame as well as luminous flame motion are to be seen, then a schlieren technique is indicated. The qualitative information gained by using a combination of single pass schlieren and high speed photographic methods has been shown to be extremely useful [72] with pre-combustion chamber diesel engines.

However, with direct injection engines, with which this work is concerned, the piston forms part of the combustion chamber and is very close to the head at the top of the compression stroke. This makes a single pass system almost impossible to use. A double pass system, similar to that used by Millar [71] would seem feasible. A plain mirror forming part of the schlieren system is placed on the piston top and optically joined to the system via a window in the head. Figure 86 shows the general arrangement.

This poses problems. Sideways movement of the piston involving tilting, and hence tilting of the plain mirror, may be too much for the sensitive schlieren system. The piston mirror must not distort. The mirror surface must be able to withstand any abrasive effects during combustion and continual cleaning after each test. Because the engine is direct injection just one combustion cycle could

foul the mirror. Means, therefore, must be found to obtain combustion conditions without this occurring.

In the initial stages of the work any changes made to the apparatus could be costly, both in money and time. Thus it was decided to do first, part of the work on a small 3-inch bore high speed engine and transfer this experience to the large 8-inch engine at a later date.

6.3. Schlieren Photography on the 3-inch Bore Engine

With the concept as laid out in the above section the peripheral equipment apart from the photographic apparatus had two major objects. One was to keep the combustion chamber clean until photography was required. The second was to enable the chamber to reach as near combustion conditions as possible.

6.3.1 Motor-Fire Technique

The first was achieved with a motor-fire technique. The engine was connected in series with two D.C. motors; Figure 87 shows the rig layout. One was a shunt wound motor which could motor the engine up to any speed between 0 and 1200 r.p.m. The second was a generator with the field coils separately excited and the load applied across the armature windings. A solenoid operated contactor could switch off the motor while another contactor applie the load to the generator. In conjunction with these motors, the conventional jerk fuel injection system was modified by making the rack movement solenoid operated. Figure 88 shows diagrammatically the arrangement.

In preliminary trials, with the engine running on load as normal at a given speed the position of the rack was marked for a given combination of load resistors. Thus when photography was required the load resistors were set,

the engine motored up to speed and then the fuel, motor and generator solenoids operated such that the motor was cut out, the fuel pump rack pulled in the required distance (set by means of a micrometer stop, see Figure 88), and the load resistors applied. The engine would then run on load until the procedure was reversed. This proved very satisfactory giving a smooth changeover with no loss of speed.

6.3.2. Change Over Heater

The second object of the peripheral equipment was obtained by using a rapid changeover air heater supply to the inlet manifold. This consisted of two pipes running into the same manifold at the inlet on the head (Figure 87). On one pipe was fitted an electric heater and a blower. The other was open to atmosphere via a filter; both were controlled by solenoid operated butterfly valves.

For the chamber to attain combustion conditions the inlet and exhaust valves were lifted open. The blower forced heated air through the open valve into the chamber and out of the exhaust pipe. When the chamber walls reached near normal working temperatures (measured by thermocouples), the engine was motored up to speed. The closed valve in the cold air pipe allowed the engine only to breathe hot air. Just before the firing cycle the butterfly valves were changed so that the engine began to breathe relatively cold air and thereby in part reproducing normal engine conditions.

In practice the heater system did not work satisfactorily. On changeover the temperature into the engine did not fall rapidly. It was found that the inlet pipe was too substantial and acted as a source of heat

after the changeover had taken place. As the engine was only being used to test the schlieren system, no modifications were carried out.

The method of measuring the transient temperatures in the inlet pipe was to insert a fast response thermocouple into the gas stream. An ultra-violet recorder was used as the output device.

6.3.3. Event Sequencer

The sequence of events in the motor-fire technique together with the triggering of the high speed camera (later described) were controlled by a programmer, similar to the one described by Hempson [73]. Figure 89 shows the principle of the unit and Figure 90 the general layout. As none were available on the market it was manufactured. The basis for the control unit was a three-bank 50-way uniselector. In the first bank the driving pulses for the uniselector coil were routed through all the contactors except one. This one was joined to the rest via a push start button. Thus when pulses were fed into the uniselector it would rotate until the arm came into contact with the separate contactor. It would then remain stationary until the start button was pressed. In this way the selector was controlled to rotate once. The other two banks provided the 'on' and 'off' pulses for a series of remanence relays, as shown in the diagram. After modification to the selector and remanence relays, the maximum satisfactory speed obtained was about 20 steps per second. The pulse was supplied from a micro-switch positioned on the end of the engine camshaft and moved by a small eccentric cam.

The outputs from the 'on' and 'off' banks were connected to a patch panel as were the inputs to the remanence relay coils. Thus the time of a number of events could be programmed in any sequence. Also on the patch panel were the relay arm contact outputs. Figure 90 shows the panel.

6.4. Modification of the Engine for Photography

The engine had a 3-inch diameter bore with side valve gear and flat top piston. It was a WB type and made by Ruston and Hornsby Limited. Because of the absence of valve gear in the head and the flat top piston, it was ideal for the testing of the schlieren system, requiring little modification.

The standard head was replaced by a special head which had a window allowing visual access to the cylinder. Figure 91 shows both heads and although the outside shape was considerably changed little modification of the combustion chamber shape was needed. Two types of window material were tried. In some direct photography tests that were tried at the outset, perspex windows were used. This meant that pre-heating the engine could not be carried out, but successful photographs were taken.

For the schlieren test quartz windows were used. Optical grade was the most successful, but industrial grade gave reasonable results. The shape and seating of the window is shown in Figure 92. It had a step machined to allow it to fit flush with the combustion chamber wall and at the same time have adequate seating arrangements. The metal seats in the head were angled against the cylinder pressure. This obviated the need for the normal 'O' ring recesses, giving a smaller seat.

The sealing rings were 'O' rings with a shore hardness number of 80. The use of these eliminated cracking of the quartz when installing the windows. Figure 92 also shows that the top clamp had a spigot. This safeguarded the quartz if the 'O' ring should collapse while the clamp was being tightened down. By machining this spigot the tension on the 'O' rings was adjusted until a satisfactory gas-tight seal was obtained. This was tested by filling the space above the window with water and running the engine. The 'O' rings were changed after 10 tests, although one pair did last 20 or more without obvious distress.

The piston mirror surface itself was a .005" layer of chrome deposited directly onto the aluminium base and polished to a flatness of ½ wave length per inch of diameter. This was found to be resistant to abrasions due to combustion conditions and to cleaning after each test run. This cleaning was done using soft wool and alcohol. One surface was used for over 50 tests and showed only slight crazing at the end. The chrome layer was recessed into the aluminium to eliminate chipping at the edges.

The major difficulty was thought to be distortion of the mirror due to heating of the piston. Figure 93 shows the chrome layer deposited on an insert held with a central pin. In this way it was hoped to obtain uniform expansion of the insert. Figure 94 compares this piston with the standard type. During initial tests it was found that the type of mirror where the chrome was deposited directly onto the piston tended to distort nearly uniformly into the shape of a concave mirror. This resulted in a slight change of focus during engine heat up period. Adjustment

of the optical system immediately prior to a run compensated for this change in focus. Due to the piston's superior mechanical reliability over the insert type, it was used in most of the tests. The insert mirror, when tested, had virtually no distortion. The shape of the combustion chamber with window and mirror in place is shown in Figure 95, together with a cutaway view of the actual engine.

When the first attempt was made to take schlieren pictures it was found that the running clearance between the piston and cylinder wall was excessive allowing the piston to tilt enough to make schlieren photography impossible over the whole cycle. This clearance was found to be about .006". (This done by measuring the deflection of the source image at the knife edge while the engine was running). To overcome this a new liner was put in and bored so that the clearance was reduced by about .0025 inches. This could be done because the engine was only fired for short periods and therefore scuffing and increased wear of the liner and piston could be tolerated. By this means movement of the mirror was reduced to an acceptable amount for ordinary schlieren photography but, as is discussed later, it did not prove enough for the colour filter technique.

A further problem that occurred during initial tests was that of lubricating oil passing up the cylinder during the short motoring period before firing. This oil fouled the piston mirror and window. To combat this more severe downward scraping rings were used in the bottom two of the three compression ring grooves. This resulted in no oil appearing on the mirror if the engine ~~were~~ was motored for

about two to three minutes.

6.5. Photographic System

6.5.1. The Schlieren System

The double pass schlieren system used is shown diagramatically in Figure 96 and the actual arrangement in Figure 97. A 4-inch concave mirror with a 48-inch focal length was used together with a 4-inch plain mirror which turned the cylinder image from the vertical to the horizontal. The slits, filters and focusing lenses were mounted on two standard optical benches as was the light source, a mercury vapour lamp, type No. AEI/ME/D P 28/25. This was used to give a point source with the linear graded filler and a slit with the step wedge filters. Because of the use of a high speed camera the lamp could not be supplied with A.C. current so a D.C. power pack was built, giving less than 1% ripple. As the schlieren system was mounted directly on top of the engine, some means had to be found of isolating it from the engine vibrations. The table carrying the schlieren system was held, via multiple rubber mounts, on a steel stand. The legs of the stand were in turn mounted on rubber isolators. After some experiments with the thickness of the isolators, it was found that most of the engine vibration could be eliminated. The method of testing this was to set up the schlieren apparatus with the plain mirror reflecting the light directly back to the concave mirror and measure the maximum amplitude of the source image at the knife edge.

In the initial stages direct photography was tried using a full height Fastax camera, running up to 8000 frames per second. Here the camera was focused into

the cylinder via the plain mirror only. The flame front movement was found to be very rapid and blurring of the image occurred. In the movie film, sequence 5 demonstrates the type of result gained. Therefore a half height 16mm Fastax camera running up to 16000 frames/sec was used on the schlieren system. After some experimentation this camera gave good results both in sharpness and in number of frames per combustion cycle using an aperture slit of 0.08 inches. The engine speed in all tests was 1200 r.p.m.

At first the camera was mounted on a pillar stand separate from the system. Due to the size of the test area this proved inconvenient. It was then placed on the schlieren table and when run caused no added vibration to the system. Subsequent runs were with the camera in this position. A small stand was constructed to allow levelling and positioning of the camera. Figure 97 shows this in position.

It was found useful to be able to correlate combustion phenomena and any piston misalignment with the position of the piston when analysing the high speed film results. To do this the crank position was superimposed on the same film frame as the schlieren. A Trafelite rim was engraved with the crank position at 2^{o} intervals. This was fitted to the flywheel as shown in Figure 98. It was then viewed by the camera via a system of prisms and lenses. The lens and prism nearest the flywheel were carried in a tube projecting above and below the schlieren table. The final lens and prism were held in separate lens holders to allow for adjustment.

The crank markings were illuminated with 750 R lamps on stalk arms. The number of lamps used depended on the film sensitivity and camera speed used.

Focusing the camera both on the schlieren image and the direct image of the crank proved difficult. The best method found was to leave the camera lens in position and to use it to finely focus the crank markings. Then the schlieren image was focused by using the final lenses in the schlieren system. When setting up the camera for the schlieren system, care had to be taken that the image in no way interfered with the edge of the rotating prisms in the camera, or cut off of part of the image occurred.

6.5.2. Beam Splitting and Filter Types

In Figure 96 the methods of beam splitting used in the schlieren system are shown. Of the three, the off axis method offers the best solution, the others having an inherent loss of illumination which proved critical when using the higher framing rates and graded filters. Due to abberations that occurred in the off axis system when tried and due to lack of space to manouevre the mirrors, much of the initial work was carried out with the half plate method, this giving the best illumination of the remaining two. It was thought that with a slight modification to the stand and optics the off axis system should work satisfactorily.

It has been mentioned that graded filters were used. These were chosen from the beginning in place of the usual knife edge. With the linearly graded filter the sensitivity of the system is independent of the position of the source image on the filter and this made it ideal for this sytem, where engine induced vibrations and piston

movement made the same image unstable. Step wedge filters were also used with success, their advantage being that they could be made in the laboratory. The process was quite simple. The film was laid flat on a sliding plate whose movement was controlled by a micrometer. Over it, and pressing close to it, was a metal mask finish in matt black paint. This mask was attached to the base on which the slide moved. The procedure was to place the apparatus under a standard enlarger with the film masked. Then by exposing the film in steps the step wedge was formed. The thickness and the density of the steps could be controlled by the micrometer and the time and/or setting of the enlarger aperture. The films were then processed and mounted between two thin plain optical glass sheets. Figure 99 shows an example of step wedge and linear graded filters.

Another advantage of using step or linear filters was that of easily controlling the range of schlieren system [74] . As is shown very clearly by Lyn [72] by positioning the source image of various points on the graded filter, each density range can be looked at without the observer being distracted by other phenomena. For example, if the image is set in the dense region of the filter the fuel vapour would become easily seen (a large deflection to the lighter region) as against air motion (a reasonably small deflection to the lighter region).

This did not prove too successful in this work, as is shown in Figure 100. On reflection, three reasons can be offered. Firstly, with the lack of illumination inherent in this system, the positioning of the source image in the dense region of the filter was limited due to under-exposure

of the film even using the fastest black and white film available. The schlieren system was too sensitive, i.e., the vapour was deflected out of the range of the lenses and filters used. Lastly, due to inadequacies in the heating system, the combustion chamber wall and probably compression temperatures were lower than on normally running engines thus not much fuel vapour was present, indicated by little burning being observed. However, as the final system was to be applied to another engine, no more steps were taken to pursue these points. Results from the graded filter technique are shown in films sequence 6 and 7.

It has been shown that the use of colour photography in schlieren [75] can help the analysis of the phenomena under observation. Two methods of obtaining colour records were tried in this work. The more simple one was to leave schlieren as before with a graded filter and just load the camera with a coloured film. A typical result is shown in the film sequence 8. The second method was that of using the coloured filter technique [75]. Here the graded filter was replaced by a filter consisting of three different colours (Figure 99). Various combinations and strip widths were tried with the basic green, red, blue and yellow colours. These filters were made from coloured 'Chance' glass cut to size with the butted edges ground to make a perfect fit and then mounted on an optical glass square by glue applied at the outer edges of the strips. In use, the source image was placed at the centre of the filter and its width, that of the centre strip.

Then any deflection of the light rays due to a density change in the cylinder would be accompanied by a sharp and well defined colour change on the photograph. In this way it was hoped to make the movement of vapour and air more distinguishable than by the previous two methods. The results are shown in film sequence 9. Unfortunately when the results were examined, the colour that would denote densities of the same order as vapour was present when no fuel was injected, and in general the colour patterns changed suddenly with piston movement. Although the piston movement was reasonably satisfactory for the black and white and first type of colour filming was still too large for this third method to be applied.

As the technique was to be moved to the larger engine and the solution of the piston movement on this large engine could be a different problem, further investigations were postponed to the larger engine system.

6.5.3. Consideration of Films Used

The camera used standard 100 foot rolls of 16mm film with 8mm perforations. The black and white films used are shown in Table 2. The speed of film was dictated by the position of the source image on the graded filter. The camera lens aperture was in all tests wide open. With schlieren it cannot be used as it acts as another knife edge.

In colour photography only one make of film was tried. That was Anscochrome. Two film speeds were used, but although the D100 (ASA 100) could be forced in development to give equivalent speed of 200 ASA, best results were obtained with D200 (200 ASA) film also allowing some in hand for

forced development.

6.6. Results

Although this phase of work was directed at developing a photographic technique and was not intended to produce results for analysis, it is nevertheless interesting to comment on the phenomena revealed by the film. Possibly the most interesting observation is the air flow pattern (see film sequence). Although this engine has in some respect directed ports the air movement imparted during the intake stroke virtually dies out as the piston approaches the top of its travel on the firing stroke. The major swirl would seem to be imparted to the air by an expansion wave issuing from the throat of the combustion chamber as the piston uncovers it. This wave eventually gives two vortices, one each side of the main cylinder.

Two types of injector nozzle configuration were tried. With the standard two-hole nozzle not much of the sprays were seen because they impinged on the precombustion chamber wall. As can be seen in film sequence 5, only two burning jets emerge from each side of the throat. With the single hole, the spray had a tendency to move to one side. As the swirl rates were low at this point it would seem that the spray is impinging on the round edge of the piston.

These observations must of course be tempered with the fact that the engine was running at 1200 r.p.m. and not its design speed of 3000 r.p.m. and that the wall temperatures were low.

6.7. Discussion

The test on the small engine had answered at least

some of the questions posed. The piston tilt could be controlled enough to get ordinary schlieren, but care would have to be taken when applying it to the large engine because the reduction to the clearances used on the small engine could not be possible due to piston seizure. Colour filter techniques looked useful but an even tighter control over piston movement than attained on the small engine would be required.

General vibrations from the engine could be reduced to an order that did not affect the schlieren system but more space would be required in order to allow other schlieren set-ups to be tried.

The mirror when deposited directly onto the piston did distort but in such a way as to allow compensation to be made in the optical system. The insert, less prone to this distortion although possibly less reliable than the first type, would prove to be useful on the large engine because of the physical size of the piston. The use of chrome deposited directly onto the aluminium piston or insert gave a good bond which did not peel. Although slight crazing occurred after many tests, the mirror could be continually cleaned with alcohol after each test.

With the engine reasonably cold, only three cycles of combustion could be tolerated before the mirror became obscured. In conjunction with this, the heater changeover circuit never worked correctly and attention would have to be given in the design of the system on the large engine.

One other problem encountered was the oil passing from the crankcase past the rings into the chamber and

misting up the mirror while the engine was running up to speed. The problem on the larger engine might be more severe due to undercrown cooling by oil but the method of using more severe scraper ring could well be employed.

In the large engine the quartz window would have to be proportionally bigger and thus expensive. These tests had shown that industrial grade quartz was adequate, thus some cost reduction could be attained.

The schlieren system was sensitive enough with the source size and focal length of the concave mirror to pick up the density variation due to air motion in the small engine. It would probably be enough for the larger engine but if a larger schlieren table was used a longer focal length mirror could easily be substituted, this increasing the sensitivity.

From the results shown in sequence 5 on the film, that of direct high speed photography, more care should be taken with the placing of the lamps used to illuminate the chamber.

Although this system had the above shortcomings, it was obvious that the basic concept was sound and that it could be applied to the larger engine. This work is described in the next chapter.

CHAPTER VII

EXPERIMENTAL WORK ON 8-INCH BORE ENGINE

7.1. INTRODUCTION

Testing of the basic concept of the schlieren technique was described in the last chapter. Work started in May, 1965 to apply this method to an 8-inch bore medium speed engine, situated in the Ruston Research Centre at Lincoln.

This chapter describes the modification of the engine and the experimental work involved in getting results of the effect of evaporation on spray penetration.

7.2. Basis for Building Engine Rig

In applying the photographic techniques to the large engine the techniques discovered on the small engine were used. The essential differences were:-

(a) physical size

(b) Hesselman shaped piston crown

(c) four overhead valves and central multi-holed injector

(d) piston with larger clearances

(e) design to contend with high b.m.e.p.s (250 lb/in^2 as opposed to 90 on the small engine).

There was also the choice of two engines, one a single cylinder and the other a 6 cylinder, both versions of the Ruston APC type of engine. This is in its normal form, an 8-inch bore engine running at 245 lb/in^2 b.m.e.p. and 750 r.p.m., turbocharged and intercooled (see Appendix VII). The six cylinder engine was chosen because one cylinder could be used for the tests, with the others used to motor it. This meant the elimination of electric motors and dynamometers and hence switching gear, a simple water brake being adequate.

The multi-cylinder also had less vibrations than the single-cylinder engine, which was also 12 feet high, due to its large antivibration mountings. This was important when it is considered that the optical system would be carried on a table level, if not above the cylinder head.

Two disadvantages with the multi-cylinder version were, the inability to measure directly the output from the test cylinder and, due to the turbocharging system, controlling the inlet manifold conditions. It was decided to cover the work using the i.m.e.p. as the function of output. This could be measured from cylinder pressure diagrams taken from electronic equipment which must be highly accurate. The second objection could be more easily overcome, that was to remove the test cylinder from the main air chest and use air from a separate supply. The next step was to reconstruct the multi-cylinder engine such that both direct and schlieren photography could be used.

7.3. General Engine Layout

Figure 101 shows the general engine layout. The cylinder nearest to the flywheel was chosen as the test cylinder, to eliminate any severe torsional vibrations when the motor fire technique was used. The schlieren table was mounted to the side of the engine and consisted of an RSJ frame with the wooden table top mounted on it via rubber pads, as in the case of the small engine. The air was supplied from the shop supply, first passing through a filter/drier and then a measuring orifice. It then branched into two, one going through an electrically heated chamber, the other passing into a damping chamber before rejoining the first and thence into the cylinder

head. Two hand valves at the beginning of each branch controlled the pressure in each, depending on the position of the two solenoid operated Butterfly valves. These valves controlled whether the compressed air passed through the heater section or straight into the engine via the cold pipe. Figure 102 shows a photograph of the rig as laid out for direct photography tests.

As with the small engine, the object was to heat the engine while stationary then start up, still on hot air, and when up to speed, to actuate the butterfly valves and switch to cold air to reproduce engine conditions. After some modification this sytem was made air tight and the pressure drop and hence the air flow, though it measured instantaneously with a SEL differential strain gauge pick up. The instantaneous temperature and pressure at the inlet to the cylinder head were measured by a fast response thermocouple and a 0 to 50 lb/sq.in. inductance Southern Instrument G301 transducer respectively and recorded with the air flow on an ultra violet recorder.

Experiments were carried out with various sizes of damping chambers to gain fairly steady flow into the head. At 200 lb/in^2 b.m.e.p. the maximum oscillation allowed was $\pm$ 1 about the mean of 16 lb/in^2 gauge this being the order of oscillation in a normal engine inlet duct at that load. The heater unit held 32 two kilowatt rings in it. Eight were separately controlled on a multi-point switch so that the air temperature could be accurately controlled up to 150°C if wanted. The rest were used to give an air temperature of 400°C at engine air flows.

It was found during the small engine work that the intake heater pipe was too thick and acted as a heat sink which when the changeover occurred, keeping the intake air at a high temperature. To try and avoid this, the intake section after the heater was made of very thin gauge steel. Tests were carried out to ensure that the air temperature and pressure at the inlet fell to the correct level within two or three crank revolutions. The sequence of events using the heater system and sequencer is the same as with the small engine. After the changeover the fuel would be injected and the camera and lights triggered.

The electrical heaters were supplemented by passing steam through the water jacket of the engine. This considerably speeded up the heat soaking process of the engine. The temperature on the cylinder head flame plate was measured by three thermocouples placed $\frac{1}{8}$" from the surface as shown in Figure 103. However, one failed and for all of the test only two were used. With this system it was still impossible to attain the average metal temperature of a normal running engine. Figure 104 shows the temperature between the exhaust valves of a normal engine together with those obtained from the test head. The mean temperature of the normal engine would be lower and this is also indicated from experimental and calculated results. Motoring the engine with hot air still passing for a few minutes before changeover bettered the position somewhat.

Thus as far as wall temperatures are concerned, they are only representative up to about 120 b.m.e.p.

A normal Heenan and Froude water brake was used but at load up to full load on the test cylinder, no load was applied by this to the other cylinders. Above this, load was applied in an attempt to reduce the torsional vibration set up when the test cylinder fired.

The exhaust from the test cylinder passed into the standard manifold of the turbocharger which thus applied a back pressure. The effect of removing the test cylinder from the engine air chest and the intermittent firing of the sixth cylinder was to unbalance the turbocharger but this did not matter, as the other cylinders were being used as motoring units only. One side effect of blowing the engine while stationary was that the turbocharger was motored round and as its oil supply was from the main engine supply frequent priming of the system by an auxilliary hand pump had to be carried out during the soaking period.

7.4. Design of Cylinder Head and Piston

The cylinder head was a four valve type with a central injector. The piston crown was a Hesselman type. One object was to leave the combustion chamber shape essentially the same as a normal engine. Although the test section of the combustion chamber would be a wedge shape, giving longer paths of light rays than others, the best compromise was to put the mirror level and parallel to the slope of the piston, angled at 25° from the horizontal. The window in the head would also be angled at 25° from the vertical. The scheme is shown in Figure 105.

7.4.1. Piston Design

Three shapes of mirror were considered. Figures 106a, 106b and 106c show the general shapes. The first,

106a, was a mirror which hardly changed the shape of the chamber at all but was limited in that the spray path was $2\frac{3}{8}$ inches as opposed to the 4 inch radius of the cylinder. This small mirror would have the advantage that, if air flow existed, it would not upset it. The second mirror, 106b, was similar to the first, except that the piston land was cut away to give a $3\frac{3}{8}$ inch spray path. This could be used if there was no appreciable air flow. Both these mirrors were designed on the lines of the small engine insert mirror - that is, an aluminium base with chrome deposited on the top and polished to $\frac{1}{2}$ wavelength per inch diameter. When the final polishing was being carried out, the central pin was pre-loaded such that when the mirror was installed in the piston, distortion, due to tightening, was reduced. A small relieved portion was allowed on the base of each mirror to allow ease of expansion. When fitted to the piston a sealing compound was applied to stop any leaks and nylon lock nuts used on the pin. Appendix VIII (a) and (b) shows the design drawings of the mirrors and (c) the type of piston.

Work was initiated on the third type because of the possibility of piston impingement. If the spray hit the piston then it would be useful if schlieren pictures could be taken to see more of the mixing mechanisms. The answer seemed to be a stepped mirror in the area of the piston land. As this held considerable difficulties, a mock mirror was made.

Machining the steps from a solid block was disregarded, as the required accuracy of the stepped surfaces could not be gained (the region of flatness being one to two wavelengths of light per inch). The next method was to machine each

step separately and lap polish then clamp them together. Figure 107 shows the test and final mirror. A simple rig was set up to test the effectiveness of this mirror under hot and cold conditions. Figure 108 shows the arrangement using the mock mirror. Although the mirror was crude the results were reasonable. However, the assembly was very sensitive to the clamping screws being tightened right down. This mirror was also subjected to heating and it was found that if it was clamped tightly, surprisingly little distortion took place.

The final design is shown in Appendix VIII, the clamping torque being controlled by the lock pins. The associated piston is also shown in Appendix VIII (e). The initial mirror finish was gained by lapping the gauge plate and then finishing with Green Stick.

Figure 109 shows the smaller of the three mirrors in position on the piston.

7.4.2. Cylinder Head Design

From the outset it was obvious that if the general shape of the combustion chamber was to be retained the basic modifications would have to be undertaken with some compromise. The first was to limit the field of view to one quarter of the chamber. This could be done by eliminating one valve. One of the exhaust valves was chosen. The reason behind this choise was, that if any air motion was present in the cylinder during the delay and combustion periods then the main factor effecting it would be the inlet valves. The exhaust valves could contribute, but to a much lesser extent.

It was also realised that the loss of one exhaust valve would reduce air flow. To counter this the remaining valve and passages were redesigned on the basis of Thornycrofts [40] work to give a better air flow. It was also borne in mind that the boost pressure to the test cylinder could be controlled and, as mentioned later, valve timing and overlap adjusted . The exhaust port could not leave the head on the same side, nor on the other side, because of the valve push rods and fuel pump. To overcome this the inlet and exhaust valves were changed round. This allowed the single exhaust port to leave over the flywheel, see Figure 101, and re-enter the normal exhaust system at the side. Figure 110 shows the flame plates of the normal and photographic heads and the location of the window hole.

The exhaust and inlet cams were changed over on the camshaft to accommodate this change and variable cams fitted. The inlet rocker gear was a normal assembly but the exhaust bridge was dispensed with, the push rod angled inwards and a short rocker fitted the length of either side of the fulerum being designed to give the same lift as the normal assembly.

The angle of the window dictated that one cylinder head stud must be short. The strong back was modified by removing two sides but still allowing three cylinder head studs to be tightened up as normal. The fourth stud was tightened on the bottom flange below the window. Figure 111 shows the rockers and strongback assembled. The position of the window seat in the head was controlled by angle of the window and the space between the injector and the remaining valve seats. At first it was

considered that the injector could be angled. But difficulties in manufacture of the nozzle and in clamping the injector between the valve springs proved overriding. The final solution was to raise the seat of the injector and fit the injector itself with a collar. Figure 112 shows the arrangement while Appendix VIII (i) shows the design of injector.

The height of the seat above the flame plate with this layout is also shown as is the shape of the window. The final window design is seen in Appendix VIII (f) and although the length of the window would make clamping difficult the optical paths were equal, an important point when using the schlieren system. The length of the window would also reduce the area of the chamber under observation due to refraction. It was considered that some optical compensation might be needed. For direct photography a second shape was designed in which the top step was eliminated. A sketch of this window is shown in Figure 113.

Two window materials were called for, one - industrial quartz, and the other, perspex. As the quartz window would be costly and fragile a prototype window for initial tests on the schlieren system was designed. Figure 114 shows the general layout. The window was a quartz step disc with an optical diameter of 2¾ inches. These were cheap and relatively quickly obtained. In this window the inner clamp was on a screw thread. In both cases 'O' rings of 80 shore hardness were specified.

The method of clamping and supporting the quartz window used in the small engine was only partially followed

in the larger head. The clamp was made as long as possible and 12 studs used to hold it. In this way the load was spread as evenly as possible. A stud at the very bottom of the head by the cylinder head stud could not be included through lack of space. Figure 111 shows the clamp assembled. The clamp could be tightened down onto a spigot and could not at any time squeeze the window. The difference in the small and large engine was the seating. The seating in the large version was by 'O' rings as mentioned above, but standard ring grooves were used on the head and clamp. These had to be modified as described later.

The only other special feature of the head was a removable tube fitted between the exhaust and inlet valves on the camshaft side. This allowed a pressure transducer to be located at the face of the flame plate. In other respects the head was normal, i.e., clamping method, liner and water passages, except that the air starter was omitted. A small test on the engine proved its ability to start on 5 cylinders, providing number 6 was not in the air starter on position.

In Appendix VIII (g) and (h) are shown the final detailed design of the cylinder head.

7.4.3. Method of Countering Piston Movement

The method used in the small engine to counter piston movement, that of reducing the bore clearance, was rejected for the large engine because of the chance of seizure and the subsequent large amount of damage. The method used was simply to place four 'Deva' metal pads on the diameters of the piston. These were accurately machined and fitted so

that a .005 inch clearance between the liner and the pads was obtained when the engine was cold. Careful running in of the pads enabled an exact fit to be obtained at test temperatures.

7.4.4. Method of Countering Oil Passing up the Bore

Initial experiments with the normal engine indicated that the source of oil appearing on the piston crown during a motoring period was two-fold. The major source was oil issuing from the gudgeon pin ends, passing through the piston ring pack into the chamber. The second was oil passing the bottom scraper and top ring pack. To counter this severe downward scraping compression rings were fitted to the second and third compression grooves and spring loaded scraper ring on the two scraper ring grooves. The piston gudgeon pin boss was machined and sealing was obtained with 'O' rings.

As a second line of defence two further modifications were planned. One was to remove the oil feed to the piston pin and allow for grease lubrication. To back this up, a flapper was designed to fit the bottom of the liner in an effort to reduce the oil spray under the piston. A third possibility was considered. This was to re-machine the piston grooves to take morganite rings which are self-lubricating. These rings had been successfuly used on air compressors of the APC size and with the short duration of running it was thought that they would withstand combustion conditions as well.

7.4.5. Injection Equipment

The experiments with a single-holed nozzle on the small engine had demonstrated the importance of getting a

representative injection period on the first one or two firing cycles due to mirror and window being smeared by fuel oil. Because of the difficulty of priming the injection equipment on the small engine coupled with the possibility that on the large engine with long pre-heat periods the oil left in the injector might boil off and leave air locks, the system shown in Figure 115 was tried initially.

In this system the first injector is in series with a second. The first is a normal type but the second has the fuel flowing in the reverse direction and the injector needle is not spring loaded but is fixed to a push rod which is in turn controlled by a solenoid. The cycle of events is such that when the engine is started up, the pump is locked into the required load position. However the solenoid is not energised so that the fuel oil is pumped through the first injector and out of the second without the pressure in the first being increased above the normal release pressure. When the solenoid is energized, the second needle valve is kept shut so that on the next pumping cycle the pressure rises as in normal operation and opens the first needle valve.

Unfortunately, due to the inability of the equipment to work correctly at high line pressures, i.e., it allowed fuel to be injected when the solenoid was de-energized, and to its unreliability, the method used on the small engine was then built. Figure 116 shows the layout of this method on the large engine. Under test this equipment gave consistent injection after the first cycle, which in itself was very close to being representative. Figure 117 shows the extent of the difference between the first,

second and third cycles at full rack.

In both these methods, the solenoid was operated as on the small engine by the sequencer.

7.5. Direct Photography

As has been stated in Chapter I, information was necessary on the effect of evaporation on liquid fuel penetration. Some initial tests with schlieren, to be described later, had shown that practically no air motion existed in the cylinder when the piston was at top dead centre. It was therefore decided to use the engine as a hot bomb and with the direct photographic technique investigate evaporation. The windows used were the perspex window shown in Figure 113 for metal temperature up to 100°C. Above this the smaller quartz window (Figure 114) was used. The camera was mounted on the table above the engine and 8 inch plain mirror angled the combustion chamber image into it. Four 750 watt Tungsten lamps were mounted on the head, focused into the window clamp hole. The position of the flywheel, which had white crank degrees numbers painted on a black background, was photographed by the camera via a periscope arrangement at the same time as the chamber. Four tungsten lamps illuminated these figures. Figure 102 shows the general arrangement. The piston was standard except that the top surface was painted with a matt black heat resistant paint. It was found that this gave better definition of the spray.

The tests were aimed at photographing the spray penetration and at the same time measuring the pressure

within the combustion chamber. Then using the program described in Appendix III the mean gas temperature over the injection period could be calculated.

This required further instrumentation. As well as the pressure in the cylinder, the fuel injection line pressure and needle lift, the intake pressure and temperature, the piston position and the crank degree markers were measured. Earlier work on instrumentation for analysis of cylinder condition [76] had shown the importance of accurately timing the pressure measurement in relation to the engine crank and care taken with the positioning of the cylinder pressure transducer. The method chosen for timing was to monitor the actual piston motion. A small permanent magnet was attached to the piston skirt with an inductive pick up in line with and attached to the liner. The position of the pick up was such that the magnet passed it when the piston was at its point of maximum velocity, thus giving a maximum accuracy. This arrangement gave a pulse equidistant from T.D.C. on the up and down stroke of the piston. The result can be seen in Figure 118. By dividing the distance between the two pulses T.D.C. can be located. The crank degrees were measured by setting 2BA steel bolts into the periphery of the flywheel at two degree intervals. Their signal was picked up by an inductive transducer.

The cylinder pressure was measured using a Southern Instruments Type G301 0 to 2000 lb/in^2 inductive transducer, and calibrated on an hydraulic rig against a Laboratory Standards Bundenberg 0 to 2000 lb/in^2 pressure gauge. The

transducer was located on the flame plate of the cylinder head by means of the removable tube mentioned earlier in this chapter. This reduced to a minimum, any passage resonance effects. The charge air pressure was also measured using a type G301 0 to 50 lb/in^2 inductive transducer. Calibration was carried out using an hydraulic dead weight tester. The location of this transducer was in the air trunking, at the head joint as also for the earlier tests on the rapid changeover air heater system. Although the mean boost pressure was constant for a test it was found necessary to use this transducer because the pressure fluctuation made use of an accurate gauge impossible. As the air inlet temperature was held steady throughout the duration of a test this temperature was measured by a mercury in glass thermometer.

The needle lift on the injector was measured by an inductive displacement type transducer. In earlier work on the cold bomb the transducer was placed on top of the injector and inaccuracy was found with long rod, transmitting the needle movement to the transducer, compressing. In the engine injector the transducer coil was set inside the injector spring with only a small rod extension from the needle. A strain gauge type transducer, similar to the one used in the cold bomb work was used to measure the fuel line pressure. The range of this transducer was 0 to 20,000 lb/in^2 and was calibrated on a hydraulic rig against a Laboratory Standards 0 to 20,000 lb/in^2 Bundenberg pressure gauge. Due to the injector being virtually buried in the head, the

transducer could not be positioned as on the cold bomb work. Experiments were carried out on the cold bomb with the transducer on the injector, at the top of the injector and at the pump end of the injector pipe. Except for a time lag which could easily be calculated using a nominal velocity of sound in oil, the shape and magnitude of the diagram appeared unchanged. Thus during tests on the engine the pressure transducer was located at the pump end of the injector pipe. The outputs of the above transducer were presented on a Southern Instrument 6-channel recording oscilloscope with a continuous feed paper film camera. The general arrangement is shown in Figure 119.

The engine metal temperature as measured by the thermocouples placed in the head as already mentioned. The fuel oil temperature was measured by putting a fast response thermocouple into the second feed pipe left in the main injector from experiments with the double injector system. This monitored the fuel temperature at the nozzle flange, the same position as on the cold bomb injector. As well as the crank degree image on the high speed film the millisecond spark timer was used as in the cold bomb work.

The object of the investigation at this point was the effect of evaporation on spray penetration. Thus to eliminate combustion effects, nitrogen was fed into the air supply to suppress or at least delay the ignition.

The method of testing was to pre-heat the engine to a set metal temperature while stationary. Then started up and set the air inlet temperature, nitrogen enriched, to that temperature and a specified boost pressure. In this

way, no heat was picked up or lost in the inlet air passing into the engine. When conditions were steady, i.e., temperature and engine speed, the sequencer was triggered, switching on the camera, lights and pulling in the fuel rack. At the end of each test the perspex window had to be re-polished but the quartz needed only a wipe. The type of photographic result gained in shown in Figure 120.

Sequence 10 and 11 on the film show the actual results gained first with a cold combustion chamber and then hot.

The analysis of the results is dealt with in the next chapter.

7.6. Schlieren Photography

The initial work on the schlieren system was done using the small quartz window described above. Figure 121 shows the arrangement of the schlieren system. With the greater space available the source and image were split by means of a prism as suggested in Chapter VI. This gave much more light at the camera and with the graded filter Trix neg film was adequate at speeds of 13000 frames/second and with no slit in the camera. Ansco D200 was used for coloured schlieren and filter schlieren. Figure 124 shows an example of the black and white results. Sequence 12 shows the results of black and white film while sequence 13 shows the colour schlieren using the step wedge filter. Again the spray looked black and there appeared to be no vapour or change in state between vapour and liquid fuel. However the tilting effect when using the colour filter technique seemed to be less than that experience on the small engine. To check the exact movement of the schlieren image due to this piston tilt the image was focused on a ground glass screen with a graticule drawn on it. The

high speed camera was then focused onto the screen and a film exposed at 13000 frames/second, while the engine was running. In this way it was found that the movement of the image was only a matter of 1mm in a planeperpendicular to the source height and thus a filter with a required central bandwidth could be made.

The most interesting result at this stage was the air flow pattern. This can be seen clearly in sequence 13. It would appear that virtually no organised air flow exists. The next step was to fit the larger quartz window.

As an initial trial the window was fitted into the head while on the bench. This was successful, and no cracking or chipping of the quartz took place. However, on fitting the quartz in the head when on the engine, the window cracked. It was thought that the difference between the bench and the engine was that the head probably bowed when tightened down on the engine, allowing the seats to come into contact with the quartz. To investigate the area of stress an araldite mock window was made and a crude polariscope set up on the engine. Figure 122 shows a sketch of the polariscope. The window clamp was tightened down in steps and the patterns formed in the window photographed. The test was carried out with the head on the bench and the engine. The thickness of the mock araldite mirror made the patterns difficult to see, but the results did indicate an area of high stress where the crack developed on the quartz window. The seats on the clamp and the head were machined down and the test repeated. The stress area had been eliminated.

A further modification was also made. It had been noticed on the film so far taken that the window rocked slightly due to the fact that too much loading could not be applied to the quartz because of the fear of shearing it. To combat this movement and to stop the quartz hitting the side wall, 'O' ring grooves were machined in the window hole walls. These modifications proved successful and no cracking of the window took place on tightening down with the cylinder head in place on the engine.

The results from the direct photography showed high rates of evaporation and the need for more information on vapour movement. Thus when it was completed the small quartz window and the same schlieren system as before were replaced and the work continued to establish the technique for investigating the movement of vapour.

Two modifications were carried out. The positioning of the camera on the schlieren system had proved difficult so a stand was made which allowed the camera to be moved by fine threaded vertical and horizontal screws. The flywheel position tube was extended so that the flywheel image could be focused into the camera at the same time as the schlieren. The method used on the small engine for setting up and focusing proved successful.

An engine condition was chosen which, under direct photography, had shown the spray completely evaporated after about one inch of penetration. This was then checked and the results found repeatable with direct and schlieren photography. The results are plotted in Figure 125 and show that there is a difference of spray penetration between the two methods. This difference must be the

vapour which is visible using the schlieren technique but invisible when using direct photography. An example of the black and white schlieren results can be seen in sequence 12. Thus the fuel vapour penetrates further than the liquid fuel and is therefore of more interest as far as prediction of spray penetration is concerned. All the test conditions used in the direct photography tests were repeated with the schlieren system and the initial analysis of them is considered in the next chapter.

7.7. Sensitivity of Schlieren System

The schlieren system had proved itself adequate for photographing the air and vapour movement and in this form was used to give information on vapour penetration. However, one fault remained, that of not being able to distinguish between vapour and liquid on the same schlieren film.

In earlier work both on the small and large engine no difference had been detected. Three possible reasons were suggested in Chapter VI. Firstly, the investigation into the dense range of the filters had been limited by lack of illumination when using the half plate beam splitter. The schlieren system was too sensitive, and there was no vapour present. On the large engine the presence of vapour was established by using both direct and schlieren photography. The schlieren system had been using a prism to split the source and image thus reducing considerably the light loss in the system.

It was therefore decided to investigate the range and sensitivity of the system. The sensitivity of a system may be defined as the change in contrast on the viewing screen produced by a unit change in deflection. The range

of a system is the displacement at the filter for a unit change in density of the fluid. In a standard Toepler system (with a true knife edge) the range is a function of source height (H) and the focal length of the first mirror (F)

i.e., $R = \frac{H}{F}$ ..... (64)

It can be shown that [77] the sensitivity (S) is inversely proportional to the range

$S = \frac{2}{R}$ ..... (65)

In a system using graded filters the range and sensitivity of the system can be controlled by the size and density gradient across the filter. The size and shape of the source is not critical and a point source is normally used [74] thus leaving only the focal length of the first mirror as a further control of range. As has been mentioned Lyn [72] applied the graded filter technique to a single pass system. He found that a step wedge of 1 cm total width was required and that by placing the image at various positions on the filter between transmission and cut off the vapour at the edges of the spray and the air movement could be detected. The vapour was more pronounced if the image was placed in the denser region of the filter and the air movement if in the less dense regions.

The air motion in the present work was visible with fairly coarse step wedge (Figure 99 (left upper)) but no distinction between vapour and liquid could be seen even with the image in the most dense region. Therefore another filter (Figure 99 (left lower)) with a greater density gradient was tried with a similar variation of image position. In all cases no difference could be seen. The combination of

a double pass system and dense spray with no appreciable air flow present to disrupt the vapour could possibly give a deflection that was out of the range for the aperture of the filter and lenses concerned. As these were at a maximum the deflection of the light ray was reduced by introducing a 50 cm focal length lens into the system to replace the 4 foot focal length mirror. Figure 123 shows the arrangement. Also a new range of filters (Figure 99) were used. The lens was mounted on V block for convenience but this made setting up difficult. To help the prism was replaced by the half plate and although this reduced the illumination successful photographs were taken in the dense regions using Kodak Tri-X reversal film.

Tests were carried out with each filter. Vapour was detected on the outside edges of the spray but not very clearly.

Two colour filters with green-red-green band arrangements (Figure 99) were also tried using Ansco D200 film and the results are shown in sequence 14. No evidence of vapour can be seen.

7.8. Discussions

The application of direct and schlieren photography to a large engine as a reliable instrument technique has proved possible. However, even with the lens system it seems difficult to identify vapour. Two possibilities for this are, that the spray is too dense and is not disrupted by the air motion. Thus the deflection of the light ray is too large except at the outer edges of the spray. The other is the fact that in reducing the range of the schlieren system the sensitivity has been impaired such that the deflection of oil and vapour are indistinguishable.

Where air and scavanging flow patterns are required in detail the mirror system has adequate sensitivity and at the same time allows investigation of the total vapourized spray while not distinguishing between vapourèzed and non-vapourized fuel.

Other points need further work if the technique is to be extended to investigations at high mean effective pressures. The large quartz window is a weak point and further re-design of seats and window shape may be necessary. The combustion chamber wall temperatures may become important and at present the maximum value is severely limited.

If spray impact on the edge of the piston is to be investigated then further work on the stepped mirror is required. The principle has been proved with bench tests but its value on the engine has not been tested.

Piston movement control by means of pads was reasonable even for colour filter techniques but the stepped mirror would demand even more reduction in movement.

The method of controlling the oil passing into the chamber by using 'O' rings on the gudgeon pin and severe scraper oil rings was successful but for test runs exceeding 3 minutes the greased con rod and flapper may be required.

The flywheel marker tube was prone to vibration and the use of glass mirrors made the image hard to focus. A possibly better solution is to use the camera oscilloscope adaptor and superimpose the crank position on top of the high speed film. The rig as a whole, proved exceptionally reliable and easy to handle, despite its size and complexity. Some 140 runs were completed in which only 9 were scrapped due to malfunction of a part of the rig. When using

quartz windows and processing film after each test, as many as five tests a day could be completed.

The development of a single shot technique similar to the one used on the cold bomb could possibly reduce the cost of each run depending on the aim of the investigation.

However the technique in its present form is established and the results obtained are considered in the next chapter.

CHAPTER VIII

ANALYSIS OF 8-INCH BORE ENGINE RESULTS

8.1. INTRODUCTION

The analysis of some initial results from the large engine rig are described in this chapter, together with the method of analysis.

8.2. Method of Analysis

The method of analysing the oscilloscope traces was as described in Chapter IV by using a travelling microscope. The T.D.C. position was accurately located from the piston marker and the analysed cylinder pressure diagram and engine conditions fed into the computer program described in Appendix III. From this the variation of density and mean gas temperature with time was calculated. These results were measured over the injection period assuming no combustion. In one or two results at high temperatures the nitrogen suppression was not adequate and the fuel ignited a few degrees before the end of injection. In these cases the density and temperature curves were extrapolated to give conditions without combustion.

The injection pressure diagram was meaned over the injection period and thus the parameters required in the equation proposed in Chapter V could be gained, i.e.,

ΔP pressure drop across orifice

ρ_g gas density

d orifice diameter

L orifice length

with the addition of the mean gas temperature.

The high speed film was also analysed in the way described in Chapter IV, that of projecting the image onto a large screen and measuring the pentration with time using

the 1000 cycles/second marker on the edge of the film.

8.3. Analysis of Direct Photography Results

The parameters obtained as above were used in the proposed equation to give the spray penetration at those engine conditions but without evaporation. These were then plotted with the actual results measured from the high speed film. Figures 125 to 135 show the results. In Chapter I it was suggested that the density and injection pressure would have little effect on evaporation. On the other hand, by increasing gas temperature and decreasing the hole size the effect on penetration due to evaporation would be increased. The control of density is limited in these initial results but by comparing Figures 125 and 127 the effect of increasing the temperature can be seen to decrease penetration.

There is a large difference between the penetration at room temperature and 1016^{o}K. This substantiates Gelalles' findings as the fuel was at the same temperature before injection. Although the gas temperature is higher, the much larger difference with the engine results indicates that its effect is more severe noting that Gelalles used a .004 inch hole, while results were gained with .012 inch to .027 inch orifices in the engine test. The largest hole used on the present test, .027 inch in diameter was found, after tests, not to be a true cylinder in length but again considering the results as the hole size increases the effect of evaporation decreases. The results from Figure 132 with the .018 inch orifice do not substantiate this trend.

It would seem that the effect of evaporation on penetration is negligible for an orifice diameter around .027 inch.

With the limited number of results obtained it is difficult to make any further observations except perhaps from Figures 128 and 129, which would indicate that injection pressure has little effect. The fact that the mean injection pressure varied by only 1000 lb/in must be borne in mind. However, an interesting observation that differs from Gelalles is that of the deviation of the spray penetration in cold and hot gas. Gelalles suggested this was a continuous and increasing deviation, while the present results show that the spray penetration is essentially the same for a period and then diverges fairly rapidly and reaches full development. There could be an effect due to the piston and head being very close to the spray and cutting down air entrainment.

At the time these results were being analysed, a paper by Parkes et al [78] became available in which work on spray evaporation on a rig was described. They based their work on Schweitzer's dimensional parameters and extended the work to include the effect of evaporation.

From results they proposed an equation

$$S = \frac{200d}{1+\Delta\rho_a}\left[\frac{\Delta\rho_a \sqrt{\Delta P}}{d}\left[1 - (1 - \frac{d}{d_o})\, 1.12 \times 10^{-3}\ (T_m - 70)\right]\right]^{0.6} t^{0.6} \quad \ldots\ldots (66)$$

where the parameters are as above except

$\Delta\rho_a$ = gas density relative to atmosphere density

d_o = a reference diameter = .0236"

T_m = gas temperature in degrees Fahrenheit.

The reference diameter was derived from the results which showed that there was no effect on penetration for orifice diameter of .0236 inches and above. Parkes also investigated the effect of restriction around the spray and came to the conclusion that only severe restriction, which did not occur in an engine, would appreciably effect the spray penetration.

His equation has been used to plot the predicted evaporation for the conditions prevailing in the large engine and these are also shown in Figures 125 to 133. The unaffected penetrations in some cases diverge from the predicted path using equation (63), the proposed equation. This may be due to the fact that they based their results on Schweitzer's work, and the way in which they gain the equation constant and powers. The results given in the paper show a fair amount of scatter.

Comparison of the curves and equation brings out three major conclusions. The findings of Parkes confirm the effects of temperature and orifice size. Orifice diameter above .0236 inches is not affected. This is somewhat lower than the value suggested by the present work but maximum gas temperature used by Parkes et al was 1000°F while the maximum mean temperature obtained in the engine tests was around 1350°F. The evaporation curves show the same trend as the results of Gelalles, that of a continuously increasing deviation from the unaffected results. This disagrees with the present observed result. Possible reasons are the fluctuations in the injection system or difference in L/d ratio, effecting the cone angle development and thus the ability of the hot gas to evaporate the incoming fuel.

Figure 134 shows the variation of cone angle with time in hot and cold gas. The final developed cone angle is reduced by some two degrees. If the results are plotted in the same way as Figure 78, Chapter V, Figure 135, there is still a large scatter but the cone angles are reduced by evaporation.

8.4. Analysis of Schlieren Photography Results

After the survey described in Chapters I and II was completed, the idea that a knowledge of the penetration of the evaporated fuel might be important was put forward (Chapter III). The results taken using the schlieren system were analysed in precisely the same manner described above. These are plotted in Figures 125, 126, 127, 129, 130 and 131 and show that the fuel when vapourized does travel in front of the liquid spray. The difference in penetration between liquid and vapour is large particularly with the smaller orifice diameters and high gas temperatures.

From the film, sequence 12, the vapour spray is still compact as was indicated by the difficulty encountered in attempting to differentiate between liquid and vapour on the schlieren system. Thus the penetration of the vapour is of prime importance and that of liquid only of secondary interest.

The schlieren results show that within the scatter predicted in Chapter V the vapour spray follows the predicted unevaporated spray penetration. Although only a few tests have been considered this shows that equation (63) will predict the total spray penetration in both cold gas and gas up to at least 1000°C.

The cone angle was also measured and these are plotted in Figure 135 together with the liquid and cold bomb results. The angles measured still have a high degree of scatter but are in general agreement with those measured in the cold bomb.

The results show that no effect in overall penetration and cone angle is apparent when a spray develops into a hot as opposed to cold gas. This finding must now be viewed in the light of the discussions in Chapters I and II.

8.5. Application of Results

The results from the cold bomb demonstrated that the effect of an actual system on the penetration of the spray was small. The large engine results have shown that the equation proposed to predict unevaporated spray penetration also predicts the total spray penetration in hot gas up to about 1000°C. The mean gas temperature for the spray shown in Figure 85 was 980 K over the period taken for the spray to reach the piston, thus the penetration given is not reduced by evaporation effects.

From examination of film taken with normal ignition delay periods the ignition point is at the edge of the spray near the nozzle as suggested in Figure 31 and no appreciable disruption takes place. The penetration can therefore be only increased by ignition disruption.

The evidence shows that the spray must therefore reach the piston wall very quickly in the vapour form. Direct photography results with the fuel burning show the spray hitting the piston and being disrupted, moving out and around the piston. As the sprays, even in the vapour form, are compact, this could lead to a better mixing of fuel and air

unless the adjacent spray is too close.

If the normal working conditions are taken for the 8-inch bore test engine, with .012 inch nozzle and average spray path of 3 inches, again, from Figure 125, the spray in vapour form reaches the piston after 11 degrees of crank (750 r.p.m.). However, these observations can only be tentative because the investigations so far have not considered the behaviour of the spray at the piston wall when burning or the fact that in normal combustion the gas temperature continues to rise rapidly after the spray reaches the wall. For instance, from the results that have already been quoted, the mean gas temperature between start of injection and the spray reaching hitting the piston was 980°K. Nine degrees later, top dead centre the mean calculated temperature has risen to 1600°K.

Bearing in mind the limitations of work, it is proposed that as well as the type of combustion where the spray just licks the wall, and the onus of mixing is on the fuel spray developing and entraining air, there is an impingement process which increases the mixing process by disrupting the spray.

Considering penetration of sprays, it is desirable for good combustion to get the air to fuel ratio within the spray greater than stoichiometric (i.e., $\lambda = 1$). In the first type of combustion or non-impingement, it would seem sensible that the spray development must be such that the $\lambda > 1$ at the outer edge and the number of holes is such as to cover all the chamber.

If however impingement is wanted, then the number of holes should be reduced because of the spreading at the piston edge. The possible importance of this last form of combustion becomes clear if the history of the 12½-inch bore

engine is considered.

The engine has an open bowl piston and a nozzle configuration of 10 holes by .018 inch diameter. As the b.m.e.p. has risen so have the fuel line pressures in an attempt to get the extra fuel in during the same period, to keep the specific fuel consumption the same. At high b.m.e.p.s this has led to very high fuel line pressures which are uneconomic to contain and reduce reliability of the engine. Increasing the orifice diameter to decrease the line pressures only led to worse specific fuel consumptions and 'over penetration' was given as the reason.

If the distribution theory developed by Wakuri [15] is used (Appendix IX) and taking the spray path between nozzle and piston to be $4\frac{1}{2}$ inches, (This is dependent on the nozzle spray angle, in this case 150°) by the time the spray reaches the piston $\lambda = .912$. With ten holes, this would seem to be an attempt at non-impingement but with the markings on the piston such as shown in Figure 24, the value of λ and the calculated penetration shown in Figure 85, it is half and half.

A survey of other engines produced a 15-inch bore engine which had an effective spray path of only 3.75 inches and eight holes of .025 inch diameter. The value of λ was .58. From the penetration equation (63) the spray would hit the piston 6 degrees after start of injection in an injection period of 30 degrees. The performance and exhaust smoke were good thus this appeared to justify the impingement theory.

8.6. Engine Tests of Impingement Theory

Some initial tests were carried out on a single cylinder version of the 12½-inch bore engine in an attempt to verify the concept of impingement. Table 3 shows the results. Tests were carried out with the normal nozzle configuration 10 holes by .018 inch diameter at a load of 200 lb/in^2 b.m.e.p. 600 r.p.m. These were then repeated with the number of holes reduced to seven and the diameter increased to .025 inches. The effective spray path was kept constant by using the same nozzle spray angle and piston shape. The results demonstrate that the line pressure has been reduced, as is expected and the specific fuel consumption has also decreased. By increasing the total orifice area injection rate R_I has been increased while f_c, the function of the combustion chamber and spray pattern, has not changed significantly.

The last point, as to whether the impingement increases or decreases, albeit small, the heat release rate cannot be resolved with the information supplied by the present work, but at least it shows the possibility of deliberately using piston impingement without ill effects on the combustion performance as an alternative to that used at present.

CHAPTER IX

CONCLUSIONS

9.1. INTRODUCTION

The work carried out and the results obtained in the present investigation are reviewed and conclusions drawn.

9.2. Literature Survey

A survey of previous work showed that equations were available that predicted the penetration of fuel spray, but that their application was limited. No account of upstream conditions and L/d ratios such as found in an actual system was considered. The effect of evaporation and combustion on penetrations had been dealt with qualitatively but not quantitatively. Although previous work showed that very high values of air motion were required to disrupt a spray only scant evidence was available on the type and value of swirl in a medium speed direct injection engine. The mechanism of combustion in a medium speed engine was considered to be the penetration of the spray till it just 'licked' the combustion chamber wall.

9.3. Rig Work

The study of penetration of a fuel spray in dense atmospheres and room temperature from an actual injection system proved possible. A hood was used which allowed the development of one spray while not restricting the flow from the other orifices of the multi-hole nozzle. Penetration and cone angle of the spray were measured without interference by using a high speed camera and viewing the spray through glass walls set in the side of a cold bomb.

The effects of varying fuel line pressure, nozzle diameter, nozzle L/d ratio and gas density were investigated. However, this work indicated that a more useful approach was to include the effects of evaporation and combustion.

The feasability of using a double pass schlieren technique in a working engine was tested on the small three-inch bore engine. This technique allowed the investigation of vapourized fuel and air motion, as well as the liquid fuel. The double pass of light was obtained by placing a mirror on the piston and a quartz window in the head. The mirror was made by directly depositing chrome on to aluminium and this proved robust enough to stand repeated test firings. Piston tilt was overcome by decreasing the bore to piston clearance. Oil passing up the bore and obscuring the mirror was countered by using severe downward scraping rings. The affect of engine vibrations was minimised by mounting the optical system on anti-vibration mounts.

The basic system was then successfully applied to an 8-inch bore engine. Fitting the quartz window in the complex four valve head proved possible with extensive modifications. One exhaust valve was removed and the injector and valve gear altered to accommodate the window. Schlieren and direct photography were carried out on a multi-cylinder engine, this being easier to control and having less vibration. Transient temperature and pressure measurements were taken which allowed the computation of conditions inside the engine cylinder and injection system. Investigations were carried out on the effect of evaporation on the penetration effect with various orifice diameters,

cylinder densities and injection pressures. The schlieren system, using mirrors, allowed the penetration of the vapour to be followed but would not distinguish between fuel and vapour. Further work with a lens system with a reduced range distinguished the difference at the edge of a spray but not very clearly. In its final form the engine allows the investigation of liquid fuel, vapourized fuel and air motion by a combination of direct and schlieren photography. It is reliable enough to be used for future combustion research.

9.4. Results

9.4.1. An equation is proposed to calculate spray penetration in cold gas at engine densities:-

$$\frac{S}{d} = 4.13 \left(\frac{t}{d} \sqrt{\frac{\Delta P}{\rho_g}} \right)^{.64} \left(\frac{L}{d} \right)^{.18}$$

This adds to work already carried out by other researchers since it is applied to an actual jerk injection system and takes into account the fluctuating pressures, upstream passage effects and change in nozzle L/d ratio. The cone angle of sprays developing from the system has been measured and found to be a function of the ratio of fuel to air density only. It is suggested that Figure 78 is used to deduce the values.

9.4.2. Evaporation of the fuel has a pronounced effect on the liquid spray penetration and results obtained are in general agreement with those deduced from Gelalles' work [32]. The major factors effecting evaporation are orifice diameter and gas temperature. After evaporation, the fuel vapour moves ahead of the liquid spray and remains compact. The penetration is the same as that in an unevaporated spray, in gas at room temperature and the same density.

The proposed equation thus holds good for predicting total spray penetration at engine cylinder gas temperatures and densities whilst Figure 78 gives the values of cone angle.

9.4.3. The air motion, in the type of medium speed engine used, is random at top dead centre (compression) and does not affect the spray after injection is complete.

9.4.4. No conclusive evidence has been gained on the effect of combustion on penetration. Ignition occurs at the outer edge of the spray between the tip of the spray and the orifice. The effect of combustion on penetration has not been considered in detail.

9.4.5. It is suggested that, in the case of the 8-inch, 12½-inch and 15-inch bore engines investigated, under normal running conditions the vapour spray must come into contact with the piston wall, and does not 'just lick' the bore as earlier work had suggested. The mechanism at the combustion chamber wall was not investigated but appreciable disruption of the spray resulted.

9.4.6. Another form of combustion is then postulated, in which the spray is deliberately impinged upon the piston wall to help fuel and air mix. The adjacent spray must not be too close such that interference will occur at the wall. This allows larger nozzle holes than those indicated by previous theories, and thus larger total nozzle hole area. This in its turn should allow fuel line pressure to be reduced.

9.4.7. Initial test on a 12½-inch bore engine using the impingement type of combustion have shown an increased efficiency and allowed nozzle configurations to be used which reduced mechanical loadings on the fuel injection system and camshaft.

CHAPTER X

FUTURE WORK

The investigations described are in no way complete. The following work is suggested.

10.1 The proposed equation is checked with more results from the schlieren system on the 8-inch bore engine. In the present investigation there are too few results to guarantee the accuracy of the equation particularly at the larger penetration distances.

10.2 The effect of combustion on spray penetration should receive attention, together with the impingement mechanism taking place at the piston wall to investigate the impingement method of combustion and to discover any limitations.

10.3 Further work should be undertaken to adapt the range and sensitivity of the schlieren system to distinguish the difference between vapour and liquid fuel even in a dense vapour spray. This would eliminate the need for taking both direct and schlieren photographs as the method for distinguishing the difference.

10.4. The injection rate should be controlled in order that the factors affecting heat release inside the combustion chamber can be investigated. This would help elucidate the part played by injection rate in the rate of heat release.

10.5. The initial tests carried out on the single cylinder $12\frac{1}{2}$-inch bore engine should be repeated on a multi-cylinder version to check the results obtained and ensure that they were not due to bad simulation of a turbo-charged engine.

10.6. The influence of droplet size and distribution should be studied, particularly at the beginning and end of

injection in relation to both performance and exhaust smoke condition. This aspect has not been covered in the present work and could strongly influence the type of combustion required in a medium speed type of engine.

REFERENCES

1. "Fuel Injection Development on a Single Cylinder AO Engine up to 1800 hours".

K. W. M. Cockburn

R. & H. Report 65-RE-3

2. "Shatter of Drops in Streams of Air"

W. R. Lane

Ind.Eng.Chem. Vol. 43, June 1951

3. "Penetration of Oil Sprays in Dense Air"

P. H. Schweitzer

Pennsylvania State College Bulletin No. 20 122, June 1934

4. "Some Characteristics of Fuel Sprays at Low Injection Pressures"

A. M. Rothrock and C.B. Waldron

N.A.C.A. Tech. Note No.399, November 1931

5. "Some Characteristics of Sprays obtained from Pintle type Injection Nozzles"

E. T. Marsh and C. D. Waldron

N.A.C.A. Tech. Note No. 465, July 1933

6. "Oil Spray Investigations of the N.A.C.A."

W. F. Joachim

A.S.M.E. Trans. Vol. 49-50 OGP-50-6 1927-28

7. "Kompressorlose Dieselmaschinen"

F. Sass

Berlin, J. Springer 1929

8. "The Atomization of Liquid Fuels"

E. Giffen and A. Muraszew

Chapman and Hall, London

9. "Penetration of Oil Sprays"

P. H. Schweitzer

Pennsylvania State College Bulletin No. 46, July 1937

10. "Disintegration and Atomization of a Fuel Jet in Diesel Engines"

A. E. Thiemann

A.T.Z. Vol. 38, No. 19, October 1935

11. "Investigation of the Injection Process in Diesel Engines"

W. Riehm

Z.V.D.I. Vol. 68, No. 25, June 1925

12. "New American and German Investigations on Pressure Injection in Diesel Engines"

F. Sass

Forsch, Geb, Ingenieurwesens A, Vol. 2, No. 10, October 1931

13. "On Fuel Atomization in Diesel Engines"

O. Holfelder

Forsch, Geb, Ingenieurwesens A, Vol. 3, September/October, 1932

14. "On the Physics of Fuel Sprays in Diesel Engines"

H. Mehlig

A.T.Z. Vol. 37, No. 16, August 1934

15. "Studies on the Penetration of Fuel Spray in a Diesel Engine"

Y. Wakuri et al

Bulletin of J.S.M.E. Vol. 3, No. 9, 1960

16. "Experimental Investigation into the Development of the Jet of an Atomized Liquid and the Generalization of Experimental results on the angle of the Jets Cone"

A. S. Lyschevskii

Trudy Novocherkasskogo Politekhnicheskogo Instituta im S. Ordzhonikidze, 1960, 107, 3-22

17. "Length of Atomized Fuel Jet in a Diesel Engine"

R. V. Rusinov

Russian Engineering Journal, Issue No. 4, pp. 13-17, 1963

18. "Flow patterns in diesel nozzle spray holes"

W. Berwerk

"Discharge coefficient of small submerged orifices"

R. H. Spikes and G. A. Pennington

Institution of Mechanical Engineers, 1959

19. "An Investigation of Coefficient of Discharge of Liquids through small round orifices"

W. F. Joachim

Report No. 224, N.A.C.A.

20. "An Empirical Function for finding Gas Specific Heat for air and fuel/air mixtures"

H. K. Kohler

B.I.C.E.R.I. Lab. Report No. P.125

21. "Method of Predicting some aspects of Performance of a diesel engine using a Digital Computer"

N. Whitehouse et al

I.M.E. Proc. Vol. 176, No. 9, 1962

22. "An Apparatus for Determining Fuel Spray Characteristics"

N. T. Meckel et al

S.A.E. Paper No. 436A, November 1961

23. "Combustion of a Single Droplet and of a Fuel Spray"

D. B. Spalding

24. "A Technique for studying the Combustion of small single drops of liquid fuel"

M. T. Monoghan

J. Sci. Instrumentation, 1964, Vol. 41

25. "Fuel Vapourization and Ignition lag in Diesel Combustion"

M. M. El Wakil et al

S.A.E. Trans. Vol. 64, 1956

26. "Experimental and Calculated Temperatures and Mass Histories of Vapourizing fuel drops"

M. M. El Wakil et al

N.A.C.A. Tech. Note 3496, 1954

27. "Experimental and Calculated Histories of Vapourizing fuel drops"

R. J. Priem et al

N.A.C.A. Tech. Note 3988, 1955

28. "Some Characteristics of Nozzles and Sprays for Oil Engines"

A. L. Bird

British Marine Oil Engine Association, 1926

29. "Effect of Nozzle Design on fuel sprays and flame formation in a high speed compression-ignition engine"

A. M. Rothrock and C. D. Waldron

N.A.C.A. Report No. 561, 1936

30. "Fuel Evaporation and its effects on Combustion in High Speed Compression Ignition Engines"

A. M. Rothrock and C. D. Waldron

N.A.C.A. Report No. 435, 1932

31. "The N.A.C.A. Apparatus for studying the formation and combustion of fuel sprays and the results from preliminary tests"

A. M. Rothrock

N.A.C.A. Report No. 429, 1931

32. "Some effects of air and fuel Oil Temperatures on Spray Penetration and Dispersion"

A. G. Gelalles

N.A.C.A. Tech. Note No. 338, 1930

33. "Ignition and Flame Development in the case of Diesel Fuel Injection"

O. Holfelder

N.A.C.A. Tech. Memo No. 790, 1935

34. "Some Effects of Air Flow on the Penetration and Distribution of Oil Sprays"

A. M. Rothrock and E. G. Beardsley

N.A.C.A. TN No. 329, 1929

35. "Effect of High Air Velocities on the Distribution and Penetration of a Fuel Spray"

A. M. Rothrock

N.A.C.A. TN No. 376, 1931

36. "The Effects of Turbulence and wind speed on the rate of Evaporation of a Fuel Spray"

R. G. Fledderman, A. R. Hanson

Report No. CM 667, U.S. Navy Depattment, Bureau of Ordnance, University of Michigan Ann ARBOR, June 1951

37. "Some more light on Diesel Combustion"

J. F. Alcock, W. M. Scott

Proc. I.M.E., No. 5, 1962-63

38. "Air Swirl in a Road-Vehicle Diesel Engine"

D. Fitzgeorge and J. L. Allison

Proc. I.M.E., No. 4, 1962-63

39. "Unsteady Vapourization Histories and Trajectories of fuel drops injected into Swirling Air"

G. L. Borman, J. H. Johnson

S.A.E. Paper 598C, November 1962

40. "A preliminary survey of the relative merits of two valve and four valve cylinder heads"

C. H. Thornycroft and J. R. Howard

B.I.C.E.R.A. Report No. 52/3, 1952

41. "Continuous Air Flow Tests"

R. G. Tull

B.I.C.E.R.A. Lab. Report No. P.123, 1962

42. "Combustion in Piston Engines"

J. J. Broeze

De Technische Vitgererijh Stan N. V. Haarlem, 1962

43. "Gemischbrildung und Verbrennung in der Bombe Wege Zur Beherreshung und Steuerung des Verbrennungsablaufes bei Einspritz-Motoren"

E. Blume

Deutsche Kraftfahrtforschung Technischer Forschungsbericht, No. 91, 1940

44. "Combustion Characteristics, Ignition Delay Bomb"

Hurn

C.R.C. Diesel Bomb Advisory Group Report, February 1951

45. "Fuel Vapourization and Ignition lag in Diesel Combustion"

E. E. El Wakil, P. S. Myers and O. A. Uyehara

S.A.E. Trans. Vol. 64, 1956

46. "On Formation and Dispersion of Oil Sprays"

K. J. Dejuhasz et al

Penn State College, Engr. Experimental Station Bulletin No. 40, August 1932

47. "Physical and Chemical Ignition Delay in an Operating Diesel Engine using Hot-motored Technique"

YU et al

S.A.E. Trans. Vol. 64, pp. 690-702, 1956

48. "Ignition delay and Propagation of Combustion in Diesel Engines with solid Injection"

L. Herele

Faschung 10, pp. 15-27, 1939

49. "Gas Temperatures during Compression in Motored and Fired Diesel Engines"

K. C. Tsao, P. S. Myers, O. A. Uyehara

S.A.E. Paper No. 272B, January 1961.

50. "Ignition Delay Analysed from Self-Ignition of Fuel Drops"
M. M. El Wakil and M. I. Abodou
S. A. E. Journal, pp. 42-45, May 1963

51. "Significant Contributions of the Diesel Research Laboratory"
G. Rosen
Proc. I.M.E.

52. "Evaluation of Reaction Kinetics Eliminates Diesel Knock"
J. S. Meurer
S.A.E., Trans. Vol. 64, 1956

53 "A new Concept of Diesel Combustion"
Schweitzer
Automotive Industries, Vol. 114, No. 12, June 15, 1956.

54. "Tests in a Combustion Bomb under conditions simulating Diesel Engine Conditions"
A. F. Pischinger
Motortechnische Zeitschrift, January 1959

55. "Pre-Flame Reactions in Diesel Engines, Part II"
F. H. Garner et al
Inst. Petroleum Journal.

56 "Pre-Flame Reactions in Diesel Engines, Part III"
F. H. Garner et al
Inst. Petroleum Journal, Vol. 42, No. 387, March 1956

57. "Pre-Flame Reactions in Diesel Engines, Part IV - the Effect of Compression Ratio"
F. H. Garner et al
Inst. Petroleum Journal, Vol. 43, 1957

58. "Pre-Flame Reactions in Diesel Engines, Part V - Study of Temperatures, Pressure and Ignition Delay"
F. H. Garner et al
Inst. Petroleum Journal, Vol. 450, June 1961

59. "Fuel Introduction into the Intake Air of Diesel Engines"

P. H. Schweitzer and M. Alperstein

Penn State University Eng. Research Bulletin, April 1958.

60. "Diesel Combustion Study by Infra-Red Emission Spectroscopy"

W. T. Lyn

Inst. Petroleum Journal, Vol. 43, No. 398, February 1957

61. "Relation between Fuel Injection and Heat Release in a Direct-injection Engine and the Nature of the Combustion Processes"

W. T. Lyn and W. Austin

Proc. I.M.E. No. 1, 1960-61

62. "Study of Burning Rate and Nature of Combustion in Diesel Engines"

W. T. Lyn

9th Symposium on Combustion Academic Press N.Y. and London, 1962

63. "Fuel Injection and Controls for Internal Combustion Engines"

P. G. Burman and F. Deluca

The Technical Press Ltd., London

64. "Electromagnetic Gas Sampling Valve"

B. Kimpton

R. and H. Report 65-RI-4, 1965

65. "Effect of Orifice Length-Diameter Ratio on Fuel Sprays for Compression-Ignition Engines"

A. G. Gelalles

Report No. 402, N.A.C.A. 1931

66. "Penetration and Duration of Fuel Sprays from a Pump Injector System"

Rothrock and Marsh

Report No. 455, N.A.C.A. 1931

67. "Flame Propagation in Spark Ignition Engines"

I. Higashino

J.S.M.E. Bulletin, Vol. 4, No. 15, 1961

68. "Measurement of a Gas Temperature in an Engine by Velocity of Sound Method"

J. C. Livengood et al

S.A.E. Annual Meeting, January 13th-17th, 1958

69. "Shock Tube Technique to study Auto-ignition of Liquid Fuel Sprays"

C. J. Mullaney

Industrial and Engineering Chemistry Vol. 50, No. 1 January 1958, pp. 53-58

70. "A new Tool for Combustion Research, a Quartz Piston Engine"

F. W. Bowditch

S.A.E. Preprint 150B, National Auto week, March 15th-17th, 1960

71. "A Photographic Study of Events in a 14-inch Two Cycle Gas Engine Cylinder"

C. P. Miller et al

A. S. M. E. Trans. January 1954, pp. 97-106

72. "The Application of High Speed Schlieren Photography to Diesel Combustion Research"

W. T. Lyn and E. Valdmanis

The Journal of Photographic Science, Vol. 10, 1962

73. "An Automatic Control System for a High Speed Cine Camera"

J. C. C. Hempson

Paper M-3, 5th International Congress on High Speed Photography, 1966

74. "Schlieren Systems using Graded Filters"

R. J. North

Fluid Motion Sub-Committee Aeronautical Research Council, F.M. 1769, 1952

75. "Colour Schlieren Photography in High-Speed wind Tunnels"

R. J. North and R. F. Cash

N.P.L. Report NPL/AERO/383 1959

76. "Instruments Used in the development of Diesel Engines"

C. H. J. Daft

Paper No. 4, Symposium on Accuracy of Electronic/

76 (continued)

Measurements in l.c. Engine Development, January 1966

77. "Schlieren Methods"

D. W. Holder and R. J. North

N.P.L. Notes on Applied Science, No. 31,1963

78. "Penetration of Diesel Fuel Sprays in Gases"

M. V. Parks, C. Polonski and R. Toye

S.A.E. Paper No. 660747, October 1966

BIBLIOGRAPHY

A major source of references was the following:-

"Bibliography on Sprays", 2 ed.

Texas Co. Refining Dept. Technical and Research Div. N.Y. 1953, 210 pages.

Further relevant information can be found in:-

"La mecanique de l'evaporation"

N. Albertson, 1956

La Houille Blanche (Paris) No. 5, 1955 pp. 704 et.req. No. 1, 1956 pp. 36 et.req. No. 2, 1956 pp. 282.

"Photographic Techniques Applied to Combustion Studies"

Altseimer, 1952

J. American Rocket Soc. March-April, 1952 pp. 86-91

"Influence of the Quality of Atomization on the Stability of Combustion of Liquid Fuel Sprays"

Anson, 1953

Fuel Vol. 32, No. 1 (1953), pp. 39-51

"Injection and Combustion of Liquid Fuels"

Members of Battelle Memorial Institute

Wright Air Development Centre Tech.Rep: 56-344 A. R. Dev. Command

"The RE-vapourization of Fuel Sprays I - theoretical treament"

Benson, 1956

(N.A.E. Canada), Laboratory Report LR-181, Nov. 1956 46 p.

"The Evaporation of Fuel Sprays II - Experimental Work"

Benson and Bresebois 1956

(N.A.E. Canada) Laboratory Report LR-189, Nov. 1956

"Induced Air Flows in Fuel Sprays"

H. Binarh, W.E. Ranz

A.S.M.E. Paper No. 58-A-284 for Meeting November 30th-December 5th, 1958.

"Ursachen der Klopffreien Dierefverbrennung"

Boettger 1958

Kraftfahrzeugtechnik Vo. 8, No. 8, pp. 284-289

"Combustion of Liquid Fuel Spray"

Bolt and Boyle, 1955

A.S.M.E. Semi-Annual Meeting Paper No. 55-5467

June 1955 or in Trans. A.S.M.E. April 1956

"Neue Erkenntnisse auf dem Arbiete geraushamer Dieselverbrannung"

J. Bottger, 1955

Kraftfahrzeugtechnik Vol. 5, No .9, September 1955, pp. 301-307

"Neue Gesichtspunkte uber Gemischbielung in Kolben-Verbrennungsmotoren, insbescondere Diesel Motoren"

J. Bottger, 1957

Kraftfahrzeugtechnik, Vol. 7, Nos. 2 and 4, 1957, pp. 46-50 and 136-138

"Methodes de Mesure des Dimensions des Gouttelettes des Jets de Combustible dans les Moteurs Attematifs a combustion et dans Turbines a Gas"

Brun, 1952

IL SIA (Paris), August 1952, pp. 191-195

"Diesel Nozzle Spray - A procedure for determining Discharge Characteristics"

Bryan, 1941

Autom. Eng. (Engl)., Vol. 31, October 1941, pp. 337-340

"Combustion of Heavy Fuel Oils"

Chang, 1941

Sc.D. Thesis M.I.T. 1941 Manuscript

"Photographic Research Aids Engine Design Development"

C. E. Cordonier

Indus. Photography, V. 7, N.1, January 1958, pp. 24-25

"Combustion in Compression Ignition Oil Engines"

S. J. Davies

Ch. Mech. Eng. V. 1, N. 1. January 1954, pp. 24-36

"Effect of Ambient and Fuel Pressures on Spray Drop Size"

Decorso, 1959

Scientific Paper No. 8-0524-P12 Westinghouse Res. Lab.

7th October, 1958

(Presented at A.S.M.E. Gas Turbine Power Conference, March 1959)

"Wasser Einspritsung in Diesel Motoren"

A. B. Delfamah

N.T.Z., V.18, No. 2, February 1957, pp. 46-8

"Fuel Injection Spray Chamber"

Dema 1948

Anon. Diesel Engine M'frs. Ass'n. Lab. Eng. Bull. No. 2, 1948

"Measurement of Rapidly Fluctuating Pressures"

E. J. Diehl, H. Visser

Int. Shipbuilding Progress, V.1, N.3, 1954

"Photographic Methods of Analysis in Chemical Engineering Research"

Dombrowski, 1956

The Chem. Engineer No. 128 (December 1956)

"A Double flasher system with variable substractive delay for High-Speed Photography"

Dombrowski and Tyley, 1959

Brit. Communications and Electronics, Vol. 6 (1959)

"Liquid Atomization and Drop Size of Sprays"

P. Eisenklah and R. P. Fraser

Inst. Chem. Eng. - Trans. V. 34, No. 4, 1956

"The Effect of Turbulence and Wind Speed on the Rate of Evaporation of a Fuel Spray"

Fledderman and Hanson, 1951

Rep. C.M. 667, University of Michigan, June 1951

"High Speed Photography in the study of Moving Fluids"

Fraser and Dombrowski, 1953

Science and Applications of Photography

The Royal Photography Socy of Great Britain,

Proc. of R.P.S. Centenary Conf., London 1952, pp. 360-370

"High Speed Photography in Fluid Kinetics"

Frazer, 1955

Journal of Photographic Science Vol. 3, 1955, pp. 21-32

"The Dependence of Interpretation on Photographic Technique in Fluid Kinetics Research"

Frazer and Dombrowski, 1956

High Speed Photography

(Proc. third Internat. Congress, September 1956)

edited by R. B. Collins

Butterworths Sci. Publ. London, pp. 376-384

"A Selection of Photographic Technique for the study of Movement"

Frazer and Dombrowski, 1957

Jl. Imperial College Chem. Eng'g Soc. Vol. II (1957), pp. 131-151

"Liquid Atomization in Chemical Engineering"

R. P. Fraser, P. Eisenklah, N. Dombrowski

Bri. Chem. Eng. V.2, Nos. 8, 9, 10 and 11. August, 1957, pp. 414-417

"Leucht dichten intensiver Funkenentladungen"

Frungel, 1948

Optik. Vol. 3, Nos. 1-2, 1948, pp. 128-136

"Spray Formation and Break-up and Spray Combustion"

Fuhs 1958

Air Force Off. of Sci. Report TN-58-414 AMF/TD N 1199

Tech. Note No. 4 February, 1958

"Precision Control of the time interval between two Electric Spark Discharges"

Geyhart and Edmonson et al, 1951

John Hopkins Univ. Report No. CM-682, July 16, 1951

"On Burning of Single Drops of Fuel in Oxidizing Atmosphere"

M. Goldsmith, S.S. Penner

Jet Propulsion V. 24, No. 4, July-August, 1954, pp. 245-251

"The Evaporation of Fuel Spray in an Airstream, and effect of Turbulence of Droplet size distribution"

Hanson, 1952

Proc. Second Midwestern Conference on Fluid Mechanics, Ohio State Univ. (1952), pp. 415-428

"An Equation for predicting a Mean Drop Size in a High Speed Spray"

Harmon, 1955

Univ. Calif. Publications in Engineering, Vol. 5, No. 5 (1955) pp. 145-153

"Zwei neue MeBokalare fur die mikroskopische Volum und Oberflachenmes-sung"

Hennig, 1957

Forsh Ing-Wesen Vol. 23 (1957), pp. 71-73

"The size distribution of Droplets in a Fuel Spray"

Hopkins, 1946

Shell Petroleum Co. Ltd., London, Techn. Report No. ICT/6 (1946)

"Study of Pressure Effects on Vaporization Rate of Drops in Gas Streams"

Ingebo, 1953

N.A.C.A. TN 2850 (January 1953)

"Note on a Laboratory Apparatus to Study the High Speed Impact between a Liquid Drop and a Surface"

Jenkins, Booker and Sweed, 1958

Royal Aircraft Establishment, Gt. Brit. R.A.E. Tech.Note Mech.Eng. 256 (N-65562) February 1958

"Methods of Atomizing Liquid Fuels"

J. R. Joyce

Inst. Petroleum - J.V.64, No. 2 May 1952, pp. 301-330

"Heat and Mass Transfer in Process of Fuel Combustion in Air Stream"

B. V. Kantorvich, G. N. Delyagin

Int. J. Heat & Mass Transfer, V. 5, January-February 1962, pp. 11-21

"Effects of Combustion on Depth of Penetration of Liquid Fuel Droplets"

Khudyakov, 1949

Izvest. Akak. Nauk SSSR Otdel Tekh. Nauk. 1949, pp. 508-513

"Messung und Darstellung der TropfengroBenverteilung in sinem Zerstaubungsstrahl"

Klein, 1958

Brennstaff-Warme-Kraft. Vol. 10 Nob. June 1958, pp. 263-269

"Combustion of Single Droplets of Fuel"

K. Kobazasi

Engr. Digest, V.16, No. 1, January 1955, pp. 223-234

"Atomization of Heavy Fuel Oil"

G. Kolupaev

Sc.D. Thesis. Chem. Eng. M.I.T. 1941

"Combustion of Fuel Sprays"

Kumagai 1957

Sixth Internat. Symp. of Combustion. Reinhold Pub. Co.,

New York, 1957, pp. 668-674

"Uber die Veranderliche Stromung in Rohrleitungen bei Hochcruckeinsprit zung insbesondere in VerbrennungShraftmaschinen"

Kurzhais 1957

VD I-Z, Vol. 99, No. 9, March 21, 1957 pp. 375-380

"Review of Theoretical and Mathematical Analysis of the performance of Atomizing Nozzles"

Laster and Doumas, 1953

Chem. Eng. Progr. Vol. 49 (1953), pp. 518-526

"Atomization of Liquids in High Velocity Gas Streams"

Lewis, Edwards, Goglia, Rice and Smith

Ind. and Eng. Chem. 40, 67 1948

"Zweitaktmotoren mit Kraftstoffeinspritzung"

List, 1940

Deutche Kraftforschg (Germ) Zwischimbericht No. 86 (1940) pp. 51-59

"Determination of gas-turbine C. Chamber efficiency by Chemical Means"

P. Lloyd

Trans. 1948, p. 335

"Combustion in the Gas Turbine"

Lloyd, 1945

Proc. Inst. Mech. Eng., Vol. 133, No. 12 (1945) pp. 462-472

"Report of Atomization Panel to Sub-Committee on Combustion"

Lucas, 1943

Anon. K. Lucas Res. Lab. Report No. L520 (1943)

"The Effect of Varying the Quality of Atomization on Combustion"

Lucas, 1944

Anon. J. Lucas Res. Lab. Report No. B 40 (1944)

"Dispositil pour l'etude micro-photographique de la pulverisation de combustibles liquides"

N. Manson, S. K. Banerjea, R. Eddi

Revue de l'institut Francais du Petrole et Annales des combustibles liquides

V. 10, No. 6, June 1955, pp. 636-656

"Review of Experiments and Empirical Correlations relating to the Production of Sprays"

Marshall, 1953

Proj. SQUID Tech. Rep. NTI-I-C

"Untersuchungen uber den Einfluss von Druck und Viskositat auf die Durchflusszahl bei Einspritzdusen fur Diesel Motoren"

Meissner 1958

Kraftfahrzengtechnik Vol. 8, No. 9, pp. 326-331

(Inst. fur Verberennung motoren und kraftfahrwesen (IVK) Tech. Hochsch Dresden)

"Fuel Injection Problems in Otto Cycle Engines"

Meyers 1952

Proj. SQUID Tech. Report NTI-I-C

"Recent Advances in Spray Technology"

C. C. Miesse

Applied Mechanics Reviews V. 9, No. 8, August 1956, p. 3214

"One Dimensional Velocity Variation of a Burning Droplet"

Miesse 1953

C. C. Miesse, Heat Transfer and Fluid Mech. Inst. Rep (1953)

pp. 223-240

"Slow-motion Study of Injection and Combustion in a Diesel Engine"

Miller, 1945

S.A.E. Journal (Trans. Vol. 53 (1945) pp. 719-735)

"High Speed Photography in Design"

Miller and Shafton, 1952

Prod. Eng. (September 1952) pp. 167-182

"Diesel Fuel Injection and Combustion"

NAGAO, 1937

Austr. Dr. Tsu and W. E. Meyer, Pen. State College (Yo Yen, Tokyo 1937)

"Some Aspects of Fuel Injection Research in England"

W. E. N. Nicolls

Koninklijk Institut Van Ingenieurs Voodrachten No. 1-11,

January 1951, pp. 93-110 and 111-113

"Experiments and Theoretical Considerations on the Evaporation and Ignition Lags of Fuel Droplets"

Nishiwaki, 1955

Proc. Fifth Symposium on Combustion Reinhold Pub. Co., New York, 1955

"Veruche Zur Frage der Kraftstoff auf bereitung durch die Einspritzduse"

Oschatz, 1941

Deutsche Kraftfahrtsforschung No. 57 (1941) (Germ)

"Effect of Turbulence of a Liquid Jet on its Atomization"

Panasenkov, 1951

Zhur. Tekh. Fiz. Vol. 21, 1951 pp. 160-166 (Revision)

"Drop Size Distributions of Fuel Sprays"

Pilcher and Thomas, 1958

Amer. Chem. Soc. Advances in Chemistry, Series No. 20, pp. 155-165

"Verfahren zur Untersuchung von Dieselein spritzstahlen"

Pischinger 1955

Maschinen bau und Warmewirt schaft Wien Vol. 10, No. 3 (1955)

pp. 61-69

"Gemischbildung und Verbrennung im Diesel Motor"

Pischinger, 1957

Vol. VII of Series Die Verbrennungskraftmaschine,

Second Ed. Springer Verlag Wien 1957

"Fuel Distribution in the Combustion Zone of a gas Turbine Combustion Chamber"

Poulston and Shepheard 1957

Report No. 179 Shell Research Ltd., July 1957

"Recent Research of Fuel Injection and Electrical Equipment for Transport Vehicles"

Priddle, 1948

Transport World, May 8th, 1948

"The Influence of Spray Particle Size and Distribution in the Combustion of Oil Droplets"

Probert, 1946

Phil. Mag. Vol. 37, No. 265, February 1946, pp. 94-105

"Injection and Combustion of Liquid Fuels"

A. A. Putnam et al

Wright Air Development Centre, W.A.D.C. Tech. Report, N. 56-344

March, 1957, pp. 786.

"Sprays and Spraying"

W. E. Ranz

Pennsylvania State Univ., Dept. Eng. Research - Bul. No. 65

March, 1956

"Fuel Injection System in Compression Ignition Engines"

A. W. Rowe

S. African Inst. Mech. Engineers - J V2, No. 1 August 1952, pp. 3-25

"Ein fluss der Luftbewegung auf die Ausbildung Kraftstoffstrahles in der Wirbelkammer"

Saeuberlich 1943

Deutsche Kraft forschong, No. 76, 1943

"Catching on a Plate Coated with a Layer of Soot as a Method for Determining the Drop-Size of an Atomized Fuel"

Salamandra and Naboko, 1957

(Russian) Soviet Phys. Vol. 2, No. 3, March 1957 from Amer. Inst. of Phys. Inc. (Translation)

"Speed Micro photography of Drops and of Atomized Liquid in Flight"

Salamandra and Naboko, 1957

Translation from Soviet Phys. Vol. 12, No. 3, March 1957, pp. 551-554 American Inst. of Phys. Inc.

"An Experiment on the Atomization of Liquid"

T. Tanasuwa, S. Nukiyama

Trans. Soc. Mech. Eng. 5, No. 18, 63 (1939)

"On the theory of Combustion Rate of Liquid Fuel Sprays"

Tanasawa and Tesmia, 1958

Bulletin of J.S.M.E., Vol. 1, No. 1 (1958) pp. 36-41

"Measuring Drop Sizes in Sprays"

E. H. Taylor, D. B. Harmon, Jr.

Indus. and Eng. Chem. Vol. 46, No. 7, July 1954, pp. 1455-1457

"Combustion of Atomized Fuels"

M. N. Thring

Petroleum Times Vol. 59, No. 1518, 1519, October 14th, 1955

pp. 1051-1054, October 28th, pp. 1103-5

"Atomization of Liquids"

H. A. Troesch

Engineers Digest, Vol. 16

"Die Zerstaeubung Von Fluessigheiten"

H. A. Troesch

Chemie Ingenieur-Technik, Vol. 26, No. 6, June 1954, pp. 311-320

"Fuel Spray Investigation at Cranfield"

E. M. Voodger

Petroleum, Vol. 19, No. 11, November 1956, pp. 387-392

"Measuring Rate of Fuel Injection in Operating Diesel Engine"

R. J. Wehrman, H. R. Mitchell, W. A. Turunen

Soc. Automotive Engineers - Trans. Vol. 61, 1953, pp. 542-552

"Effect of Fuel Viscosity on Injection Equipment"

J. C. Whithers

Gas and Oil Power, Vol. 45, No. 537, June 1950, pp. 146-148

"Spray Combustion and ATomization"

F. A. Williams

Physics of Fluids, Vol. 1, No. 6, November/December, 1958, pp.541-545

"Photographic Analysis of Sprays"

York and Stubbs, 1952

Trans. A.S.M.E. Vol. 74, No. 7 (October, 1952) pp. 1157-1162

PUBLICATIONS

The work described in Chapter VI was thought to be original enough for publication. A concise version was accepted by, and read to, the International Congress on High Speed Photography at Zurich in September, 1965.

Reference:-

"The Application of a Double Pass Schlieren System to a Small High Speed Diesel Engine"

D. H. C. Taylor

Paper G-16

Proceedings of International Congress on High Speed Photography, 1965

ACKNOWLEDGEMENTS

The author gratefully acknowledges the encouragement and advice given throughout this work by Dr. P. H. Broadhurst (Loughborough University), Mr. A. J. Glasspoole (Ruston and Hornsby, Limited) and Mr. R. J. North (N.P.L.).

The author also wishes to thank Messrs. K. W. Topley, P. Reynolds, B. Walsham and K. Rainsforth for their continual high standard of craftsmanship shown in manufacturing the various rigs.

Thanks are also due to the Department of Mechanical Engineering of Loughborough University of Technology for facilities to carry out part of the work, and to the Directors of Ruston and Hornsby Limited for further facilities and financial assistance.

TABLE I

Coefficient of discharge of orifice	$c = .7$
Nozzle orifice diameter	$d = .018$ inches
Nozzle orifice length	$L = .07$ inches
Mean injection pressure	$= 6900$ lb/in^2
Mean density of gas	$\rho_g = .00072$ lb/cu.in.
Mean gas pressure	$= 1100$ lb/in^2
Density of fuel oil	$\rho_o = .0308$ lb/cu.in.
Viscosity of fuel oil	$\mu_o = 6$ centistrokes at 80°F
Mean pressure drop across orifice	$\Delta P = 5800$ lb/in^2

TABLE II

Type of films used on small Engine work

Film type (100 ft)	Film Speed	
TRI X Reversal (B & W)	160 ASA	Tungsten light
TRI X Neg. (B & W)	250 ASA	
Plus X Neg (B & W)	64 ASA	
ANSCO D 100 (colour)	100 ASA	Daylight Film
ANSCO D 200 (colour)	200 ASA	

TABLE III

12½-inch Bore Engine Test Results

Type of Combustion	B.M.E.P. lb/in	Speed R.P.M.	Nozzle Configur-ation	Injector period °crank	Max. Fuel pressure lb/in	Specific Fuel Consump'n lb/BHP	Smoke Colour
Original type	200	600	10 holes .018 ins. diameter	26.4	16000	.352	clear
Impinge-ment type	200	600	7 holes .025 ins. diameter	23.2	13000	.340	clear

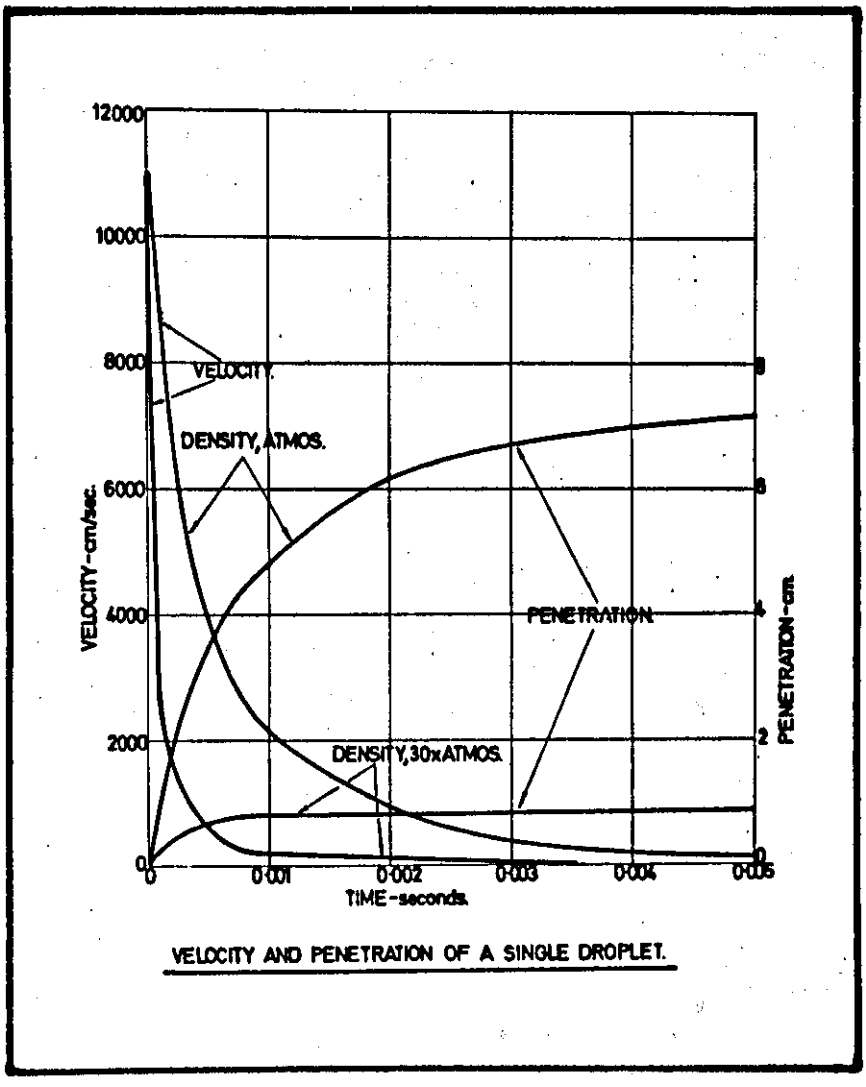

Figure 1 Velocity and penetration of a single droplet at engine cylinder density. From [8]

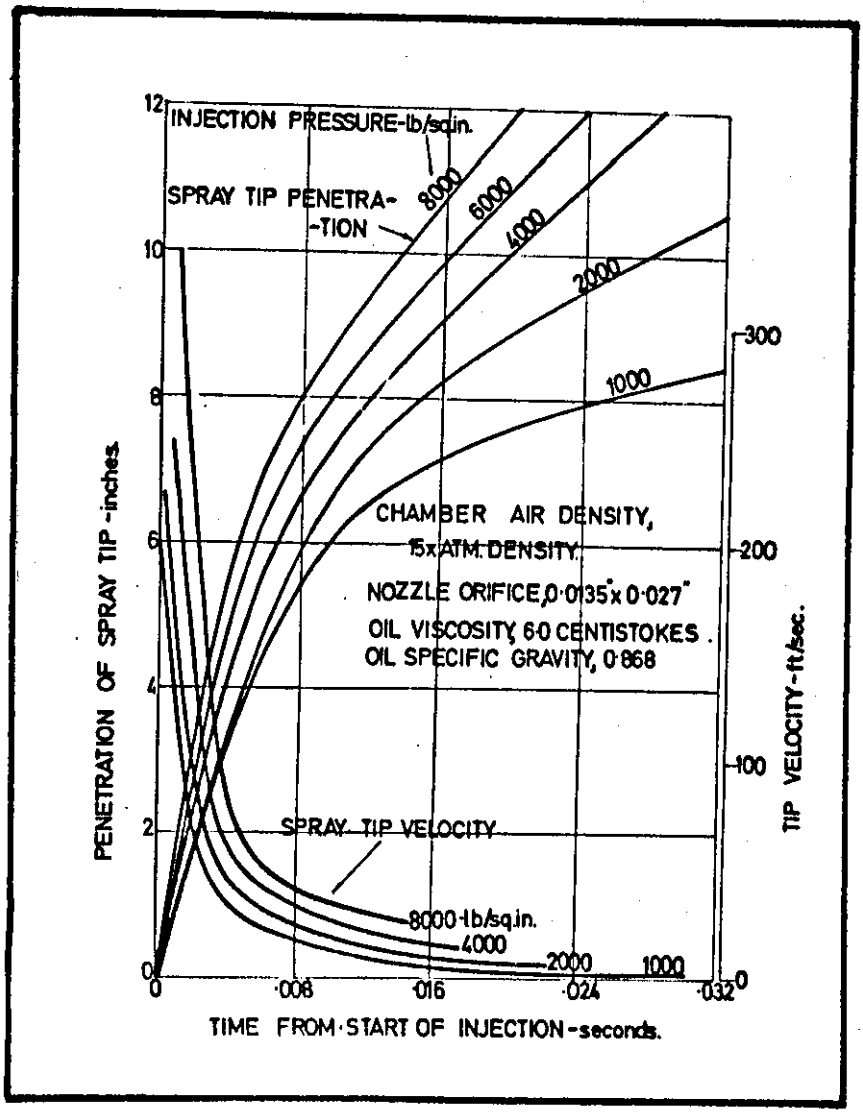

Figure 2 Variation of spray tip velocity and penetration at various injection pressures. [3]

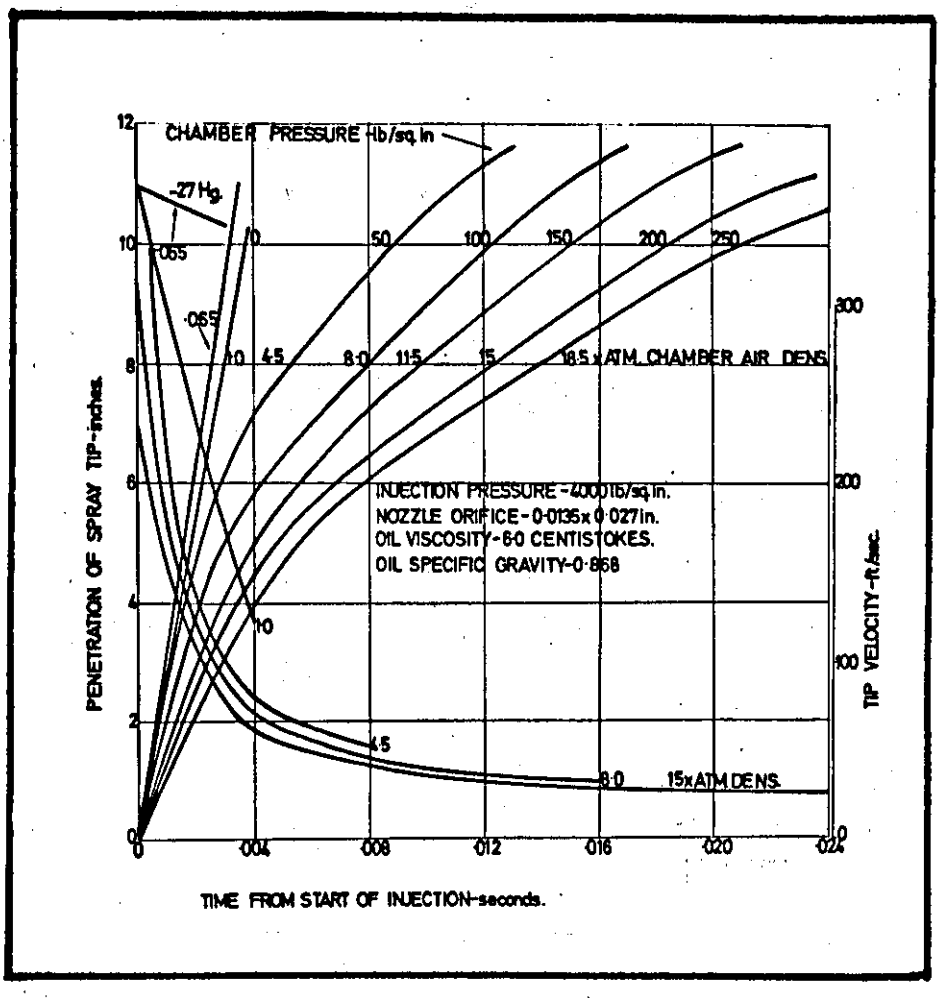

Figure 3 Variation of spray tip velocity and penetration at various chamber air densities.[3]

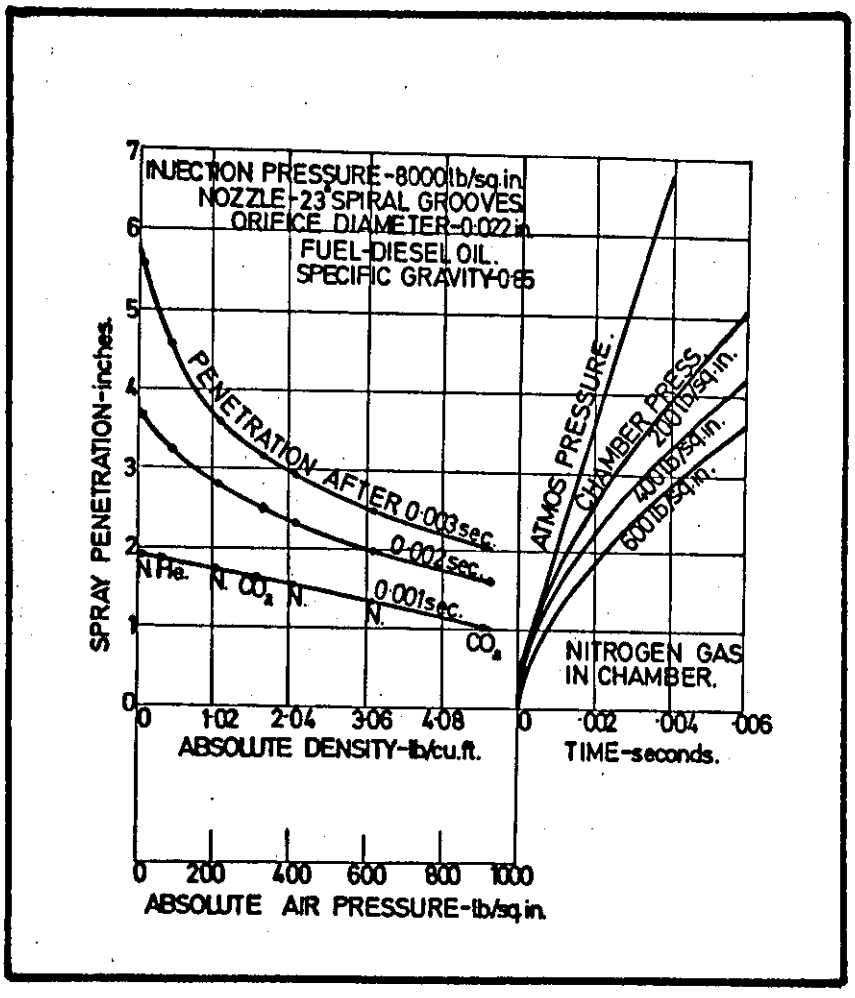

Figure 4 Effect of gas density on spray penetration, gas in chamber: Nitrogen, carbon dioxide and helium. [6]

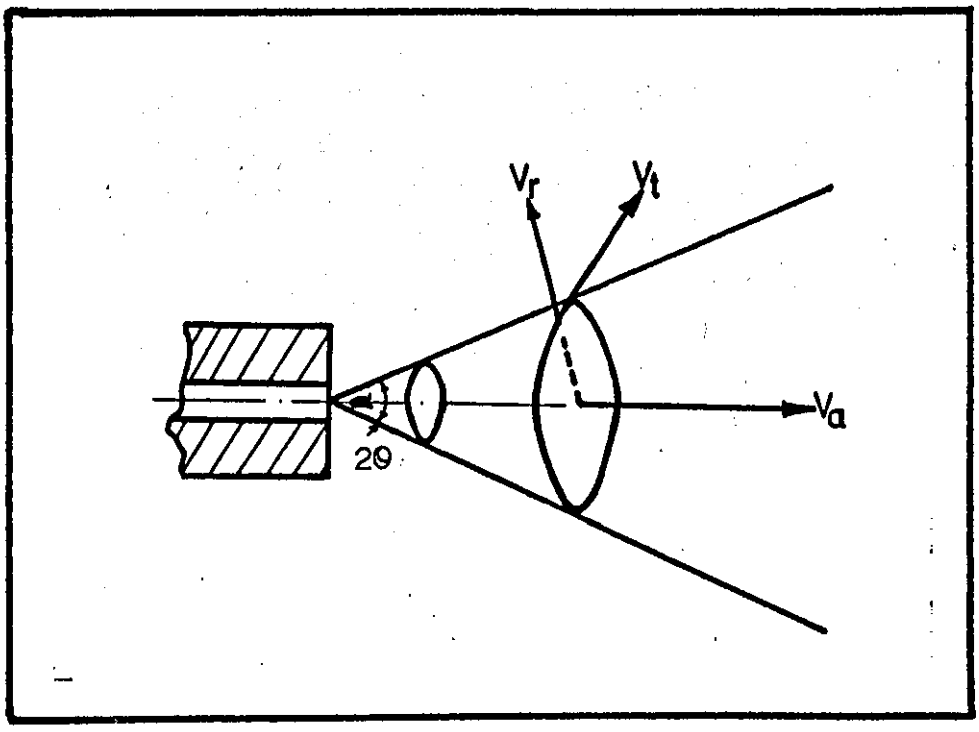

Figure 5 Diagram of velocities imparted to the fuel by the nozzle.

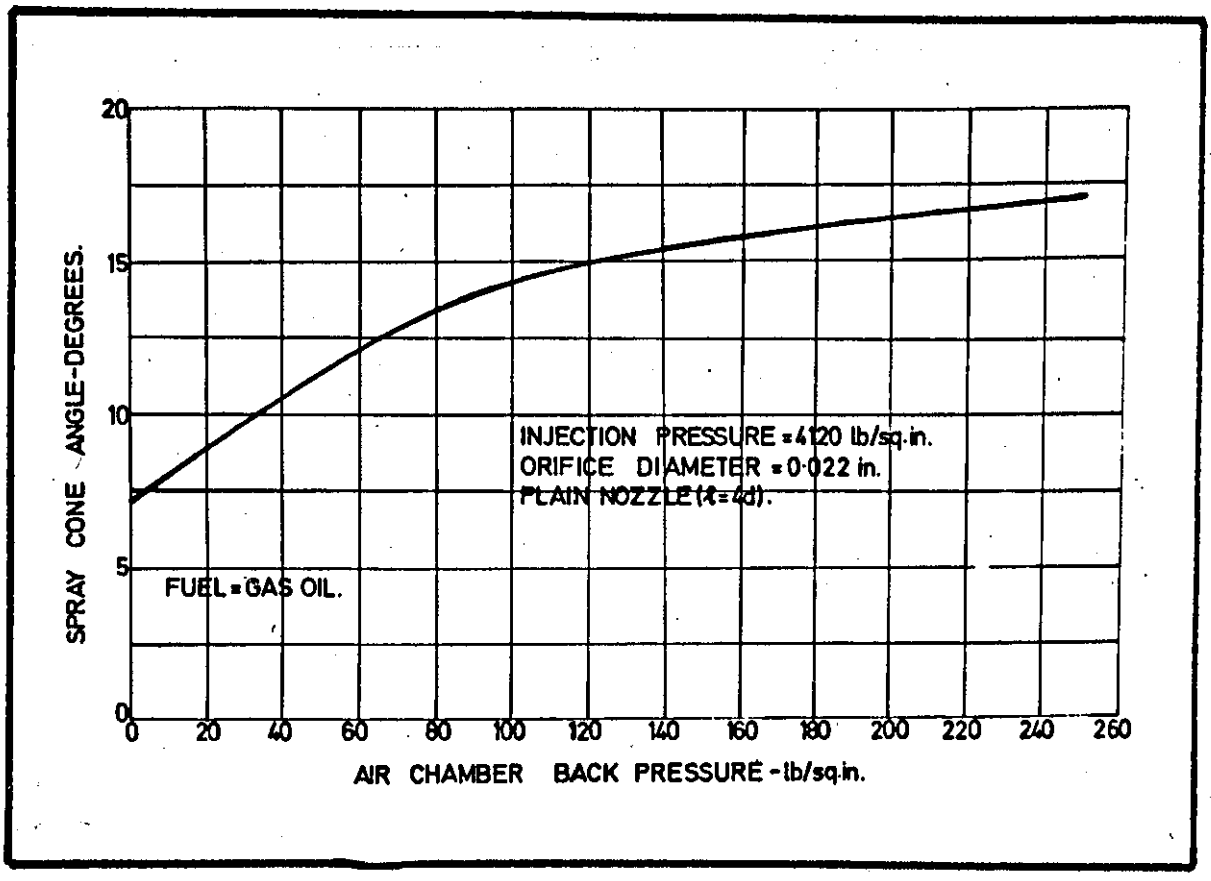

Figure 6 Change in spray cone angle with air pressure. [7]

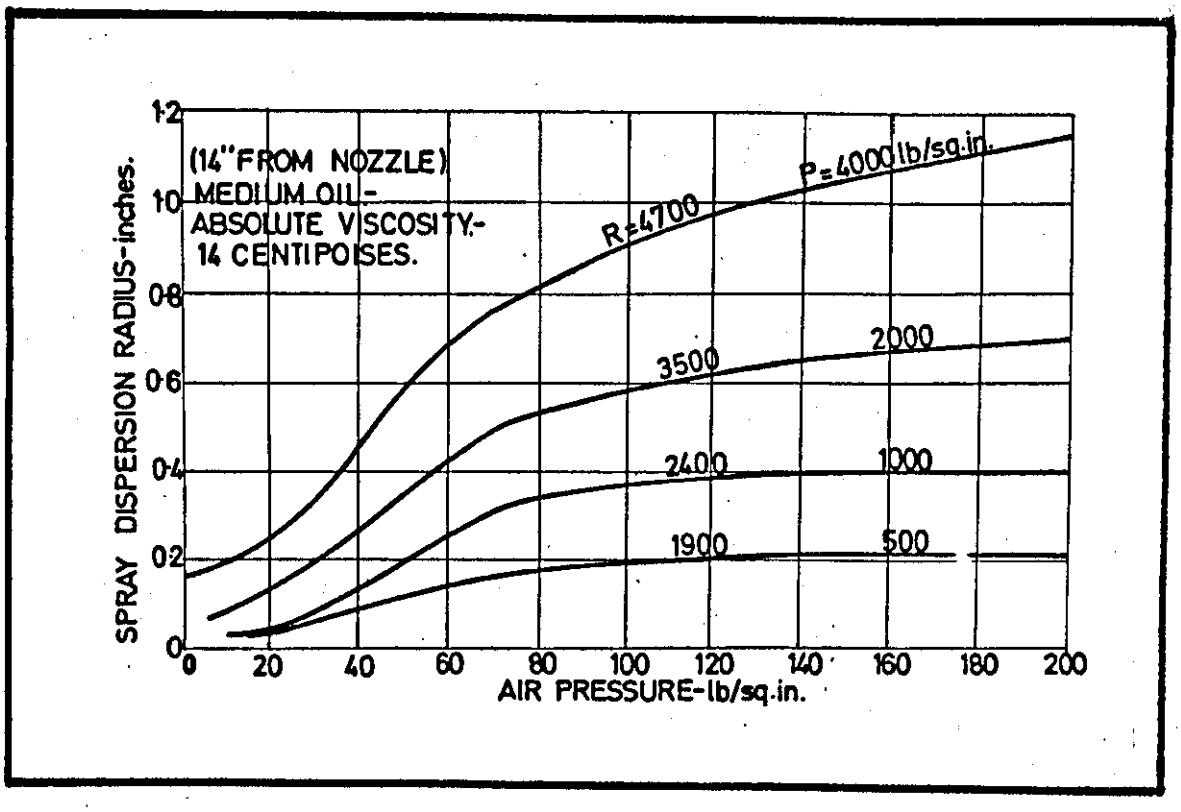

Figure 7 Dispersion radius of a spray with various chamber air pressures.

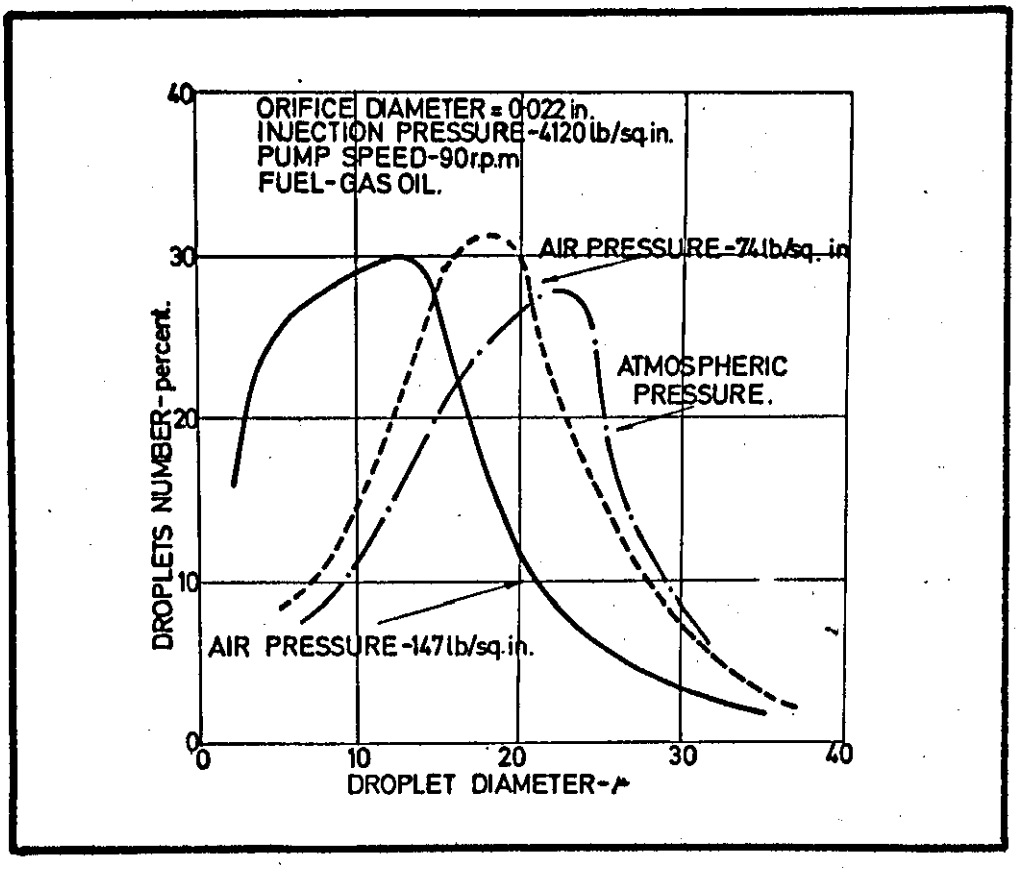

Figure 8 Effect of air density on atomisation.[8]

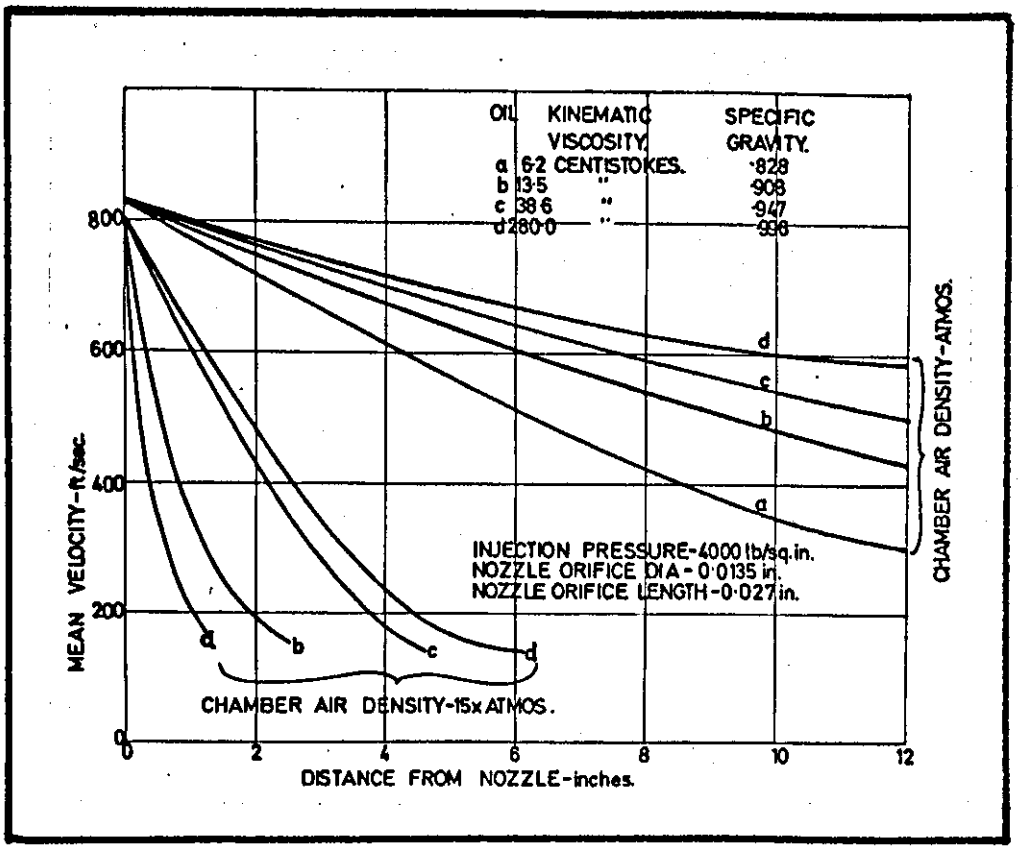

Figure 9 Effect of oil viscosity on penetration.[9]

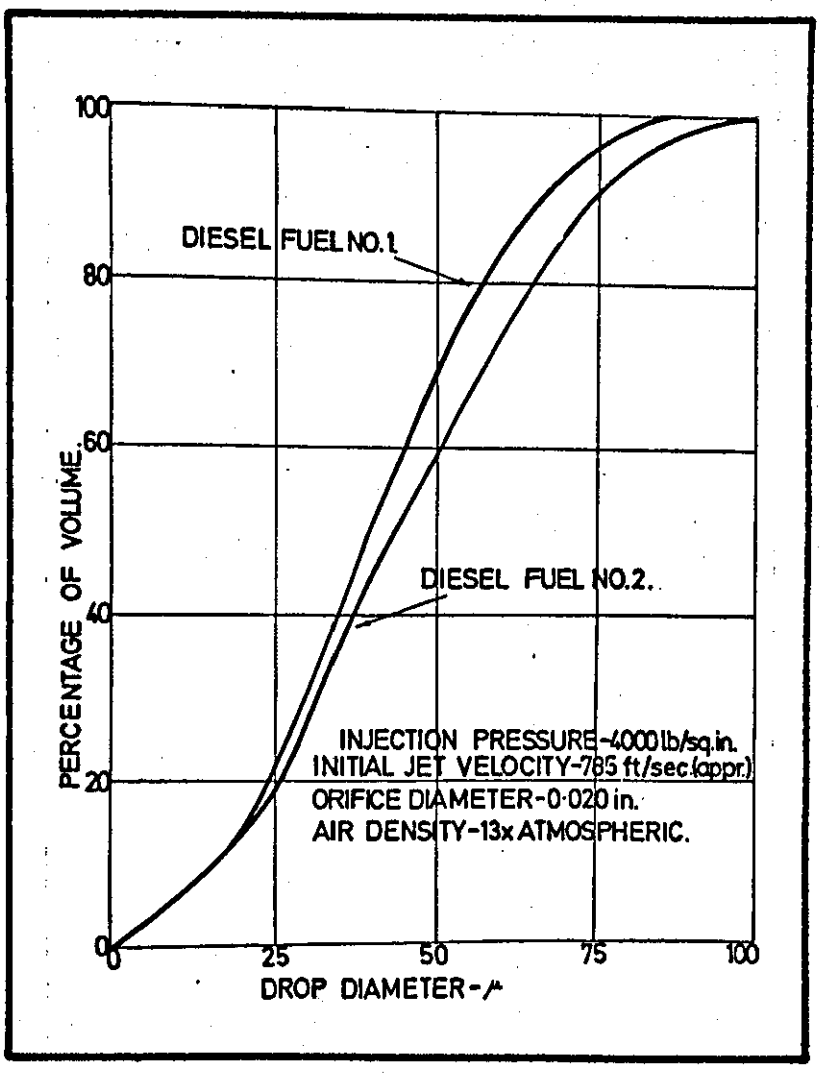

Figure 10 Effect of fuel viscosity on the fineness of atomisation.

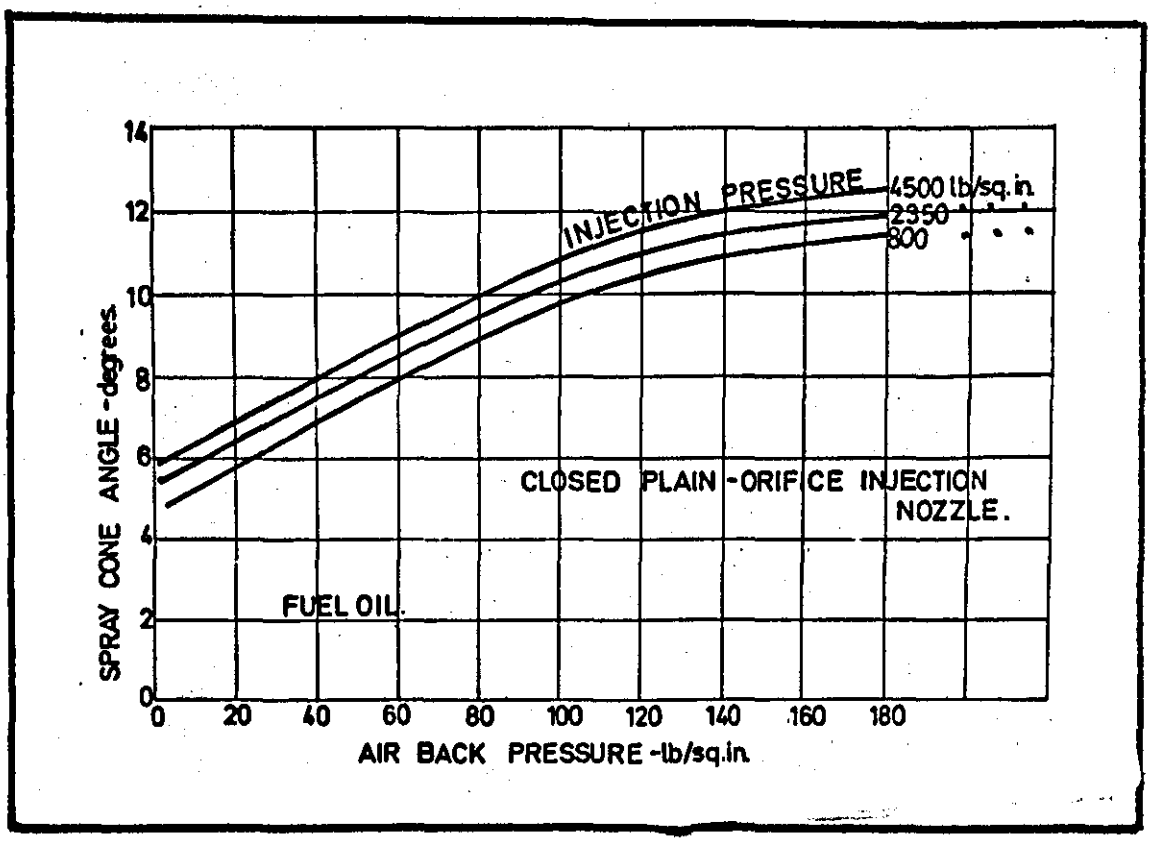

Figure 11 Change in spray cone angle with back pressure at various injection pressures.[13]

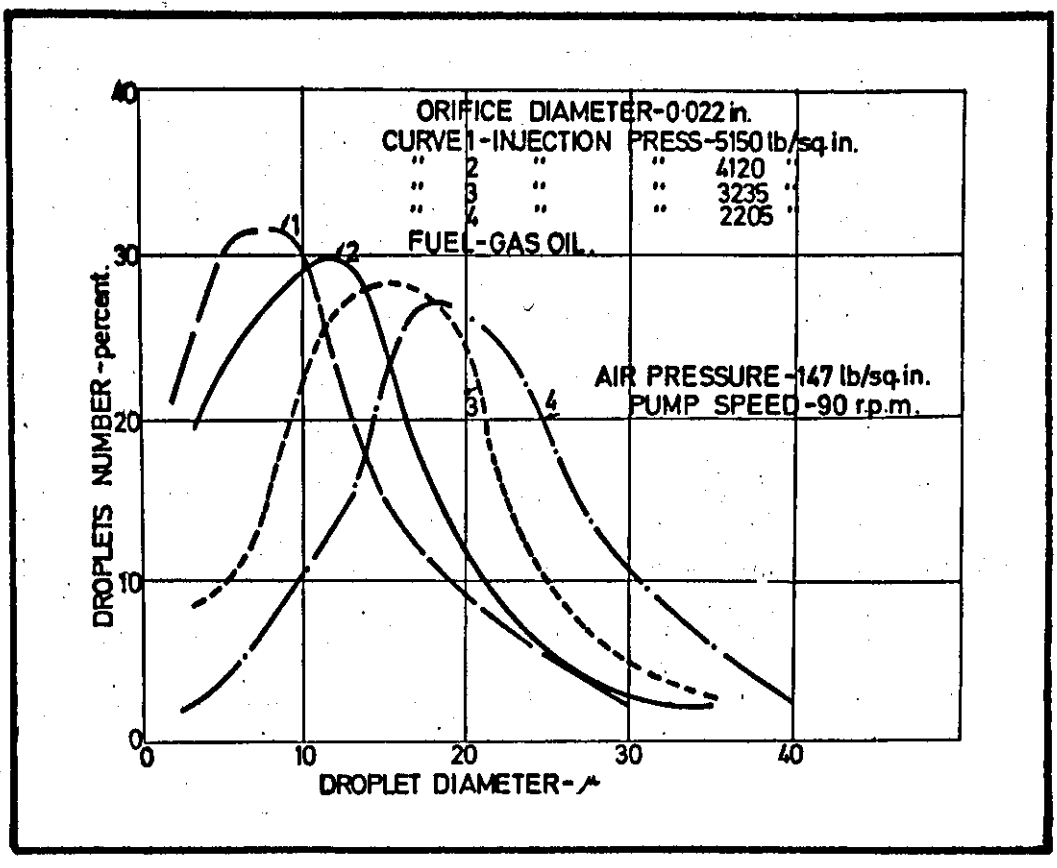

Figure 12 Effect of injection pressure on atomisation.[7]

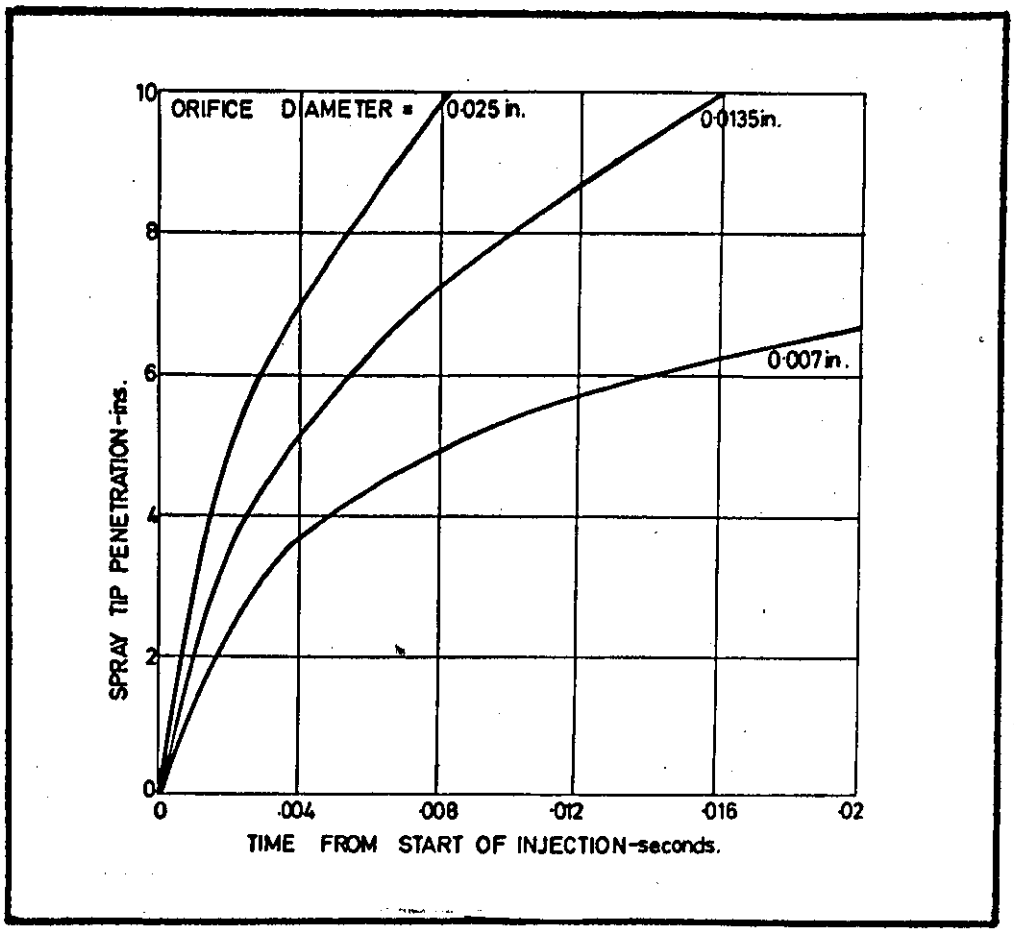

Figure 13 Variation of spray tip penetration with orifice diameter. [9]

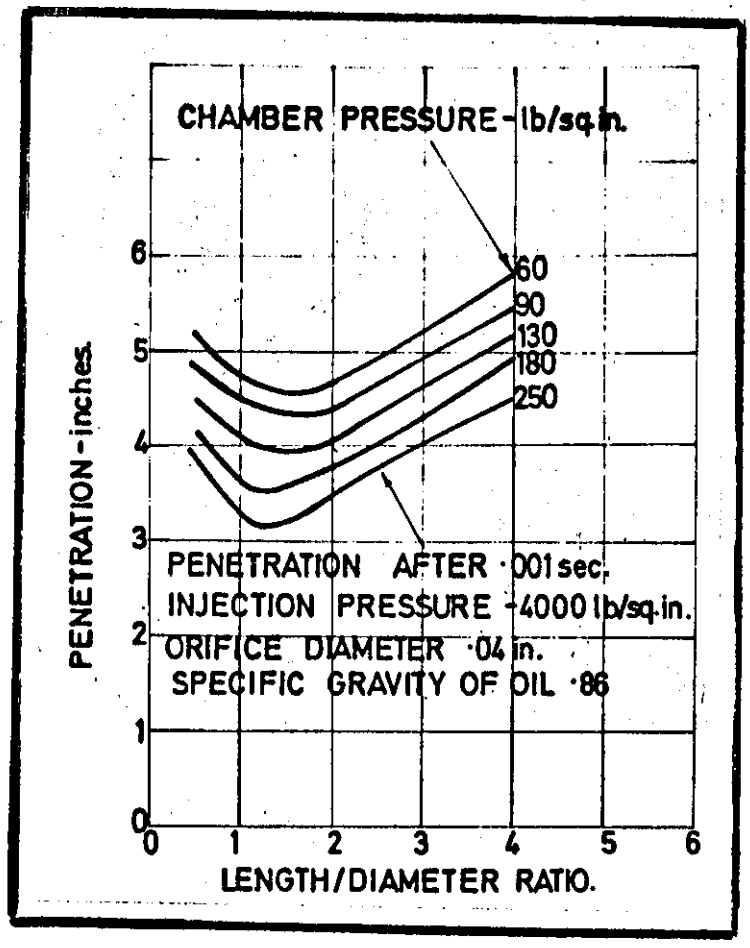

Figure 14 Effect of length/diameter ratio on spray penetration.

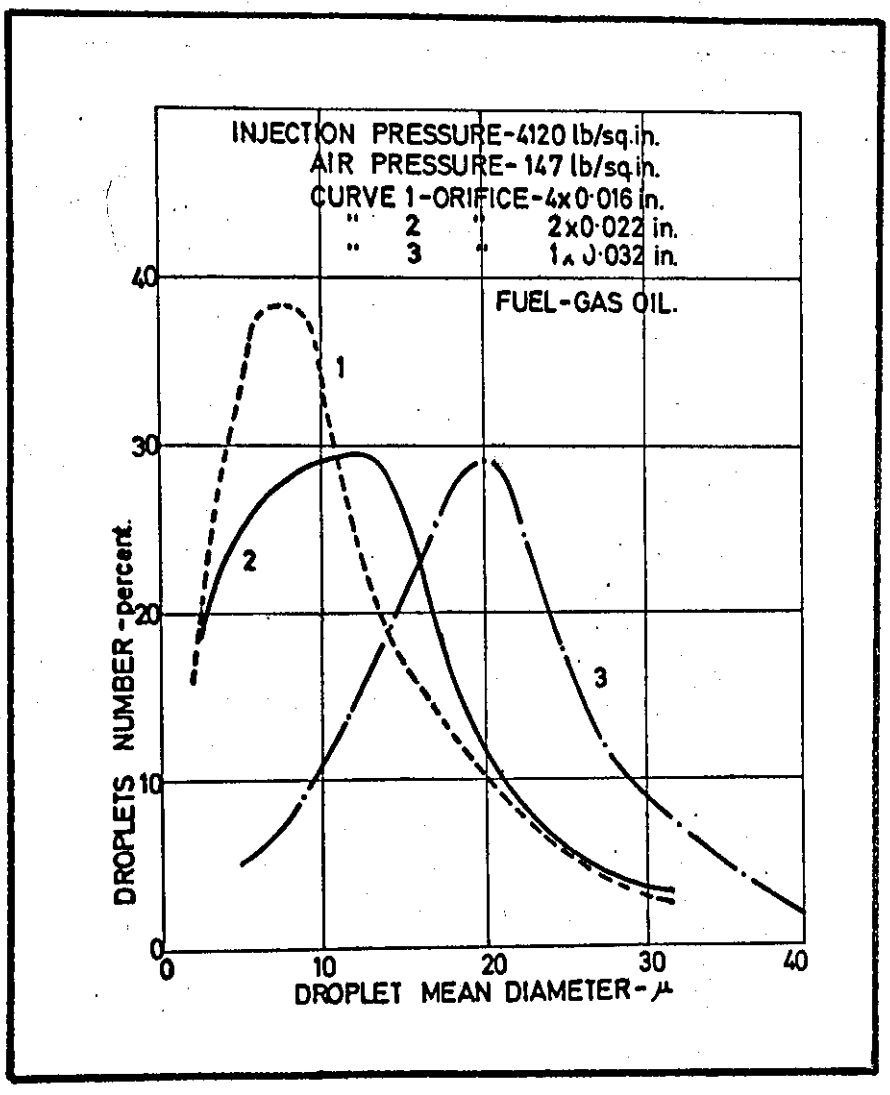

Figure 15 Effect of orifice diameter on atomisation.[7]

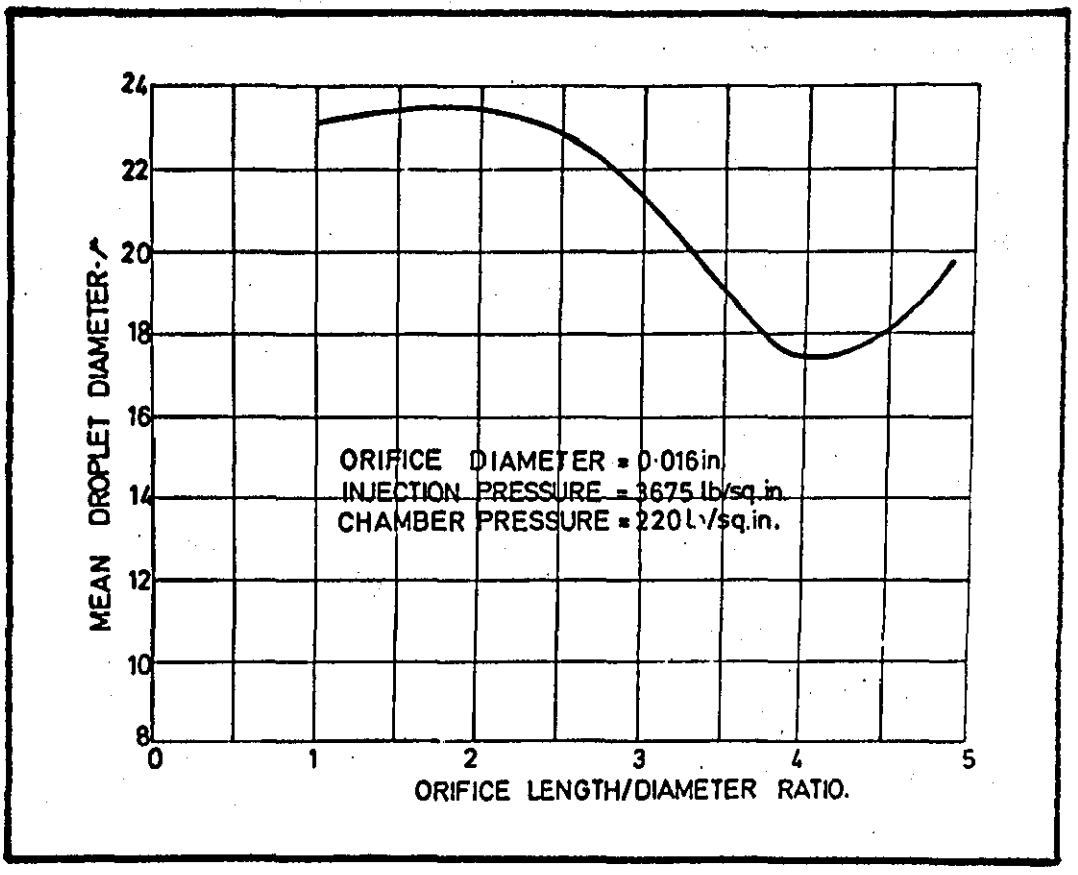

Figure 16 Effect of orifice length/diameter ratio on mean droplet size. [16]

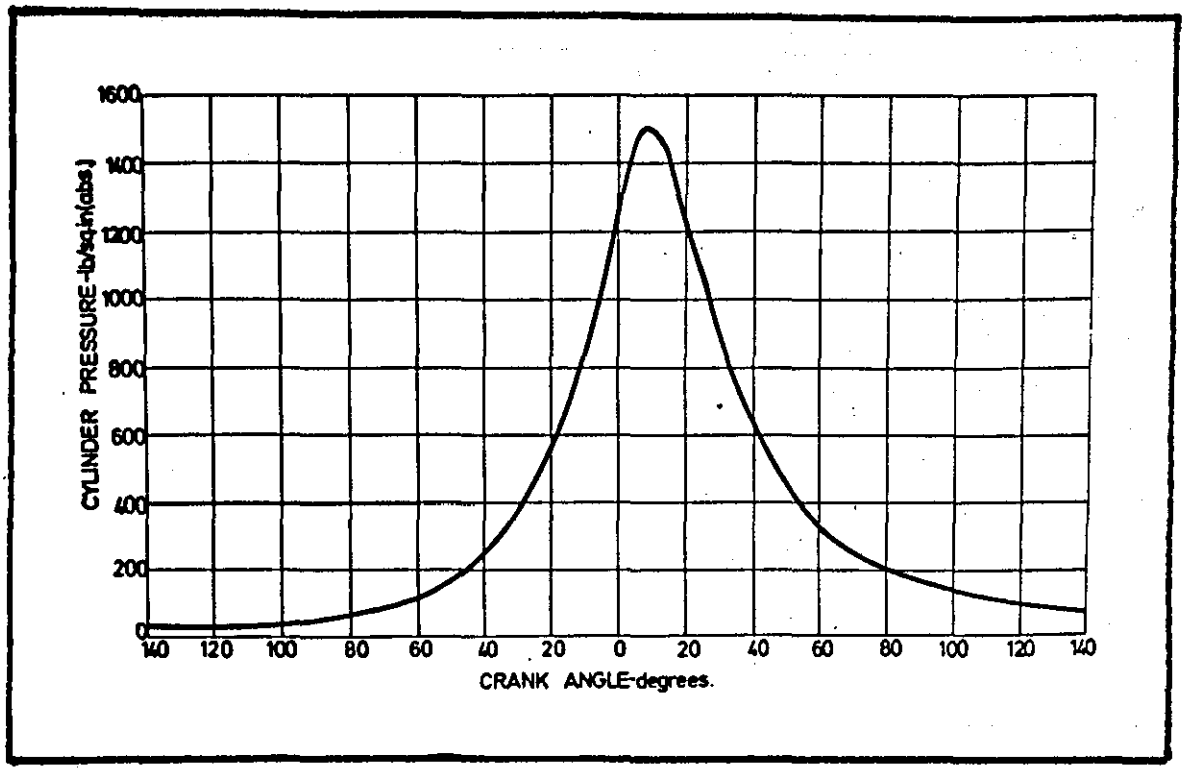

Figure 17 Cylinder pressure V crankangle diagram for 12" bore engine.

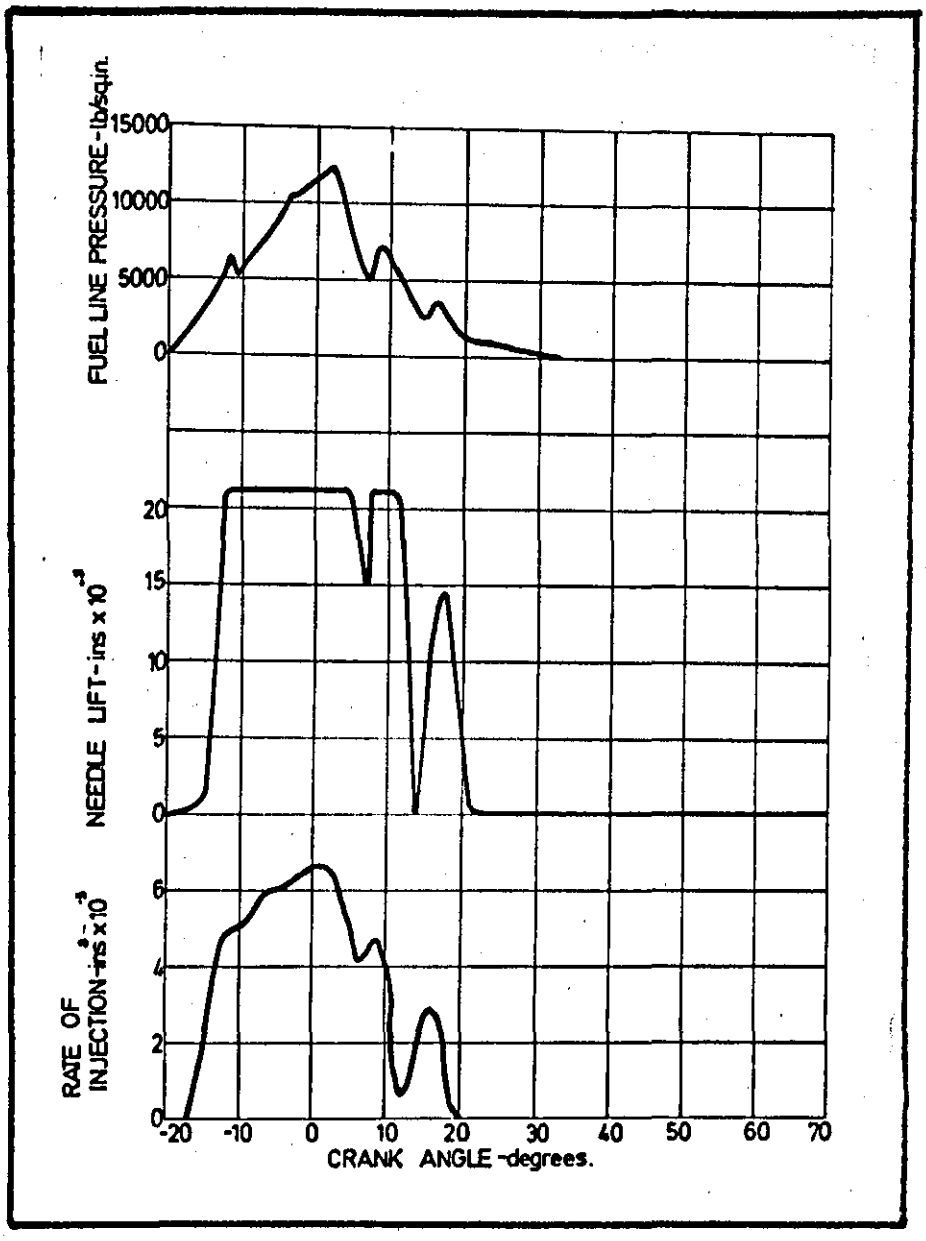

Figure 18 Fuel injection pressure, needle lift and rate of injection for 12" bore engine.

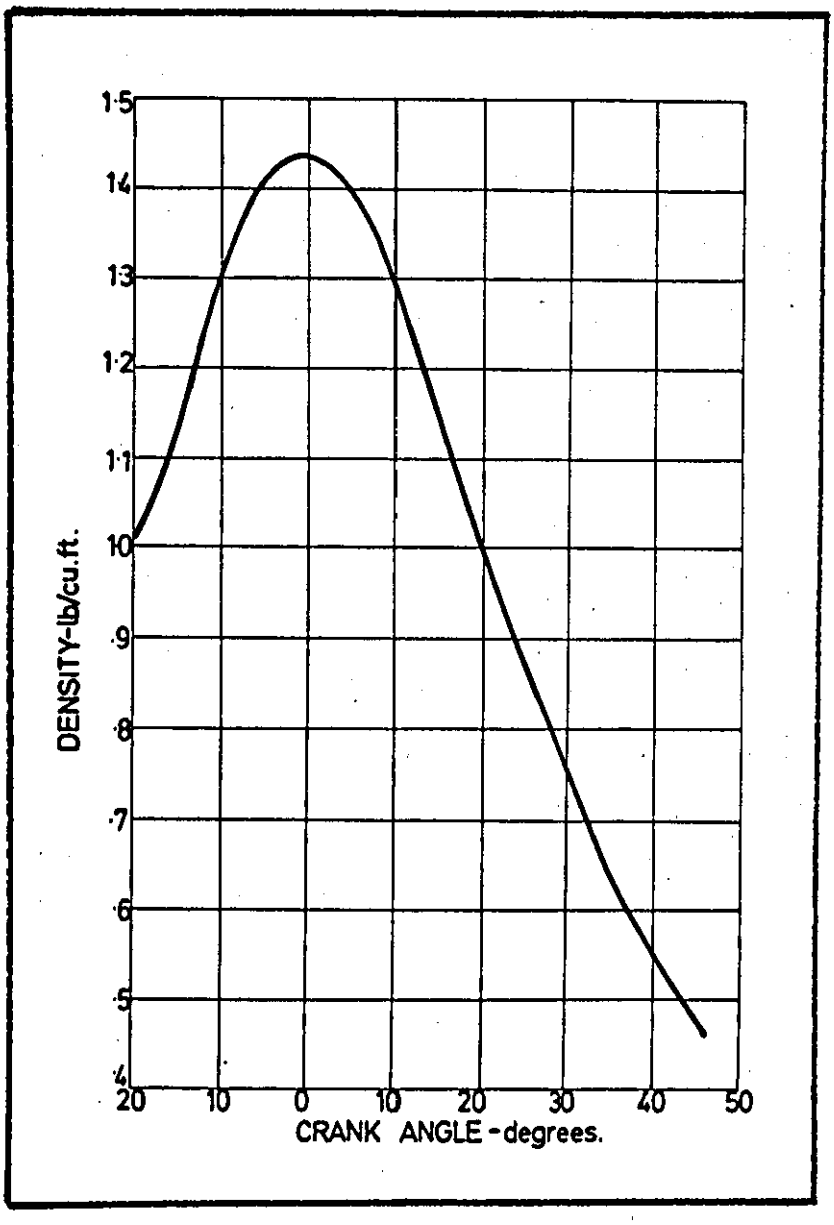

Figure 19 Calculated variation in cylinder density for 12" bore engine

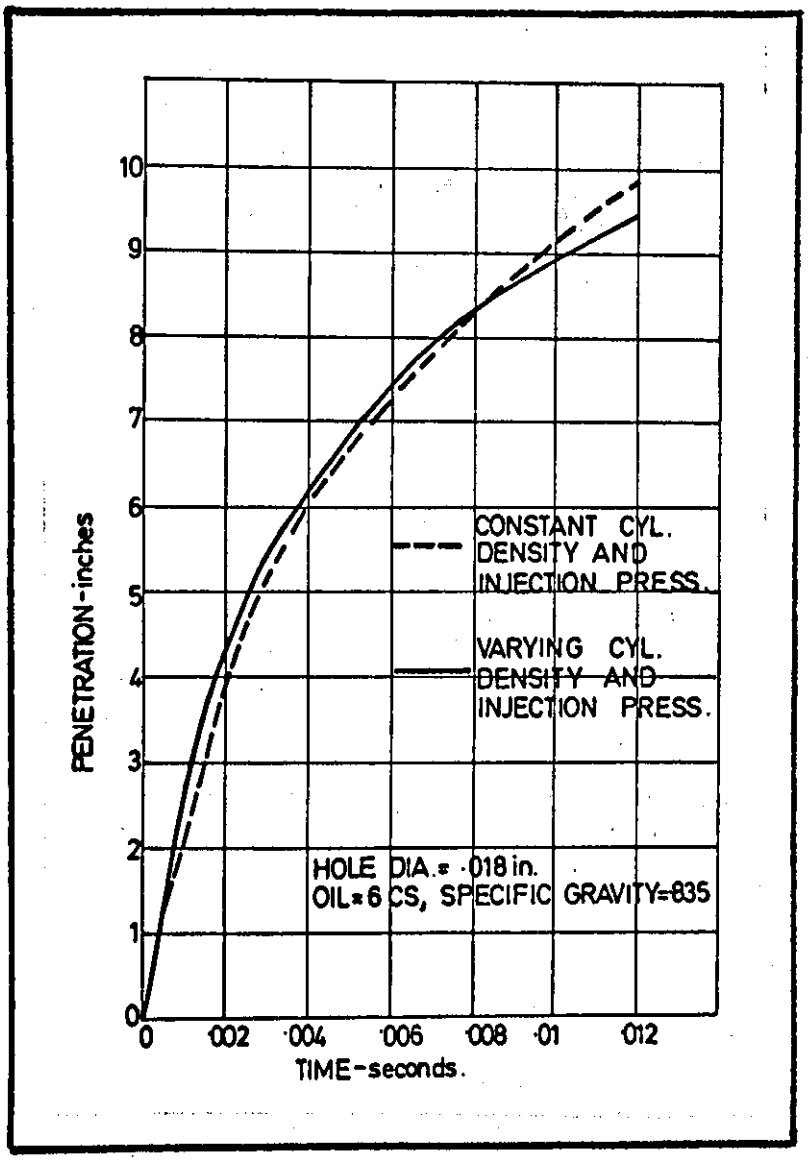

Figure 20 Comparison of spray penetration using time mean pressures and densities, and actual variations as per Schweitzer.

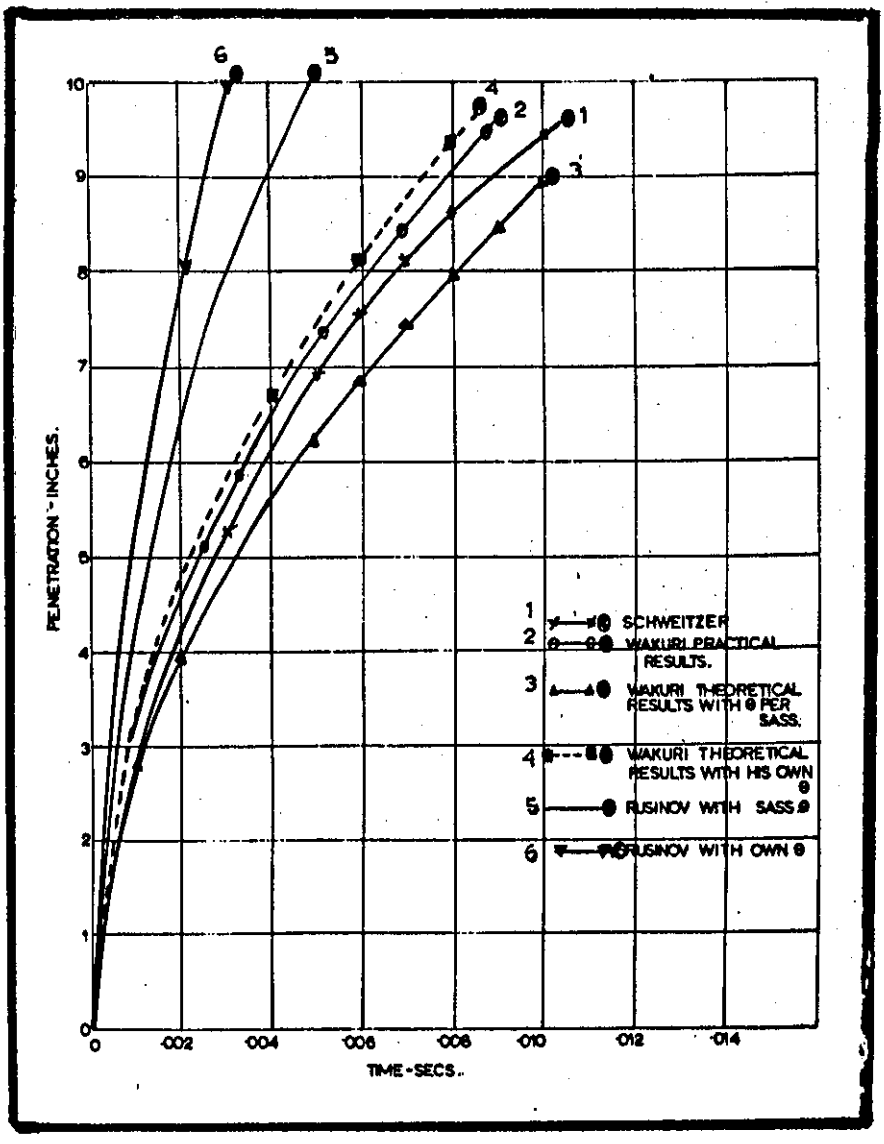

Figure 21 Comparison of calculated fuel spray penetration by various workers.

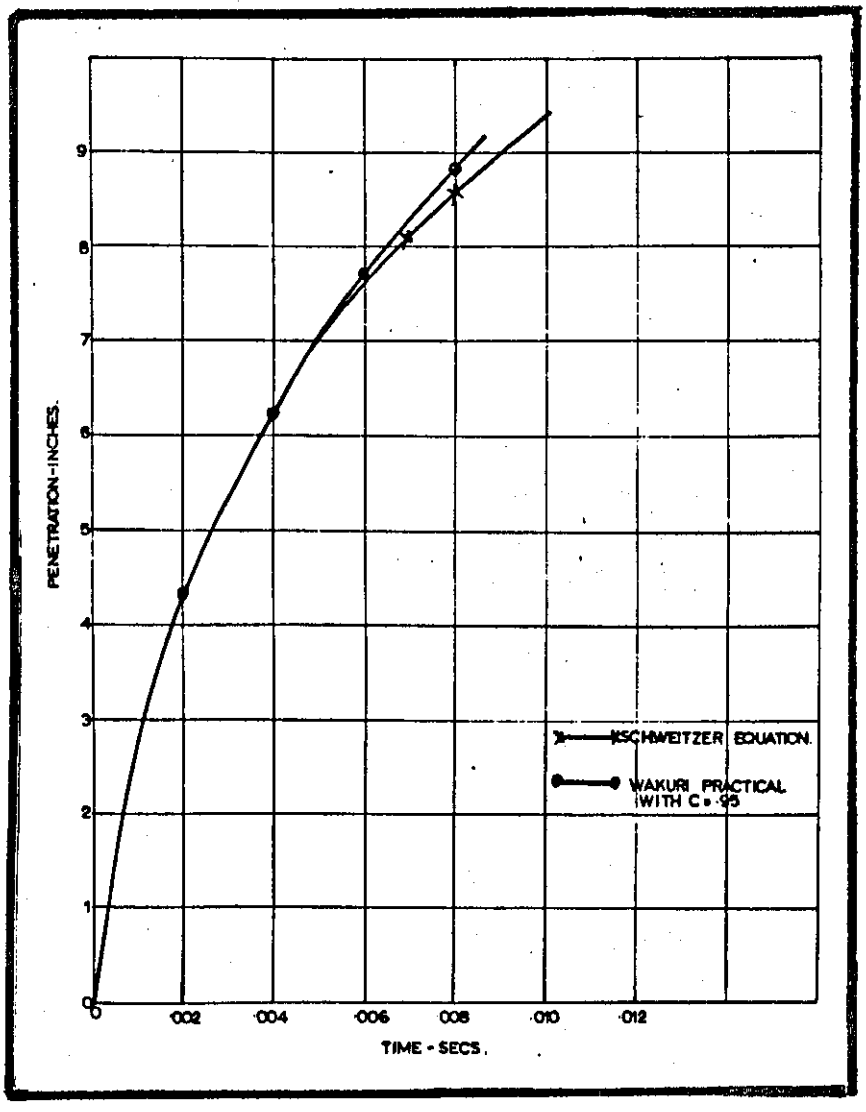

Figure 22 Comparison of equations derived by Wakuri [15]. and Schweitzer [9].

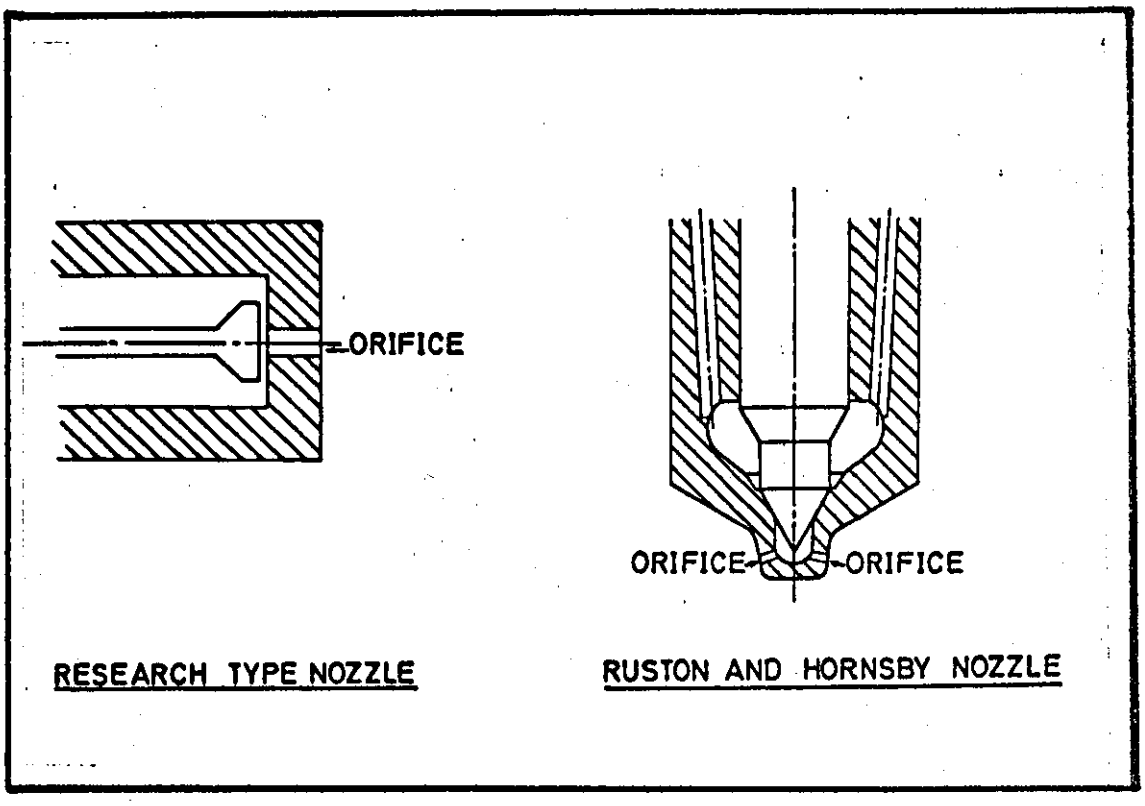

Figure 23 Comparison of a normal diesel injector with the type of nozzle used by Schweitzer.

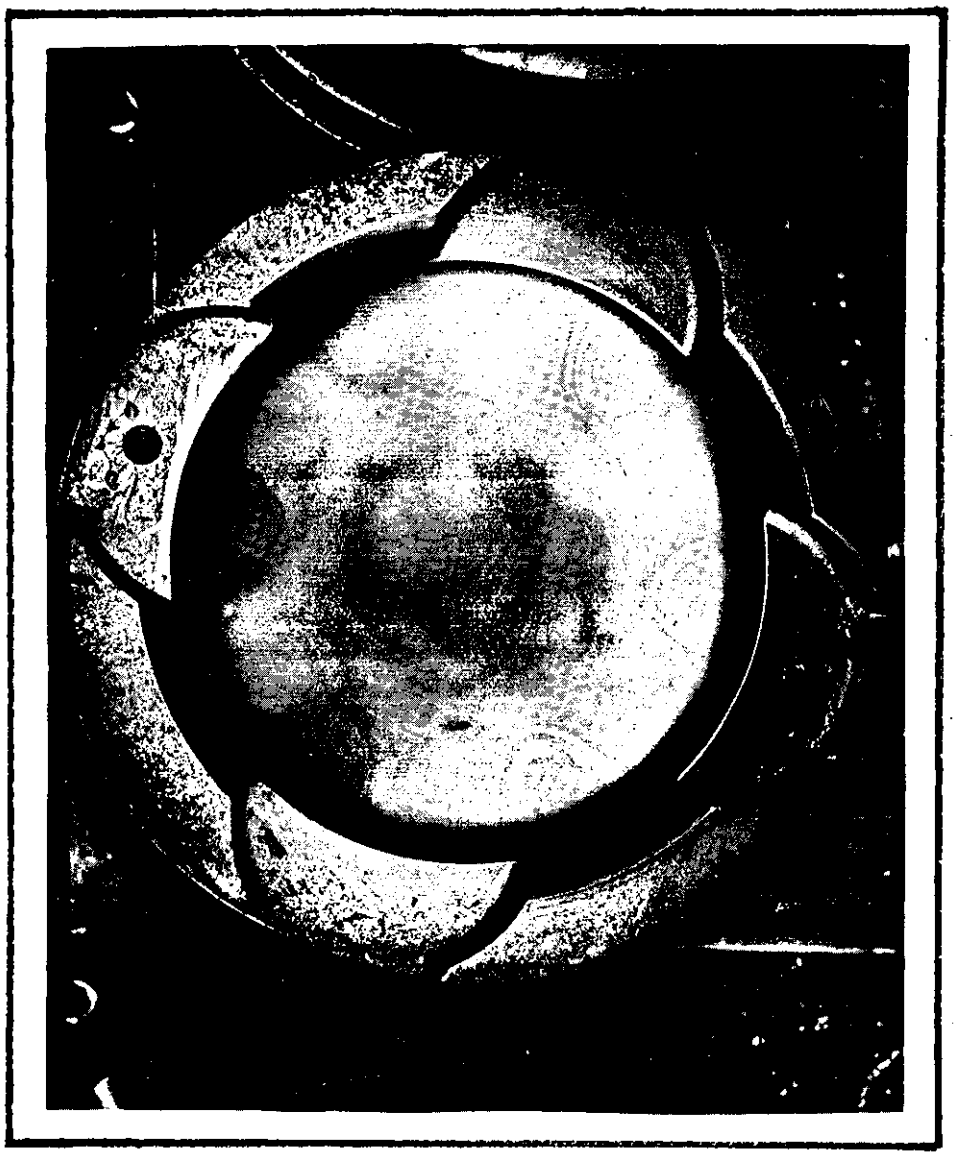

Figure 24 Spray impingement markings on AT type engine piston.

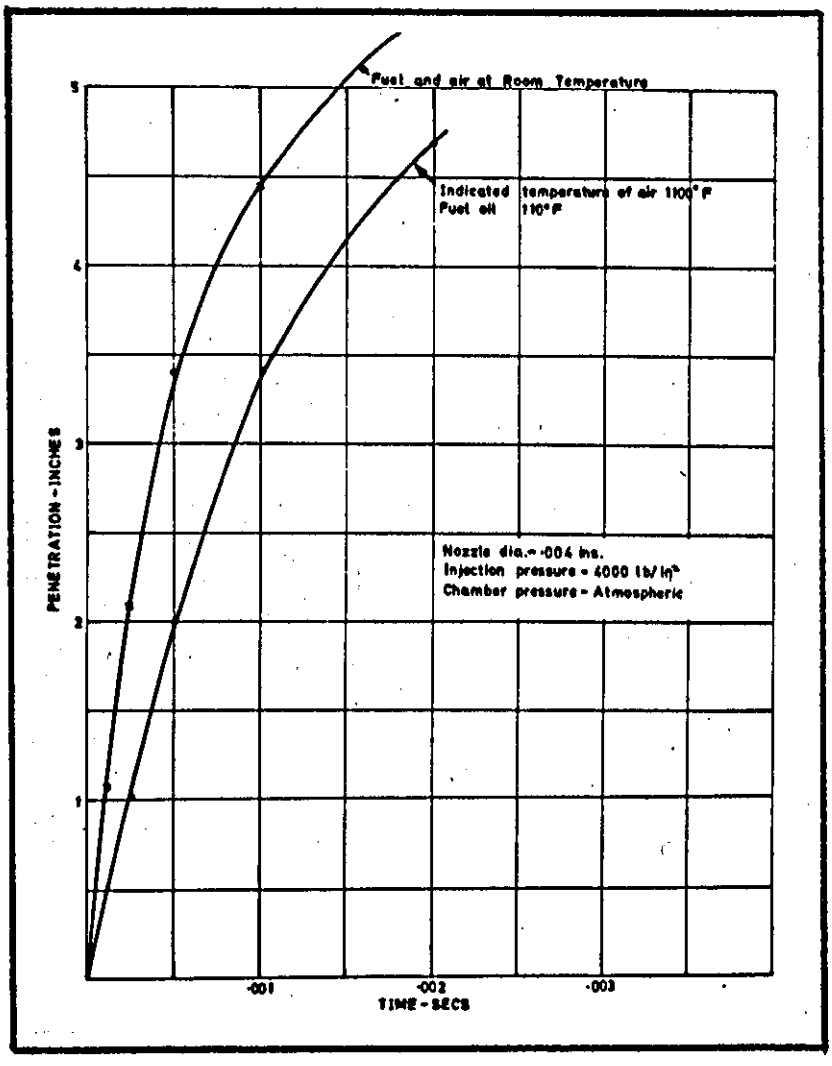

Figure 25 Effect of evaporation according to Gelalles [32].

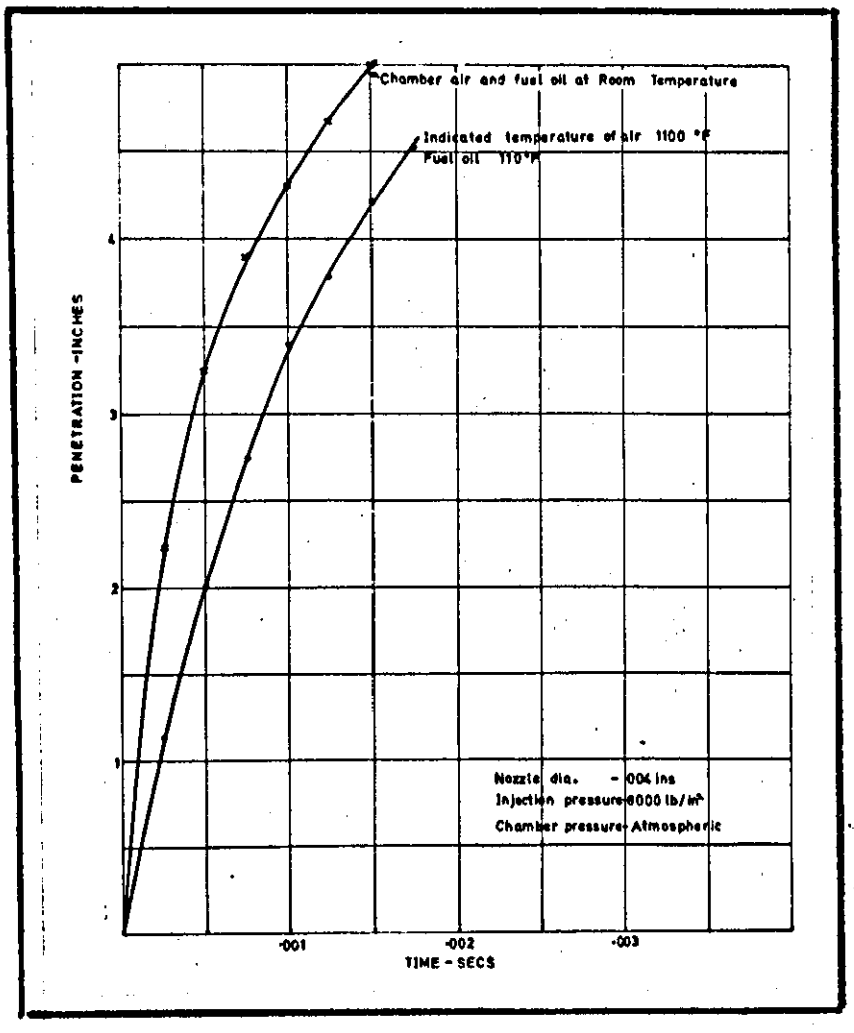

Figure 26 Effect of evaporation according to Gelalles [32].

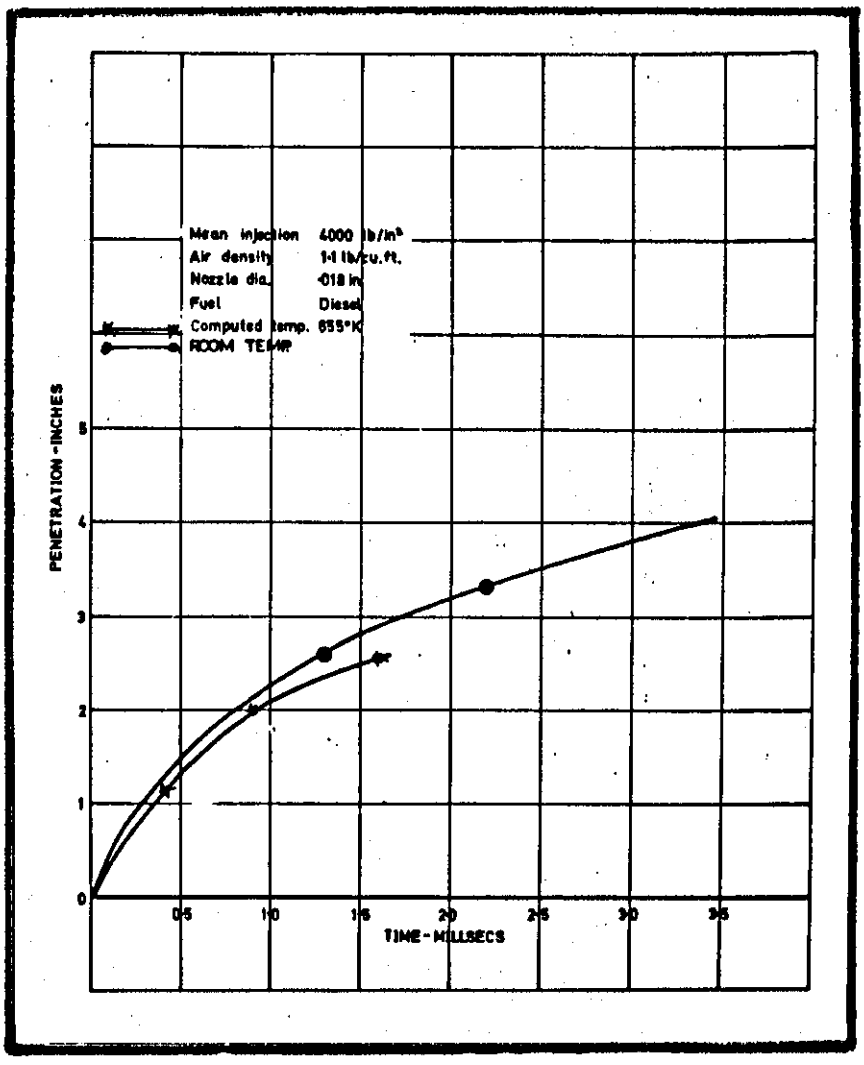

Figure 27 Effect of evaporation according to Rothrock [31].

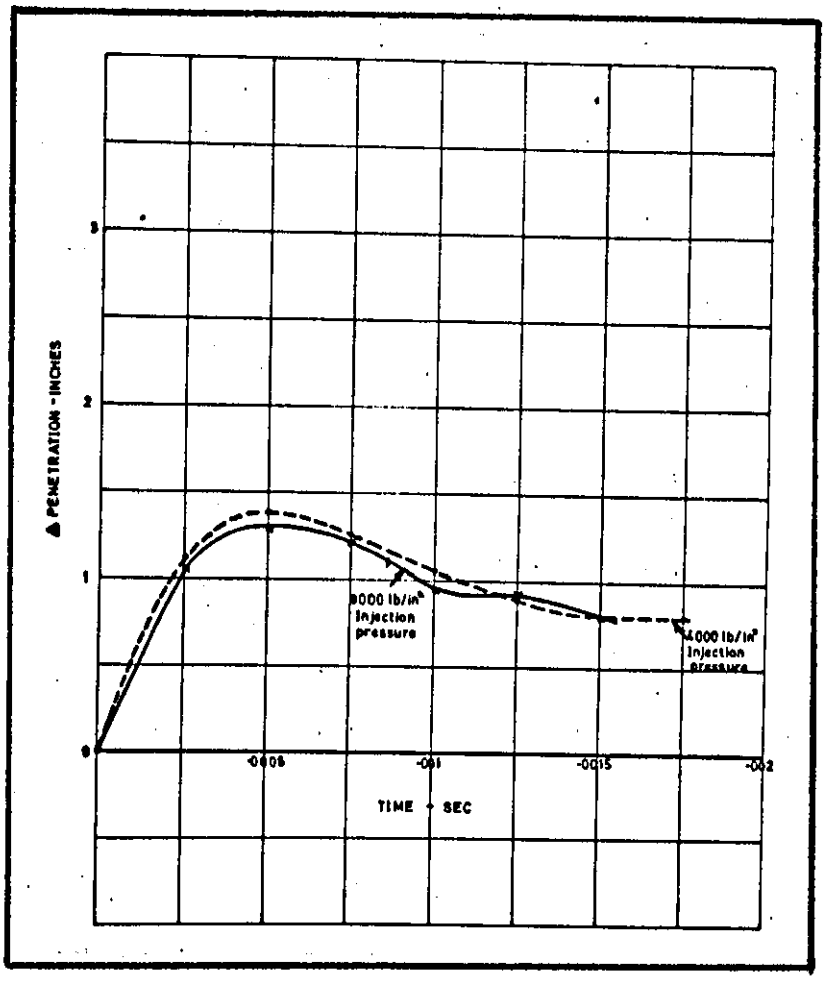

Figure 28 The effect of injection pressure on spray penetration from Gelalles. [32]

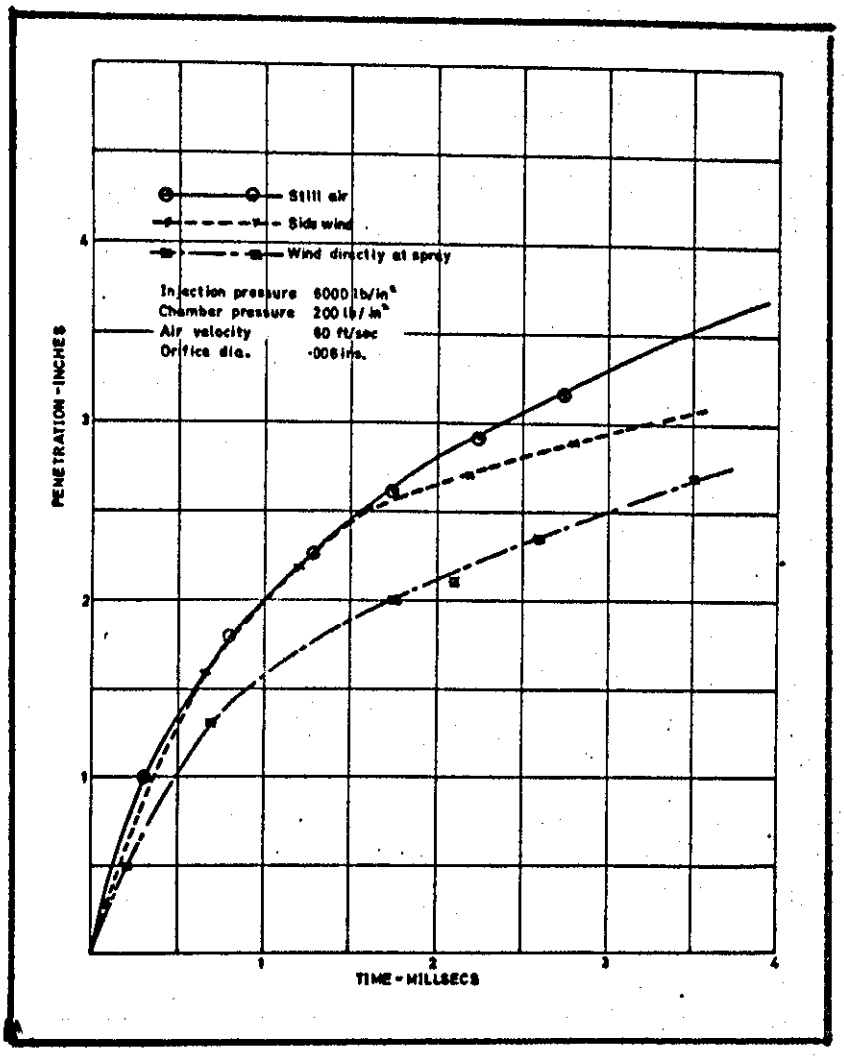

Figure 29 Effect of air motion on spray penetration plotted from Rothrock [34].

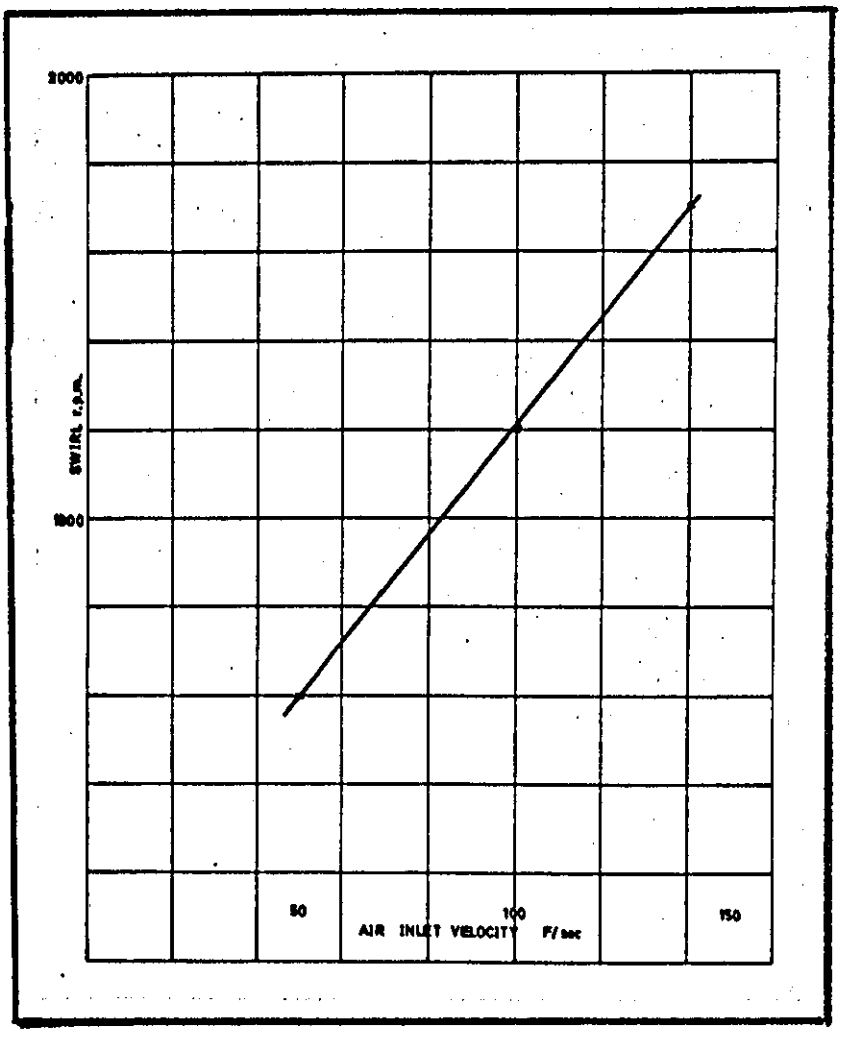

Figure 30 Swirl rate V inlet velocity taken from Tull [41].

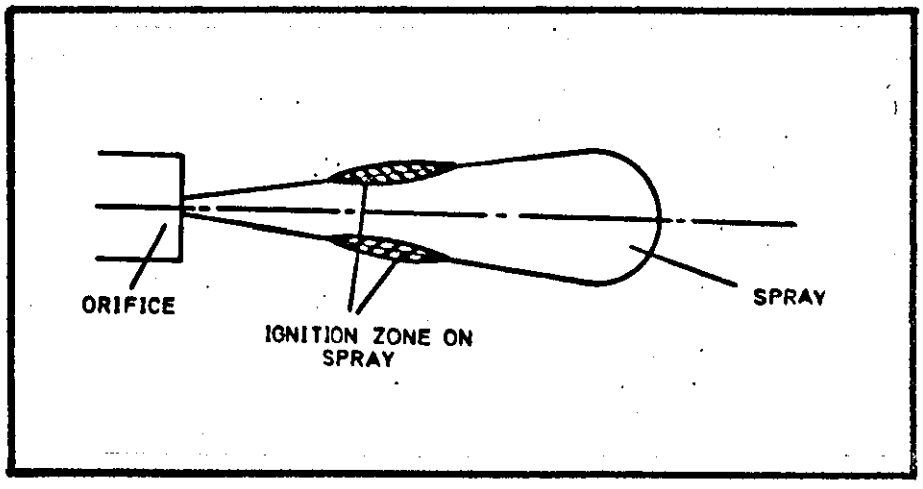

Figure 31 Suggested area of ignition on a fuel spray due to Blume [43].

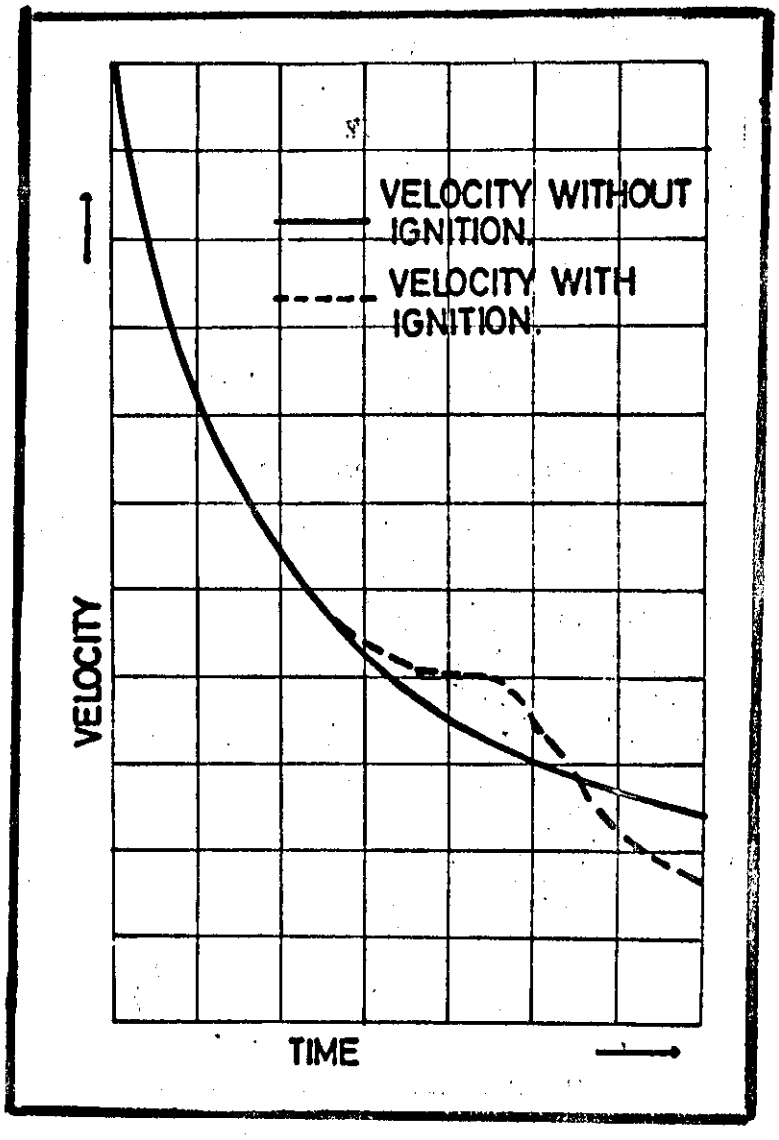

Figure 32 The effect of combustion on spray tip velocity taken from Holdfelder [33].

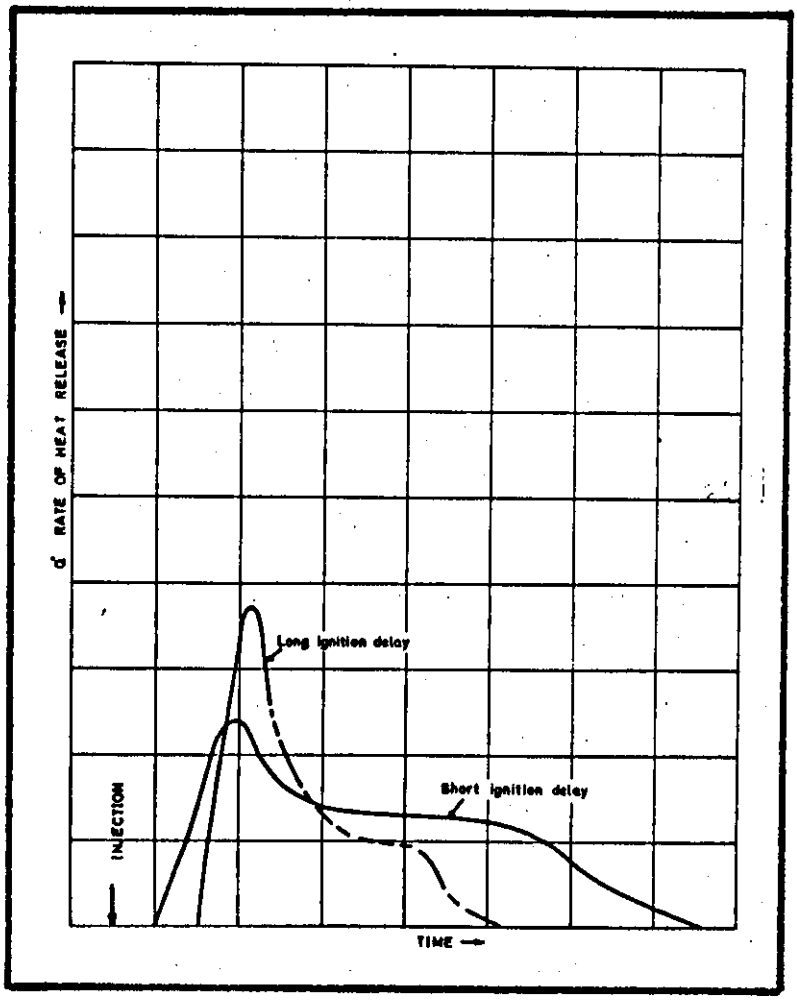

Figure 33 The effect of length of ignition delay on heat release Broeze [42].

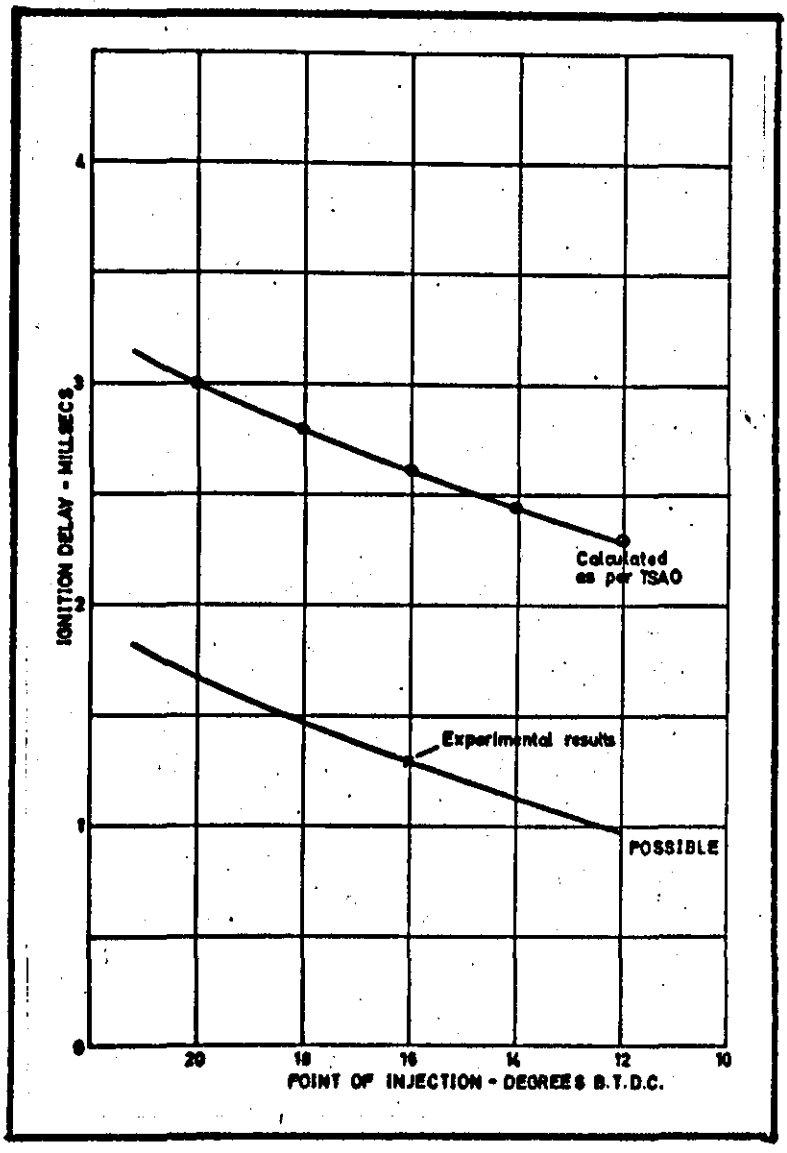

Figure 34 Calculated ignition delay for $12\frac{1}{2}$" bore engine using Tsao's work [49].

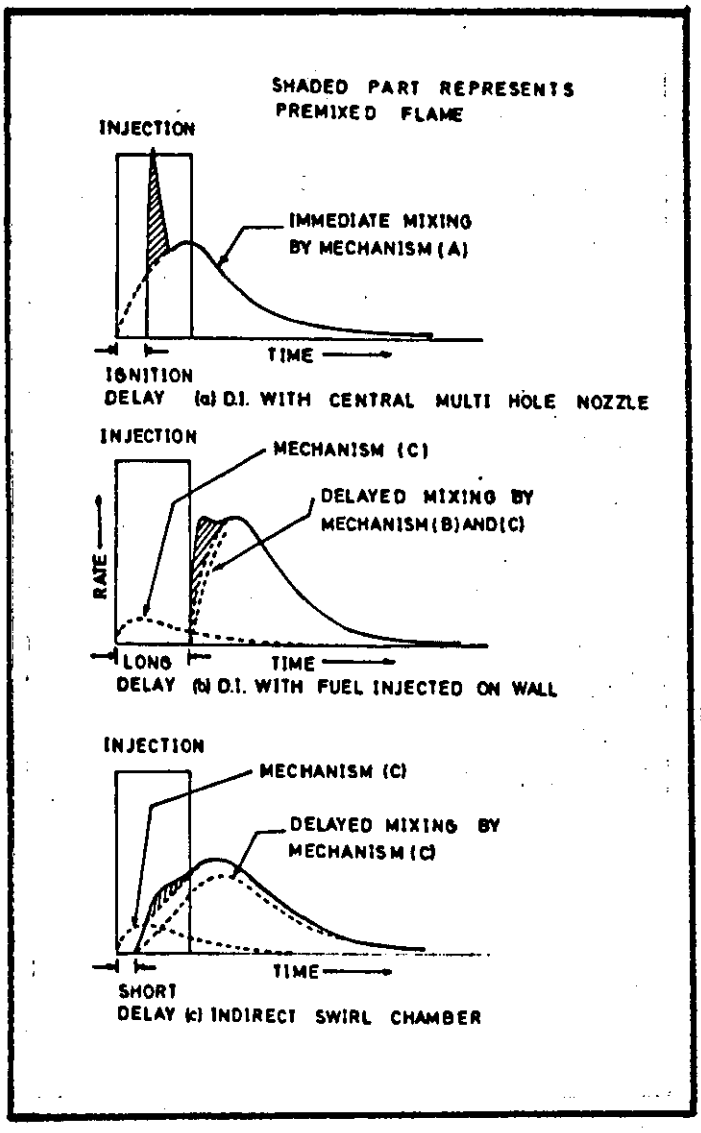

Figure 35 Heat release rates calculated from pressure diagram of various types of engine. Lyn [62].

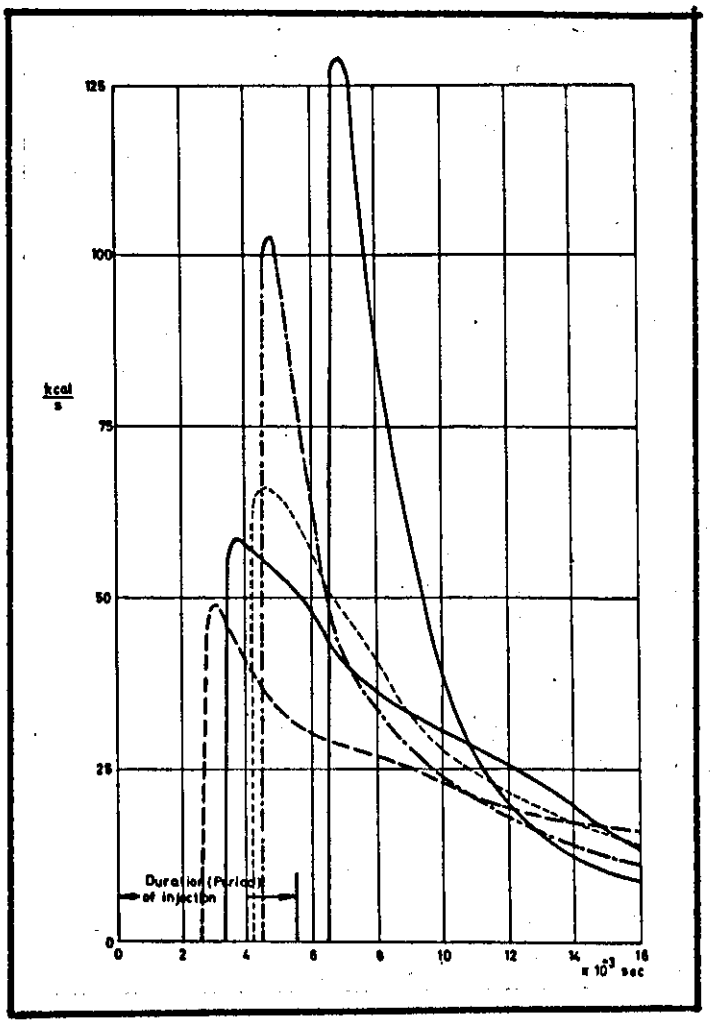

Figure 36 Heat release rates calculated from constant volume bomb results of Blume [43] with varying ignition delays. Diagram indicates effect of increase in delay period, dashed line through to full line gives increasing ignition delay. Injection period constant.

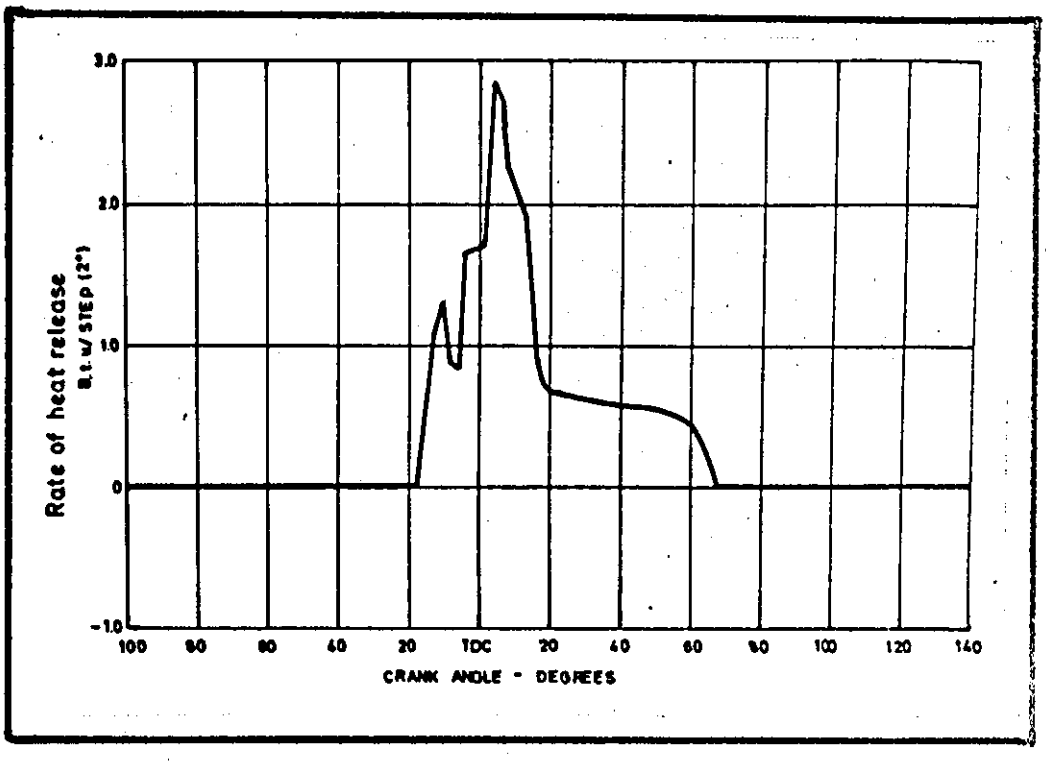

Figure 37 The heat release pattern calculated from the cylinder pressure diagram of a 10" bore engine.

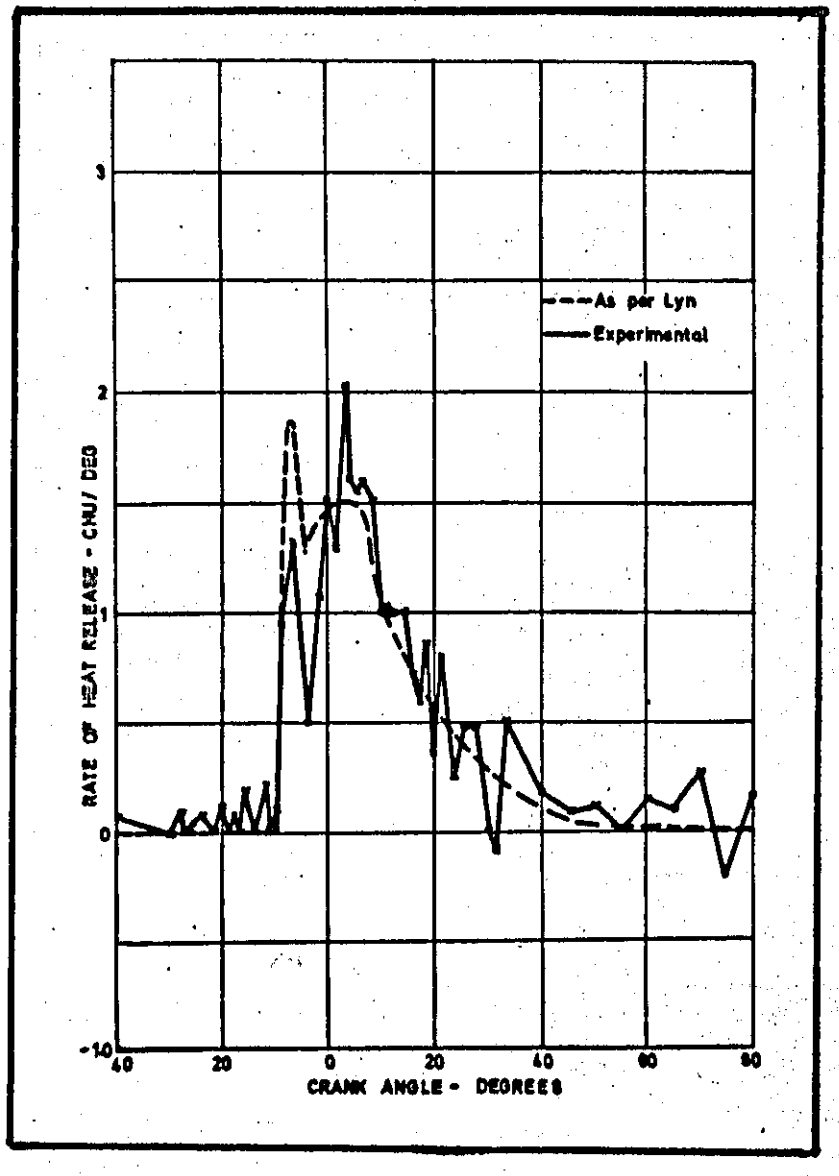

Figure 38 The heat release pattern calculated from the cylinder pressure diagram of a $12\frac{1}{2}$" bore engine together with the predicted shape as per Lyn [62].

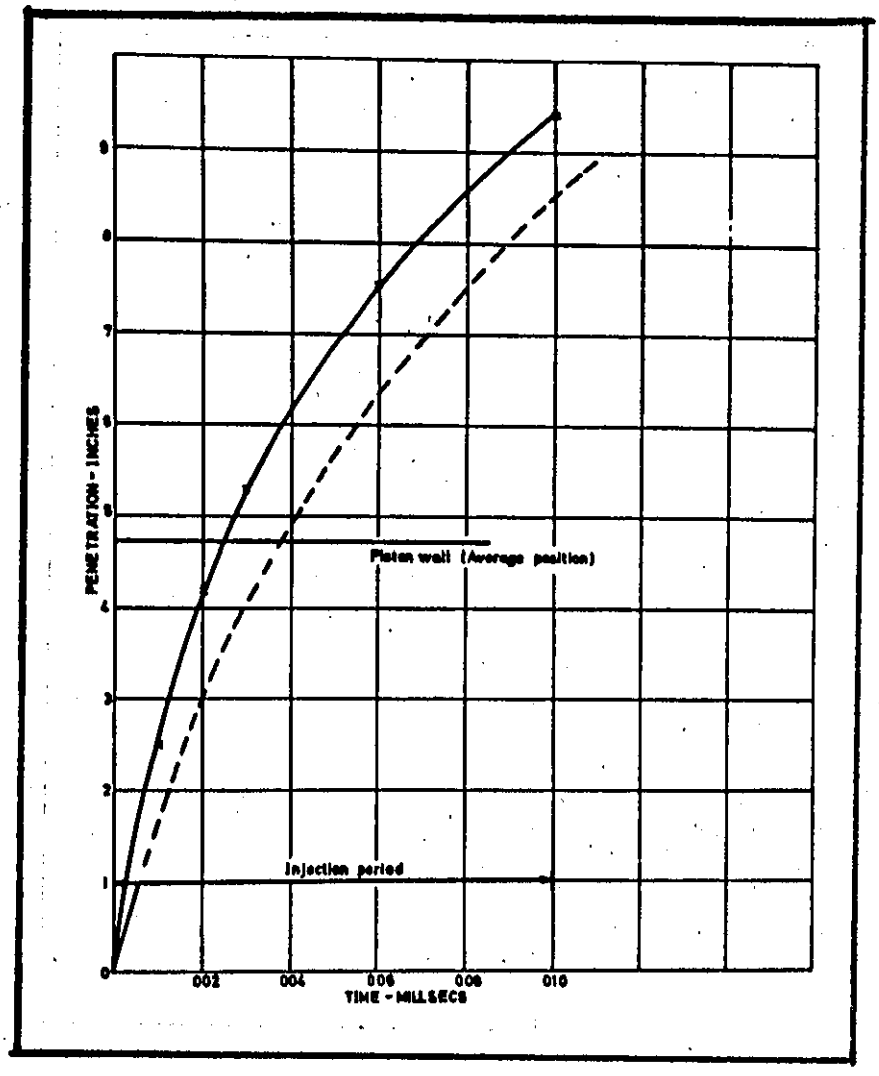

Figure 39 Possible spray penetration with evaporation on the $12\frac{1}{2}$" bore engine.
Full line calculated penetration, dashed line possible penetration with evaporation.

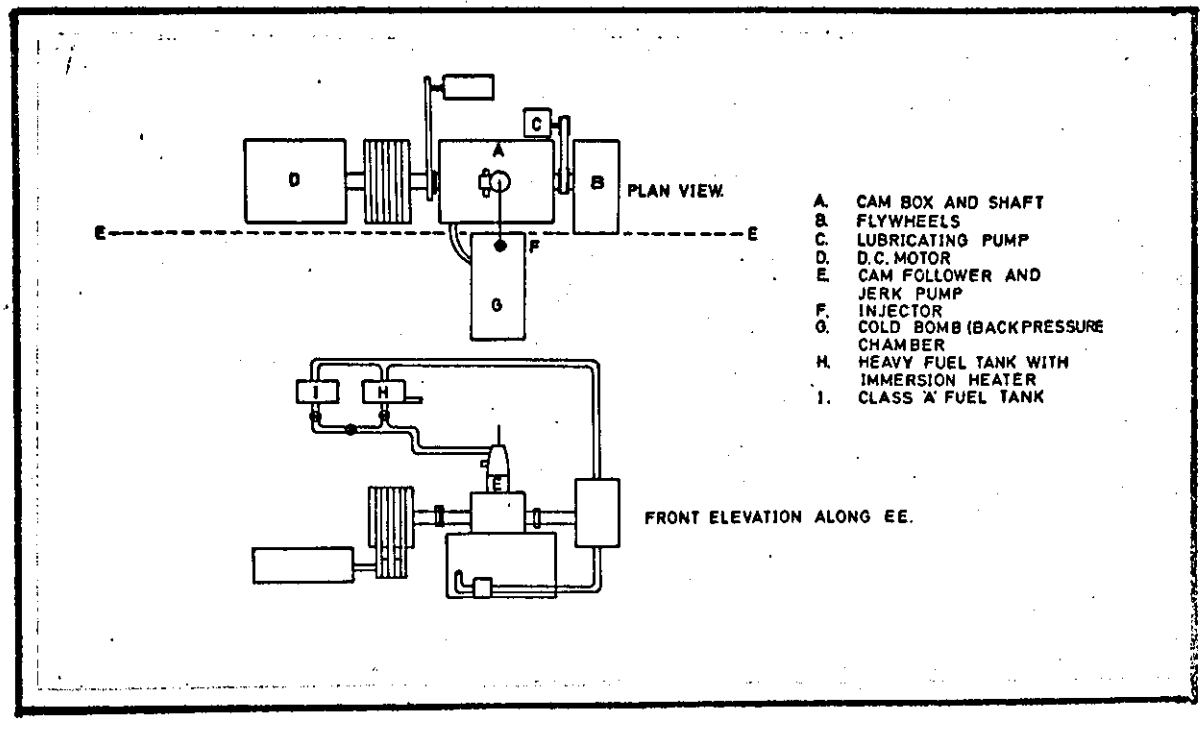

Figure 40 Diagrammatic layout of spray chamber rig.

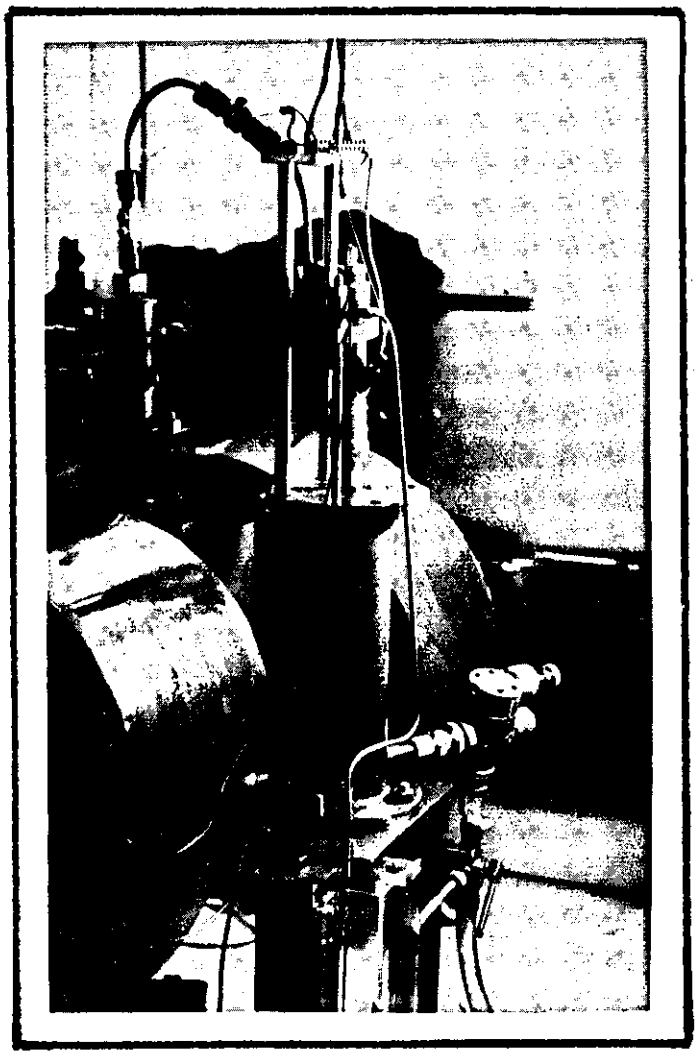

Figure 41 Back pressure cylinder with Stein-Atkinson-Vickers valve in place.

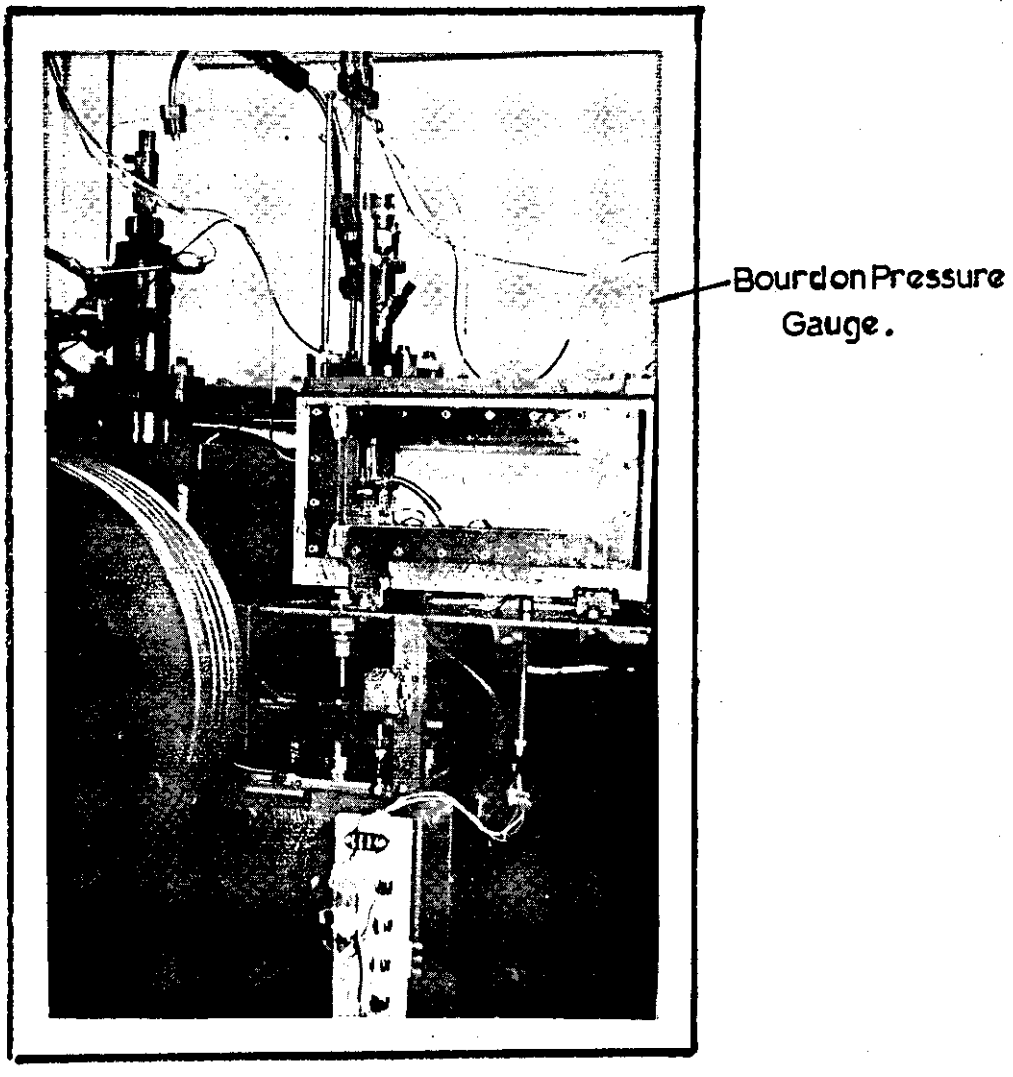

Figure 42 Pressure Chamber.

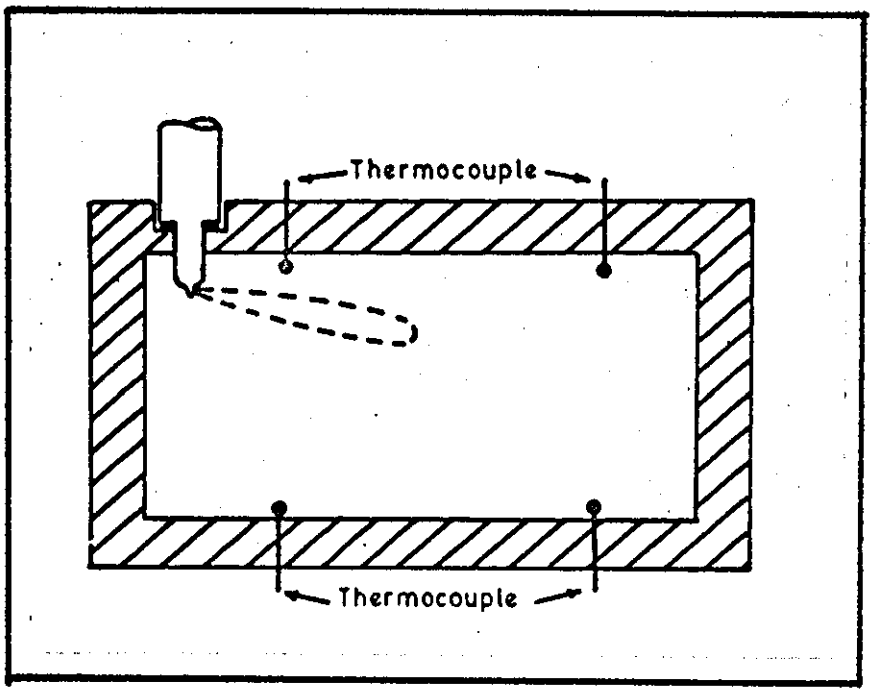

Figure 43 Diagrammatic layout of thermocouples in pressure chamber for measuring nitrogen gas temperature.

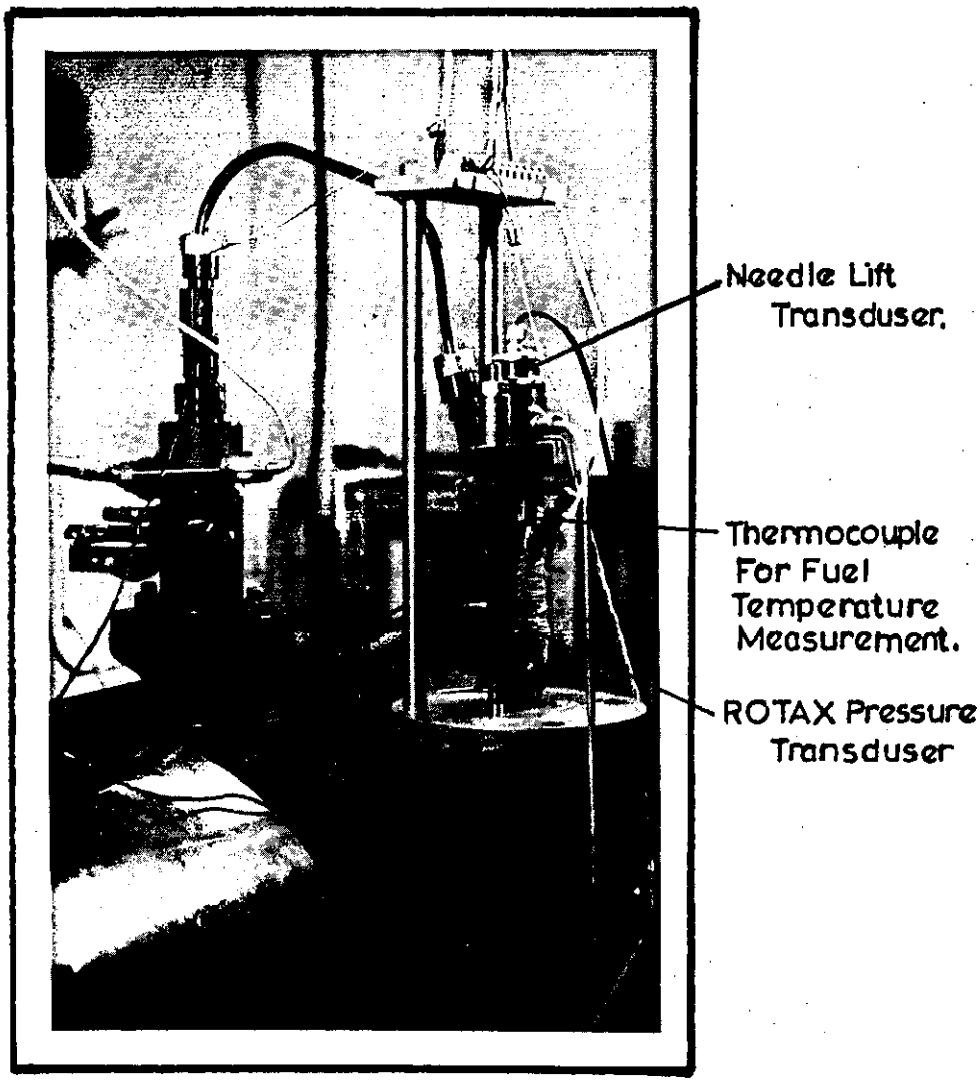

Figure 44 Positions of thermocouple to measure fuel temperature in the injector nozzle. Also the Rotax pressure transducer to measure fuel line pressure and needle lift transducer.

Figure 45 Proximity probe used for cam shaft speed measurement.

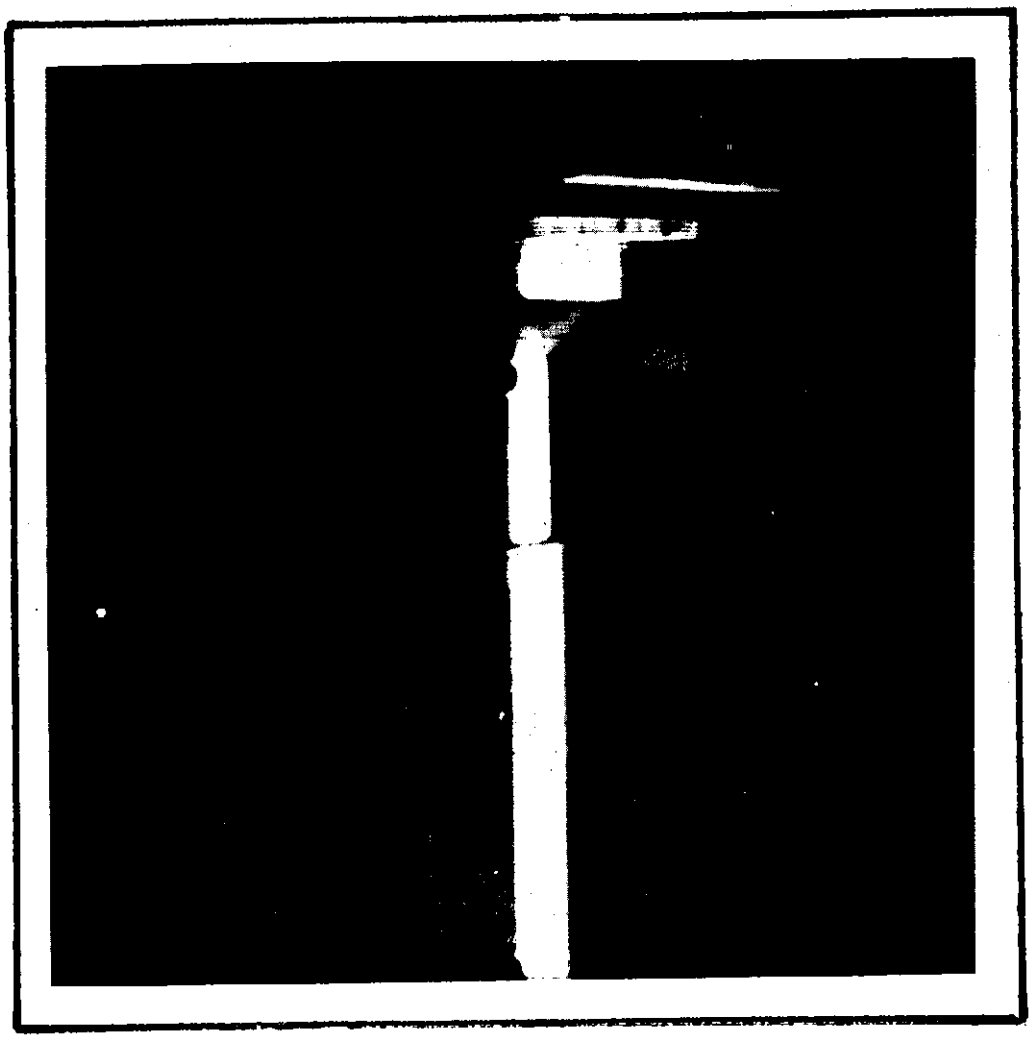

Figure 46 Nozzle hood in position in the pressure chamber.

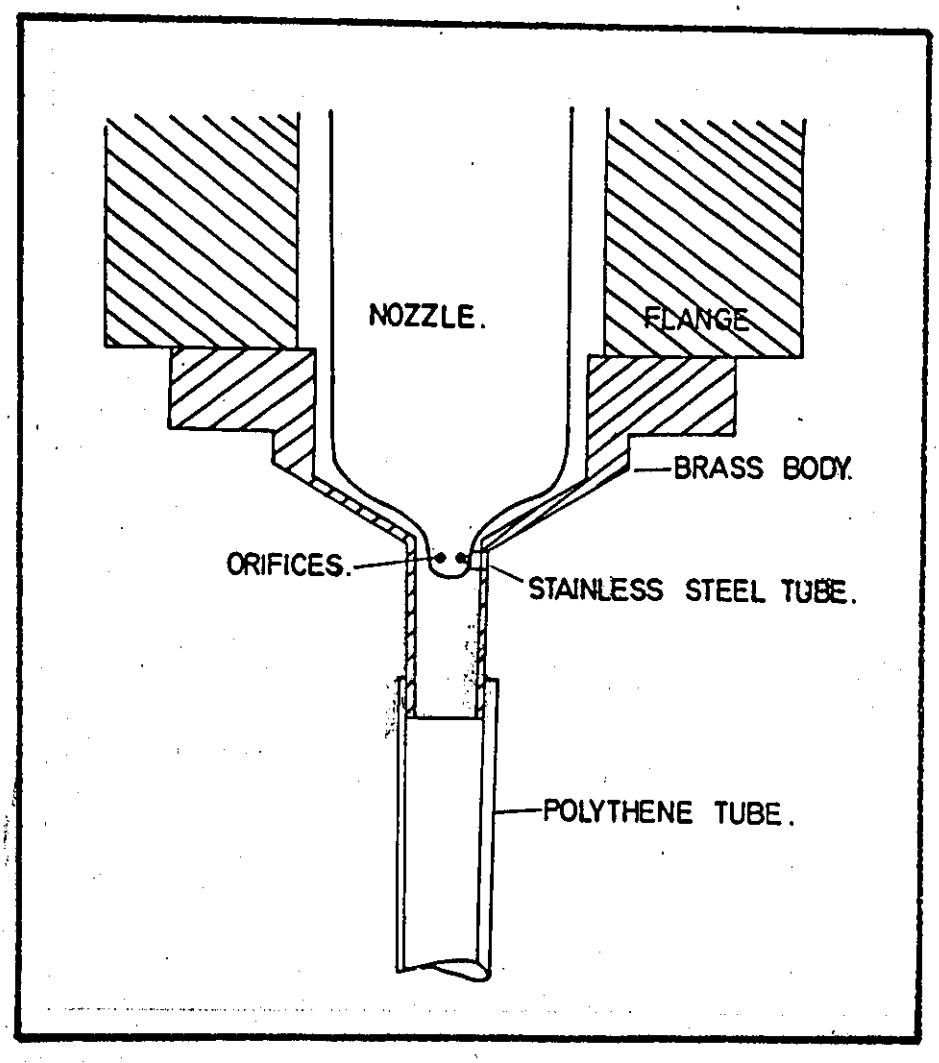

Figure 47 Cross section of nozzle hood assembly showing the stainless steel insert.

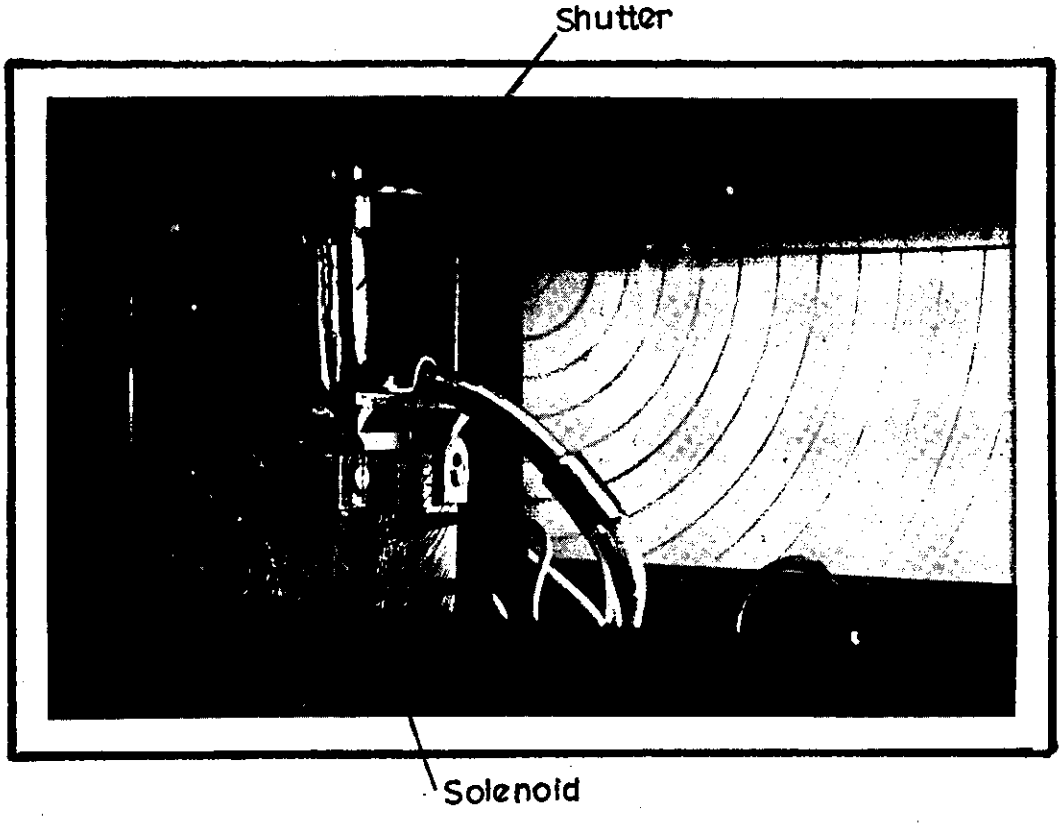

Figure 48 Fast response shutter and solenoid assembly.

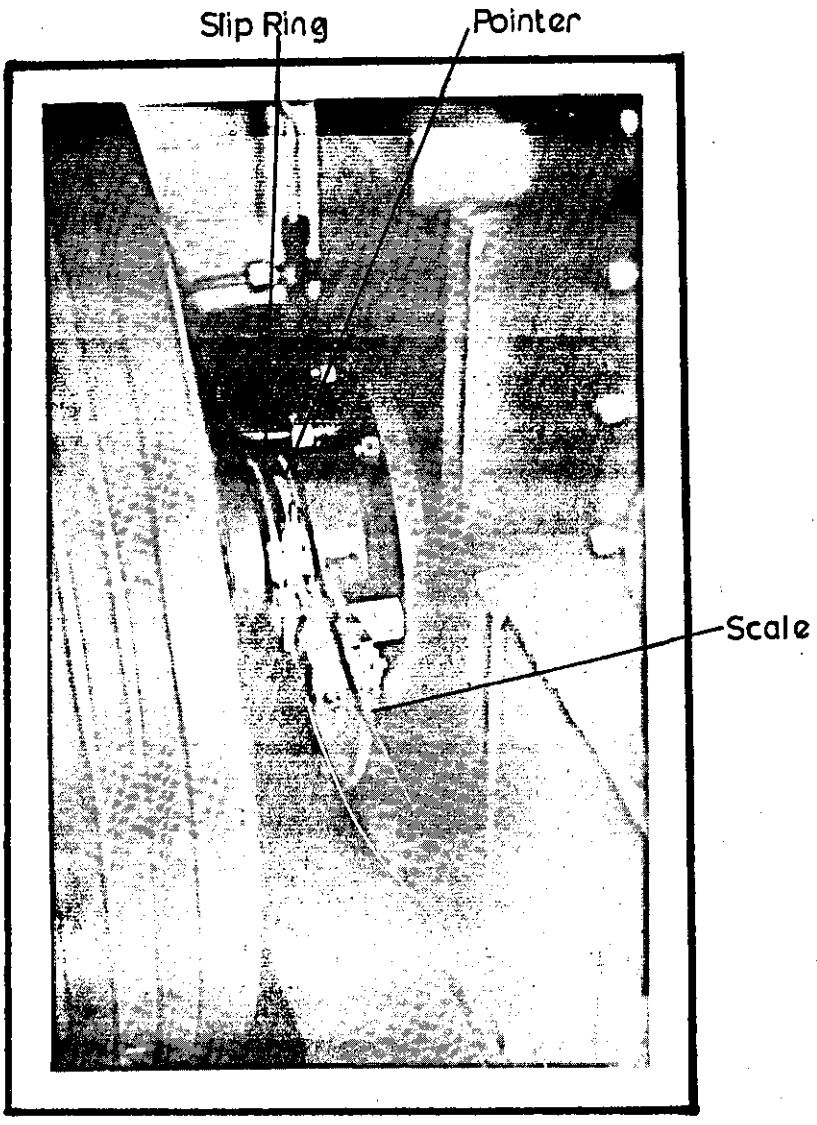

Figure 49 Slip ring switch in place on the cam shaft.

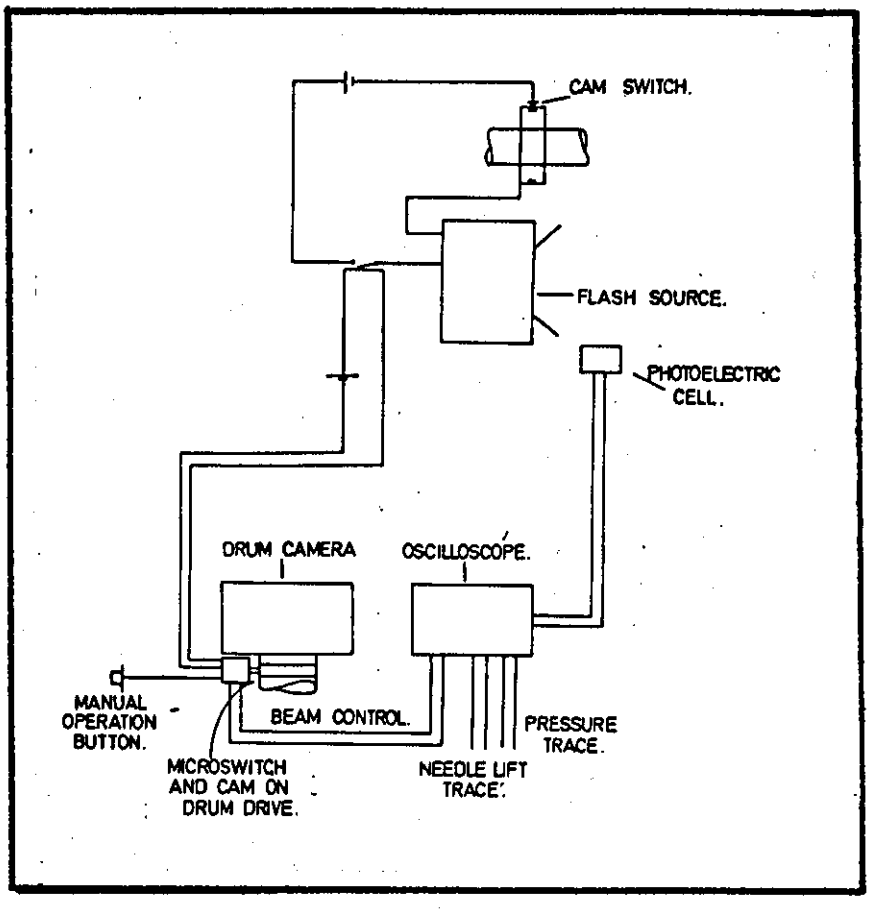

Figure 50 Diagrammatic arrangement of camera and flash trigger circuit.

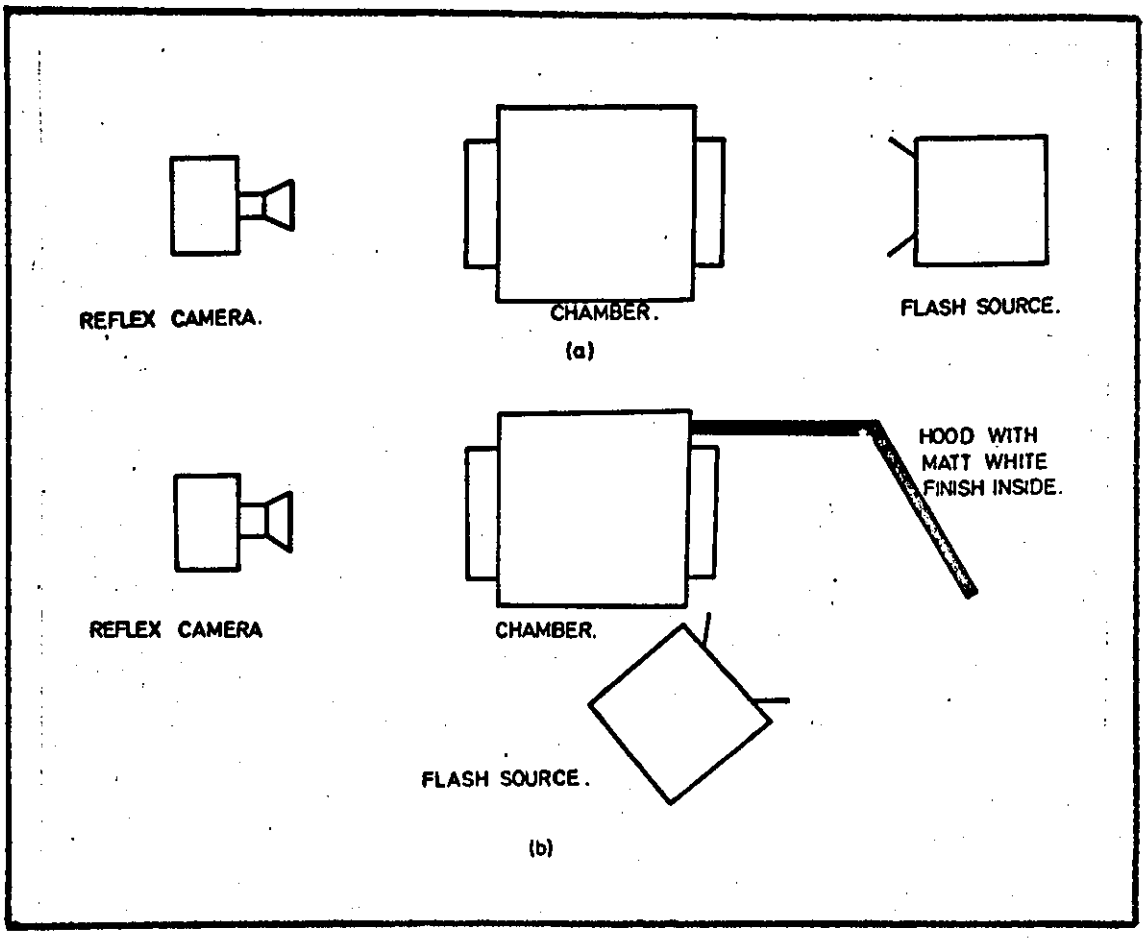

Figure 51 The two types of illumination tried with flash photography.

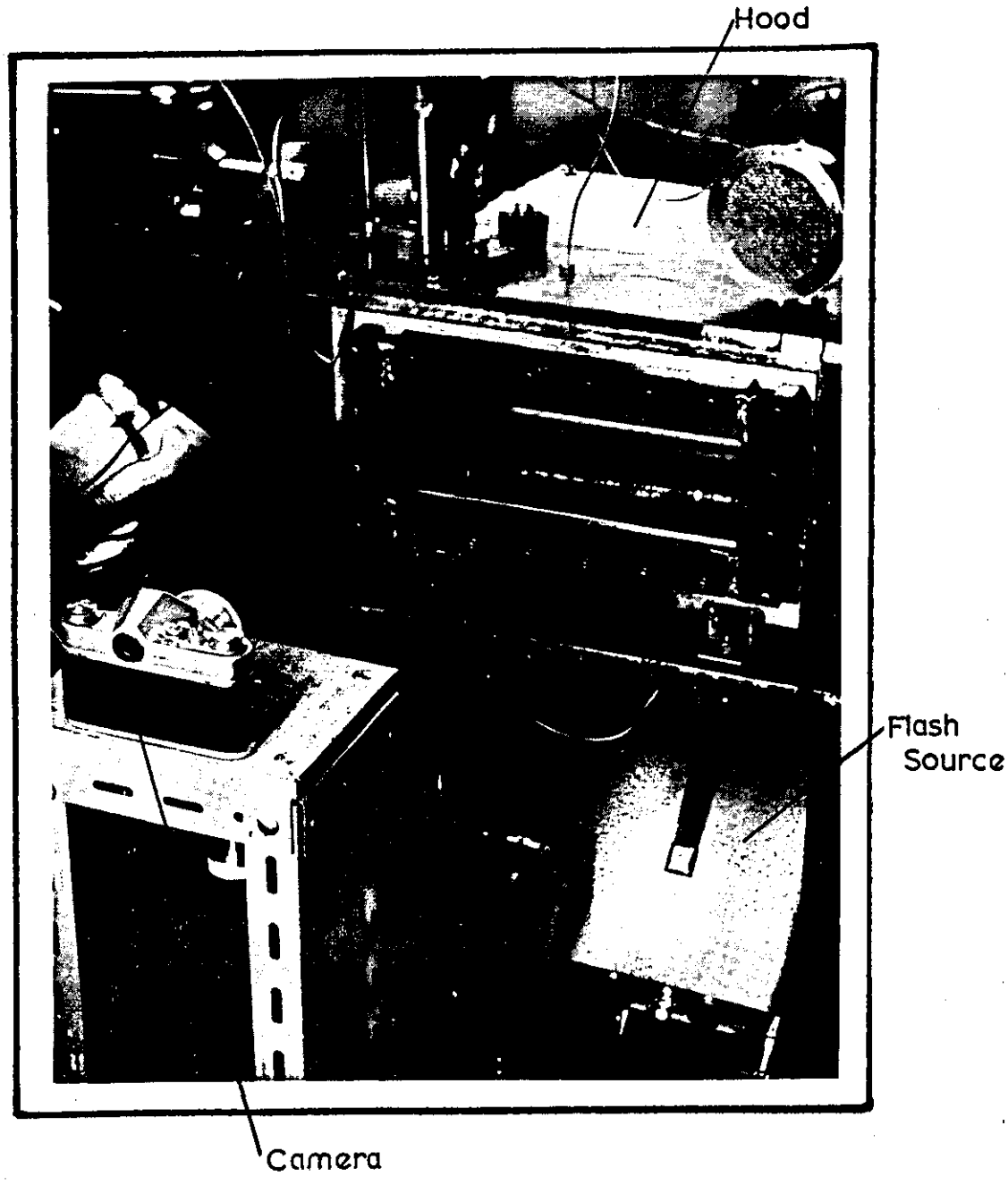

Figure 52 The flash photography apparatus in place on the pressure chamber.

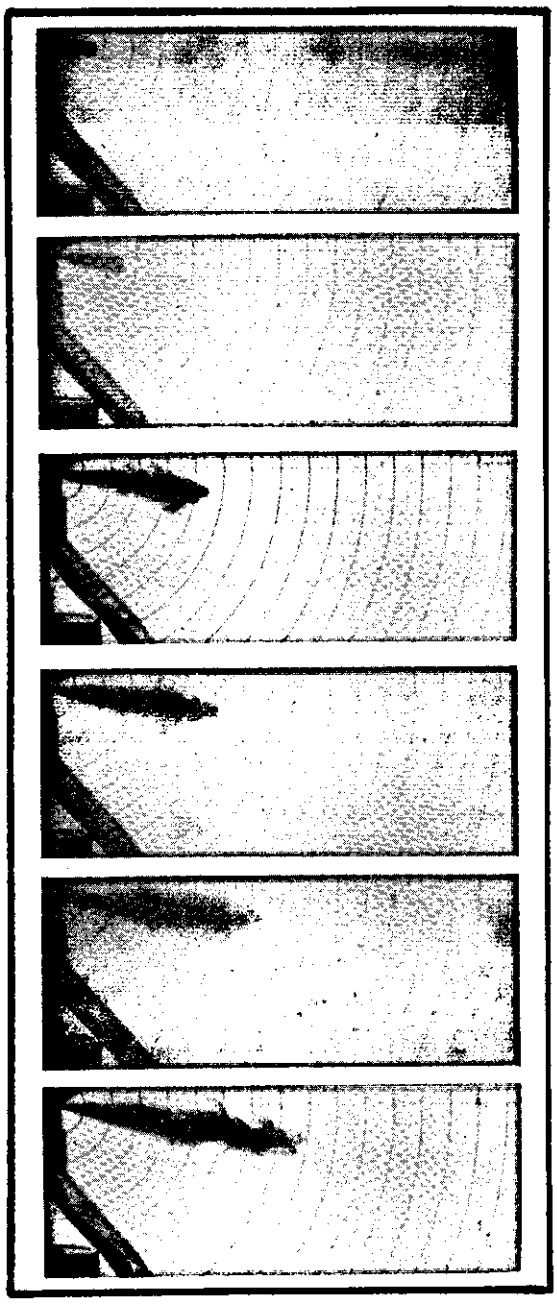

Figure 53 Still sequence of spray development using flash photography.

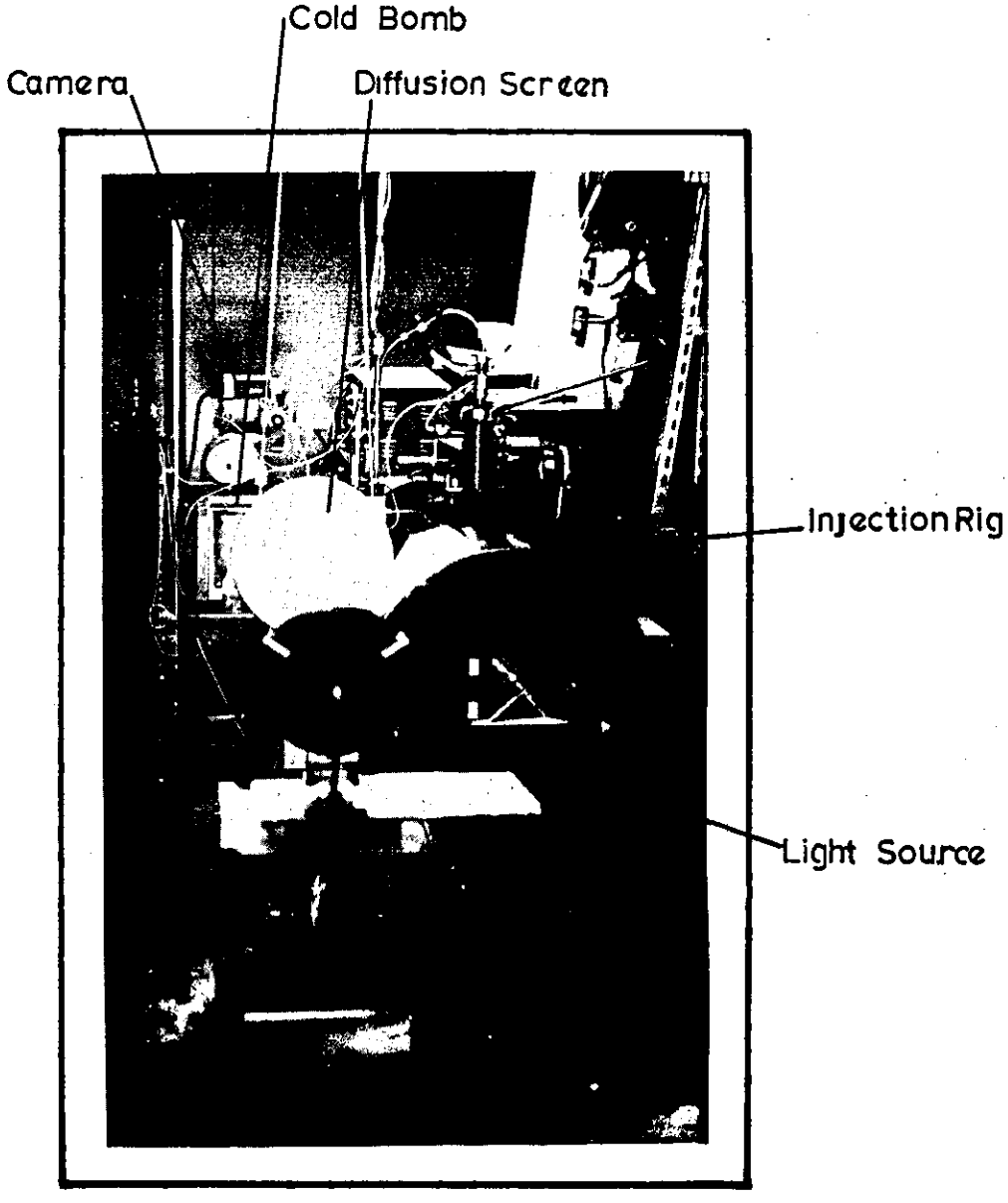

Figure 54 Pressure chamber rig with high speed photographic apparatus in place.

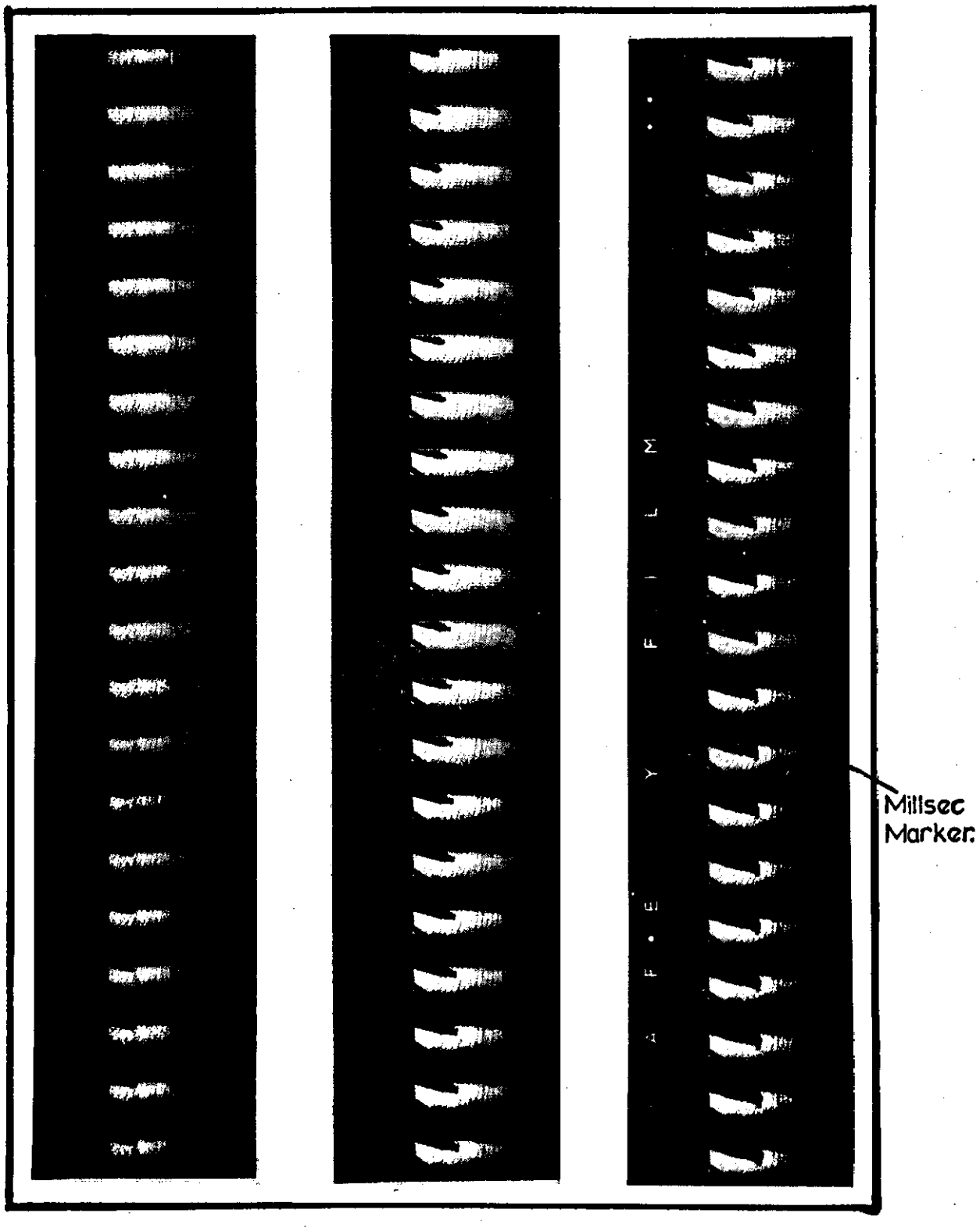

Figure 55 Spray development using high speed camera.

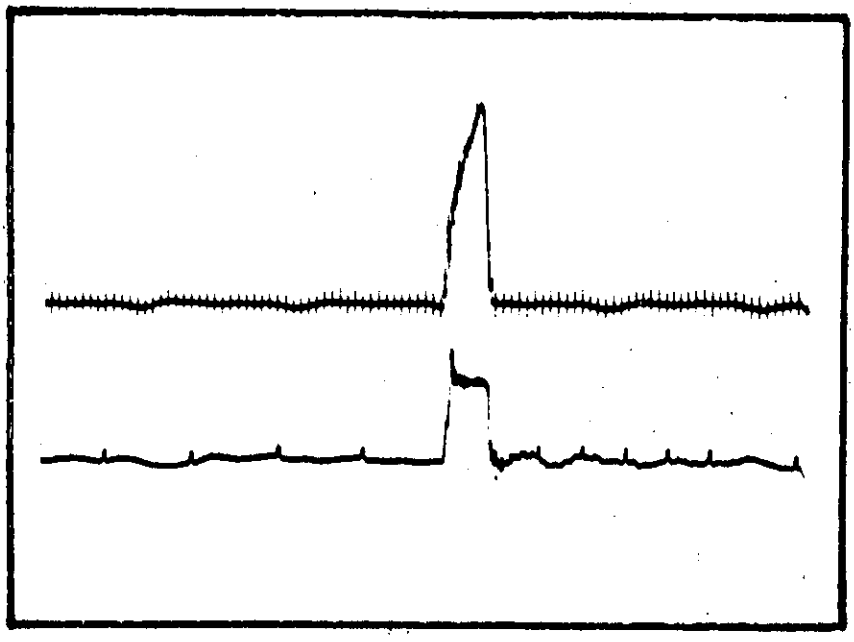

Figure 56 Example of paper trace result showing fuel line pressure and injector needle lift.

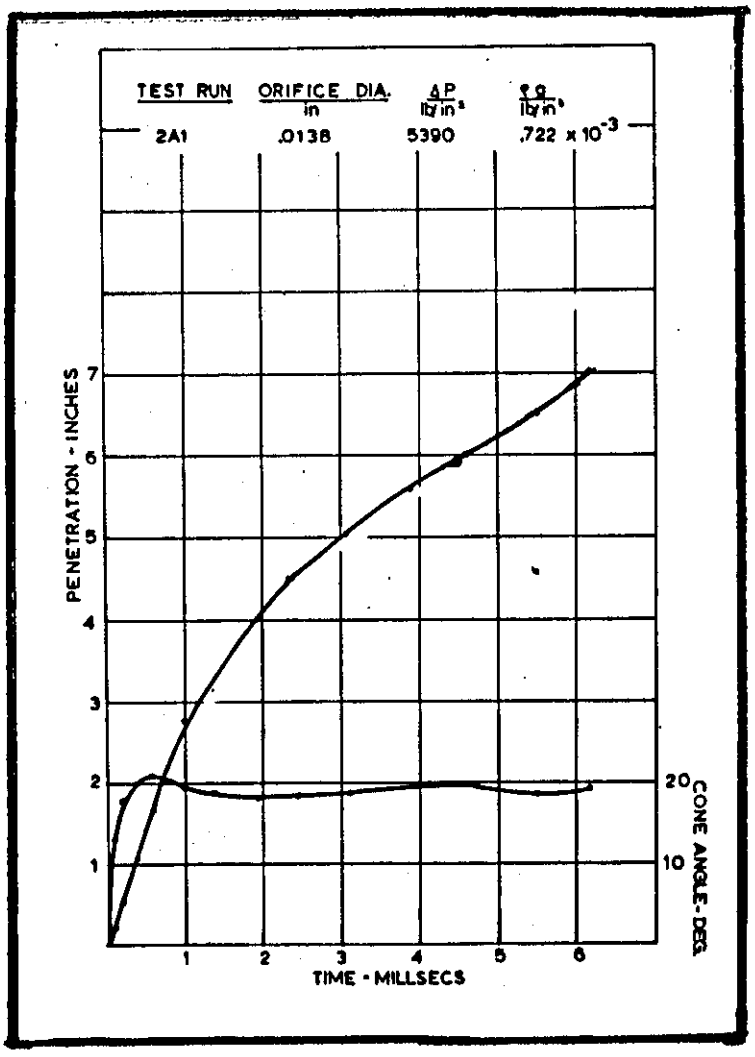

Figure 57 Results of high speed film plotted out.

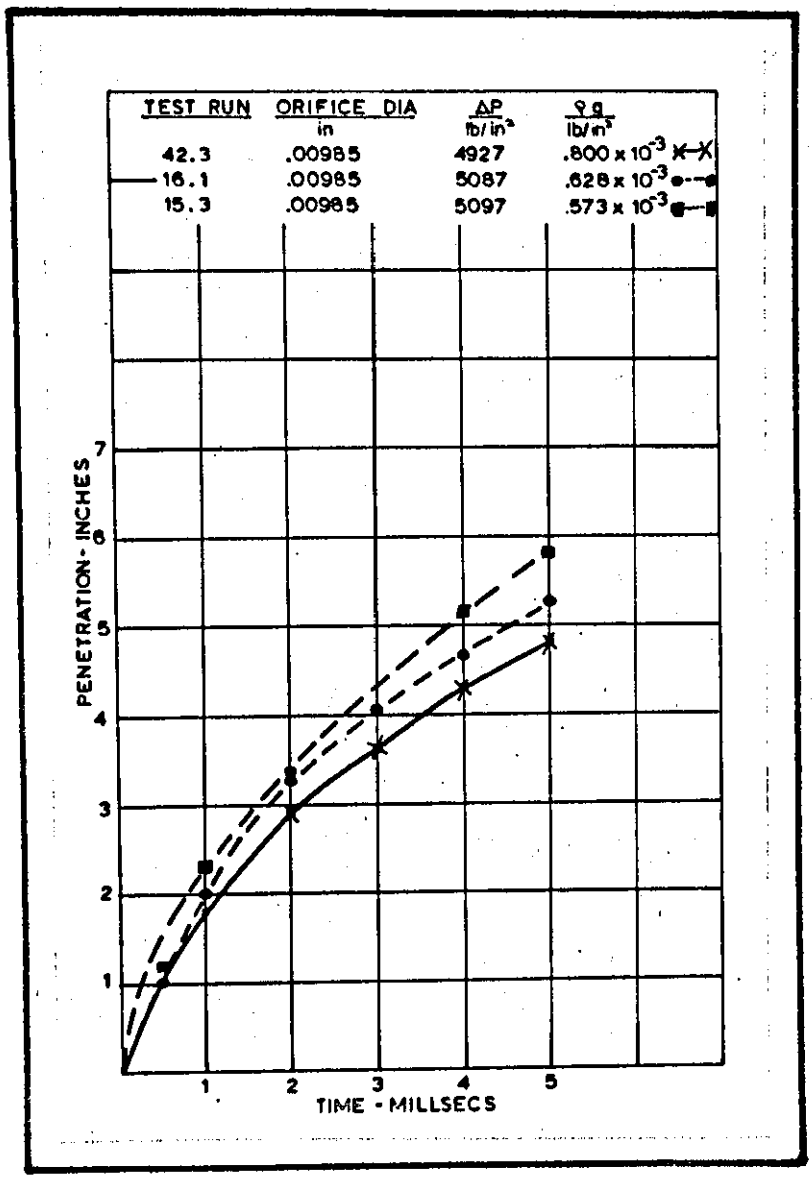

Figure 58 Effect of increasing gas density on spray penetration.

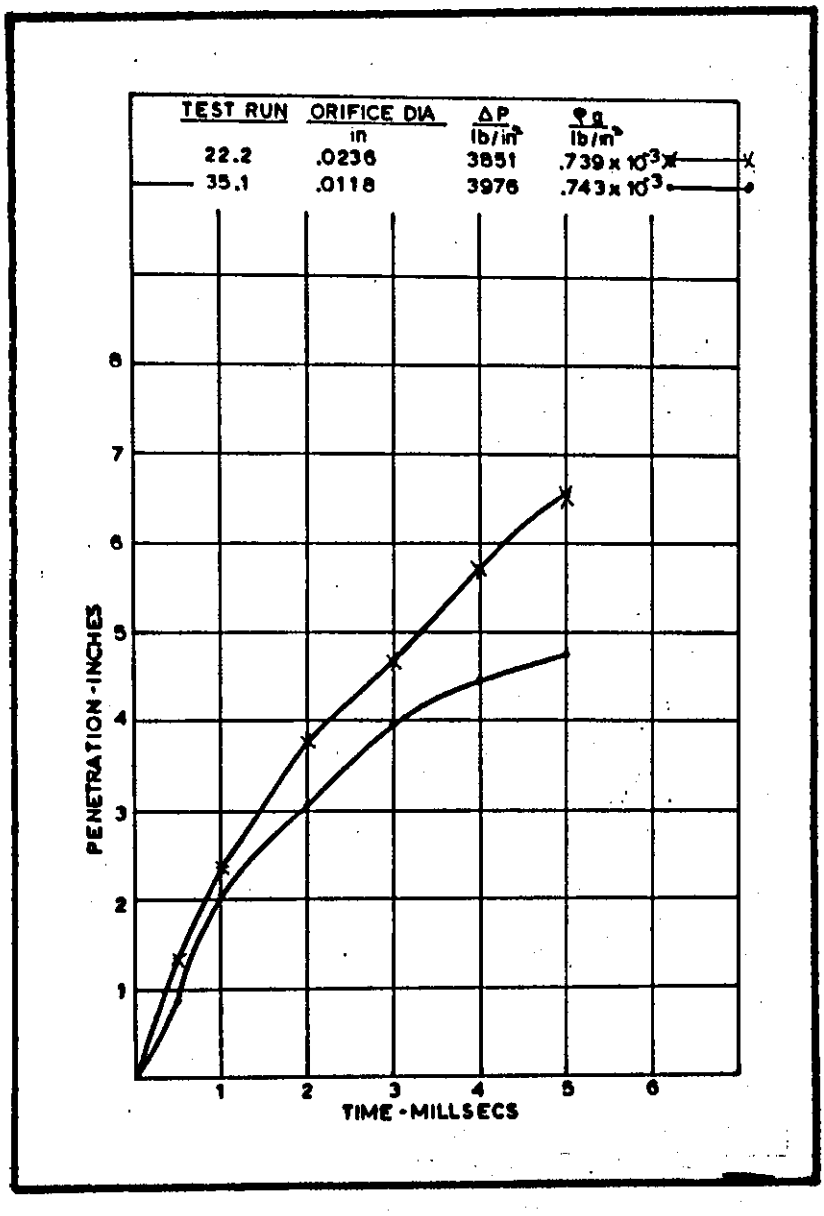

Figure 59 Effect of hole size on spray penetration.

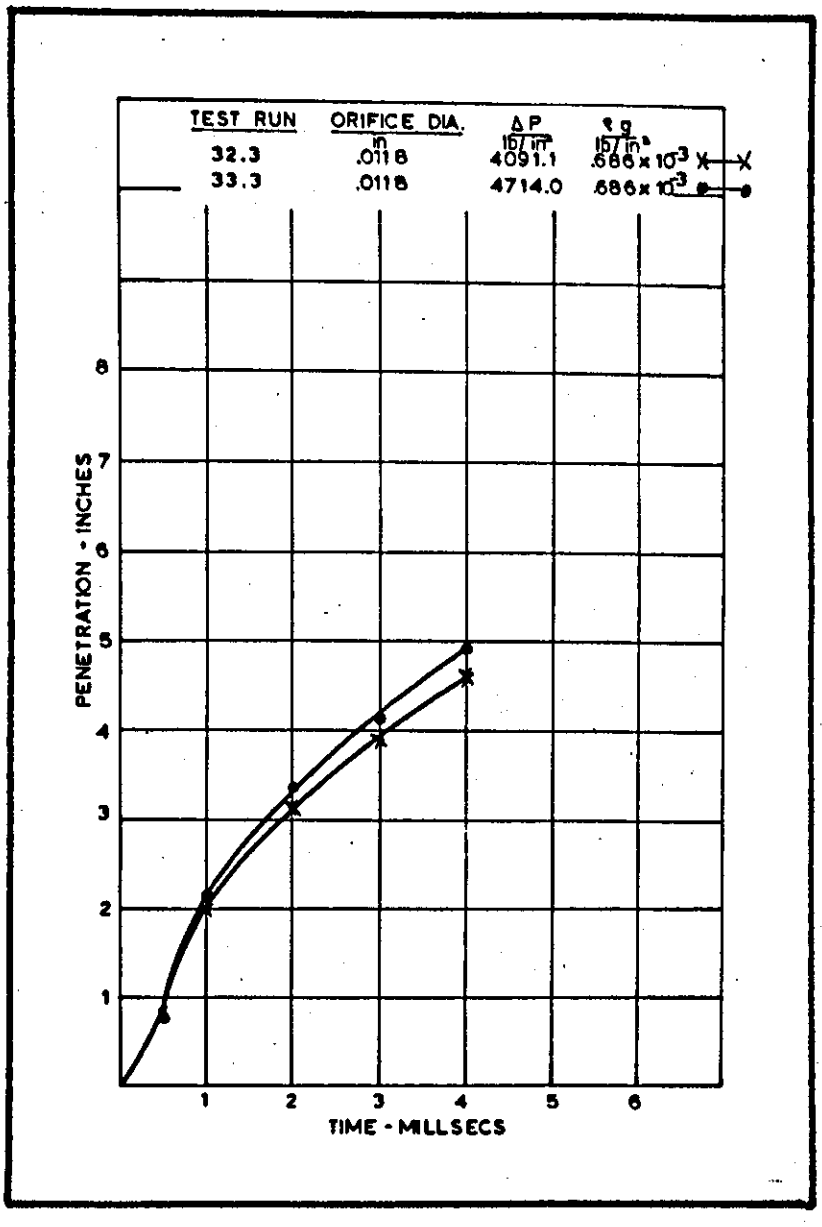

Figure 60 Effect of pressure drop across the orifice on penetration.

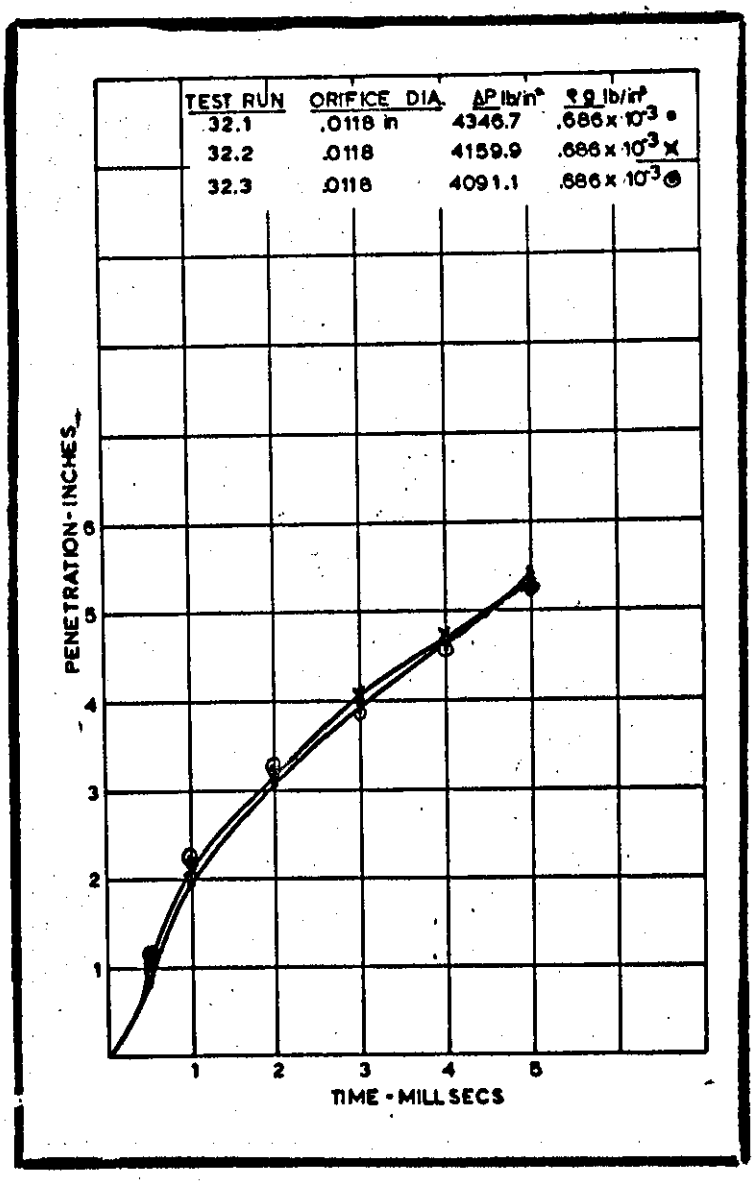

Figure 61 Random nature of spray development readings.

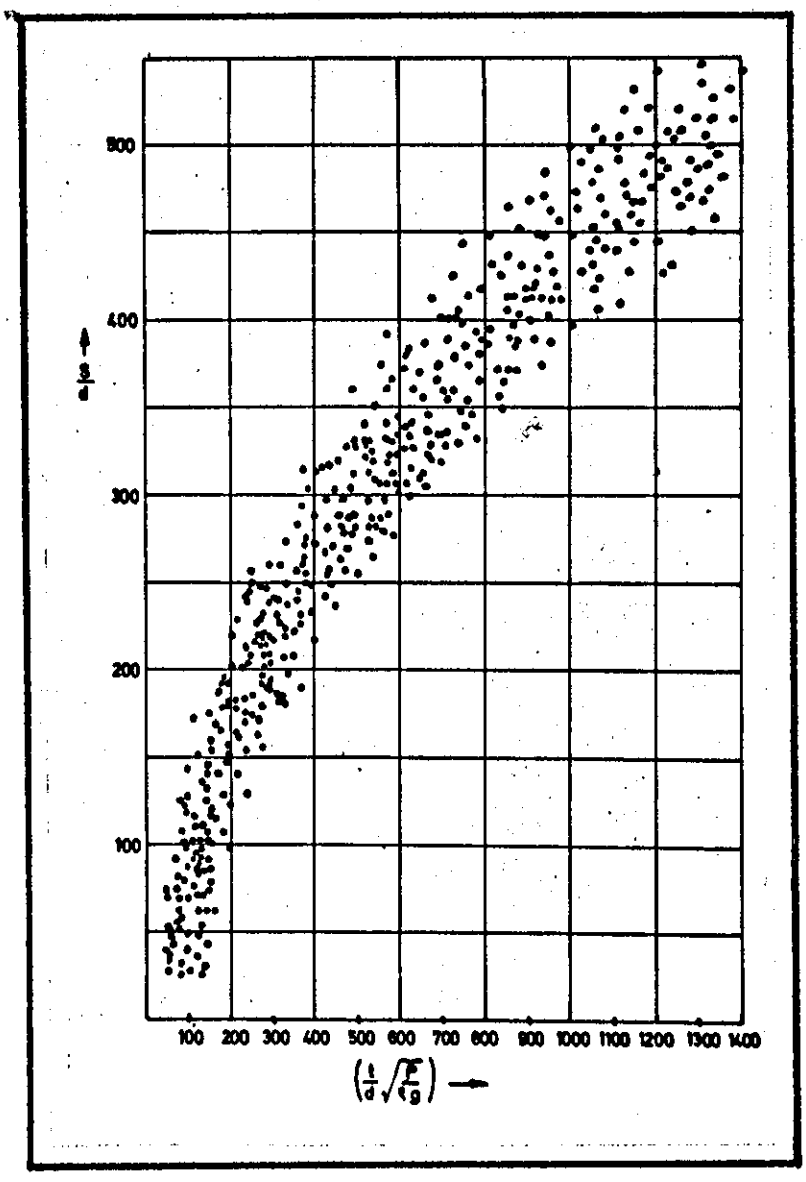

Figure 62 Dimensionless parameter $\frac{s}{d}$ plotted against $\frac{t}{d}\sqrt{\frac{P}{\rho g}}$ for all results.

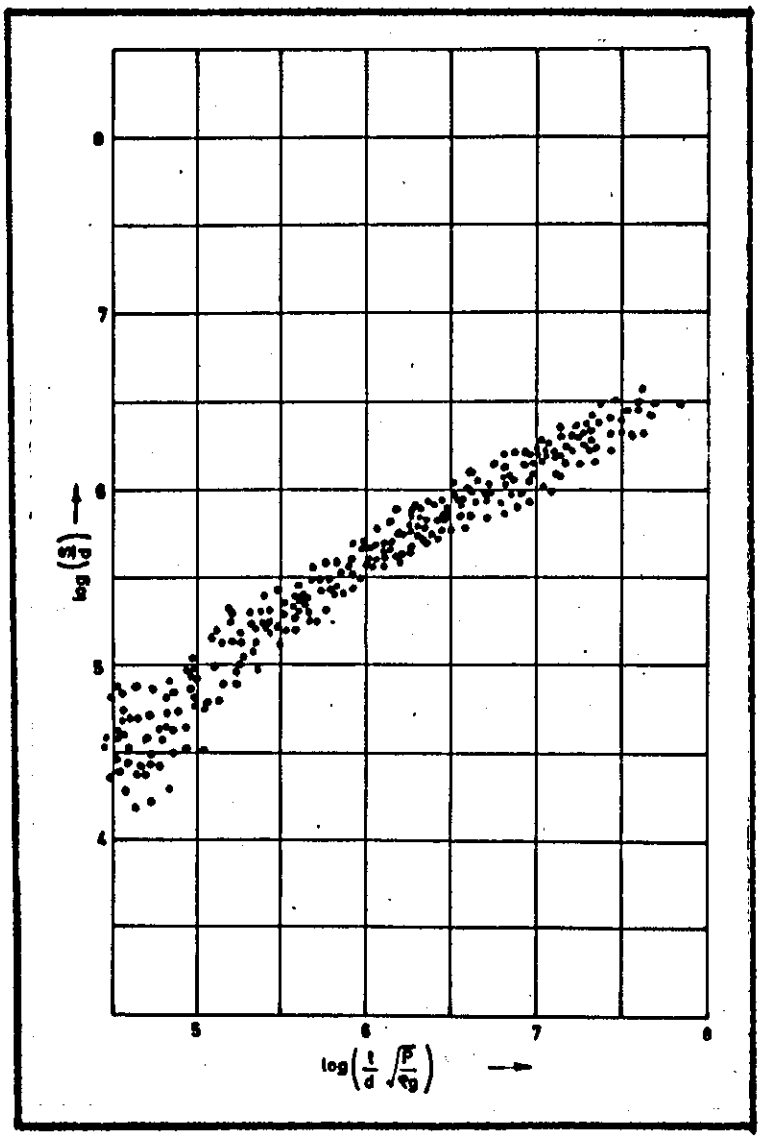

Figure 63 Dimensionless parameter $\log \left(\frac{s}{d}\right)$ plotted against $\log \left(\frac{t}{d}\sqrt{\frac{P}{\rho g}}\right)$ for all results.

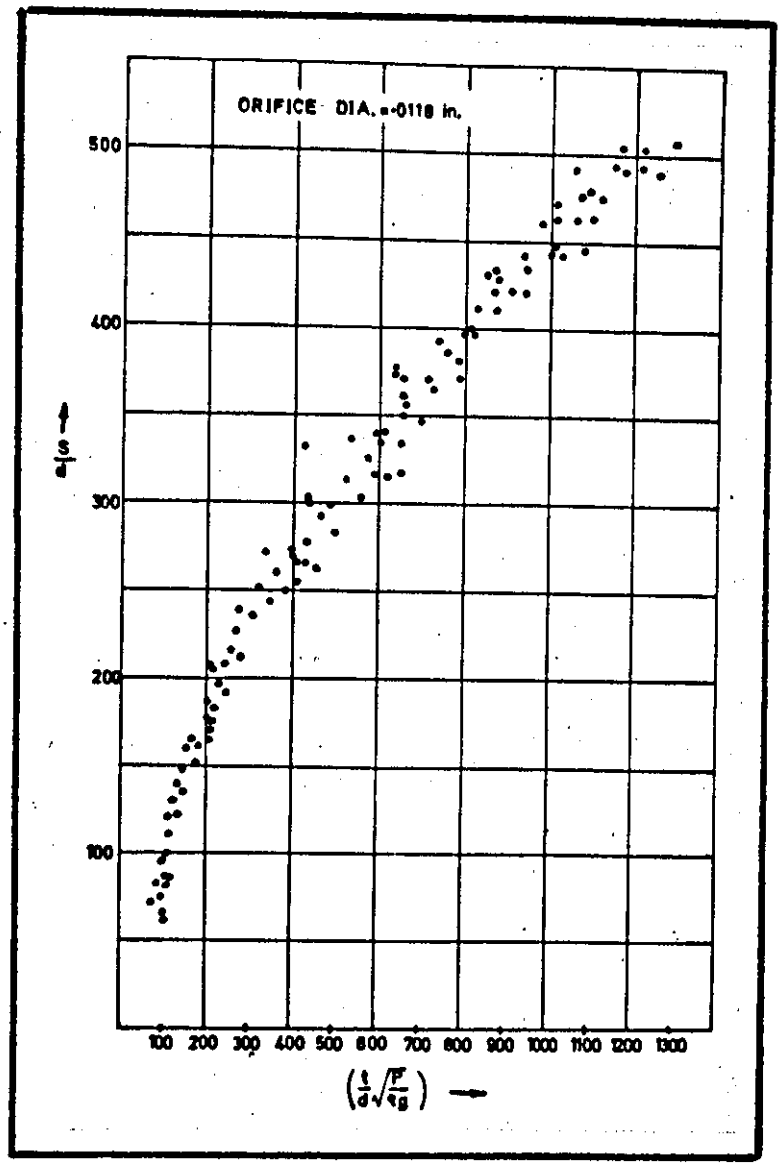

Figure 64 Dimensionless parameter $\frac{s}{d}$ plotted against $\frac{t}{d}\sqrt{\frac{P}{\rho g}}$ for the .0118" orifice

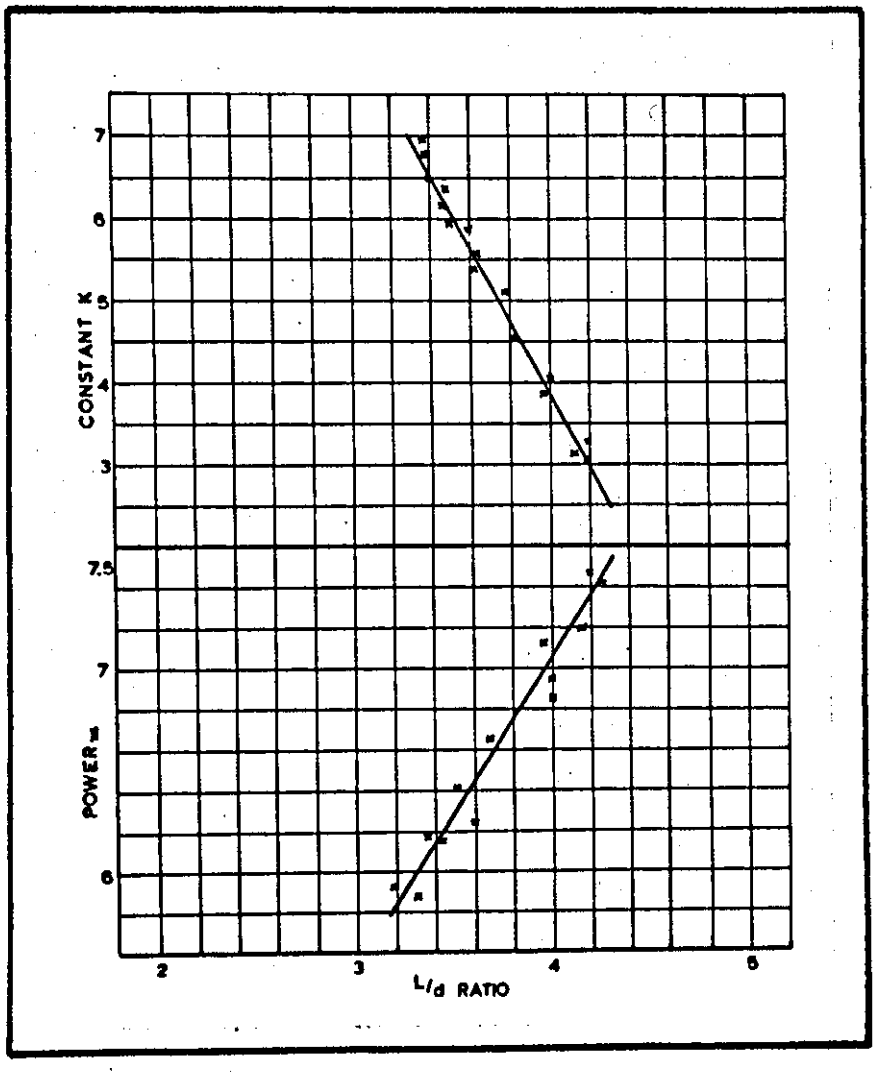

Figure 65 Constant K and power x plotted against L/D ratio.

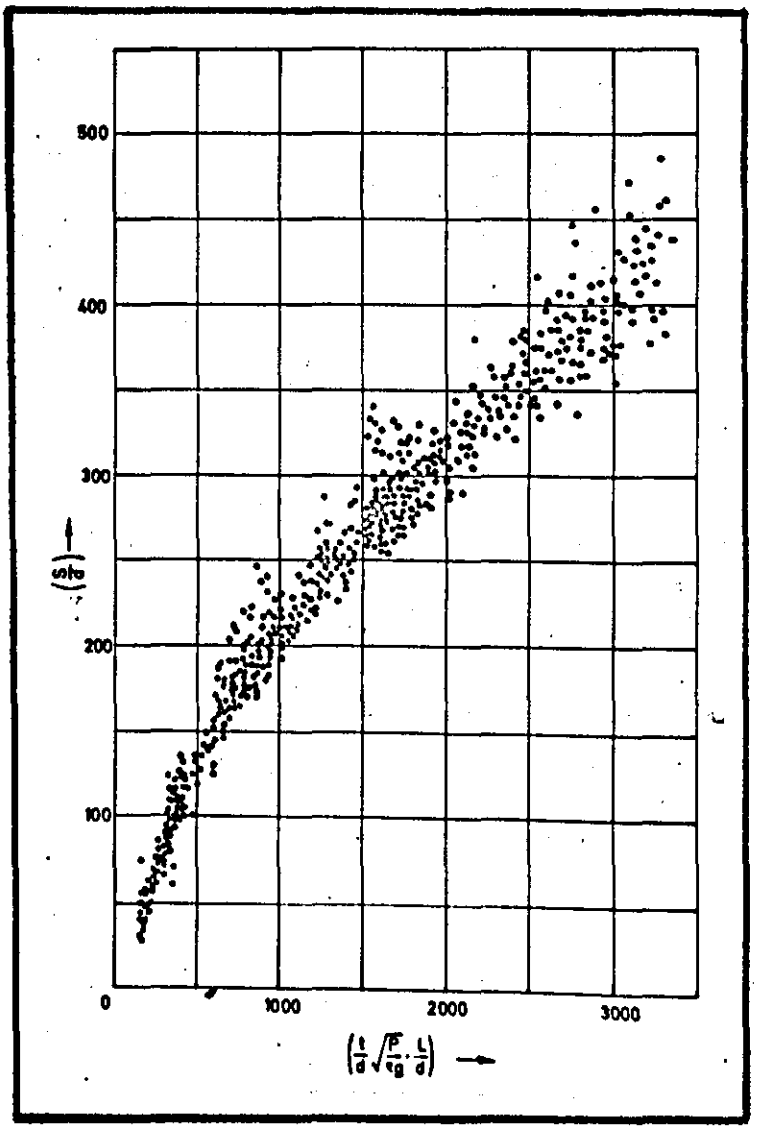

Figure 66 Dimensionless parameter $\left(\frac{s}{d}\right)$ plotted against $\left(\frac{t}{d}\sqrt{\frac{P}{\rho g}}\right)\left(\frac{L}{d}\right)$ for all results.

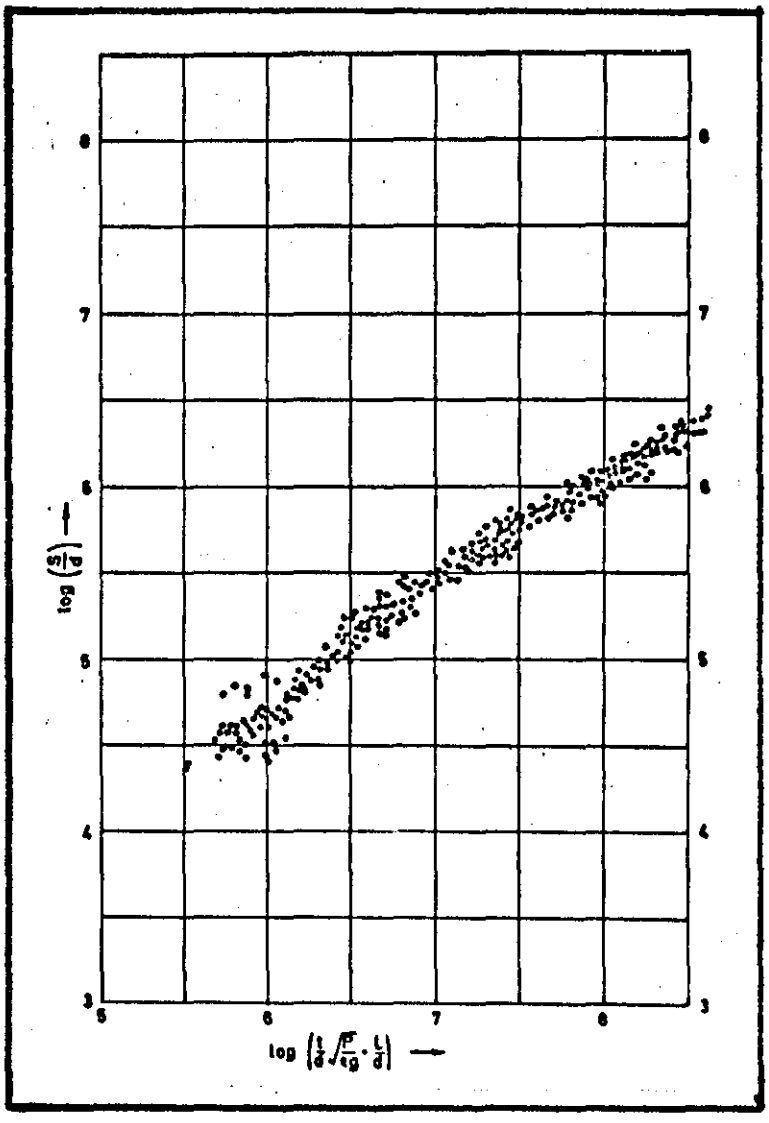

Figure 67 Dimensionless parameter $\log\left(\frac{s}{d}\right)$ plotted against $\log\left[\left(\frac{t}{d}\sqrt{\frac{P}{eg}}\right)\left(\frac{L}{d}\right)\right]$ for all results.

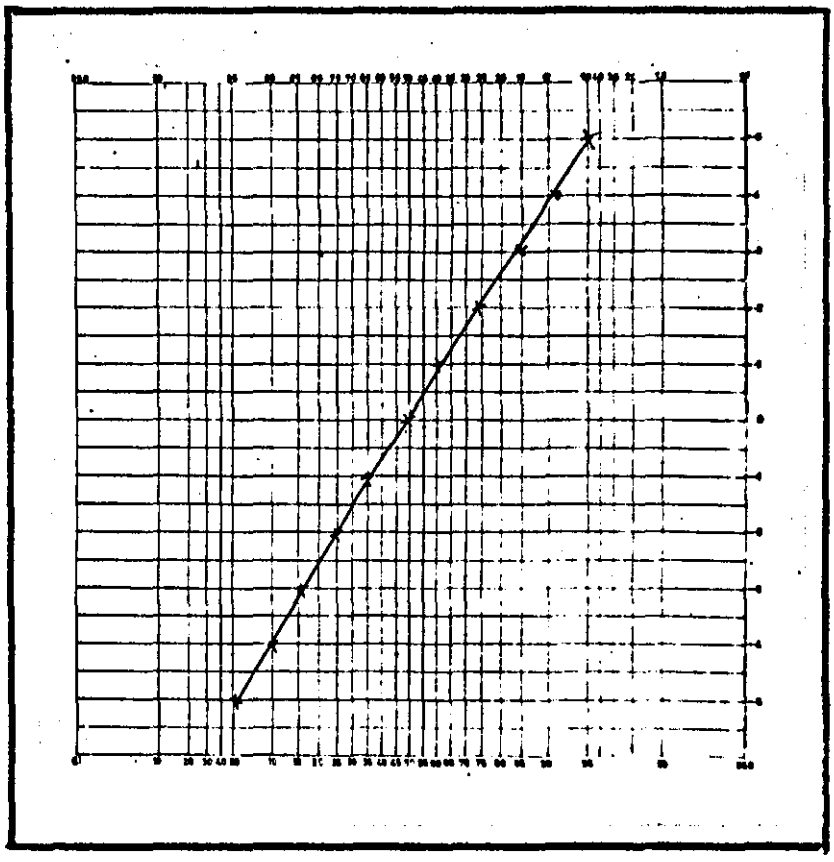

Figure 68 Probability plot of error results from proposed log fitted equation.

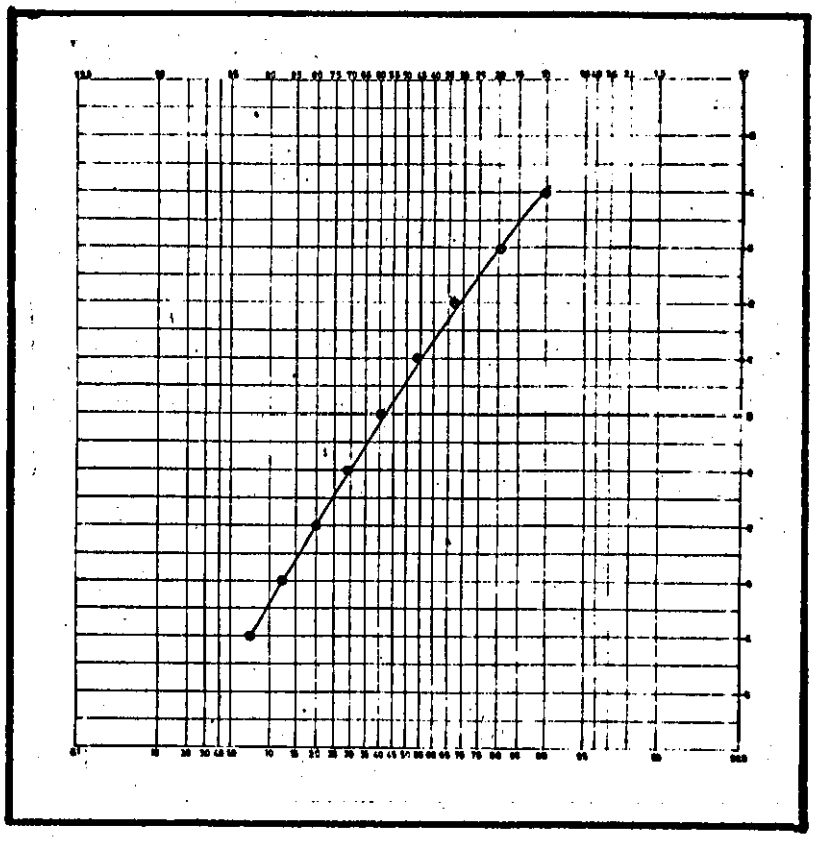

Figure 69 Probability plot of error results from proposed power fitted equation.

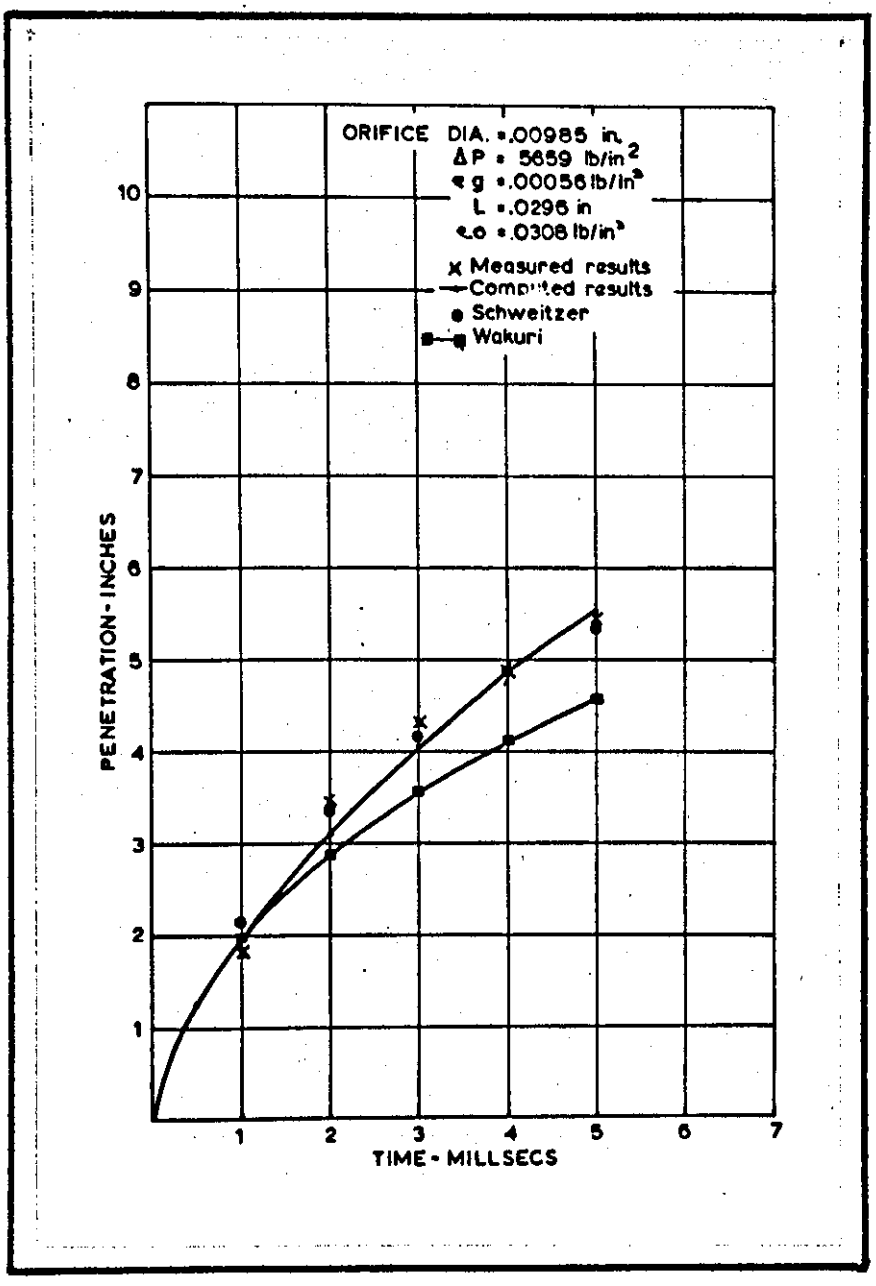

Figure 70 Comparison of measured, predicted spray penetration together with predicted curves from Wakuri [15] and Schweitzer [9] for a .00985" diameter orifice.

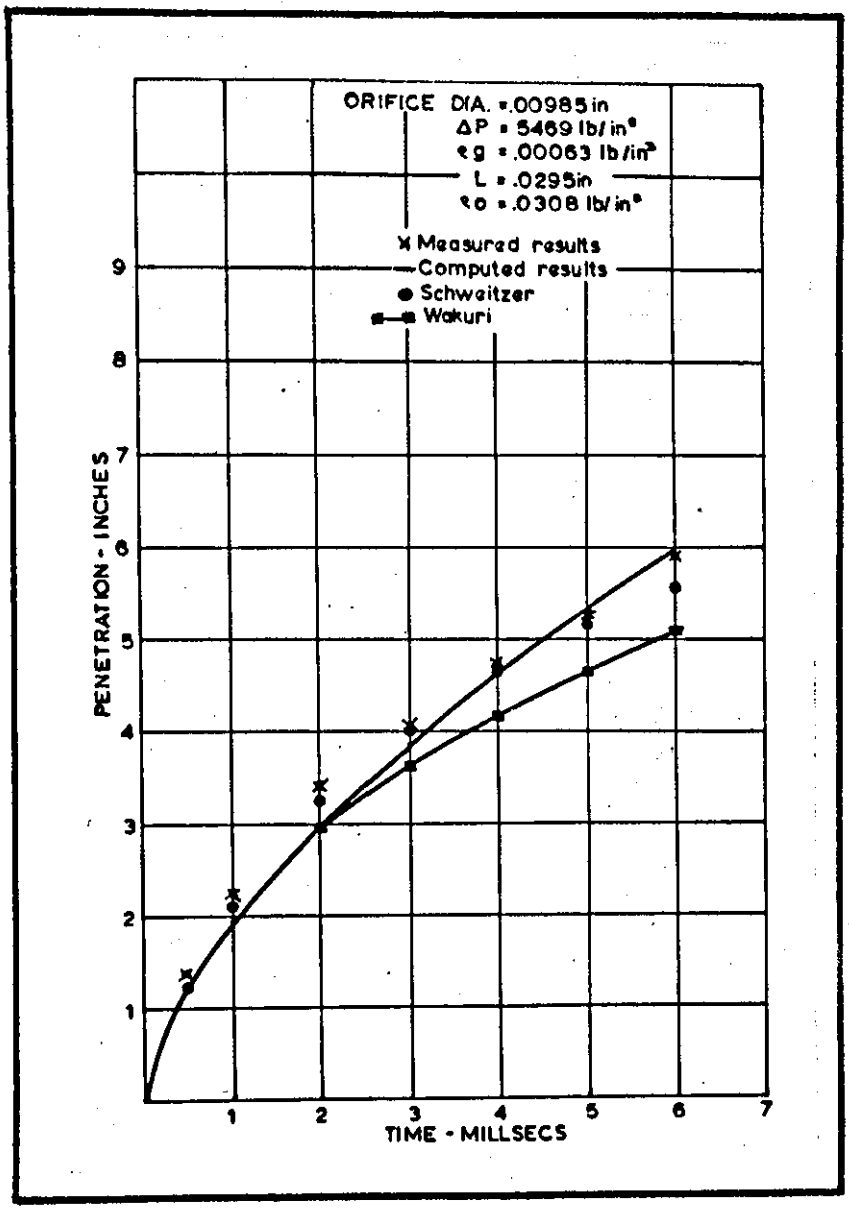

Figure 71 Comparison of measured, predicted spray penetration together with predicted curves from Wakuri [15] and Schweitzer [9] for a .00985" diameter orifice.

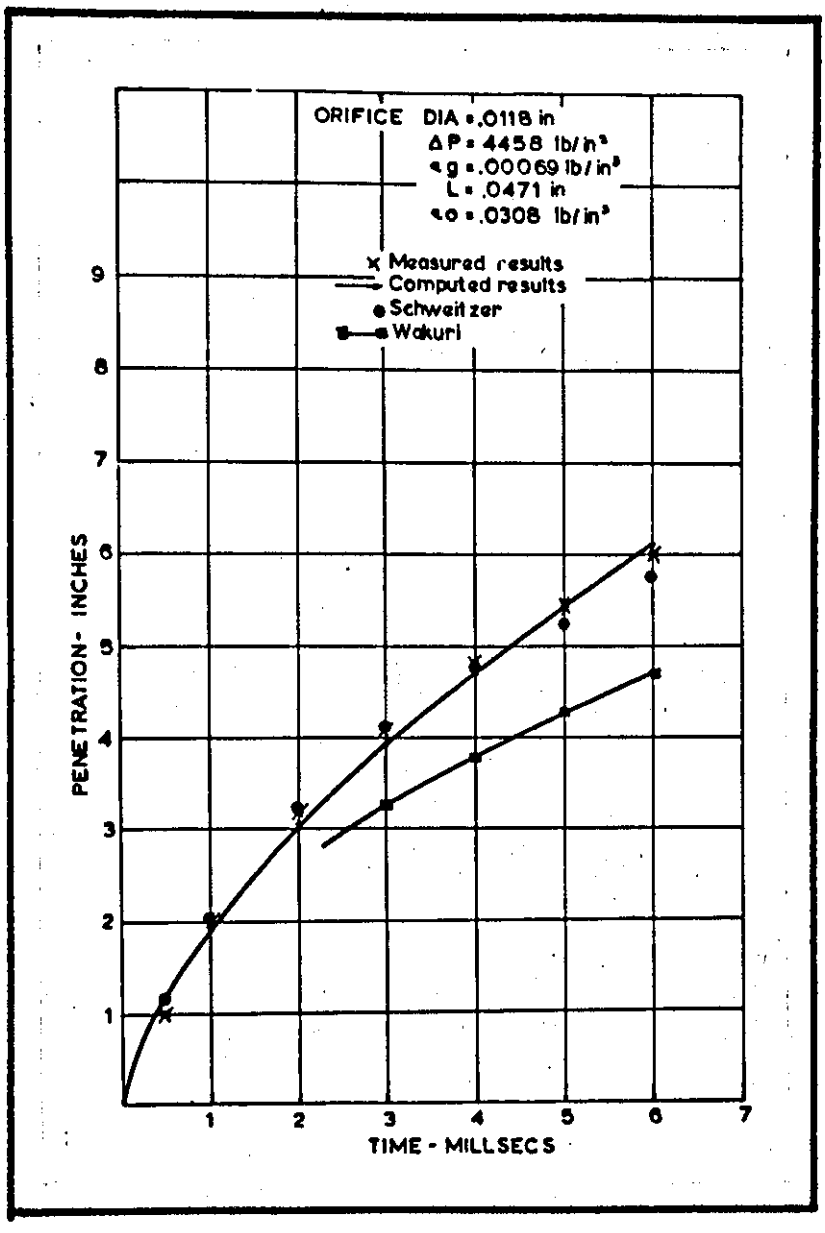

Figure 72 Comparison of measured, predicted spray penetration together with predicted curves from Wakuri [15] and Schweitzer [9] for a .0118" diameter orifice.

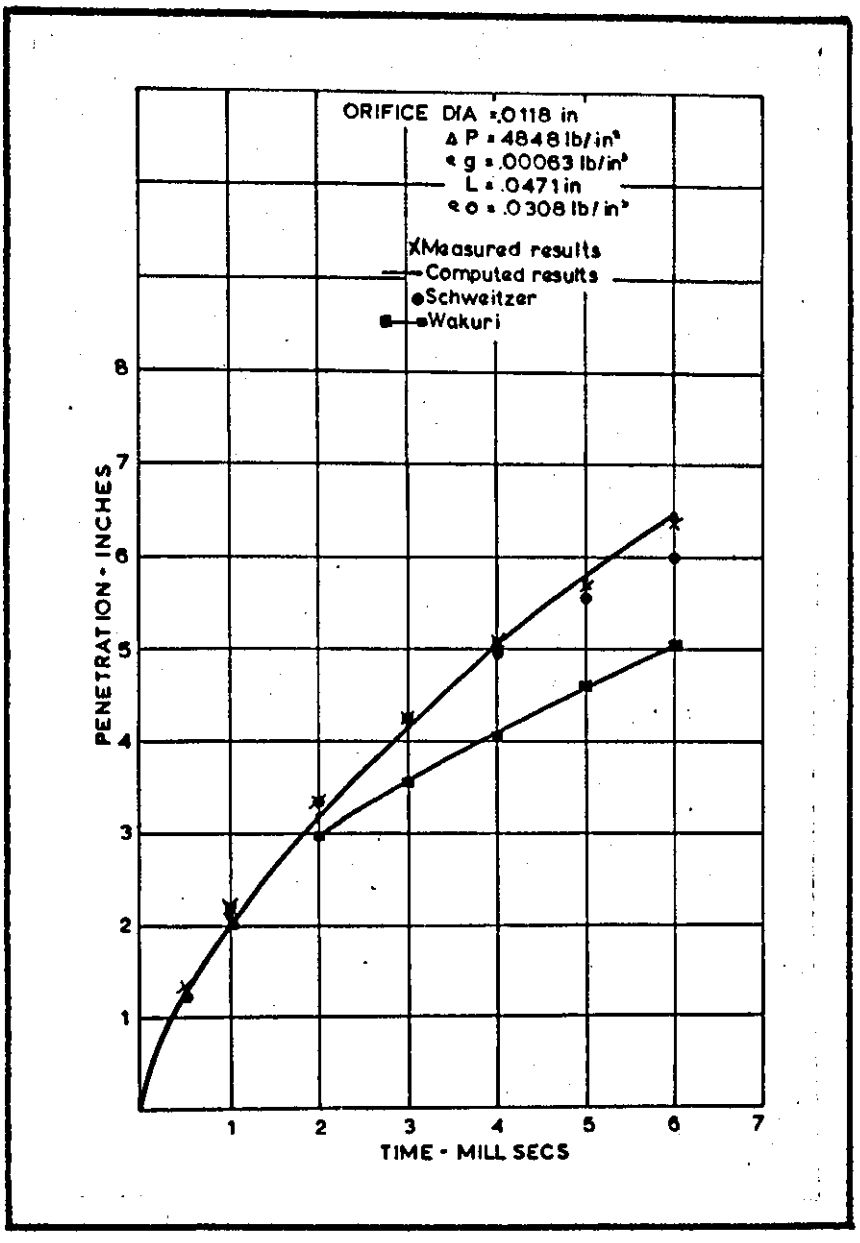

Figure 73 Comparison of measured, predicted spray penetration together with predicted curves from Wakuri [15] and Schweitzer [9] for a .0118" diameter orifice.

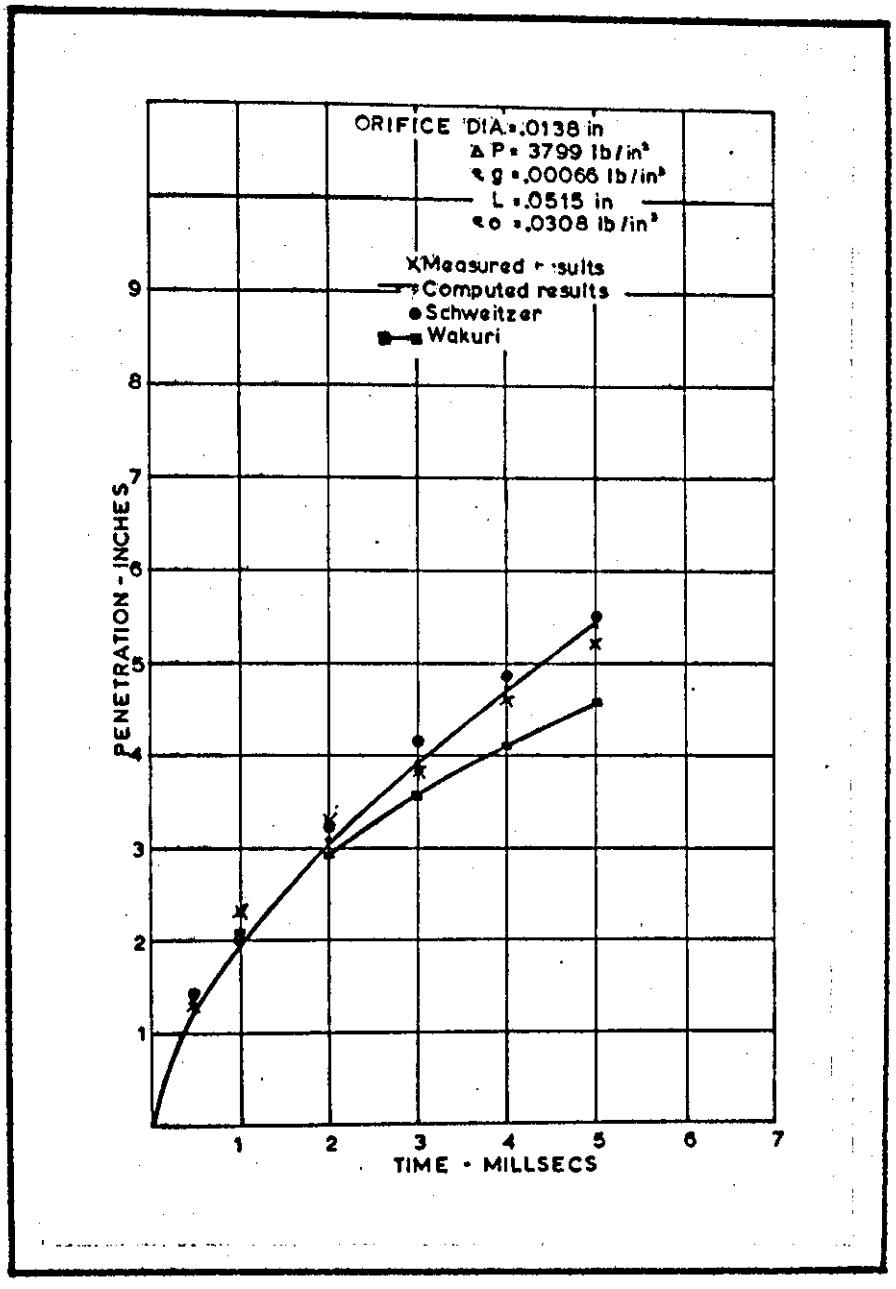

Figure 74 Comparison of measured, predicted spray penetration together with predicted curves from Wakuri [15] and Schweitzer [9] for a .0138" diameter orifice.

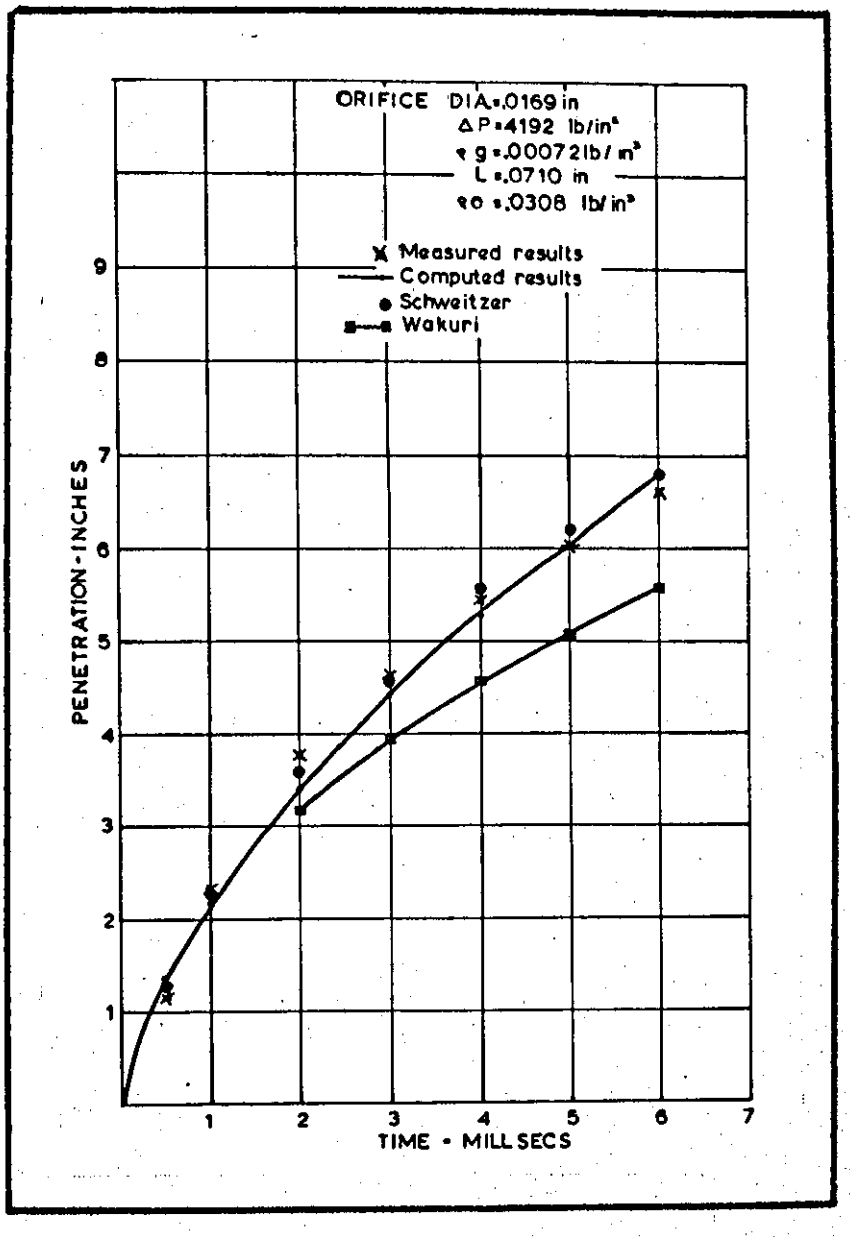

Figure 75 Comparison of measured, predicted spray penetration together with predicted curves from Wakuri [15] and Schweitzer [9] for a .0169" diameter orifice.

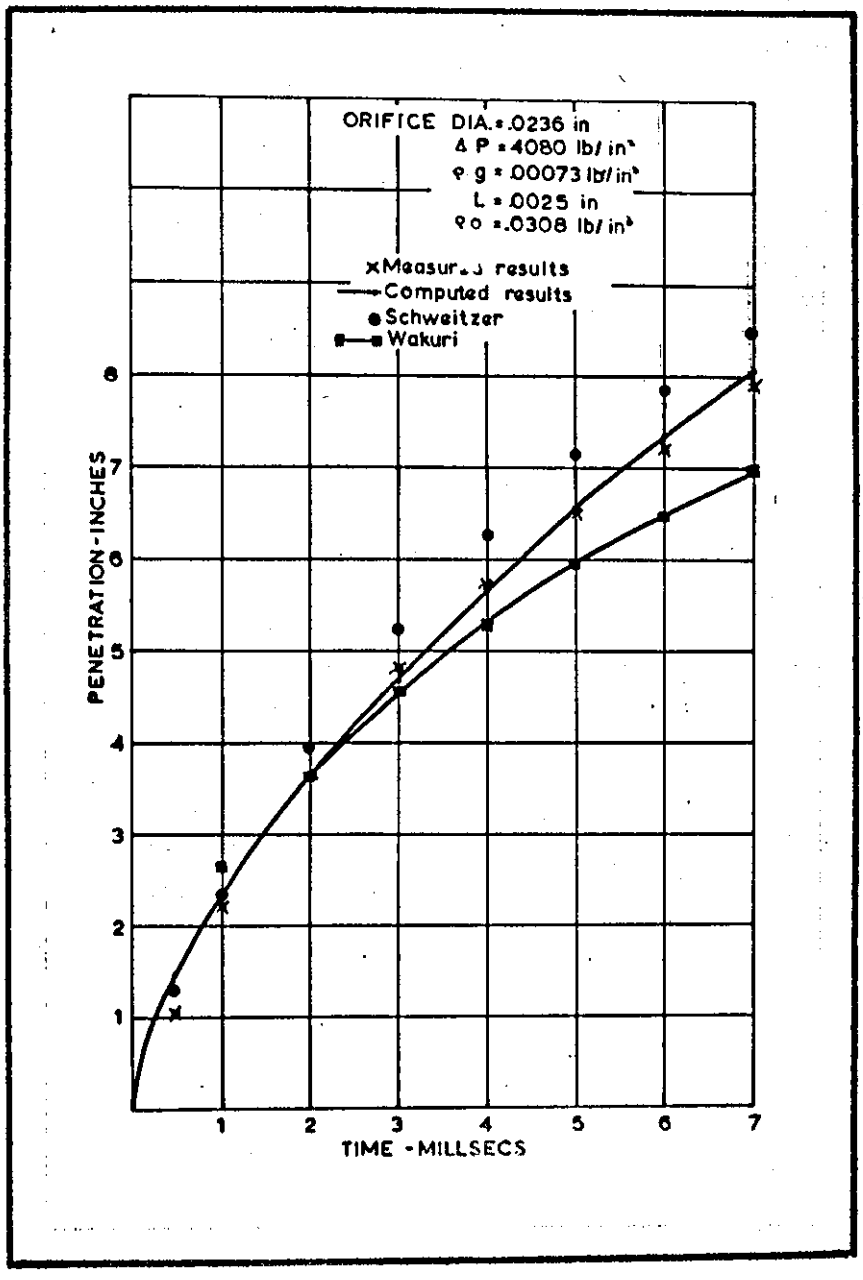

Figure 76 Comparison of measured, predicted spray penetration together with predicted curves from Wakuri [15] and Schweitzer [9] for a .0236" diameter orifice.

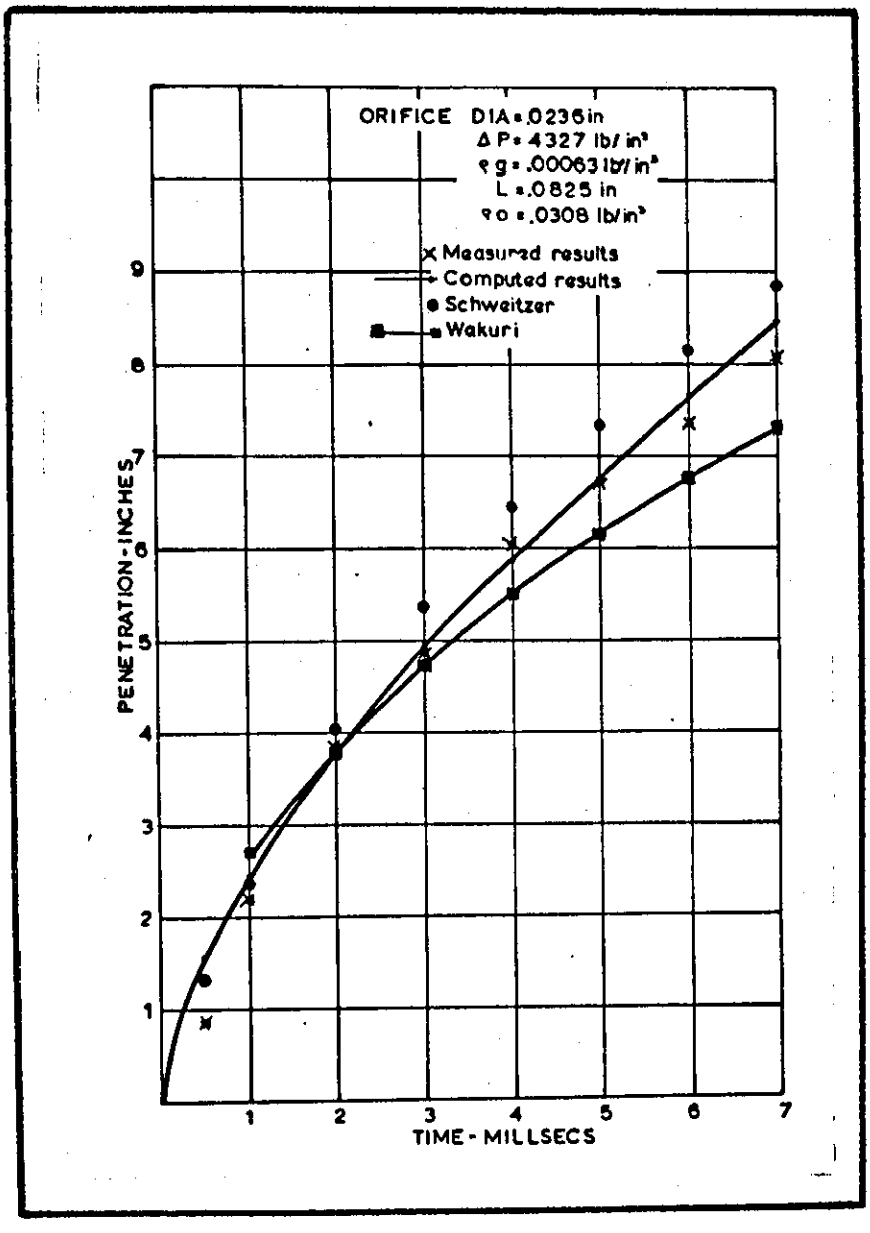

Figure 77 Comparison of measured, predicted spray penetration together with predicted curves from Wakuri [15] and Schweitzer [9] for .0236" diameter orifice.

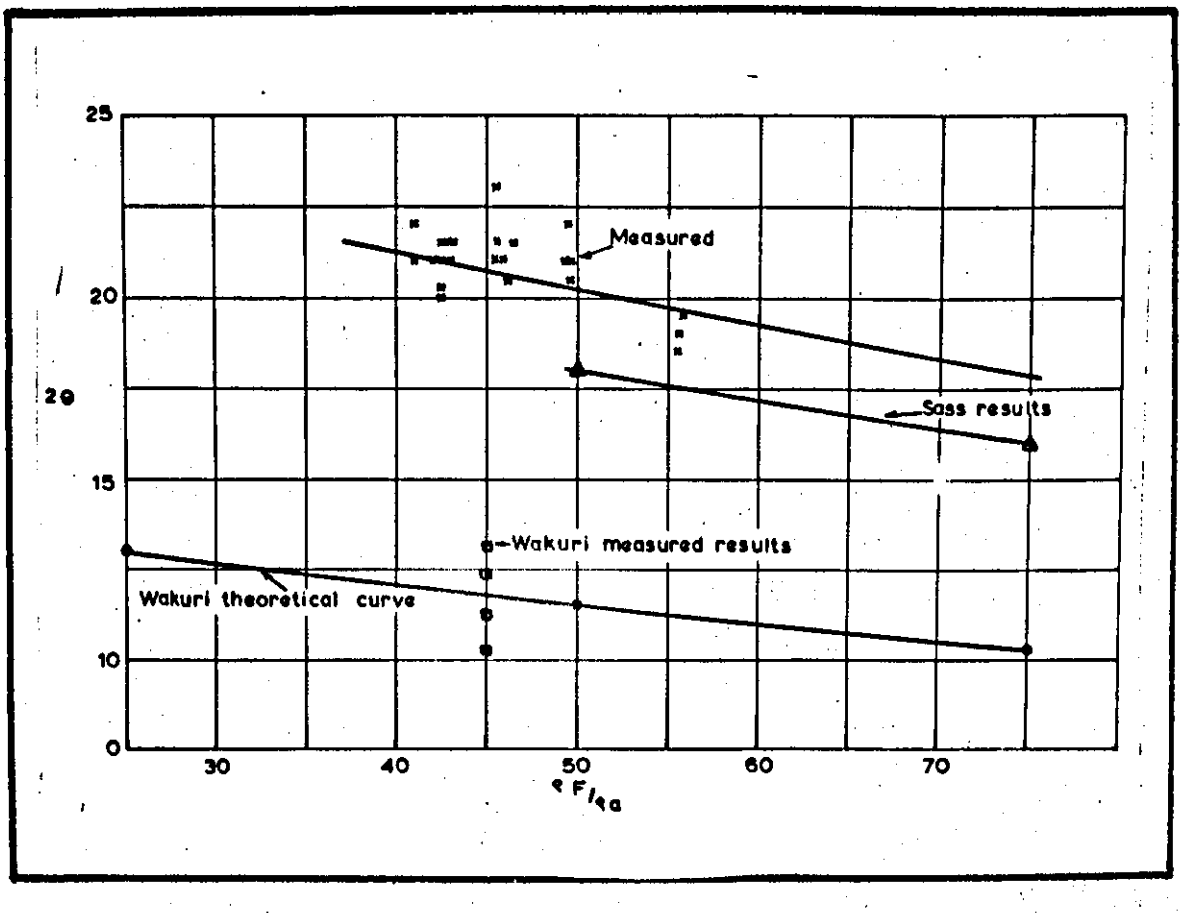

Figure 78 Spray cone angle against the ratio of fuel and air density.

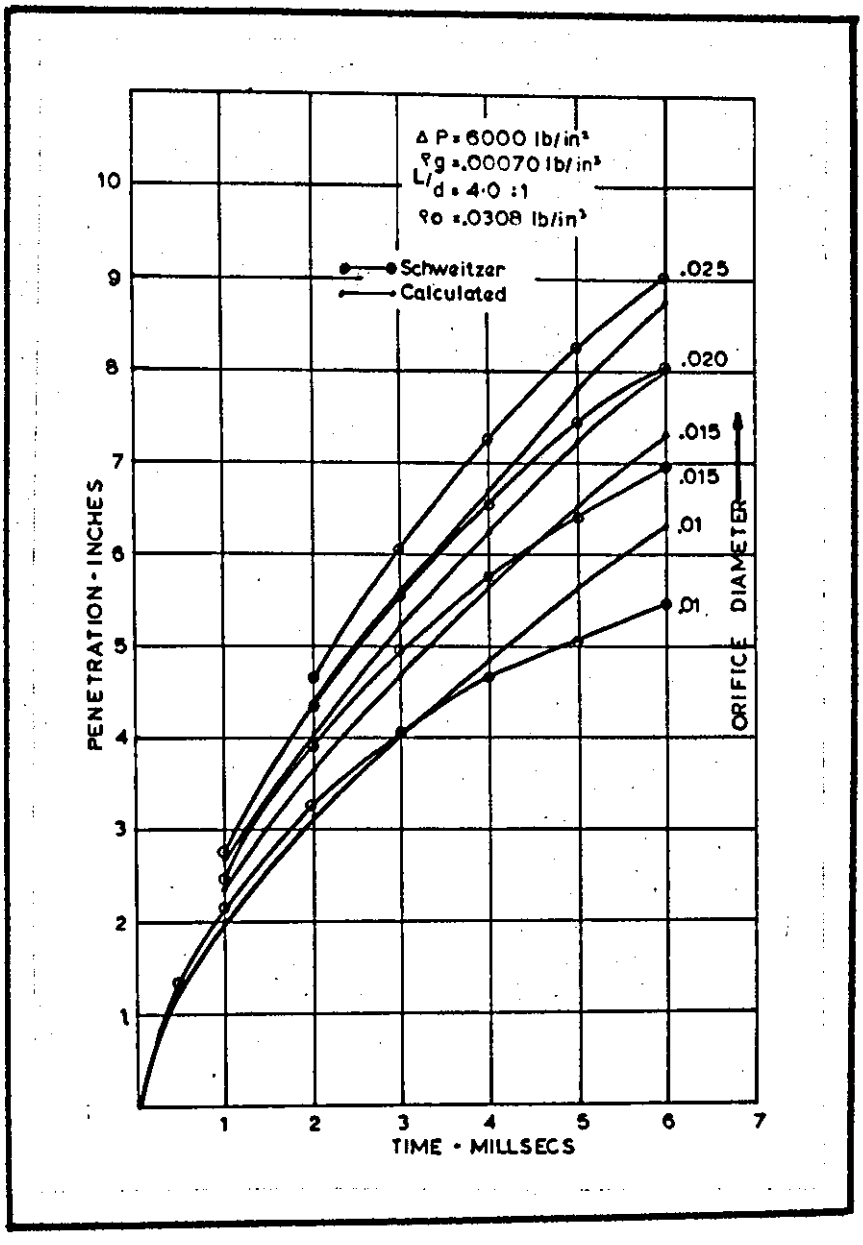

Figure 79 The effect of orifice diameter on spray penetration. Comparing Schweitzer and proposed equation.

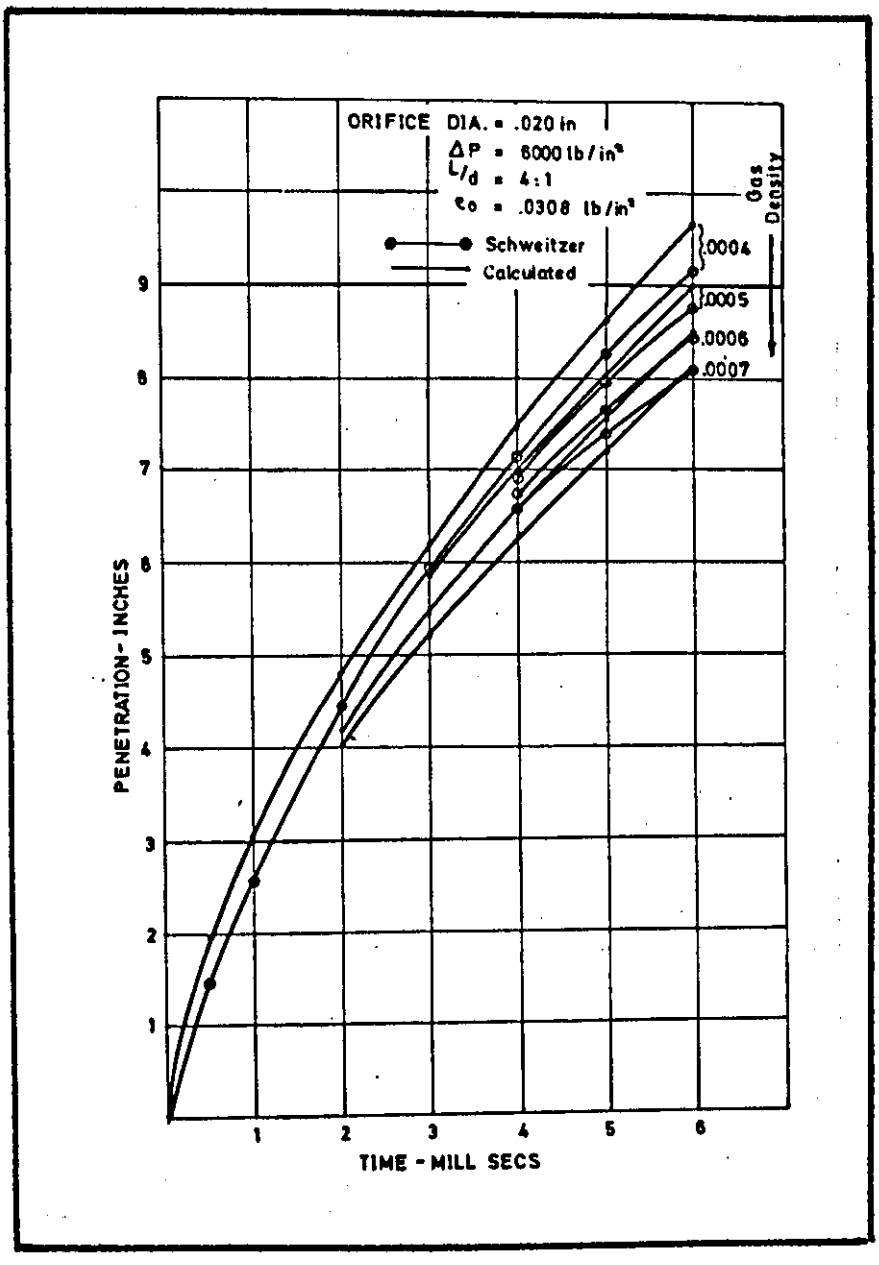

Figure 80 Effect of gas density on spray penetration comparing Schweitzer and proposed equation.

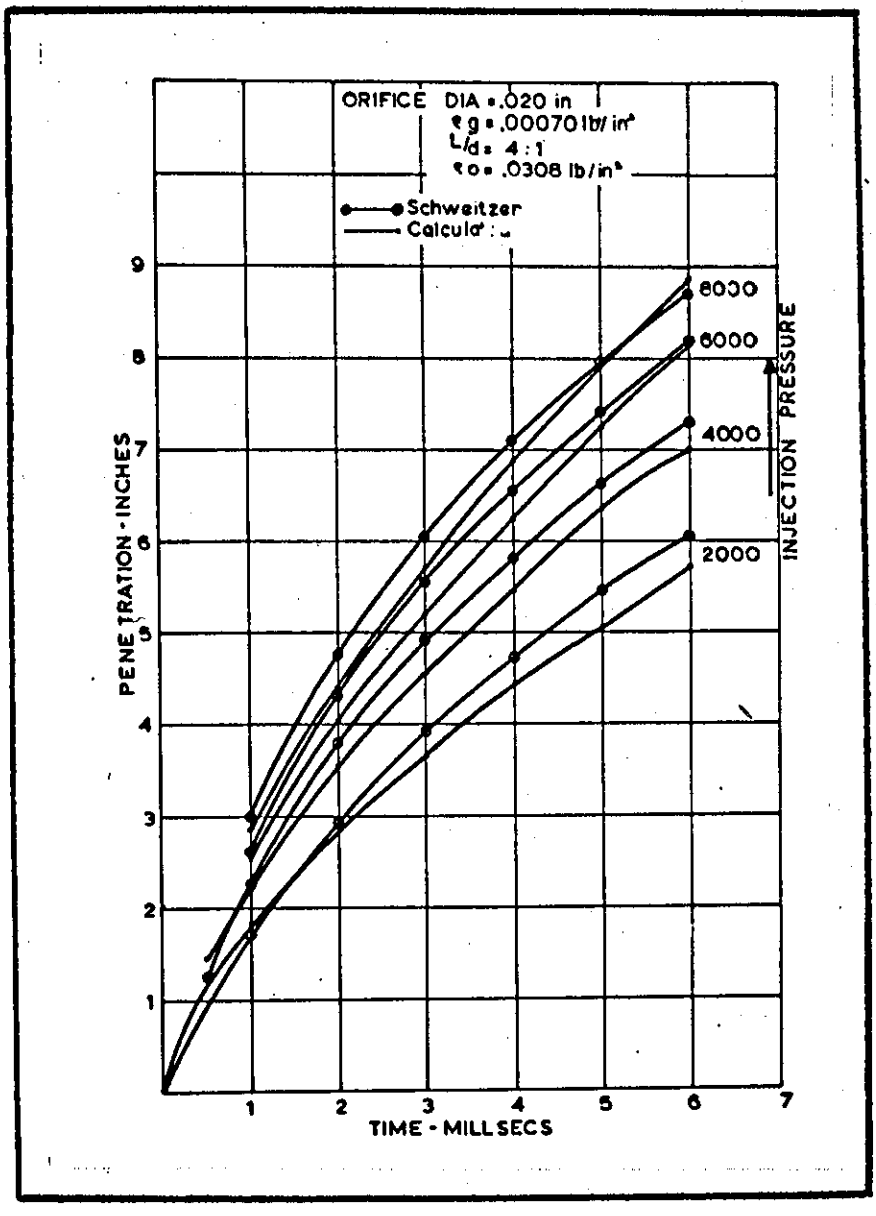

Figure 81 Effect of injection pressure on spray penetration comparing Schweitzer and proposed equation.

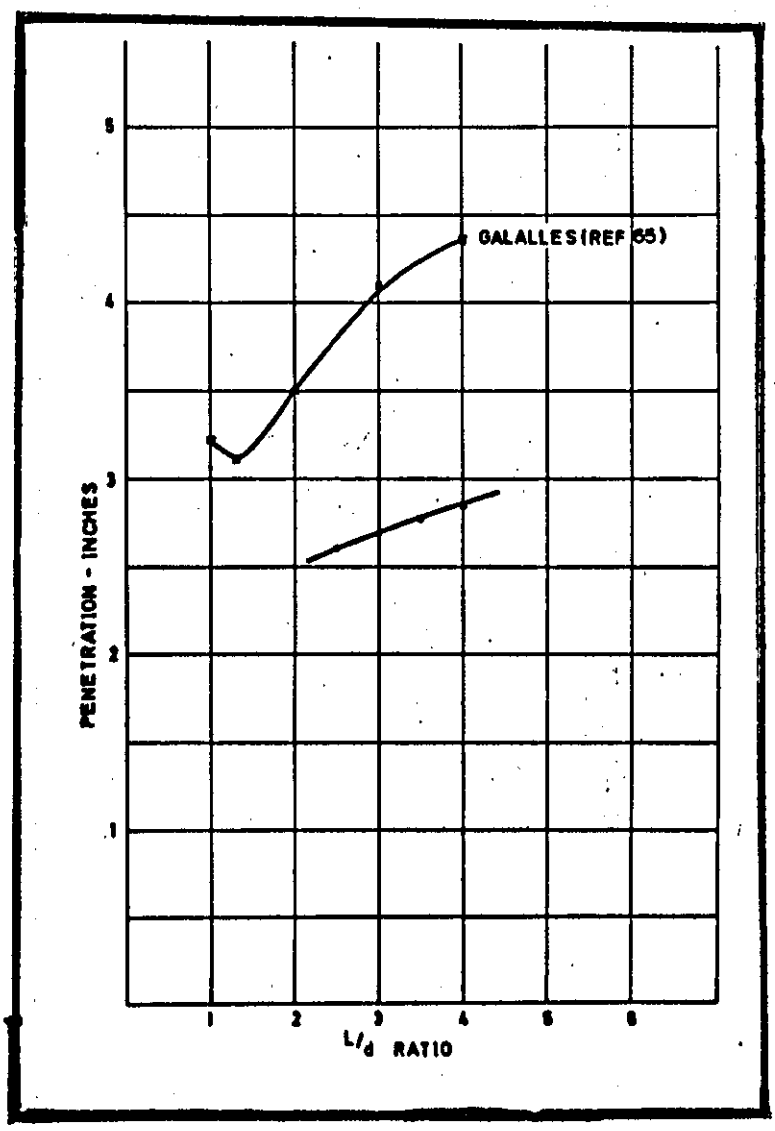

Figure 82 The effect of L/D ratio on spray penetration as found by Gelalles and compared with predicted results.

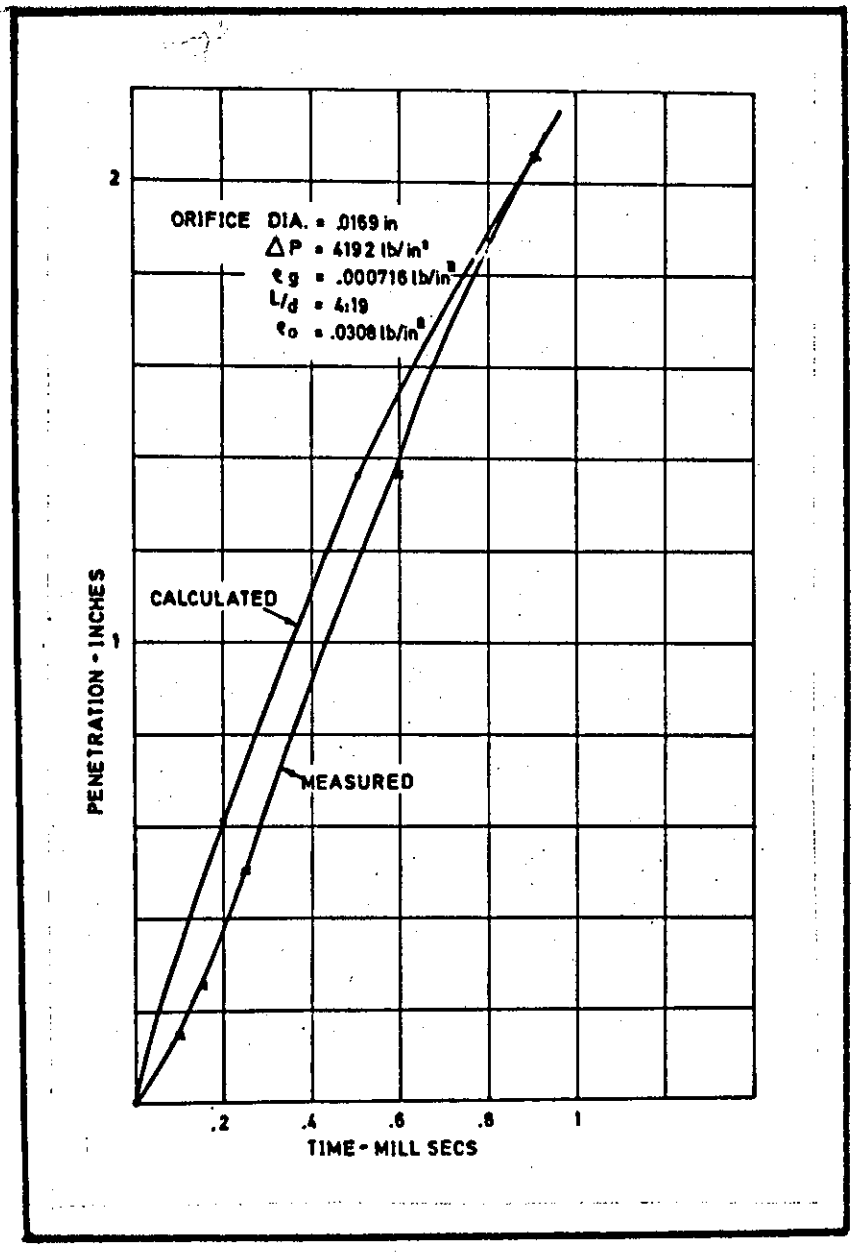

Figure 83 Deviation of calculated penetration from the measured during the initial part of the spray history.

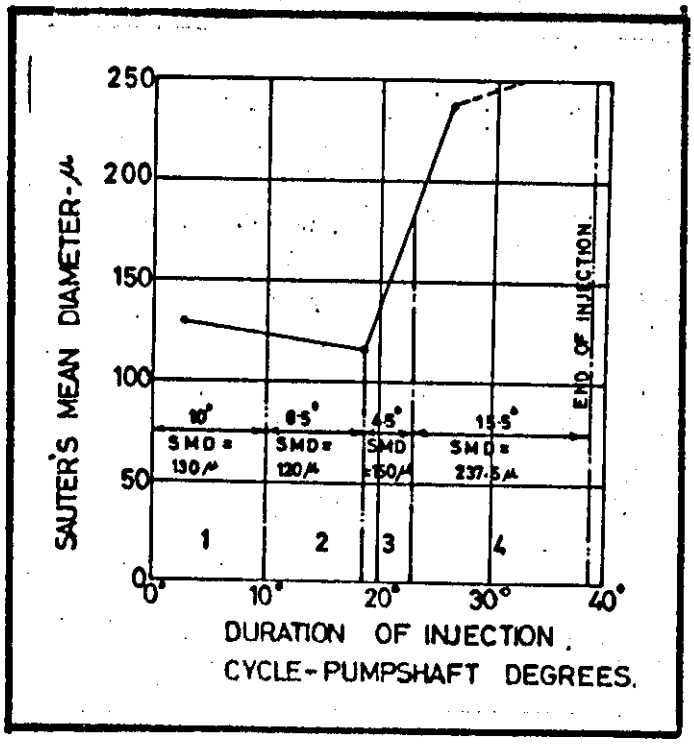

Figure 84 Variation of mean droplet diameter throughout the injection period. Giffen and Muraszew [8].

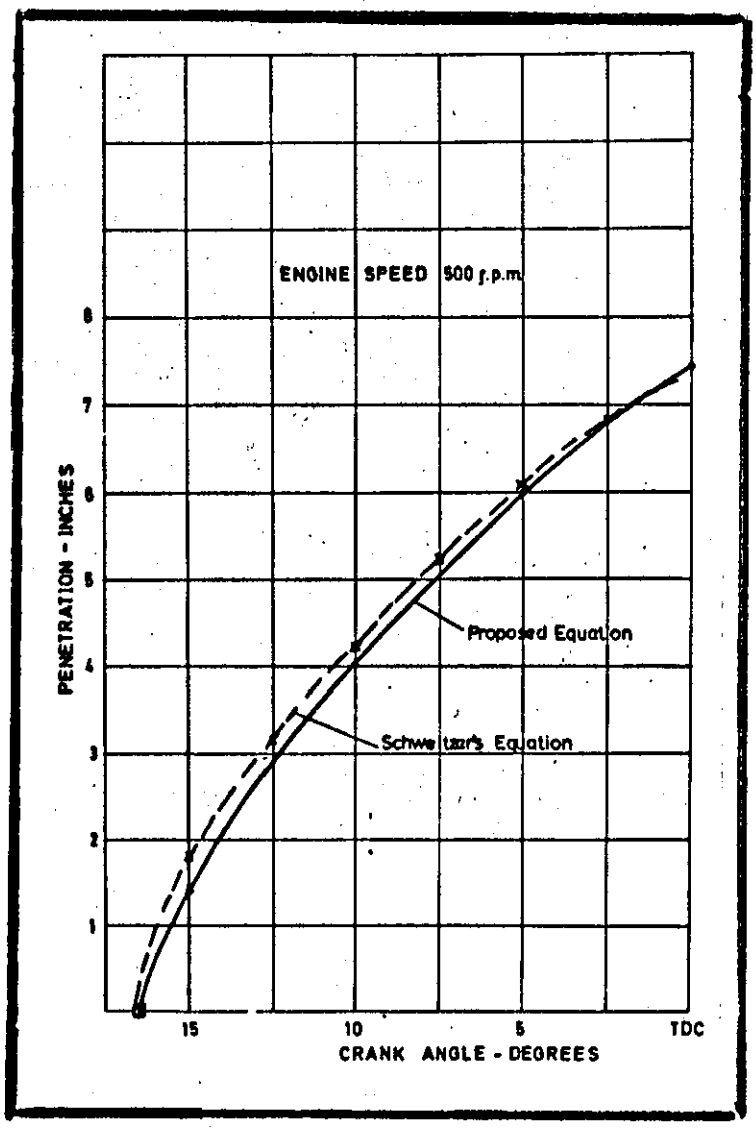

Figure 85 Penetration of spray calculated by the proposed equation for conditions in the 12½" bore engine.

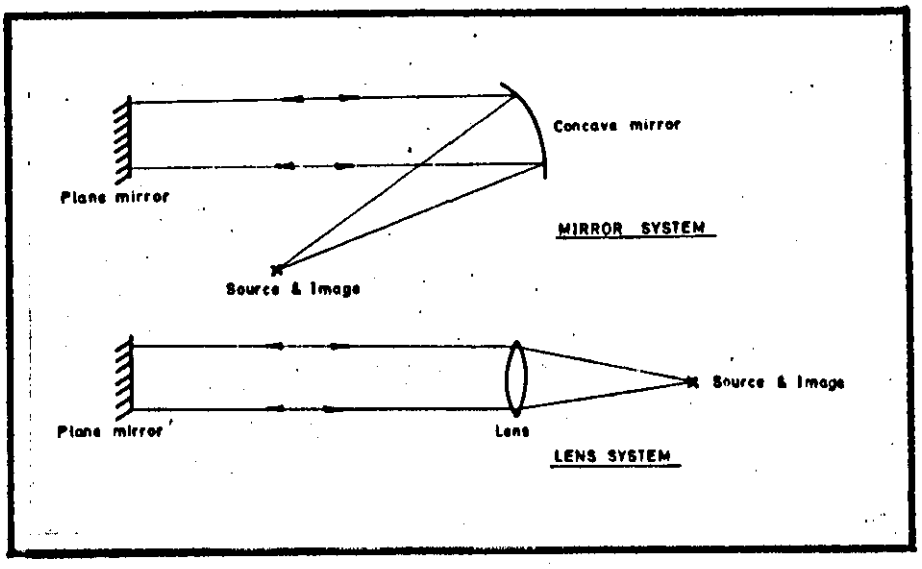

Figure 86 Simple layout of a Double Pass Schlieren system.

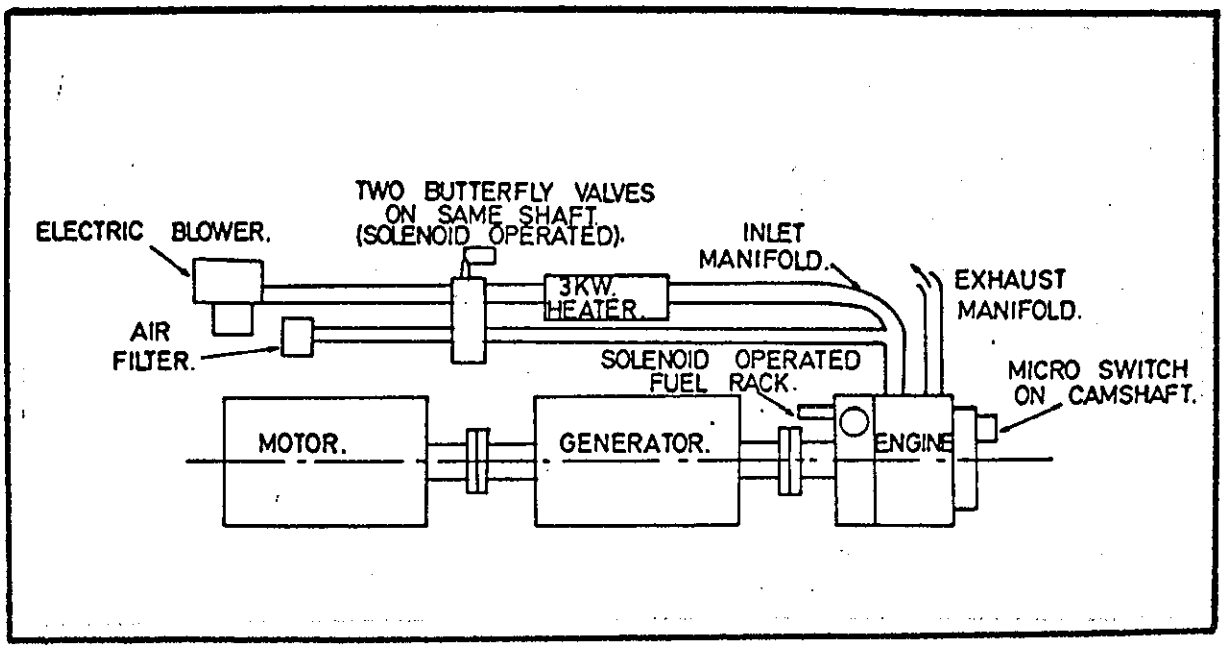

Figure 87 General layout of Small Diesel Engine Rig.

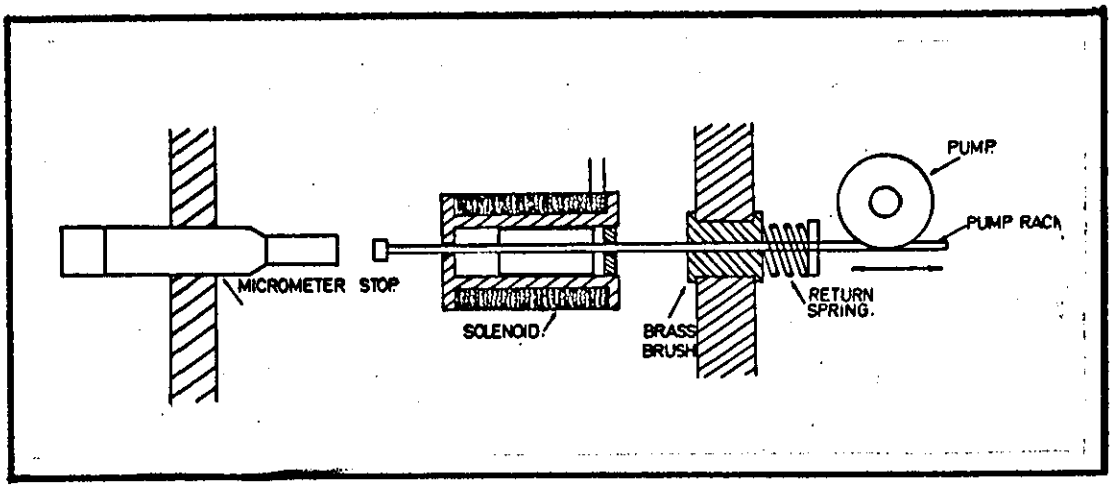

Figure 88 Layout of Solonoid Operated Fuel Rack.

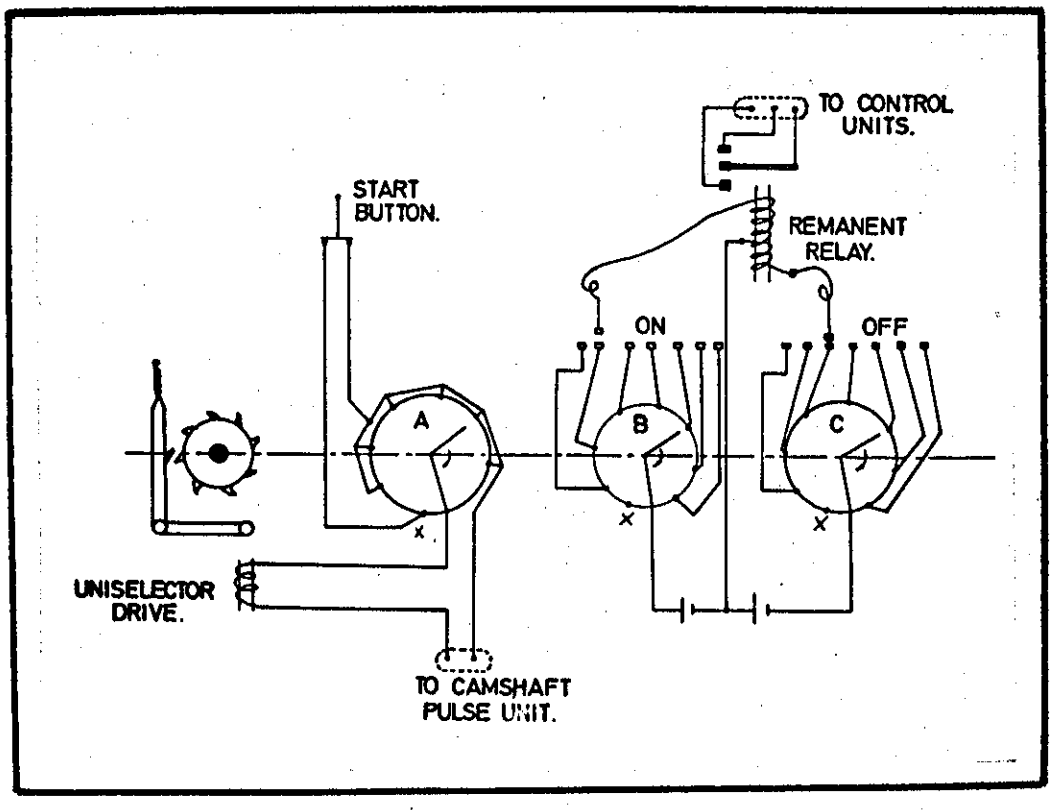

Figure 89 Principle of circuit for sequencer.

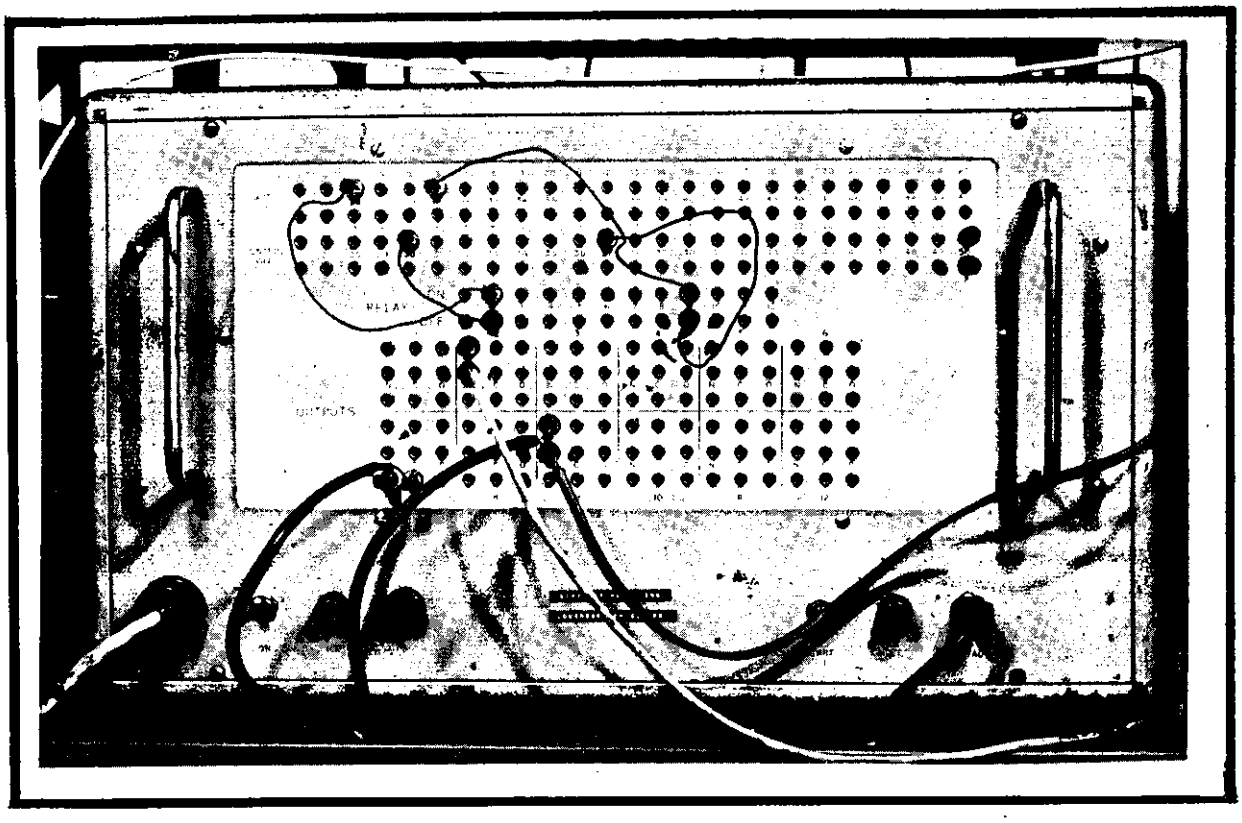

Figure 90 General view of sequencer.

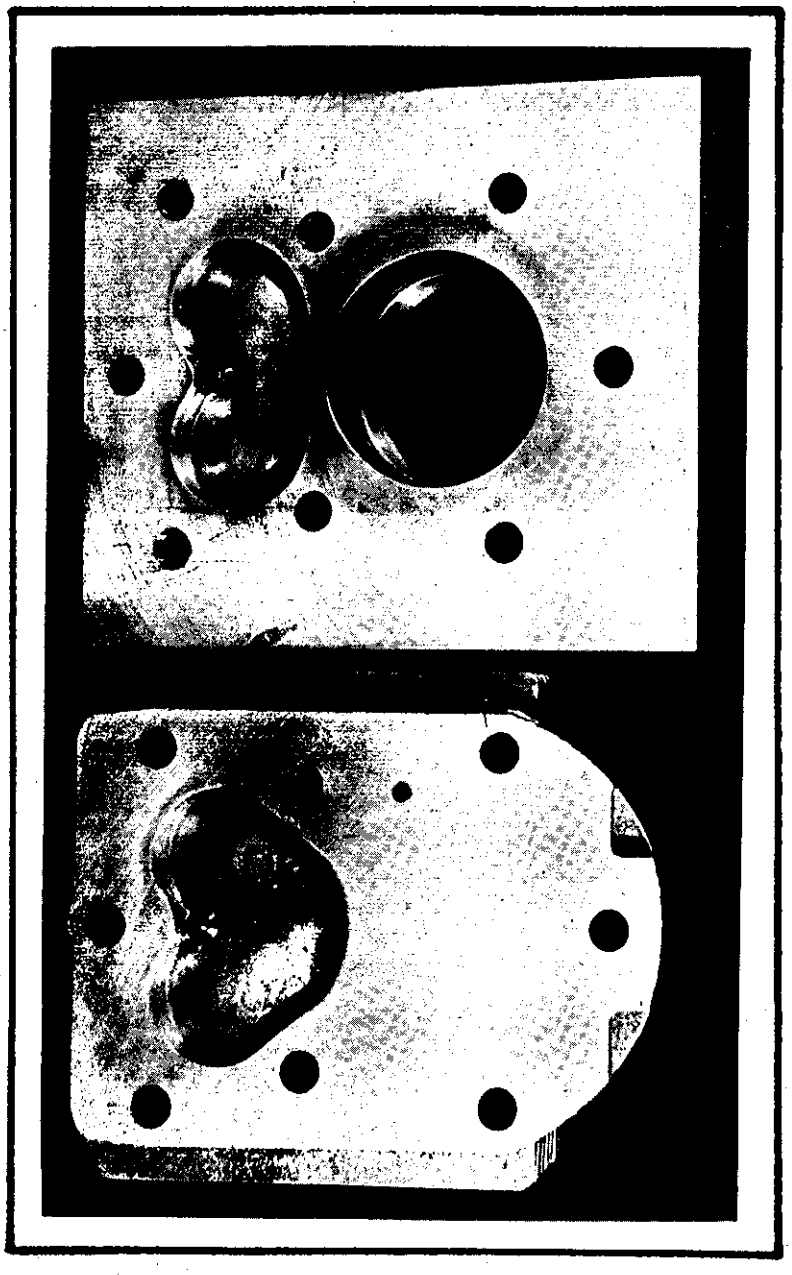

Figure 91 Comparison of standard cylinder head (right) and photographic head.

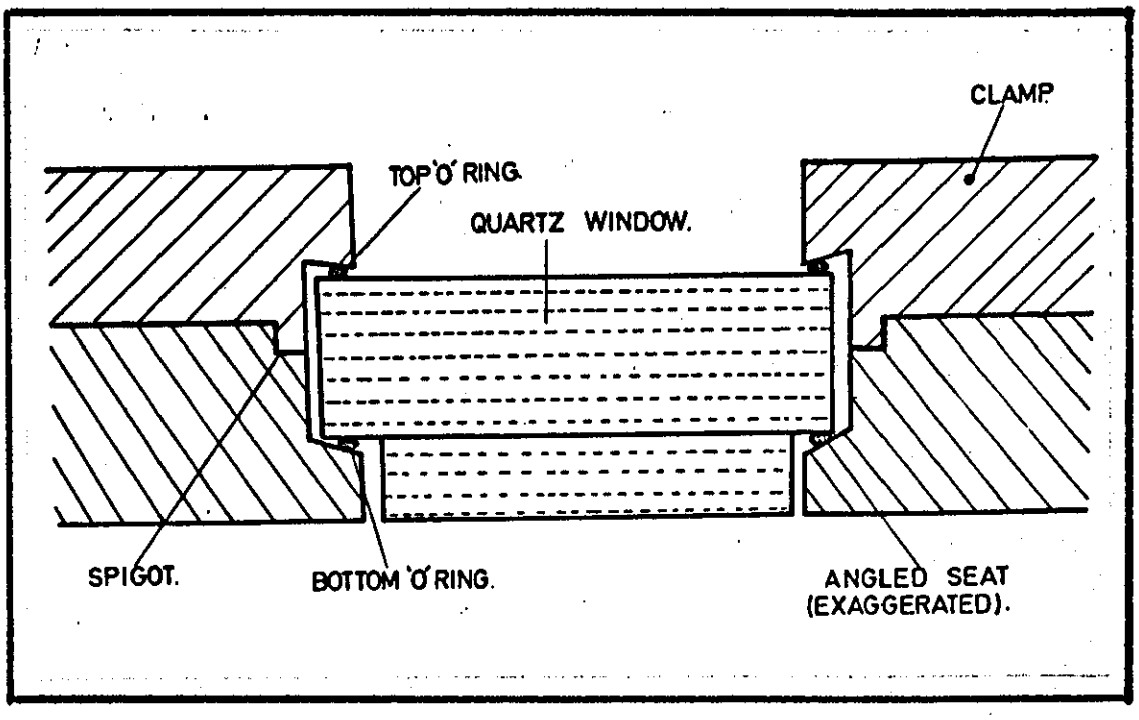

Figure 92 Diagram of cylinder head window.

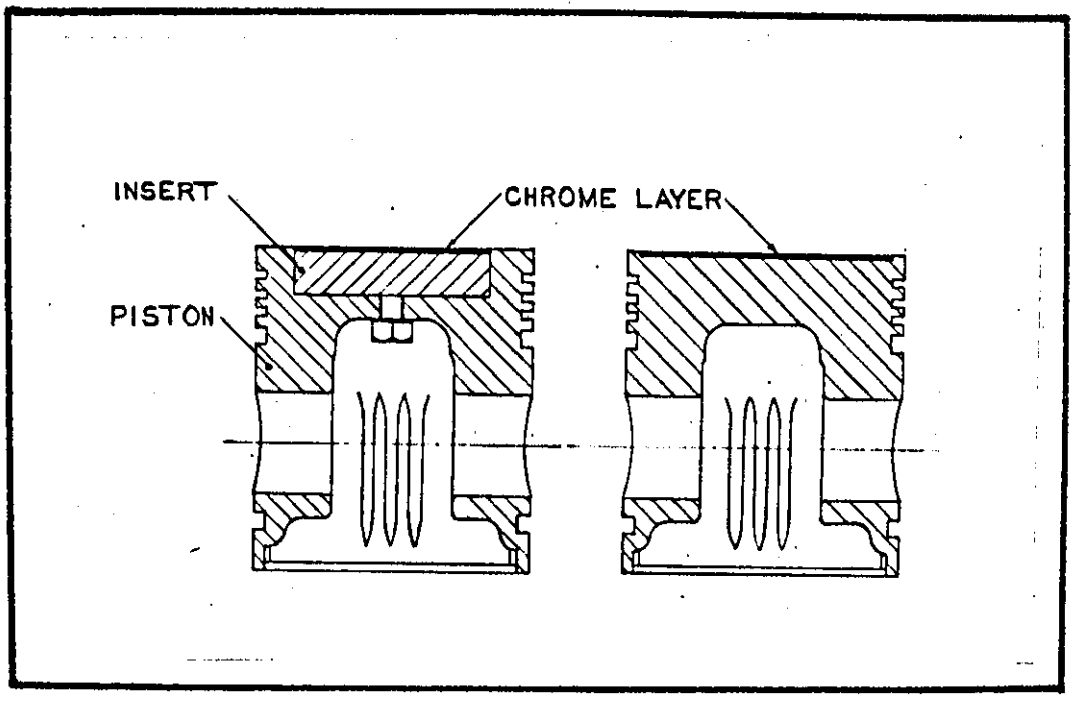

Figure 93 Method of mounting piston mirror. Insert method (left) and directly deposited method.

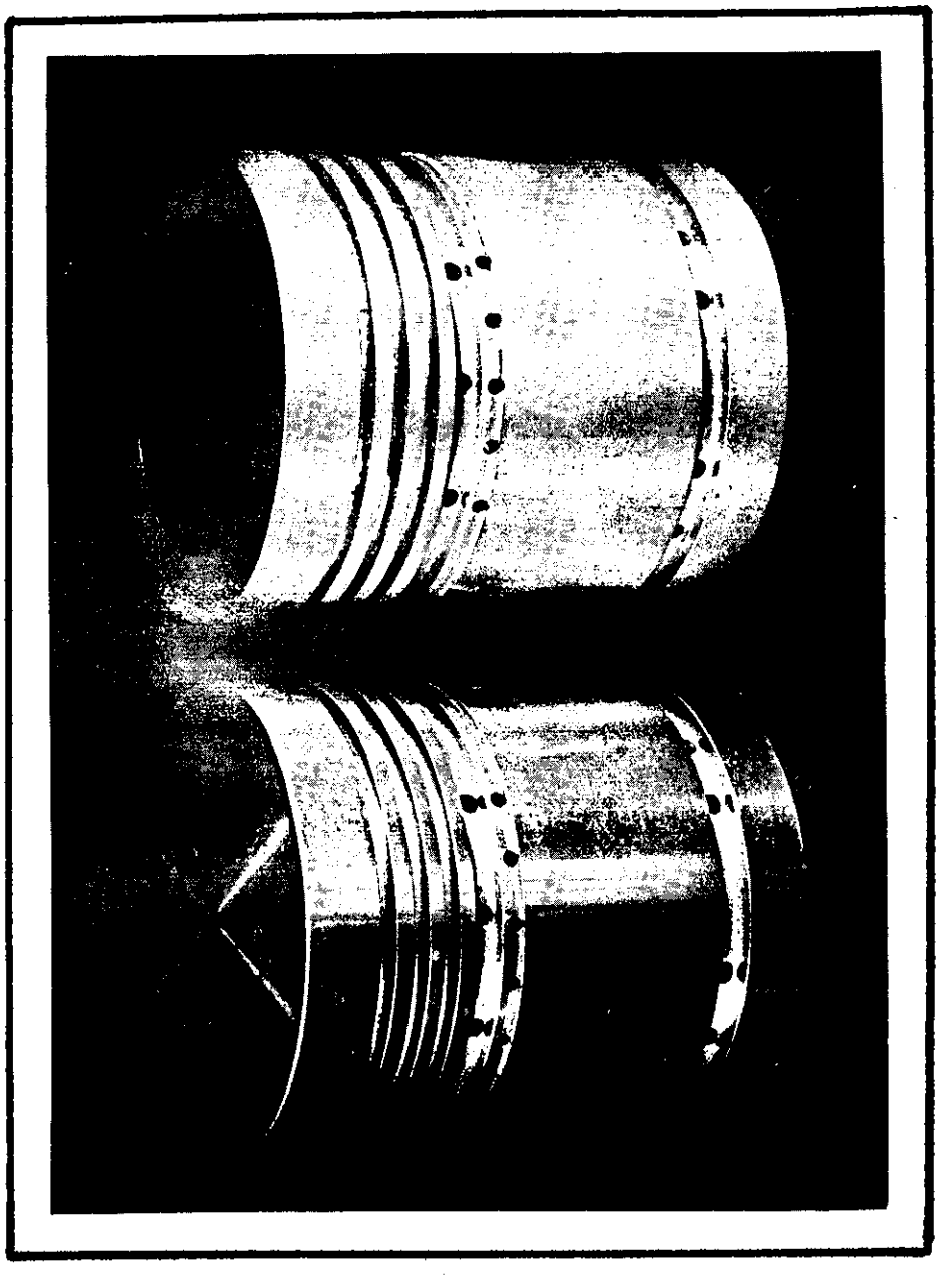

Figure 94 Comparison of standard and mirror piston.

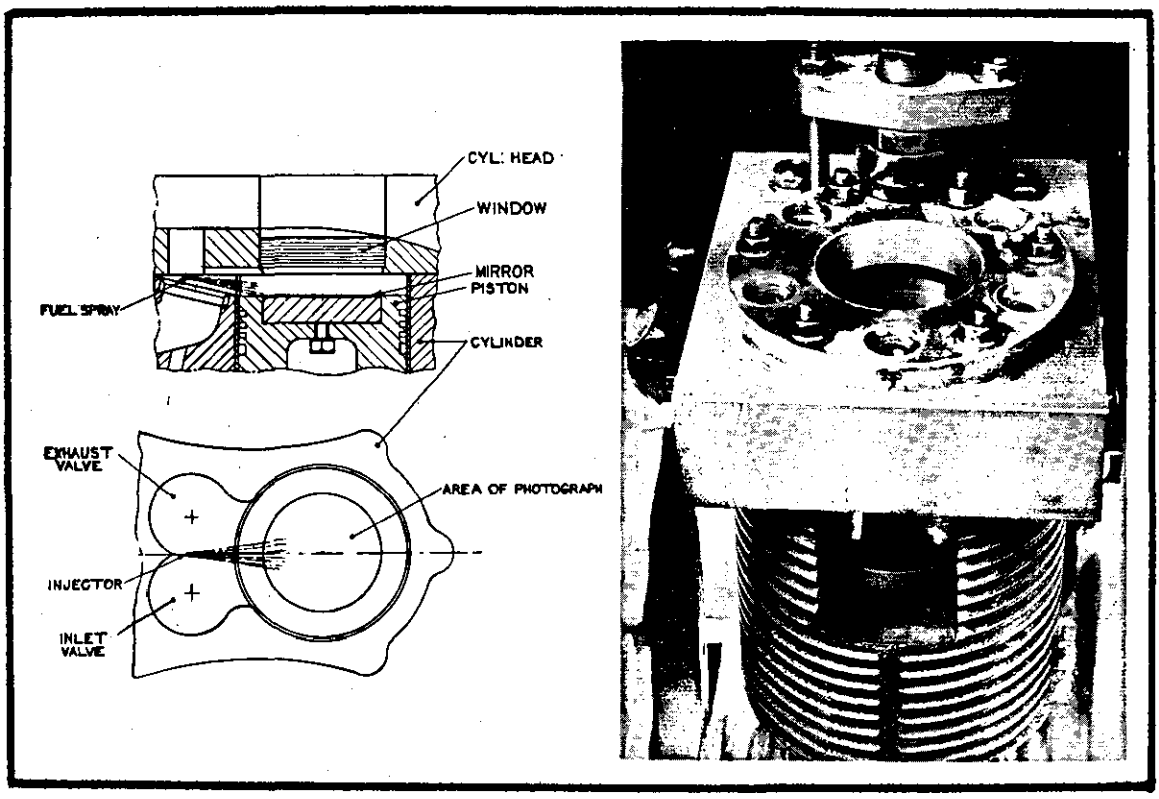

Figure 95 Sketch of combustion chamber shape together with cut away assembly of the small engine.

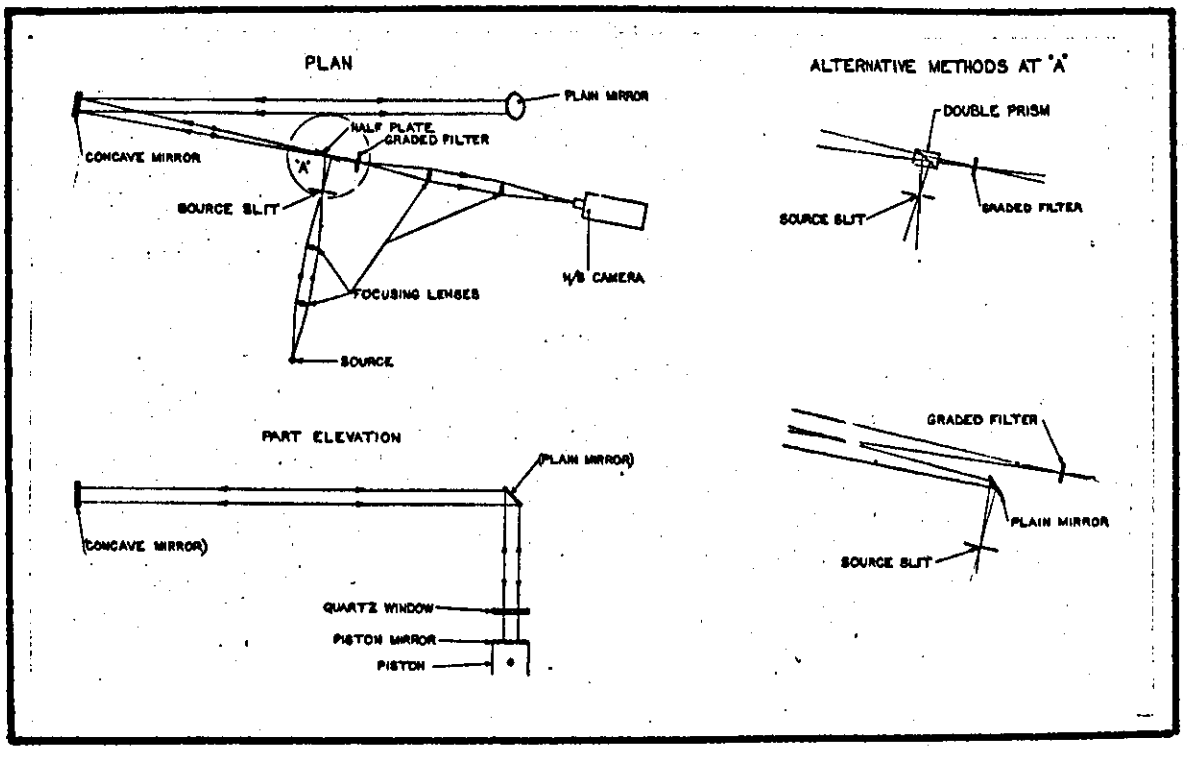

Figure 96 Diagrammatic arrangement of small engine rig.

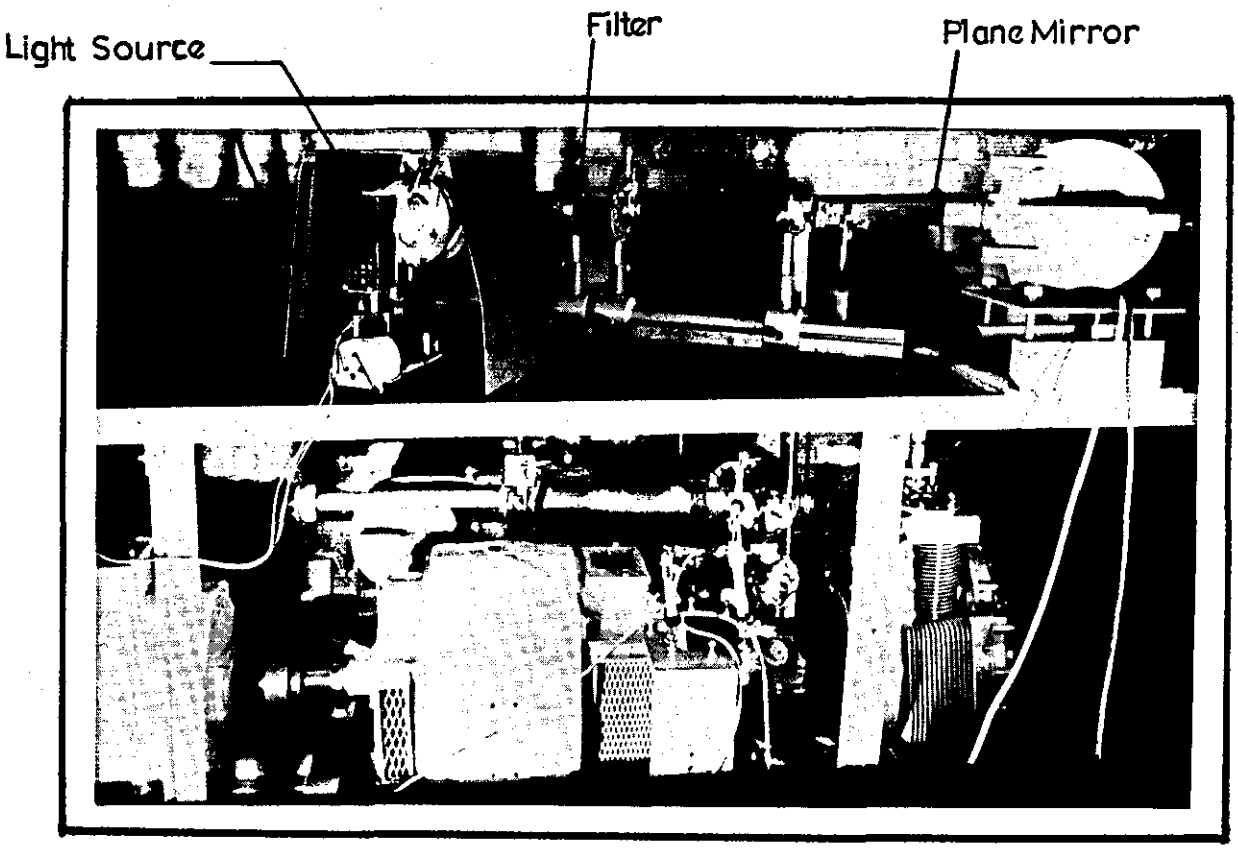

Figure 97 Actual arrangement of small engine rig.

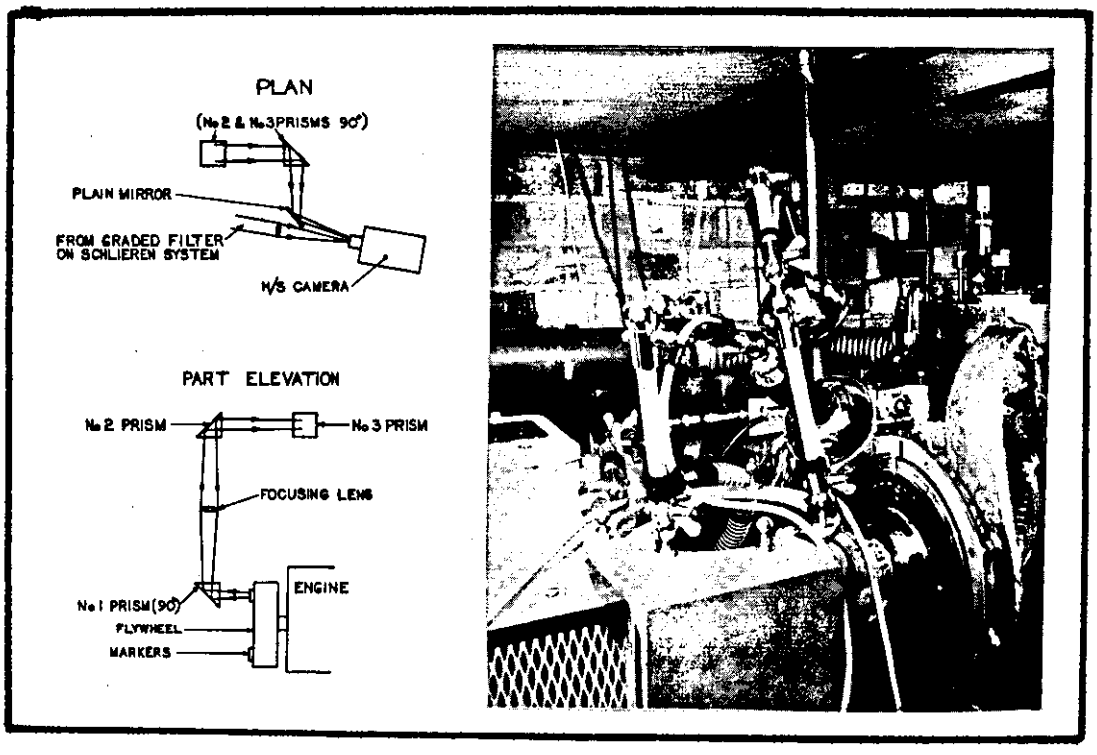

Figure 98 Diagrammatic and actual layout of crank degree system.

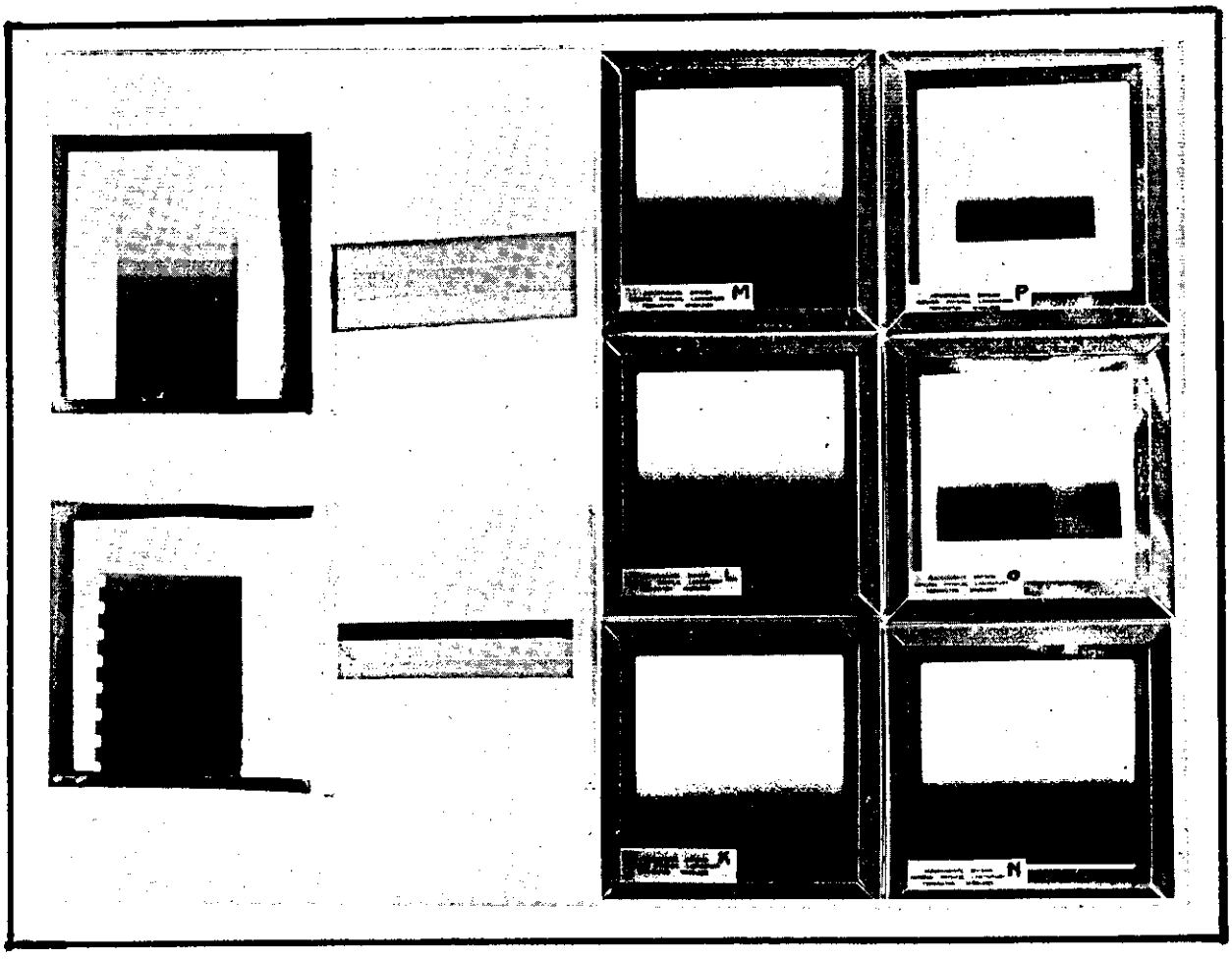

Figure 99 Example of filters used. Left, stepped wedge (black and white), centre, colour filters, right, range of graded filters (black and white).

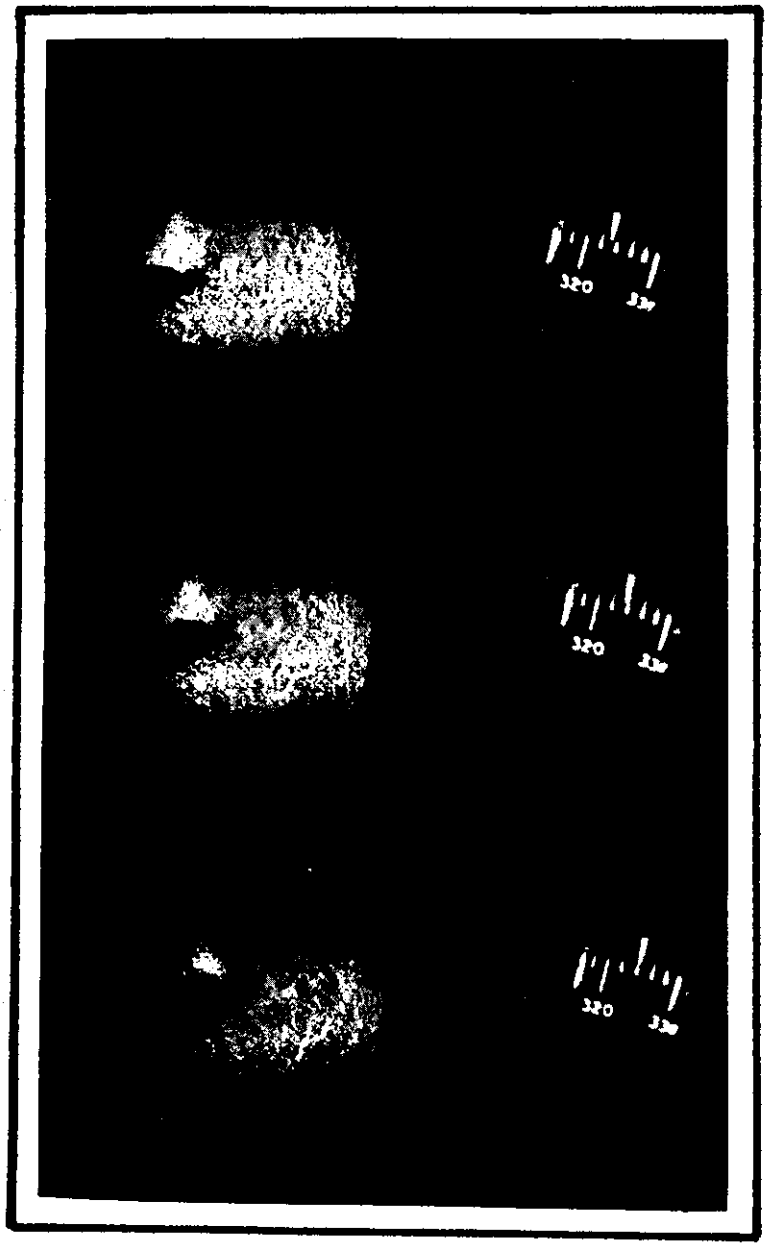

Figure 100 Example of schlieren photograph of fuel spray.

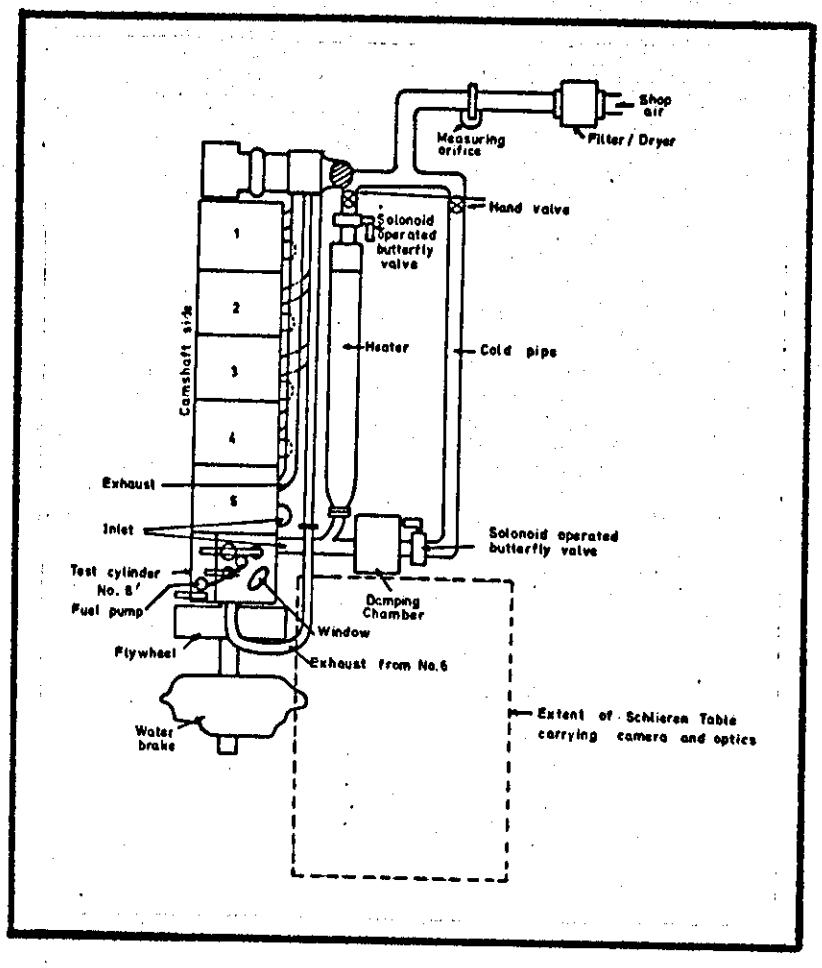

Figure 101 Diagrammatic layout of large engine rig.

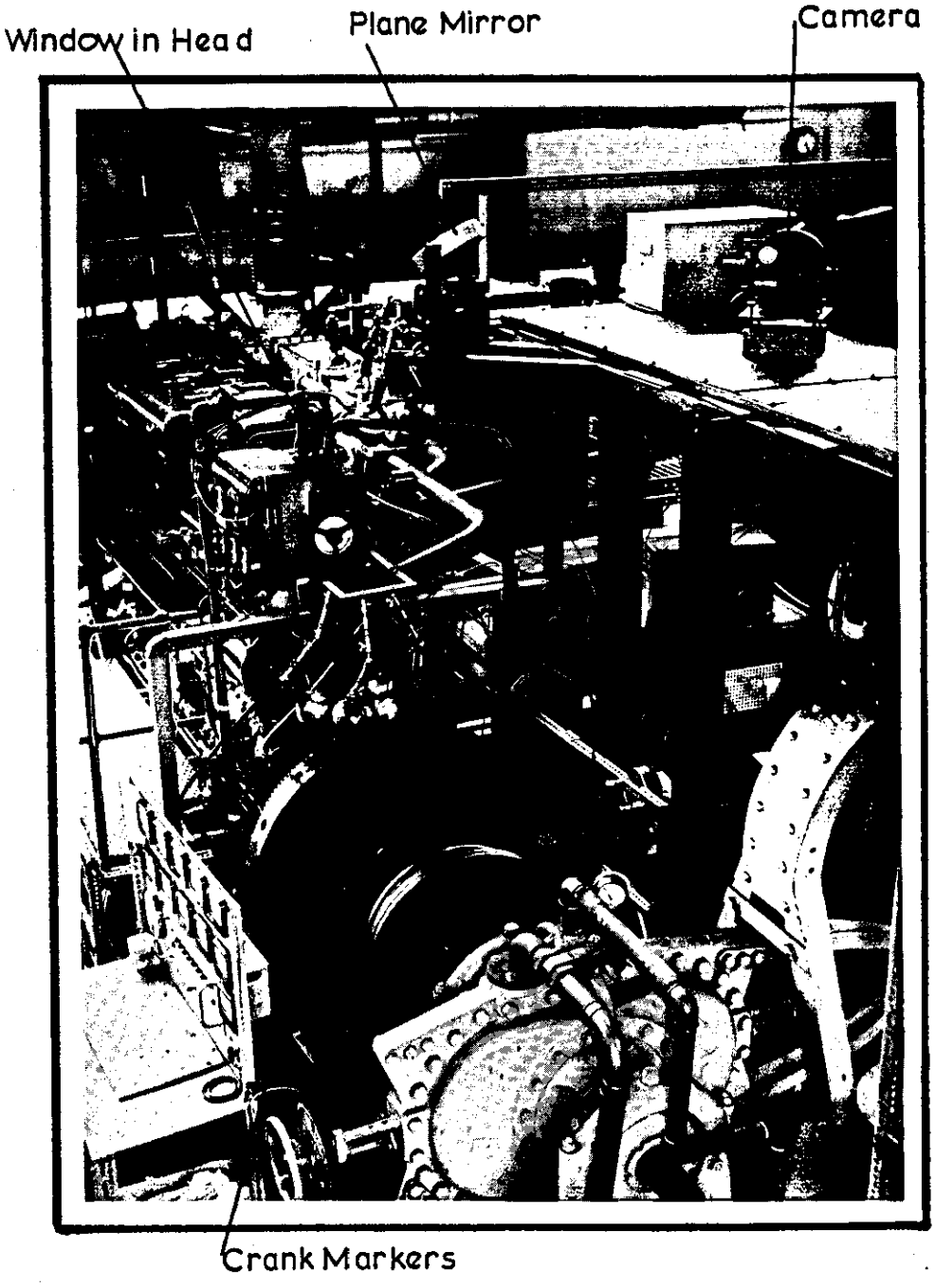

Figure 102 Large engine rig set up for direct photography.

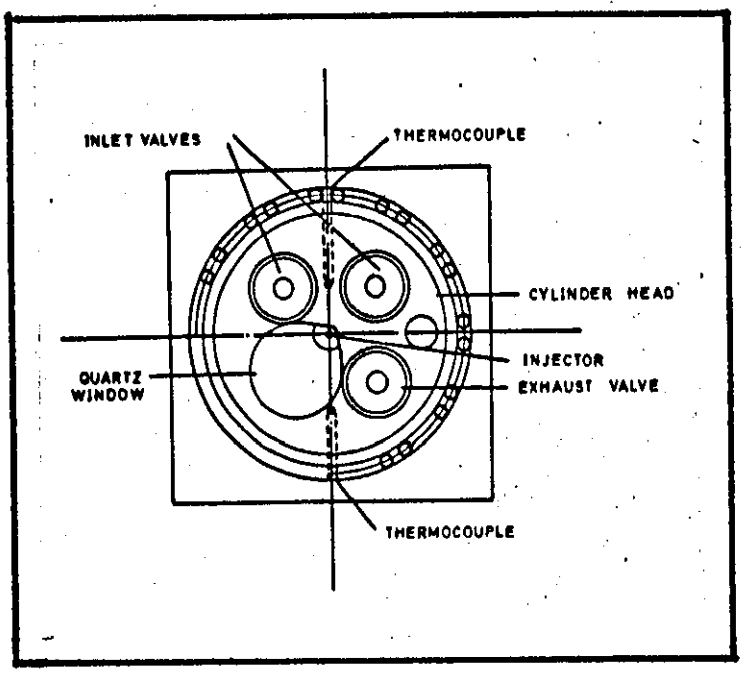

Figure 103 Sketch of large engine cylinder head and position of thermocouples.

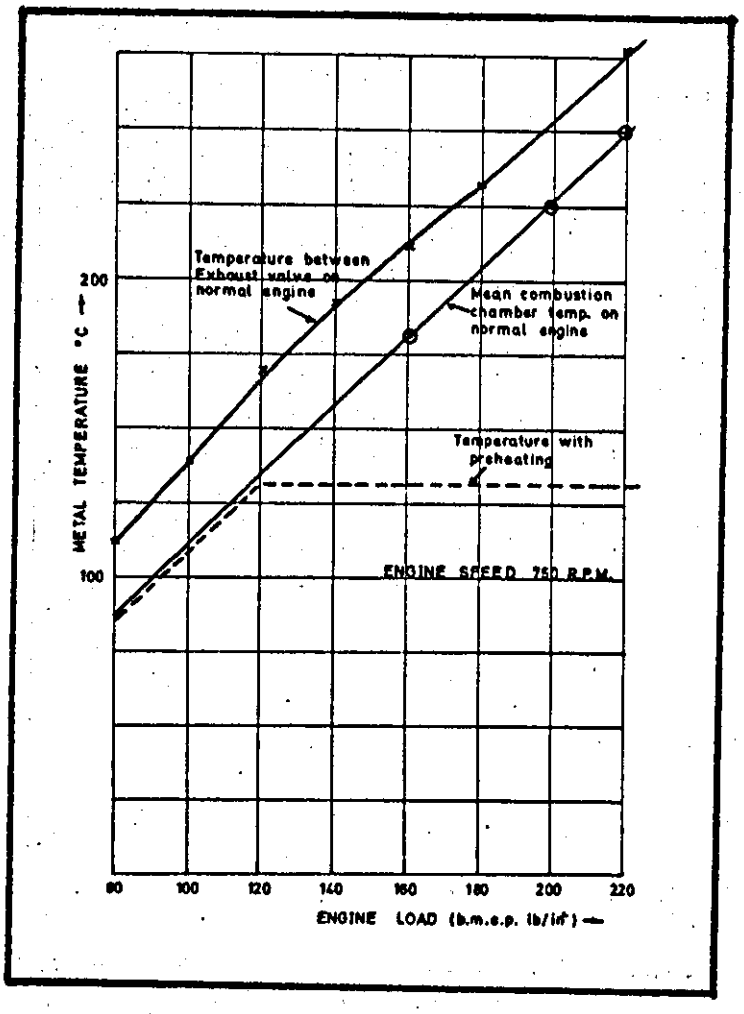

Figure 104 Variations of temperature with load between the exhaust valve of a normal engine together with the mean metal temperature gained on the experimental cylinder.

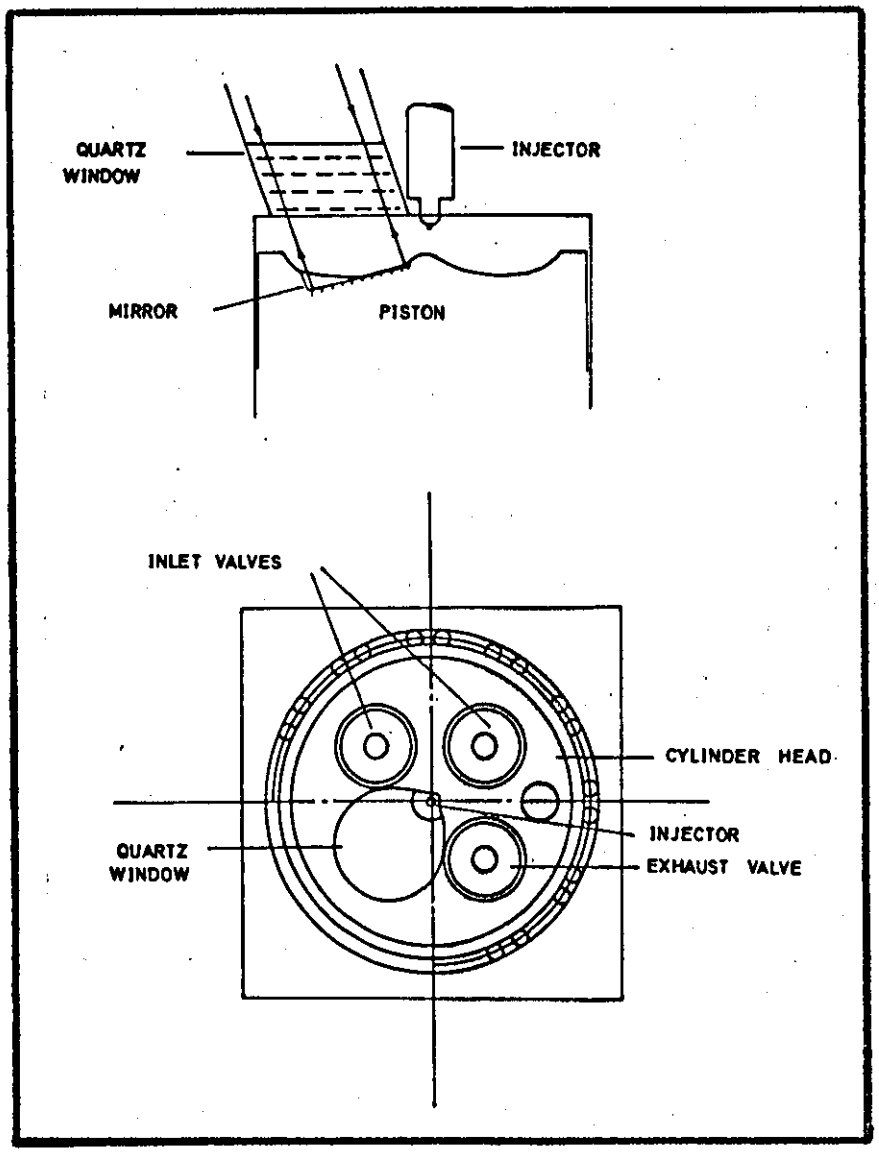

Figure 105 Scheme of combustion chamber design showing the angled window and mirror.

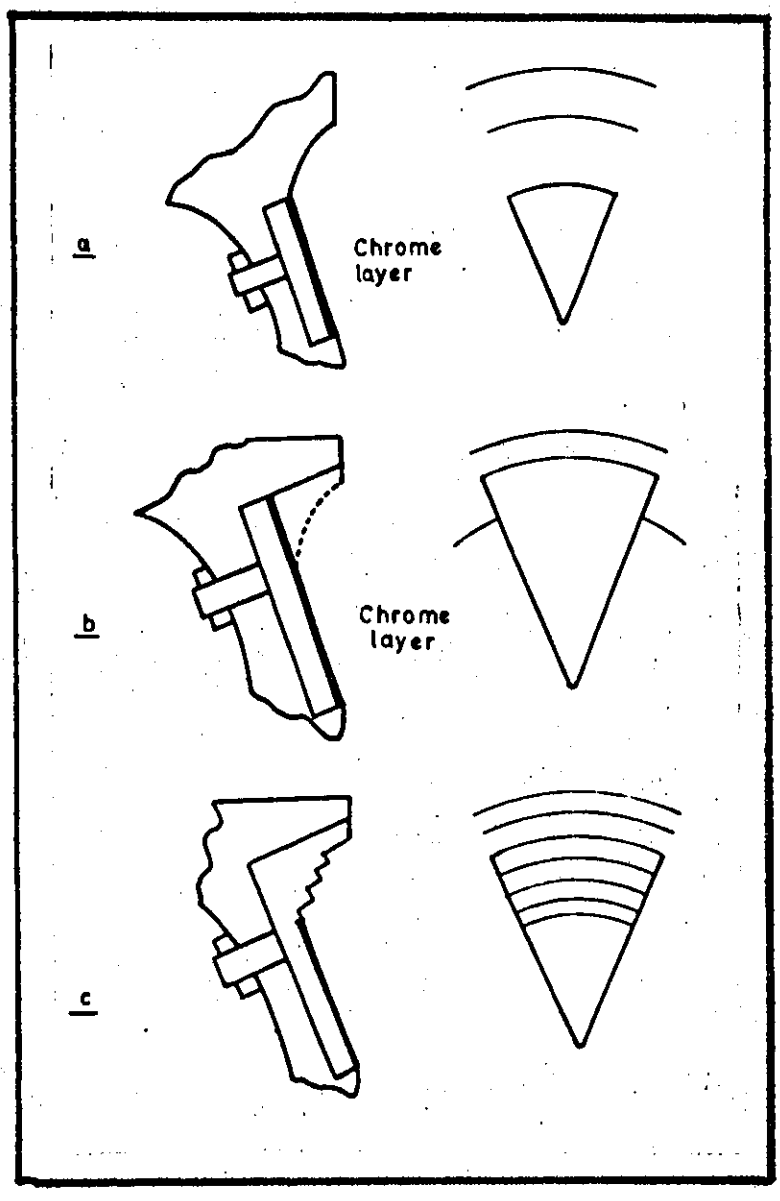

Figure 106 Three shapes of piston mirror intended for use on the large engine

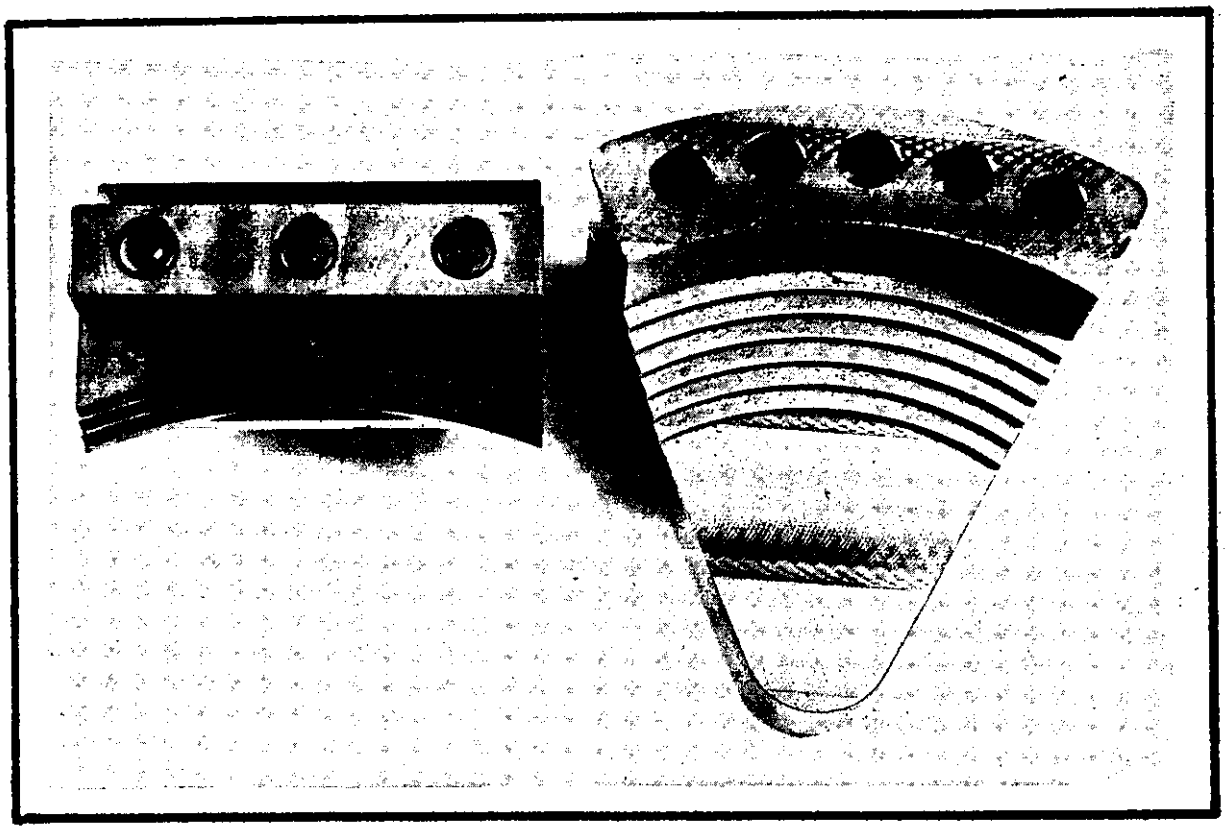

Figure 107 Mock mirror used to test the principle of a stepped mirror together with the actual piston mirror.

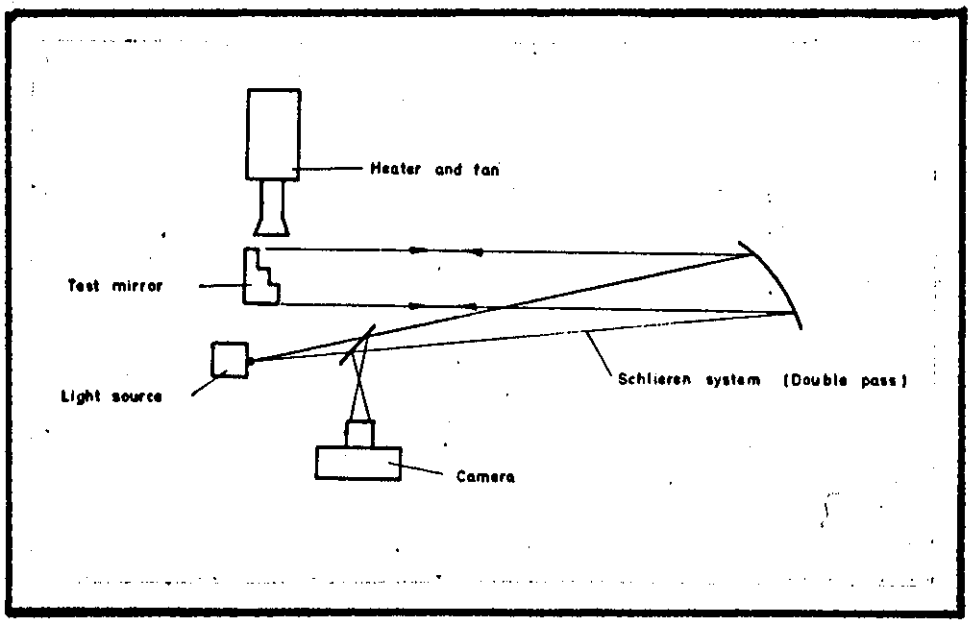

Figure 108 Sketch of test arrangement for the mock up stepped mirror.

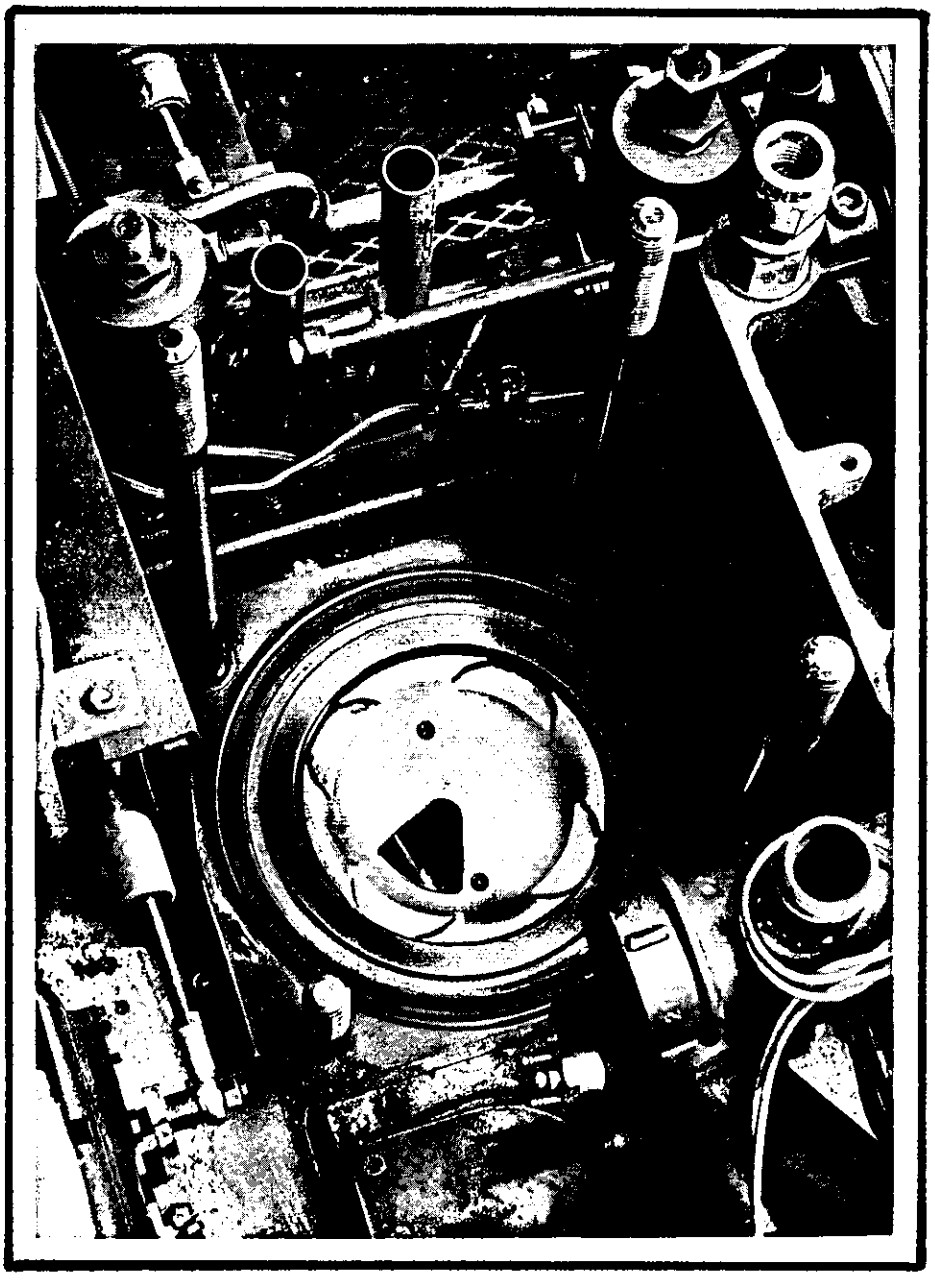

Figure 109 The small mirror in place on the piston.

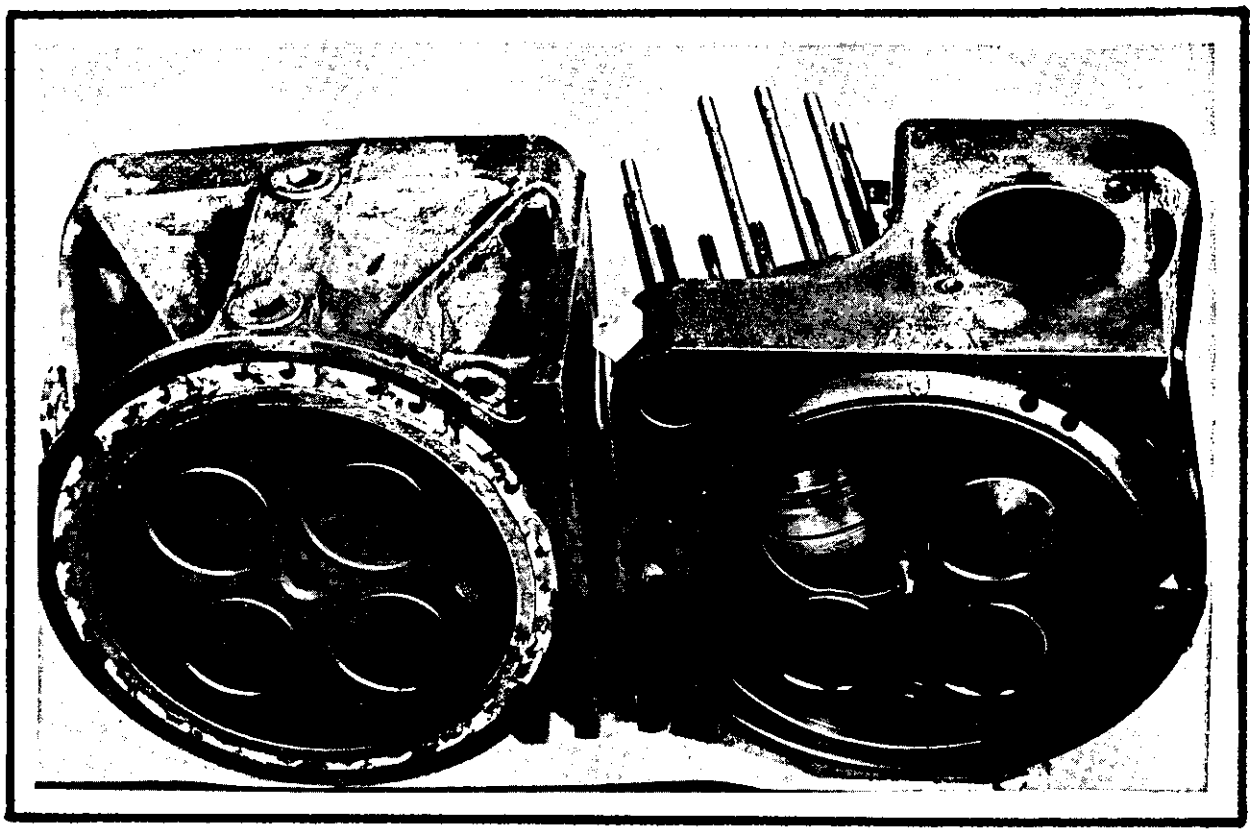

Figure 110 The normal and photographic head showing position of window.

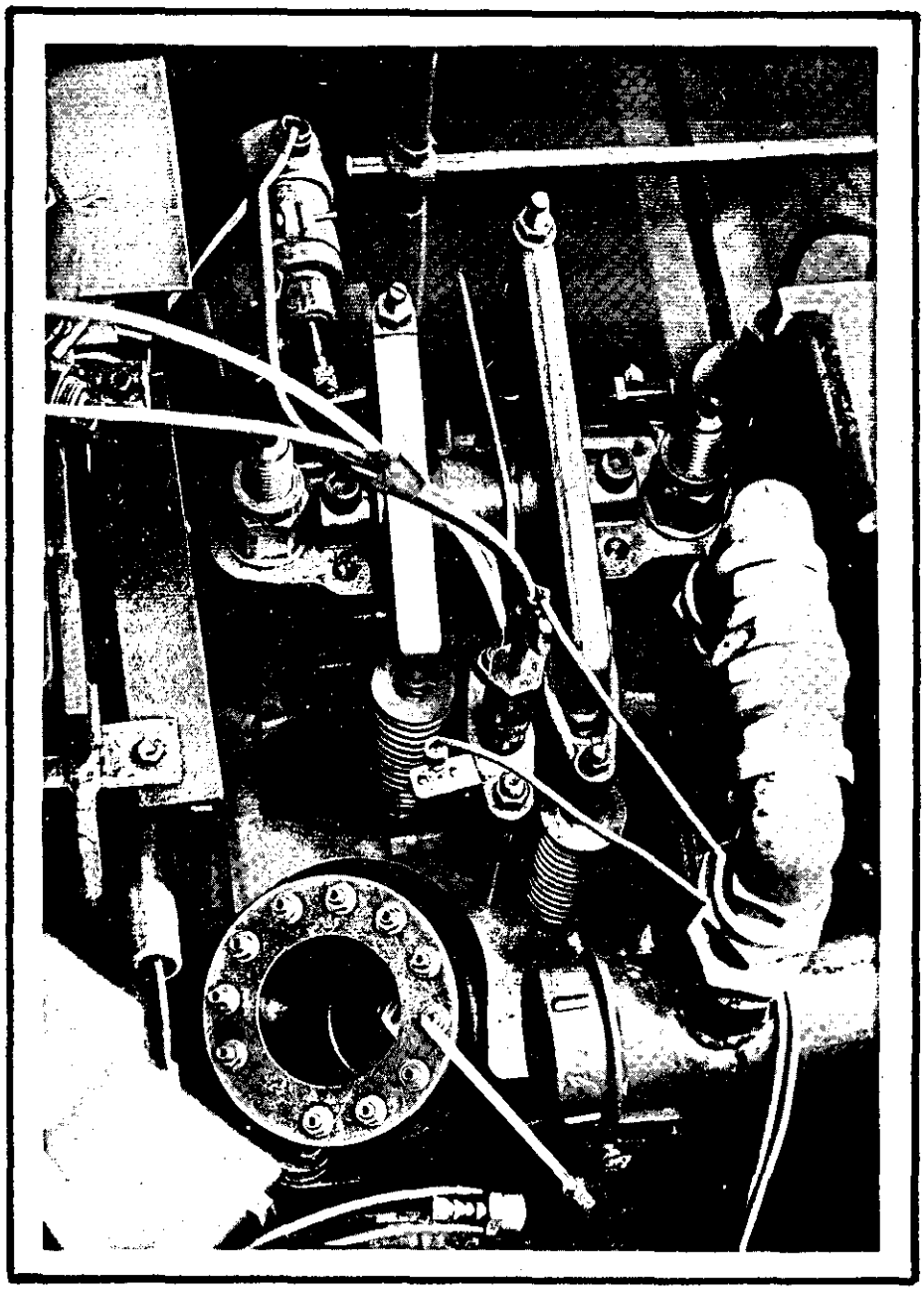

Figure 111 Strong back and valve gearing assembly.

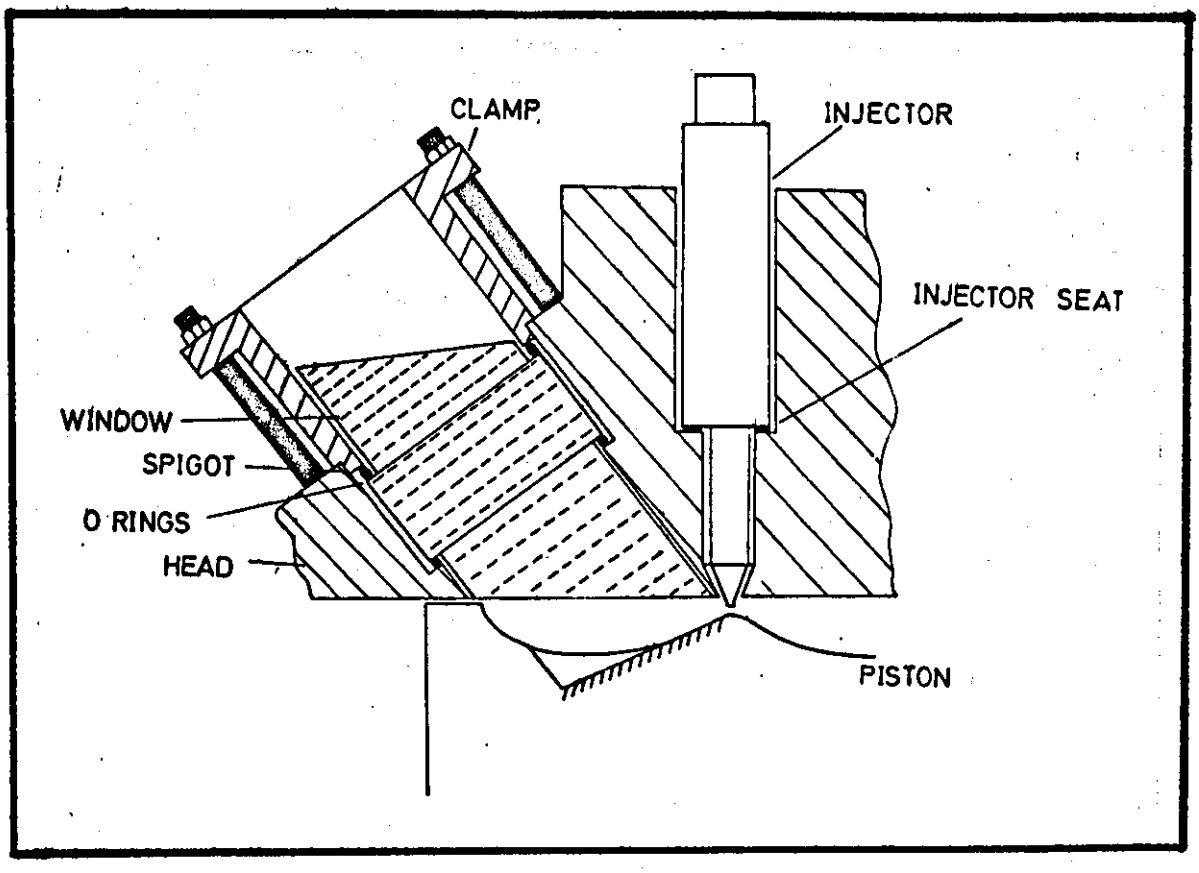

Figure 112 Sketch of window and injector arrangement.

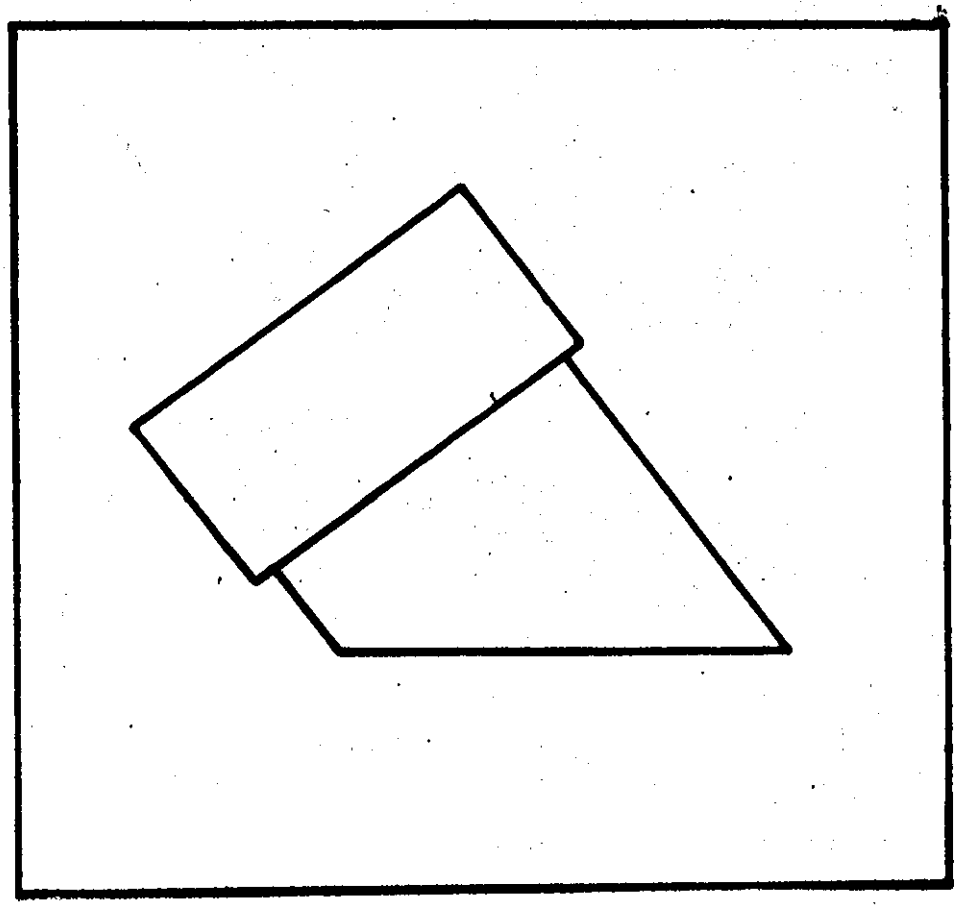

Figure 113 Sketch of direct photography window.

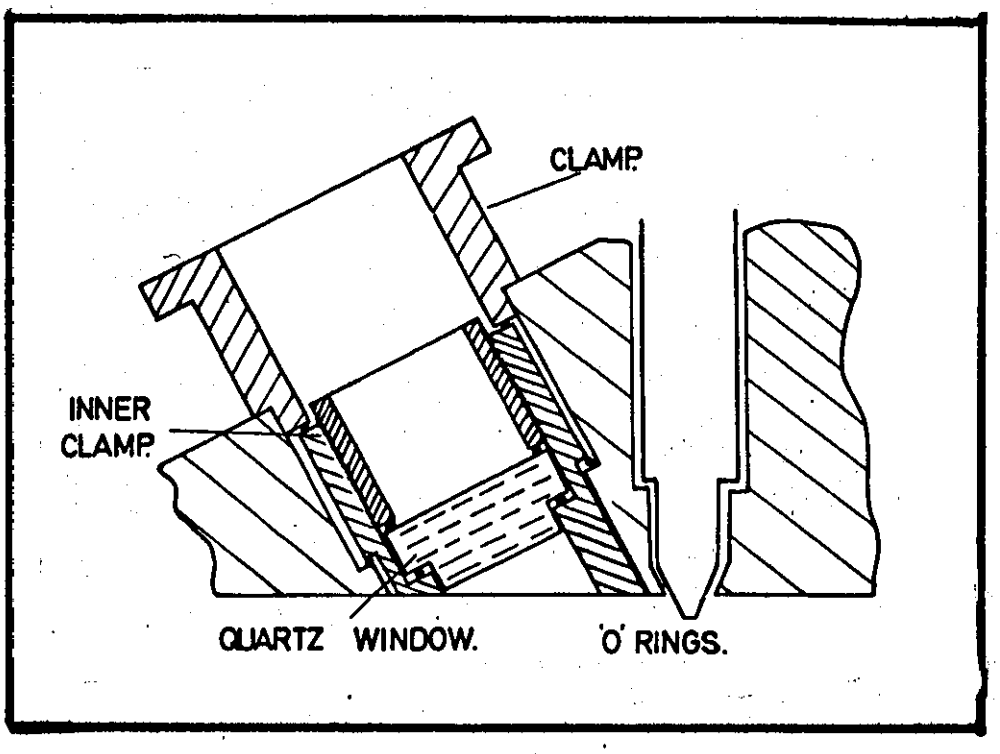

Figure 114 Sketch of the small window assembly.

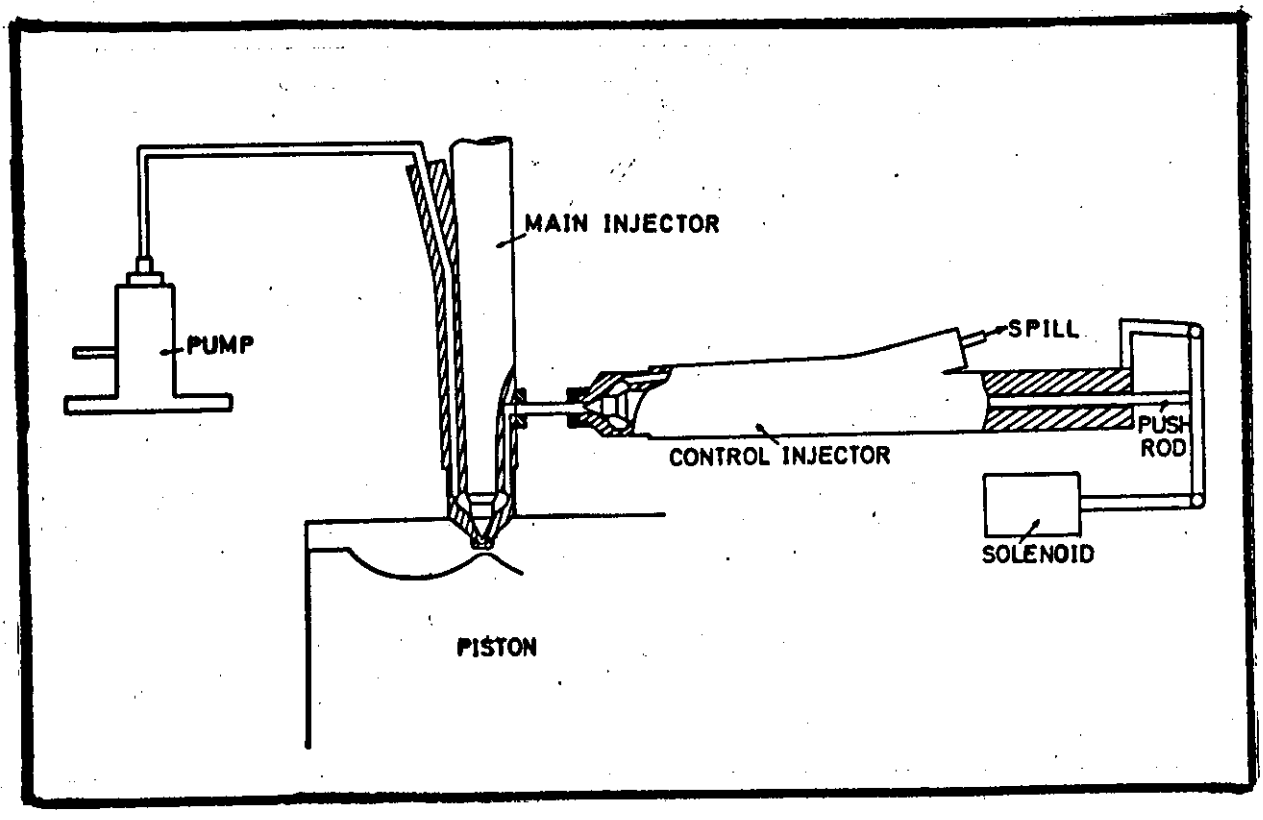

Figure 115 Diagrammatic arrangement of double injector fuel injection system.

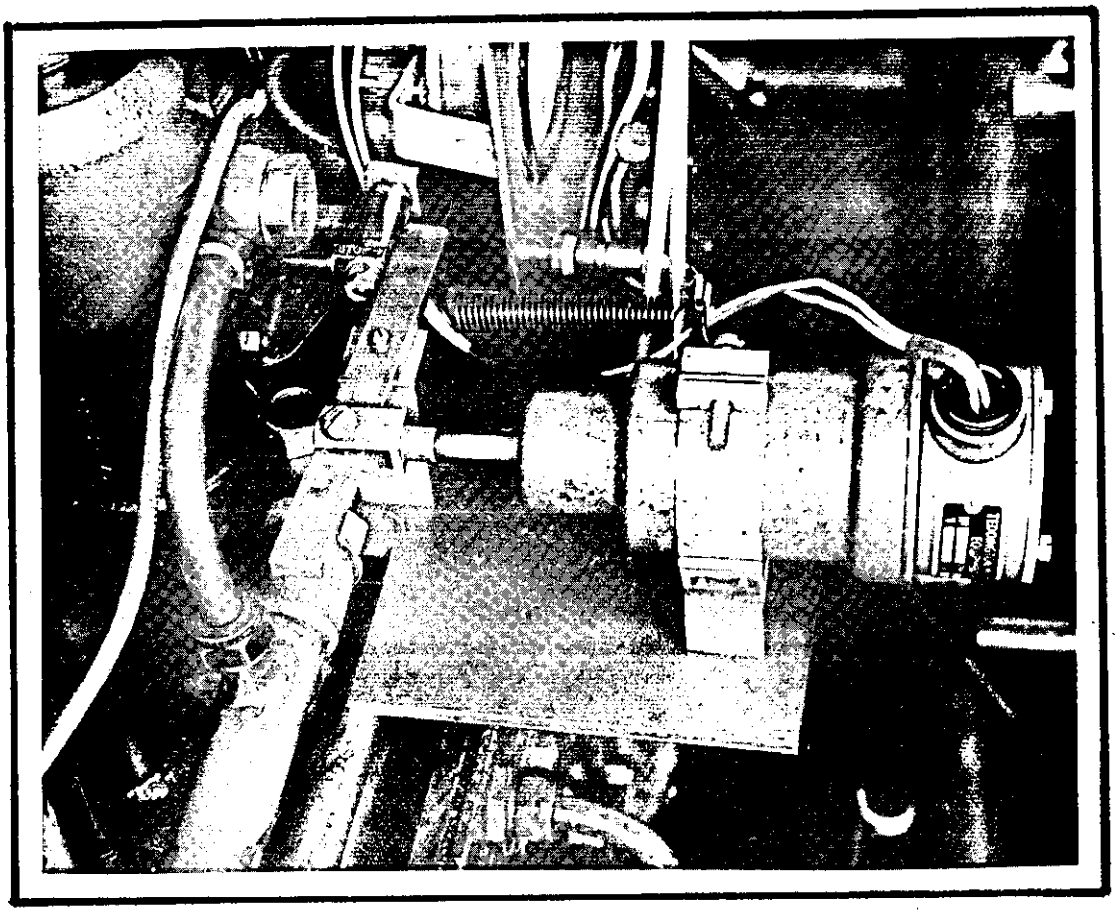

Figure 116 Fuel injection pump with solenoid operated rack.

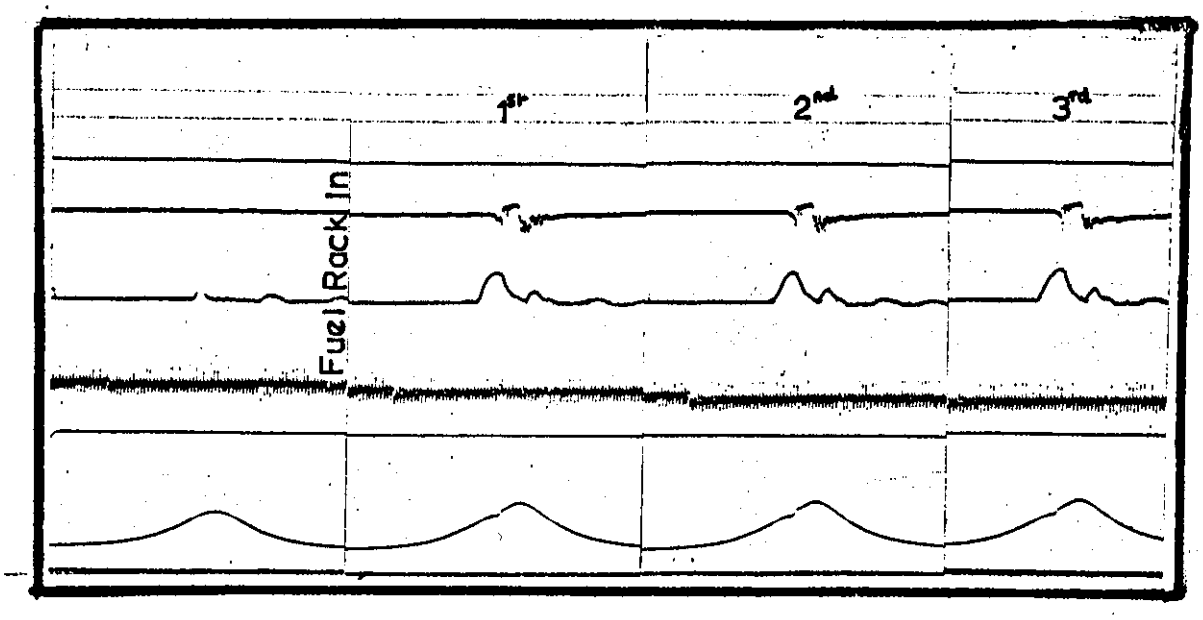

Figure 117 Fuel line pressures measured over the first 3 cycles after the fuel rack is pulled in.

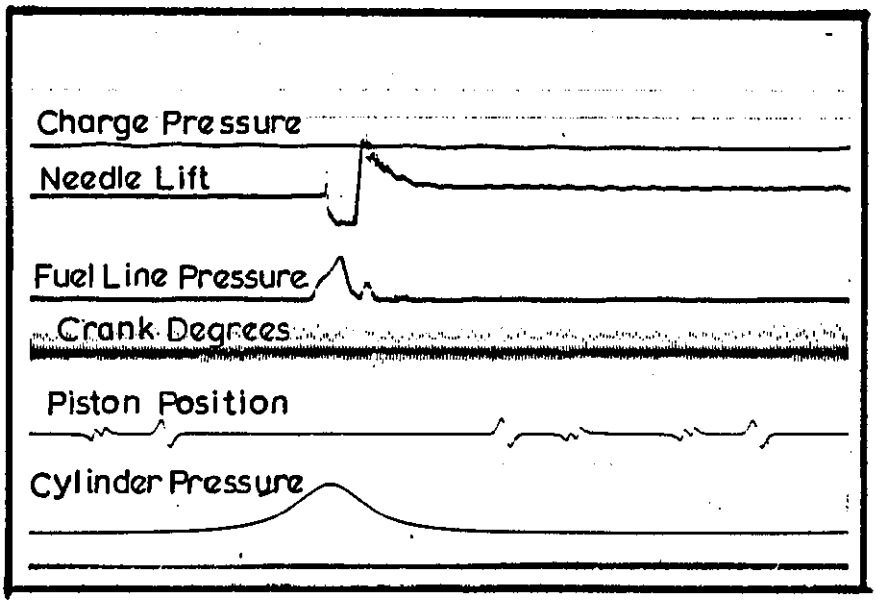

Figure 118 Example of trace giving piston position, fuel line pressure, needle opening, cylinder pressure, boost pressure, and crank degrees.

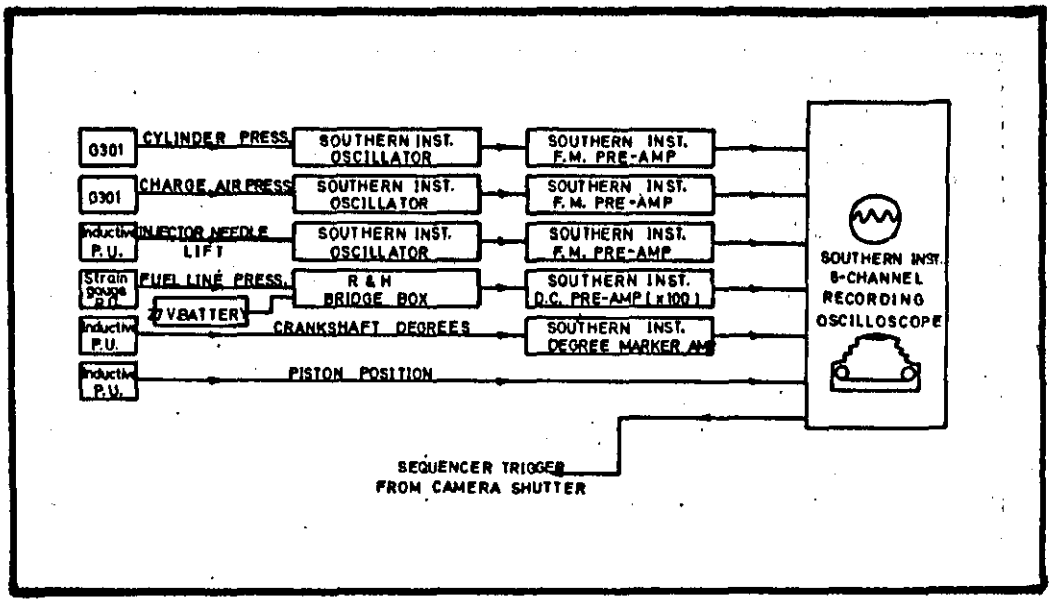

Figure 119 Diagrammatic layout of engine instrumentation.

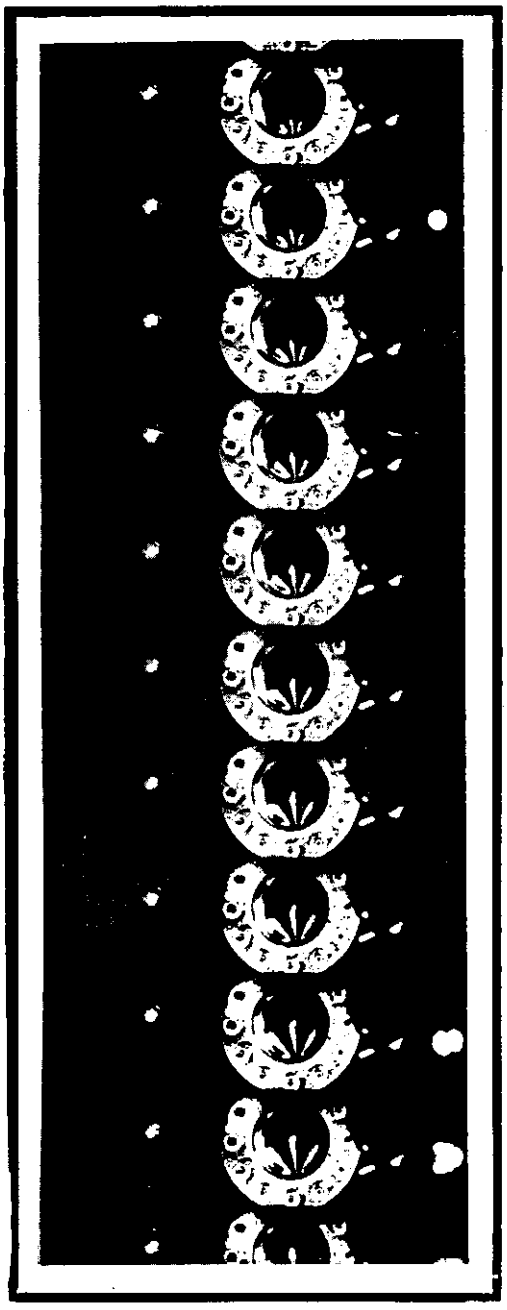

Figure 120 Example of photographic results obtained using direct photography.

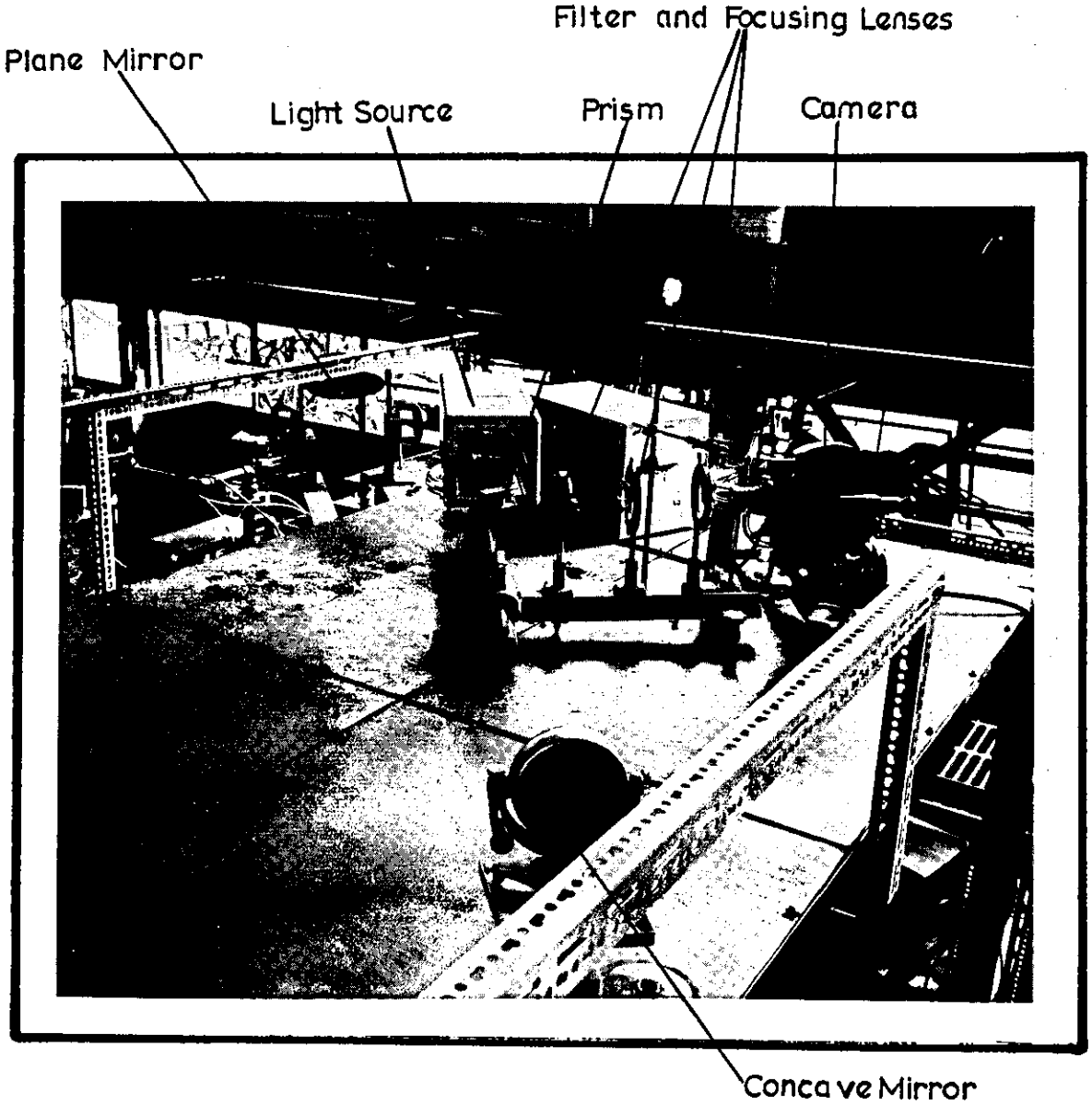

Figure 121 Arrangement of rig for schlieren photography.

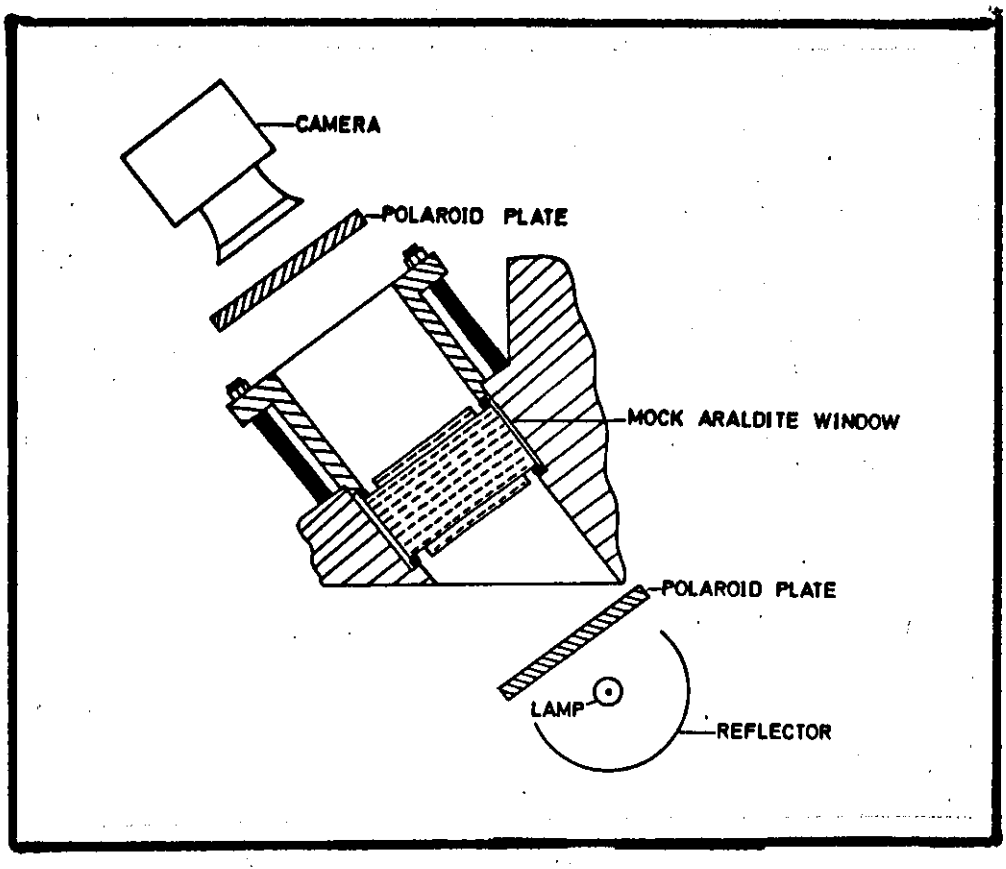

Figure 122 Polariscope arrangement on the large engine.

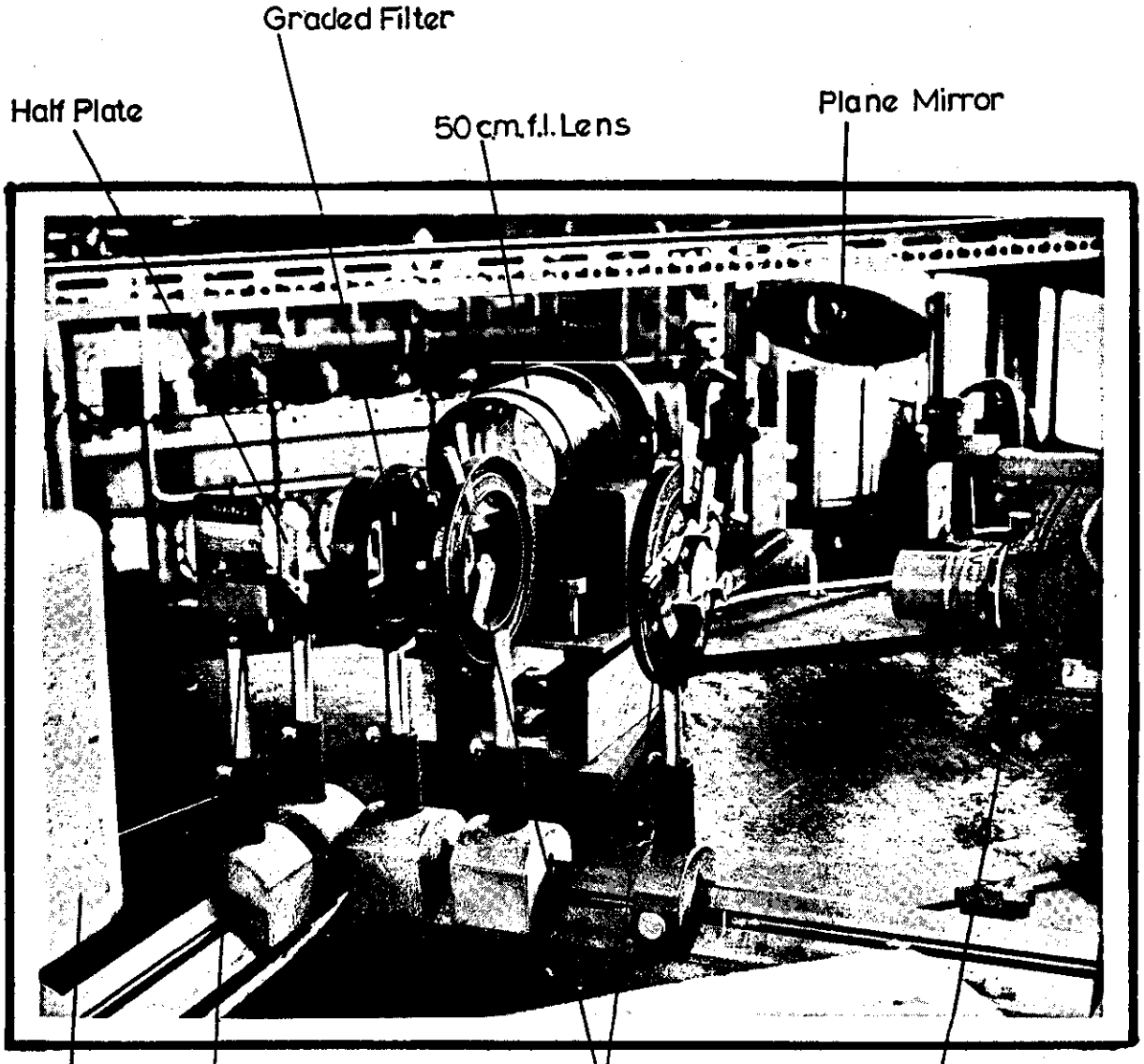

Figure 123 Schlieren system with 50 cm focal length lens.

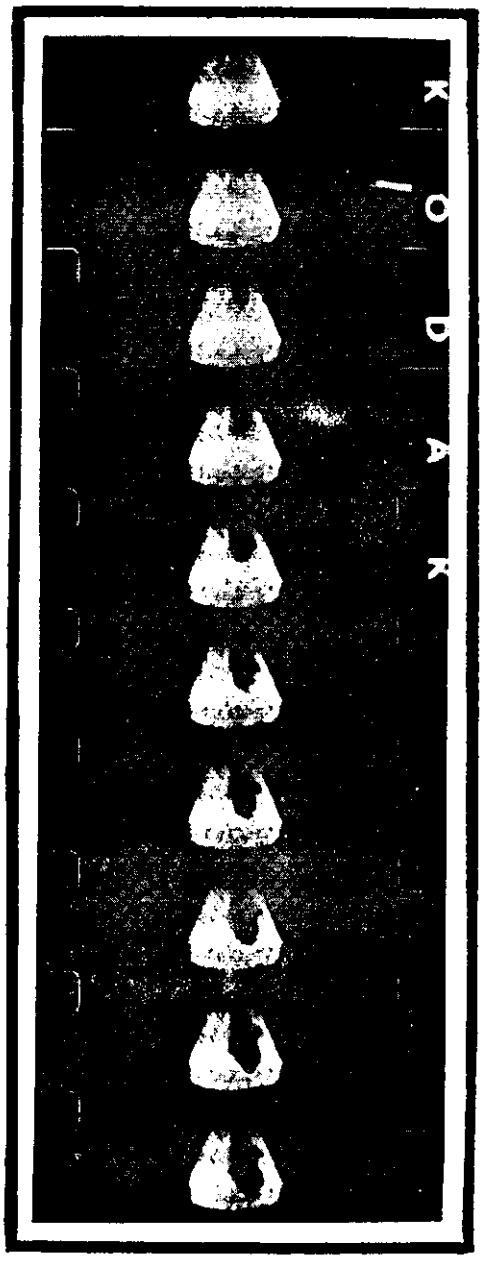

Figure 124 Example of photographic results obtained using Schlieren photography.

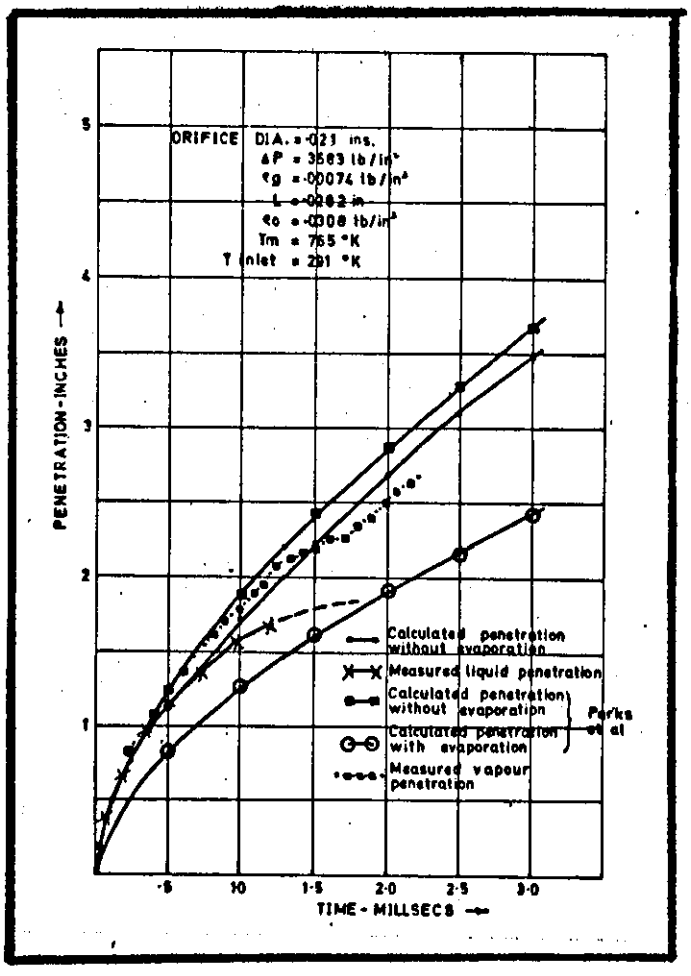

Figure 125 Penetration of vapour and liquid sprays gained from proposed equations, measured results, and Parks et al [78], for a .012" diameter orifice.

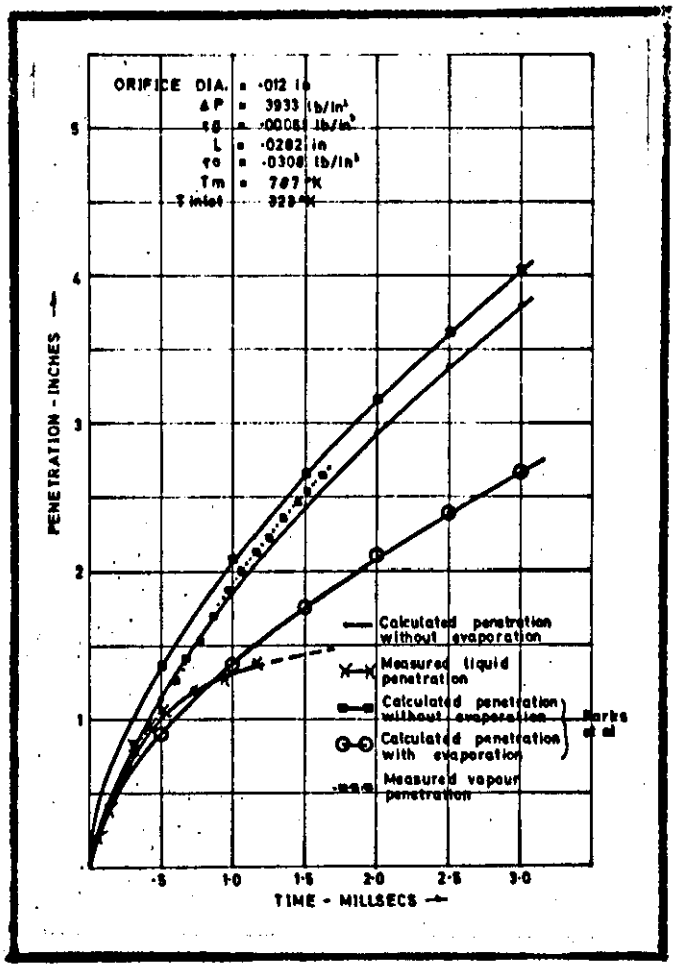

Figure 126 Penetration of vapour and liquid sprays gained from proposed equations, measured results, and Parks et al [78], for a .012" diameter orifice.

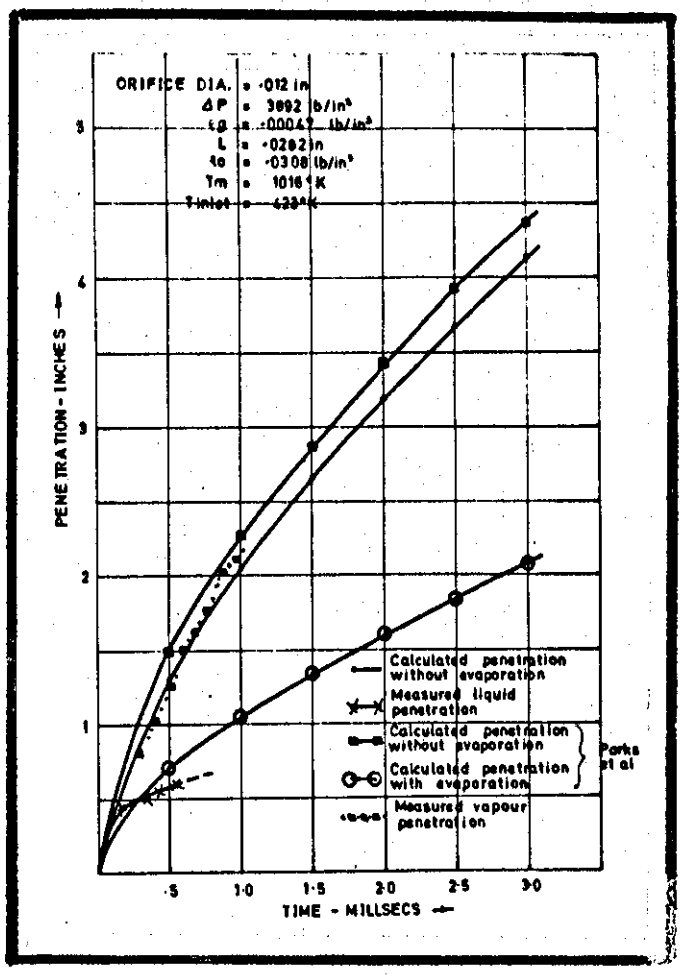

Figure 127 Penetration of vapour and liquid sprays gained from proposed equations, measured results, and Parks et al [78], for a .012" diameter orifice.

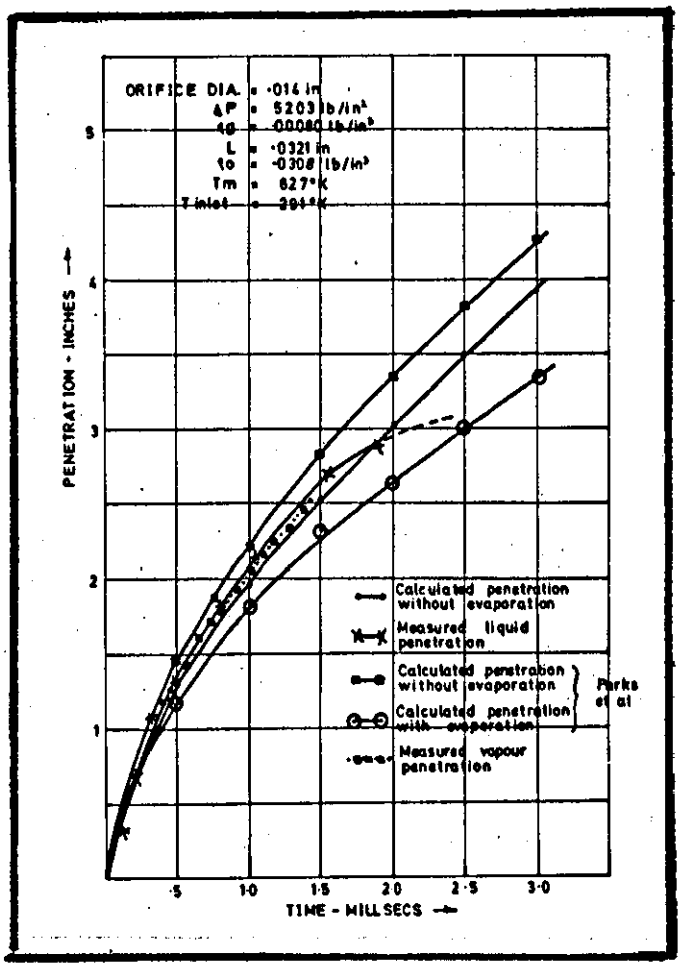

Figure 128 Penetration of vapour and liquid sprays gained from proposed equations, measured results, and Parks et al [78] for a .014" diameter orifice.

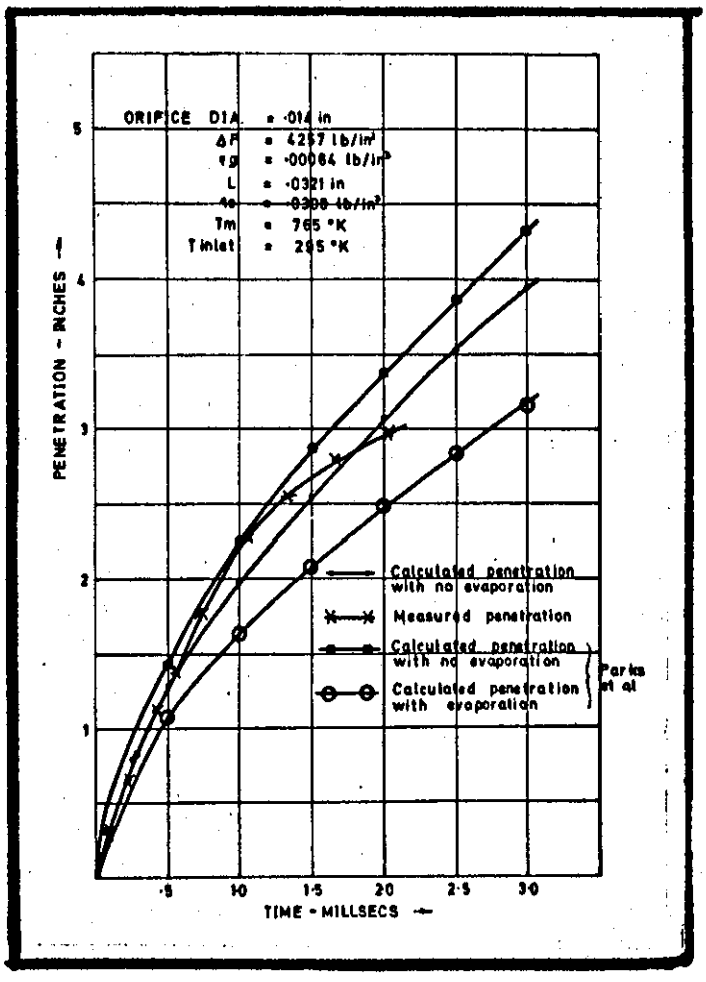

Figure 129 Penetration of vapour and liquid sprays gained from proposed equations, measured results, and Parks et al [78], for a .014" diameter orifice.

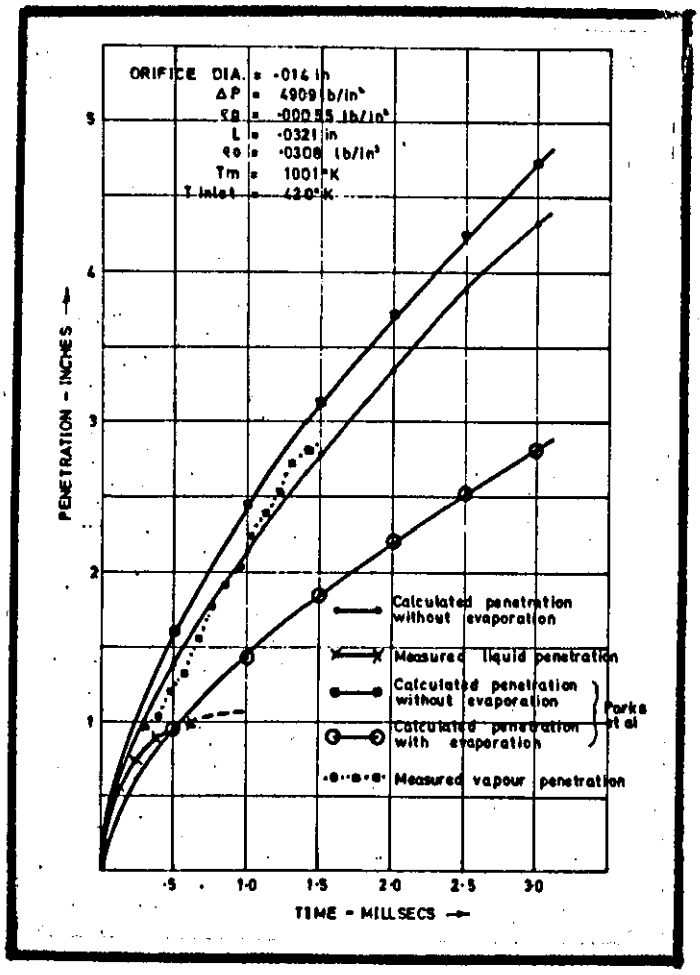

Figure 130 Penetration of vapour and liquid sprays gained from proposed equations, measured results, and Parks et al [78] for a .014" diameter orifice.

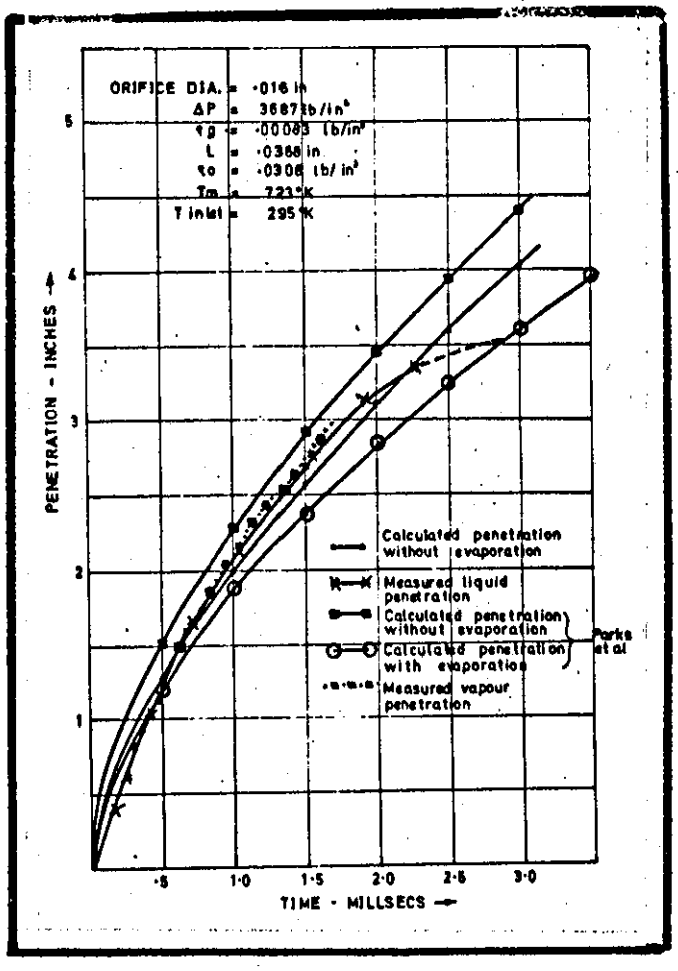

Figure 131 Penetration of vapour and liquid sprays gained from proposed equations, measured results, and Parks et al [78] for a .016" diameter orifice.

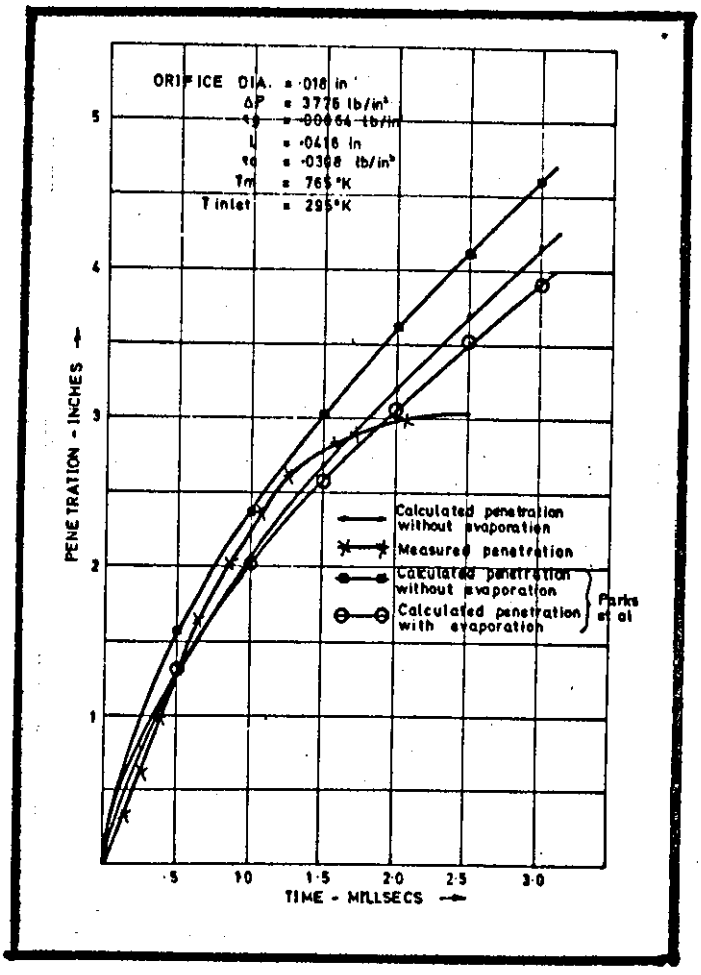

Figure 132 Penetration of vapour and liquid sprays gained from proposed equations, measured results, and Parks et al [78] for a .018" diameter orifice.

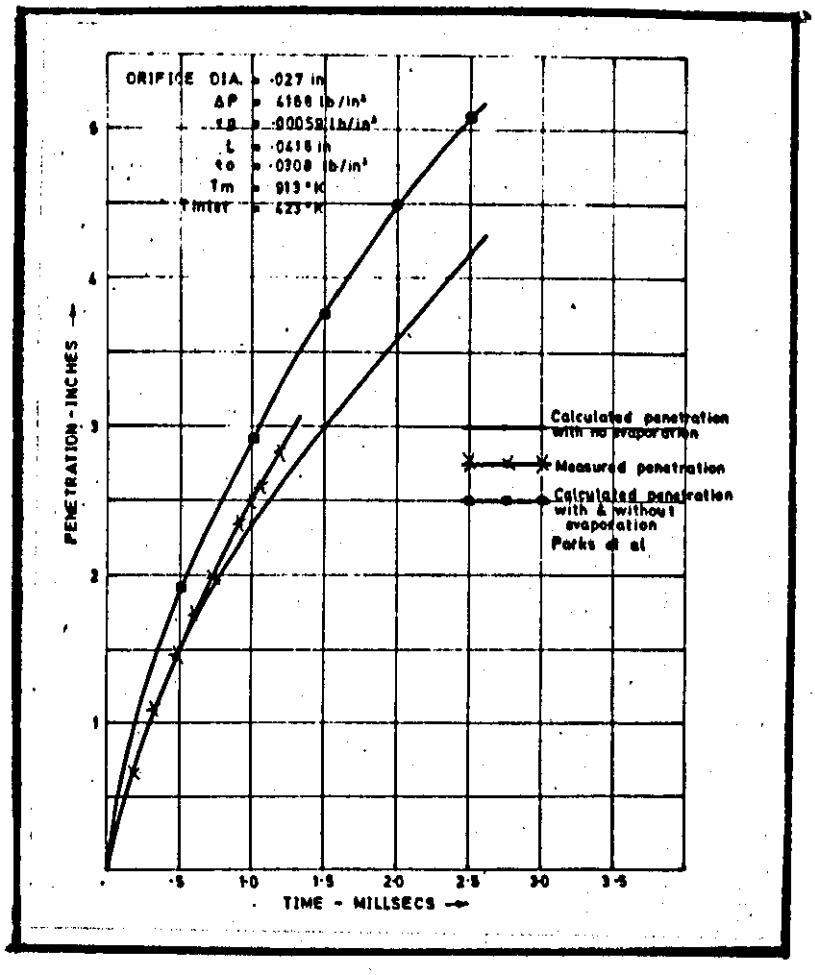

Figure 133 Penetration of vapour and liquid sprays gained from proposed equations, measured results, and Parks et al [78], for a .027" diameter orifice.

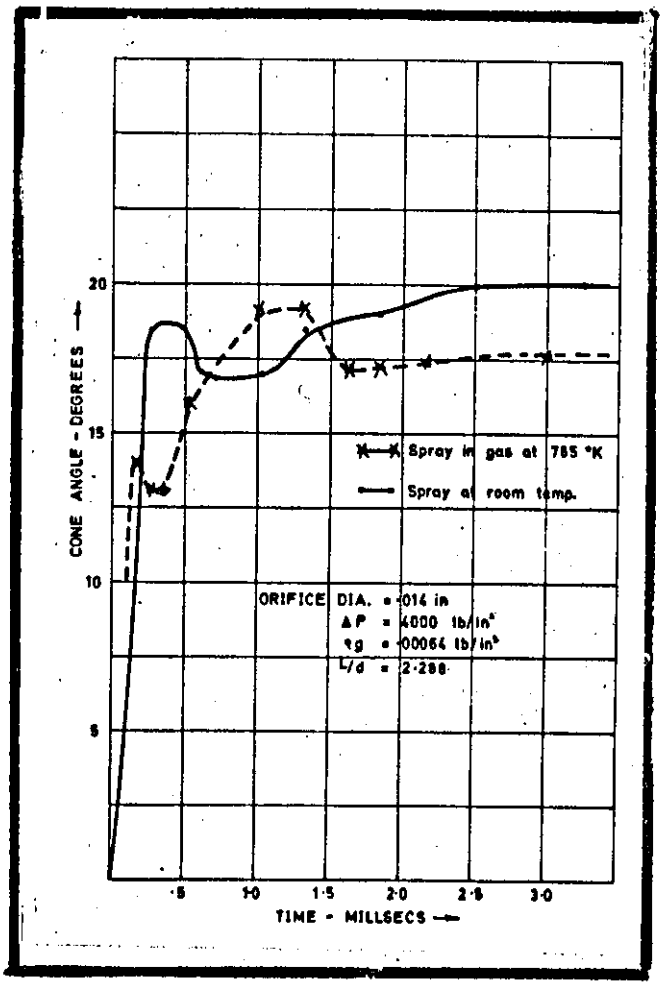

Figure 134 Build up of spray cone angle with time for a .014" diameter orifice.

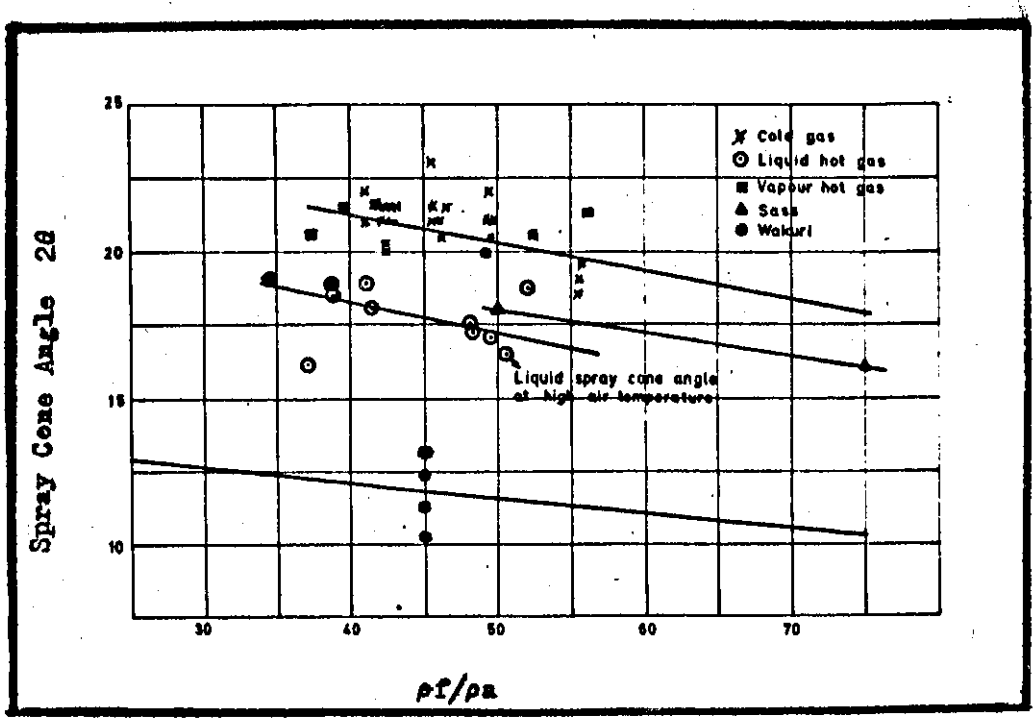

Figure 135 Spray cone angle against the ratio of oil and gas density.

APPENDIX I

Specification of 12½" bore engine

Designation number	6AT
Number of cylinders	6
Bore	12½ inches
Stroke	14½ inches
Piston Displacement	1785 cubic inches
Nominal Compression Ratio	12.5:1
B.M.E.P.	175 lb/in^2
R.P.M.	500

Intercooled and Turbocharged

APPENDIX II

Method of Calculating Mass Flow

Assuming 1) Incompressible flow

2) The following model for the nozzle:-

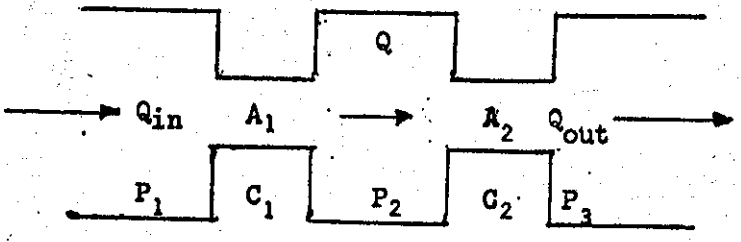

Where P_1 = Upstream pressure

A_1 = Area of seat orifice (Varies with time)

C_1 = Coefficient of discharge for seat orifice

P_2 = Sack pressure

A_2 = Total nozzle orifice area

C_3 = Coefficient of discharge for nozzle orifice

P_3 = Cylinder pressure

Q_{in} = Fuel input

Q_{out} = Fuel output

If incompressible flow

$$Q_{in} = Q_{out}$$

$$\therefore A_1 C_1 V_1 = A_2 C_2 V_2$$

It can be shown that:

$$Q = A_2 C_2 \sqrt{\frac{2g}{e}(P_2 - P_3)}$$

Where $$P_2 = \frac{A_1^2 C_1^2 P_1 + A_2^2 C_2 P_3}{C_2^2 A_2^2 + A_1^2 C_1^2}$$

and $$A_1 = \pi L \sin \theta/2 \, (d - L \sin \theta/2 \cos \theta/2)$$

Where L = Needle lift

d = Sack diameter

θ = Needle tip angle

The coefficient of discharge for the seat orifice was taken as .75.

The coefficient of discharge for the nozzle orifice was taken as .65.

These figures are taken from work done by W. Berwerk [18] and Joachim [19] . Figure 18 shows the results of a calculation for an AT engine at 176 lb/in^2 b.m.e.p. at 500 r.p.m. A computer program was written to calculate the fuel injected. From fuel consumption readings fuel input per injection = .00469 lbs. From calculation fuel input per injection = .00454 lbs.

Appendix III

Indicator Diagram Analysis

1. OBJECT

Given values of cylinder pressure against crank angle, to calculate gas temperatures, heat release rates, heat transfer and power output.

2. THEORY

2.1. List of Variables

p	Pressure of gas in cylinder	psia
T	Temperature of gas in cylinder	^{o}K
m	Mass of gas in cylinder	lbs
V	Volume of gas in cylinder	ft^3
dP	Incremental change of pressure	psi
dT	Incremental change of temperature	Kdeg
dV	Incremental change of volume	ft^3
dL	Heat lost to walls during step	Chus
dU	Incremental change in energy	Chus
dW	Work done during step	Chus
dQ	Heat released during step	Chus
ΣL	Cumulative total heat lost	Chus
ΣU	Cumulative total of energy	Chus
ΣW	Cumulative total of work done	Chus
ΣQ	Cumulative total of heat released	Chus
We	End work done	Chus
Wt	Total work done	Chus
Cm	Mean piston speed	m/sec
C_v	Specific heat at constant volume for gas in cylinder	$Chu/lb^{o}C$
h	Instantaneous heat transfer coefficient	$Chu/ft^2hr^{o}C$

N	Engine speed	r.p.m.
r	Crank radius	ins
D	Bore diameter	ins
l	Conrod length	ins
V_{CL}	Clearance volume	ins^3
A	Exposed cylinder wall area	ft^2
A_{PISTON}	Exposed piston area	ins^2
A_{LINER}	Exposed liner area at TDC	ins^2
$A_{CYL.HD.}$	Exposed cylinder head area	ins^2
A/F	Air:Fuel ratio	
T_{wall}	Mean temperature of cylinder wall	^oK
ρ	Density	lb/ft^3

The program adopts a step-by-step process:-

Suffix 1 denotes beginning of current step

Suffix 2 denotes end of current step

2.2. Preliminary Calculations

The trapped mass is calculated from the charge air pressure and temperature:-

$$m = \frac{144pV}{RT} \text{ lbs} \quad \text{where } R = 96 \text{ ft lb/lb}^oC$$

The mean piston speed $C_m = \frac{N \times 4r}{60 \times 12 \times 3.281}$ m/sec

2.3. Step-by-Step Process

$$V_2 = \frac{1}{1728}\left\{ V_{CL} + \frac{\pi b^2 r}{4}\left[1 + \frac{1}{r} - \cos\theta_2 - \sqrt{\left(\frac{l}{r}\right)^2 - \sin^2\theta_2} \right]\right\} ft^3$$

$$dV = (V_2 - V_1)\ ft^3$$

$$T = \frac{144\ p_2\ V_2}{mR} \quad ^oK$$

The programme uses Eichelberg's relationship for heat transfer coefficient:-

$$h = \frac{2.205}{10.765} \times 2.1 \sqrt[3]{C_m} \sqrt{\frac{P_1}{14.7}}\ T_1 \quad Chu/ft^2hr^oC$$

$$A = \frac{1}{144}\left\{ A_{PISTON} + A_{LINER} + A_{CYL.HD.} + \pi Dr\left[1 + \frac{1}{r} - \cos\theta_2 - \sqrt{\left(\frac{1}{r}\right)^2 - \sin^2\theta_2}\right]\right\} \text{ ft}^3$$

$$dL = hA\,(T_1 - T_{wall})\,\frac{d\theta}{N \times 60 \times 360} \quad \text{Chus}$$

$$A/F = \frac{m \times \text{Cal. Val}}{\Sigma Q}$$

The program calculates C_v from the following:-

If T<480

$$C_v = .1617 + 2 \times 10^{-5}\, T_1$$

If 480<T<600

$$C_v = .1507 + 5.3 \times 10^{-5}\, T_1$$

If T>600

$$C_v = .1378 + 8.8 \times 10^{-5}\, T_1 - 2.1 \times 10^{-8}\, T_1^2 + 16.7\, F/A\left[8.3 \times 10^{-3} + 2.06 \times 10^{-5}\, T_1 - 3.4 \times 10^{-9} T_1^2\right] \quad \text{Chu/lb}^\circ\text{C}$$

Where F/A = fuel/air ratio

$$dU = m\, C_v\, dT \quad \text{Chus}$$

$$dW = \frac{144}{1400.7}\, P_1\, dV \quad \text{Chus}$$

$$dQ = dU + dW + dL \quad \text{Chus}$$

$$\rho = \frac{144\, P_1}{RT_1} \quad \text{lb/ft}^3$$

2.4. Other Calculations

$$\text{Let } W_e = \frac{144}{1400.7}\left(\frac{P_{final} - P_{initial}}{2}\right)\frac{\pi D^2 r}{4}\left[2 - \left[1 - \frac{1}{r} - \cos(IVC) - \sqrt{\left(\frac{1}{r}\right)^2 - \sin^2(IVC)}\right]\right] \quad \text{Chus}$$

$$\therefore W_t = \Sigma W + W_e \quad \text{Chus}$$

$$\therefore IMEP = \frac{W_t \times 1400.7 \times 4 \times 12}{\pi D^2 \quad 2r} \quad \text{lb/in}^2$$

$$ISFC = \frac{\Sigma Q \times 33000 \times 60}{\text{Cal.Val.} \times Wt \times 1400.7} \quad \text{lb/IHP hr}$$

$$\text{Mean HTC} = \frac{\Sigma(h \times d\theta \times T_1)}{\Sigma(h \times d\theta)} \quad {}^\circ K$$

3. PROCEDURE

3.1. Preparation of Data

The data should be entered on the standard MAC data sheets (Form X498); each line of data should contain a 'D' in column 4 and a sequence number in columns 5, 6 and 7. The data should commence in column 9. One blank should be left between each number - if more than one blank is left the rest of that card will be ignored. It is permissible for a number to start at the end of one card and continue at column 9 of the next card. Should a number end in column 80 of one card, column 9 of the next card must be left blank.

3.2. List of Data

The data should be listed in the following order:-

D0	Identification Number		
D1	Clearance Volume		ins
D2	Bore diameter		ins
D3	Stroke		ins
D4	Conrod		ins
D5	Engine Speed		r.p.m.
D6	Charge air temperature		^{o}K
D7	Temperature correction	$(C \times P_{cor})$	K deg.
D8	Charge air pressure - P	+	
D9	Calibration constant - C	P_{cor}	psia
D10	Pressure correction - P_{cor}		
D11	Ang 1 (= IVC)	The range of	^{o}C/A TDC firing
D12	Step 1	crank angle to	C/A deg.
D13	Ang 2	be calculated	^{o}C/A TDC firing
D14	Step 2	is divided into	C/A deg.
D15	Ang 3	three divisions	^{o}C/A TDC firing
D16	Step 3	each of which may have a different step size.	C/A deg.

D17	Angle correction	C/A deg.
D18	Temperature cylinder wall	^{o}K
D19	Calorific value	Chu/lb
D20	Eichelberg constant (normally 2.1)	
D21	Area liner above TDC	ins^2
D22	Area piston	ins^2
D23	Area cylinder head	ins^2

This list is followed by the integer T (= number of pressures) and the list of pressures (units as for charge air pressure). The pressures are read one-by-one into D24 starting from the pressure at the end of the first step.

APPENDIX IV

H/S Camera

W.F.I. 8mm Fastax Camera

Technical Specification

Film Capacity	-	100 ft. daylight loading spool
Film	-	16mm with 8mm perforations
Speed	-	300 to 16000 P.P.S.
Shutter	-	8 sided High Index Glass Rotating Prism
Effective Shutter Speed	-	$\frac{1}{3 \times \text{Film Speed}}$
Lens	-	f2
Lens Mount	-	F x 1 Fastax Bayonet
Timing Light	-	See Appendix VI
Cut-off Switch	-	Automatically cuts off power to camera at end of film run
Motors	-	Two (115 volts AC-DC 60 cycle) One for drive, one for take up.

APPENDIX V

Continuous Light Sources

The High Speed camera with this extremely short exposure time of 5 microseconds needs very high intensity illumination particularly when using standard films. The two standard light sources used are specified below

1) Tungsten 750 watts 750 R lamp

Internally silvered photospot with clear front surface

ES Cup

750 W at 115 V

Produces an accurately focurred spot of light three inches in diameter at a distance of approximately twelve inches.

Two transformers were used in conjunction with the tungsten lamp

Type HF 911

Type	-	Double wound-centre tapped, 50 cycle
Rating	-	3 kVA (intermittent)
Input	-	200-250 V (tapped)
Output	-	Switch tapped 0 - 58 - 115 volts
Outlets	-	Four 3-pin Bulgin sockets
Auxiliary outlets	-	Two American hat sockets

The switch on the output could be used to give one to eight power light for housing and setting up the camera. This facility pre-heats the lamp and so reduces thermal shock on the filaments when switched to full power and thus prolongs lamp life. Universal stall lighting brackets were used to support the lamps.

2) Xenon Pulse Lamp Unit

Lamp Source	-	B.T.H. Compact Source Xenon Lamp type XE/D
Source Size	-	5 mm
Colour temp.	-	5700 K
Envelope	-	Quartz

Lamp Head

Reflector	-	Parabolic aluminium mirror (Alzac)
Focus	-	Adjustable between spot and hood
Lamp Mounting	-	On reflector optical axis for efficient light collection
Front cover glass	-	Toughened and etched glass to reduce harmful U.V. light efficiency

Control Unit

Contained in portable desk type console.

Circuitry - a high voltage striking circuit makes use of a 25 kV repeating pulse unit to present the lamp with 25 kV pulses each with a current flow of 25 amps. The lamp simmers at 500 watts. Pulsing power is selected on the panel. Each power selects a period - limiting circuit.

2½ kW pulse for 10 seconds

5 kW pulse for 5 seconds

7½ kW pulse for 2 seconds

An over-riding safety circuit prevents repeat pulsing at shorter intervals than once every 30 seconds.

Power Supply - Six 6 volt batteries in series

Operation - The lamp is struck and simmers at 500 watts which gives sufficient light for focusing and setting up the camera. The required pulse power is selected and when required, fired. In this case manual firing was used but it can be pulse from the camera.

APPENDIX VI

R.A.R.D.E. Spark Times

In sections 4.8.2 and 4.8.5., mention has been made of timing and event marks being superimposed on the high speed film. These are applied by the above unit. It is designed to give a highly accurate method of time marking on one margin of the film and a mark to indicate a second event in the other margin. This second mark occurs only once when the circuit is triggered. The control box provided this trigger once in one test run. The specifications are as follows:-

Oscillator	-	Crystal controlled at a frequency of 1.0 hilocycle/second, accuracy better than 1 part per million over temperature range - 20°C to +70°C.
Pulse Transformer Unit	-	Contains transformer and capacitor for each of the two spark gaps.
Spark Gap Head	-	Consists of two spark gaps each with its own lens. The sparks originate from the tip of a tungsten wire electrode which from the time measurement datum points.
Spark Image Intensity	-	Controlled by three water house stops to cover the complete range of emulsion speeds.
Electrical requirements	-	200-240 V AC 50 cycles
Consumption	-	120 watts

APPENDIX VII

Specification of 8" bore engine

Designation number	APC
Number of Cylinders	6 (or single)
Bore	8 inches
Stroke	$10\frac{3}{4}$ inches
Piston Displacement	541 inches^3
Nominal Compression Ratio	12.4:1
B.M.E.P.	200 lb/in^2
R.P.M.	750

Intercooled and Turbocharged

APPENDIX VIII

Detailed drawings of 8" Bore Engine Components

Appendix VIII a. Small piston mirror.

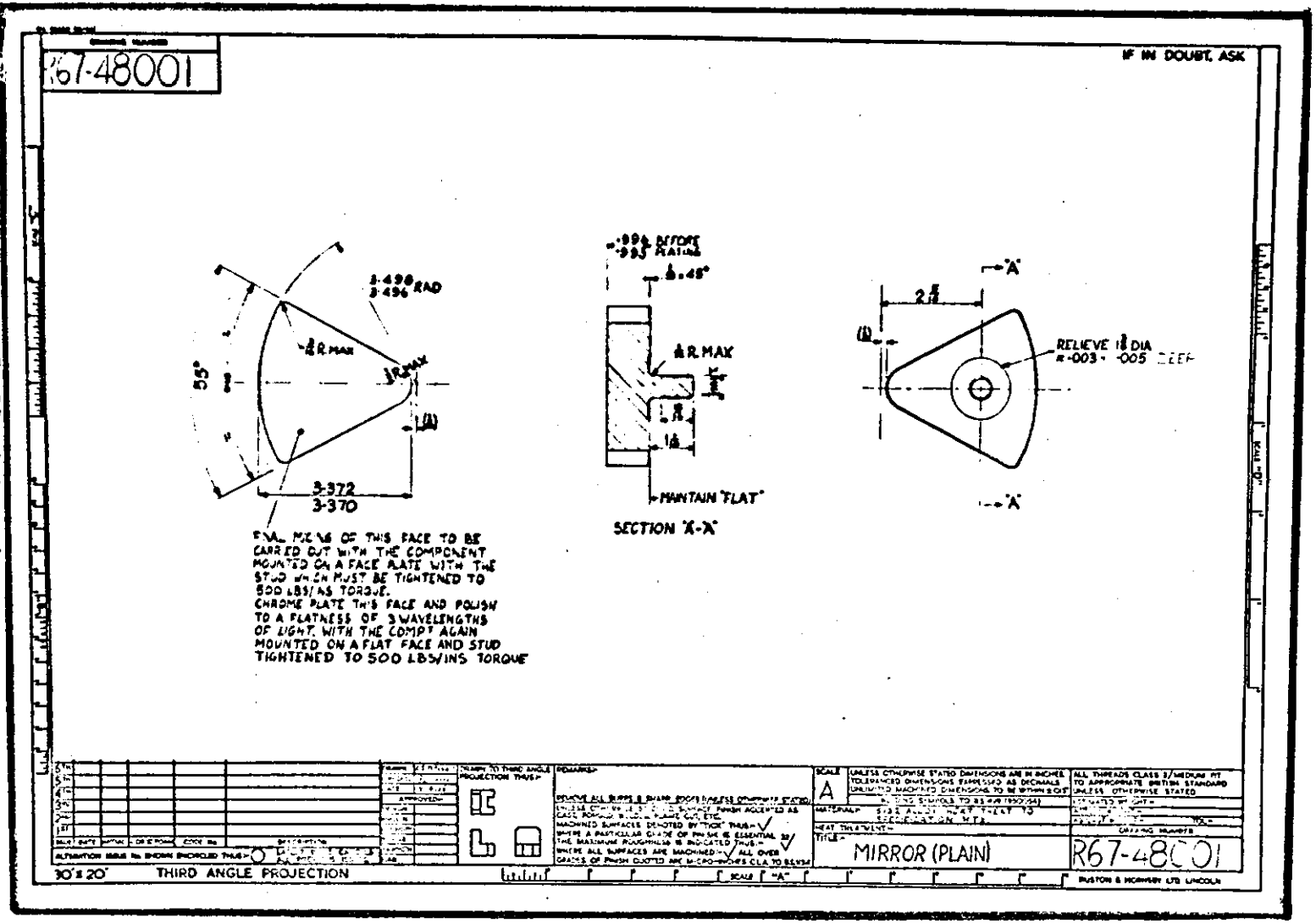

Appendix VIII b. Large piston mirror.

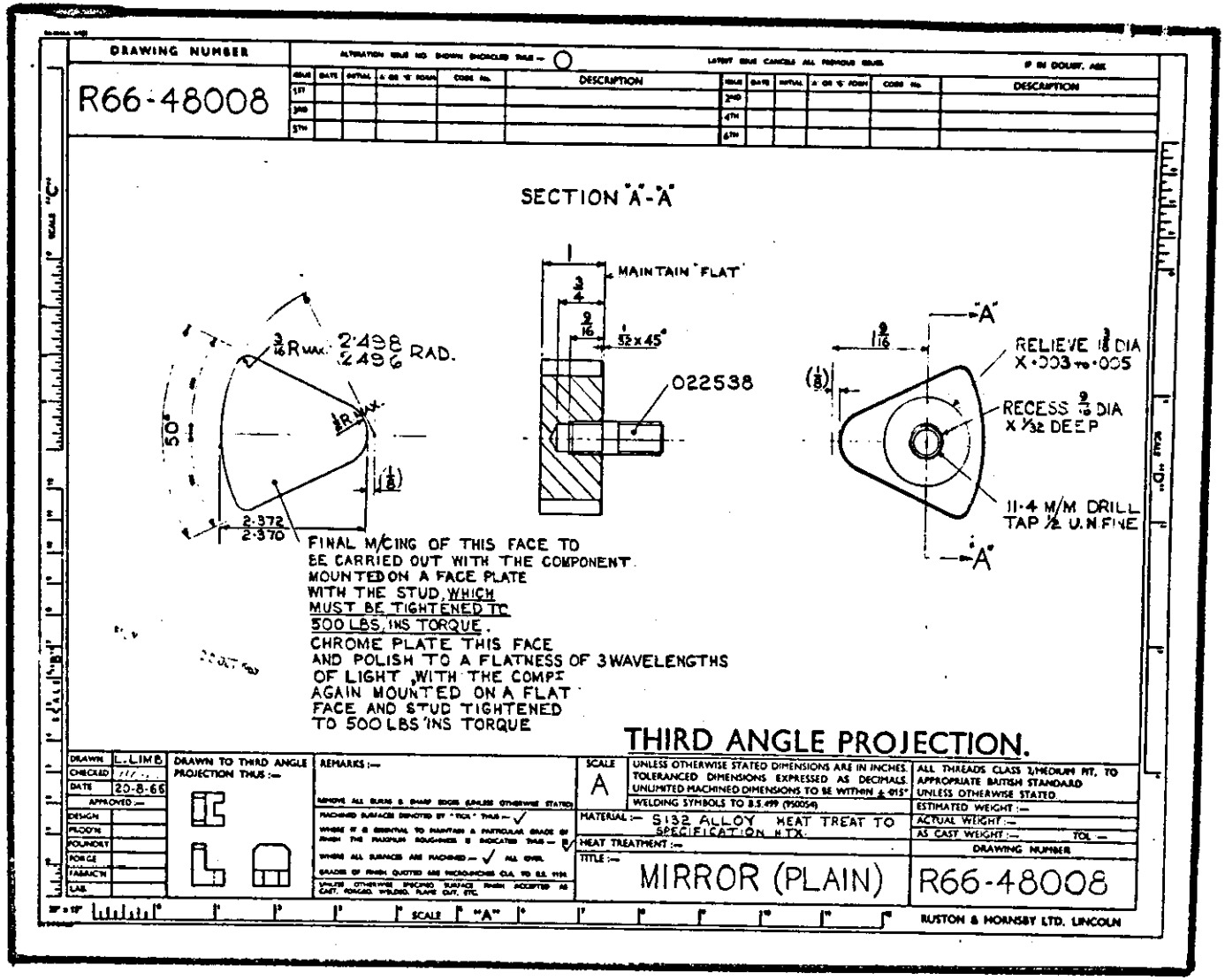

Appendix VIII c. Piston for plain mirrors

Appendix VIII d. Stepped mirror.

Appendix VIII e. Stepped mirror piston.

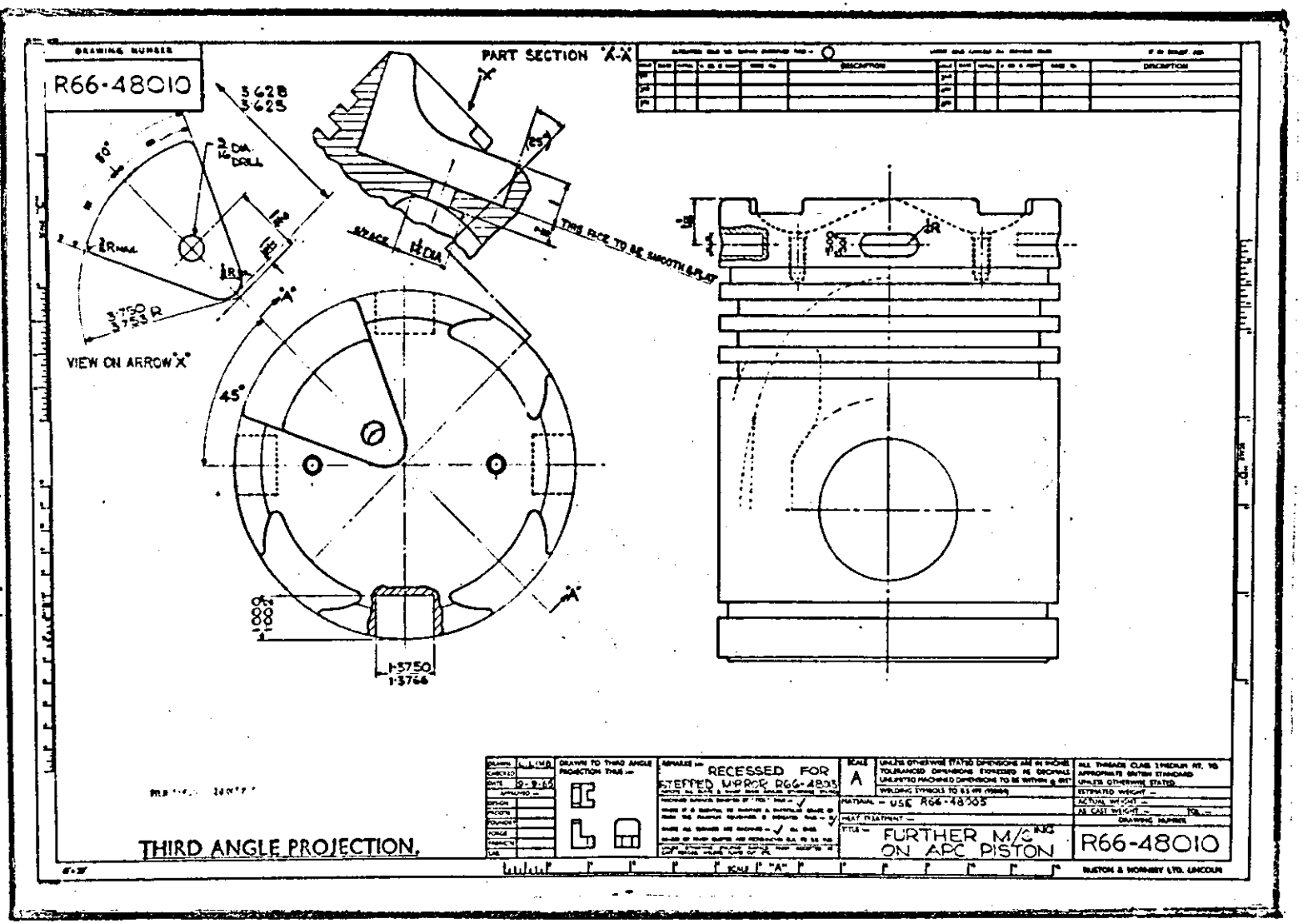

Appendix VIII f. Quartz window design.

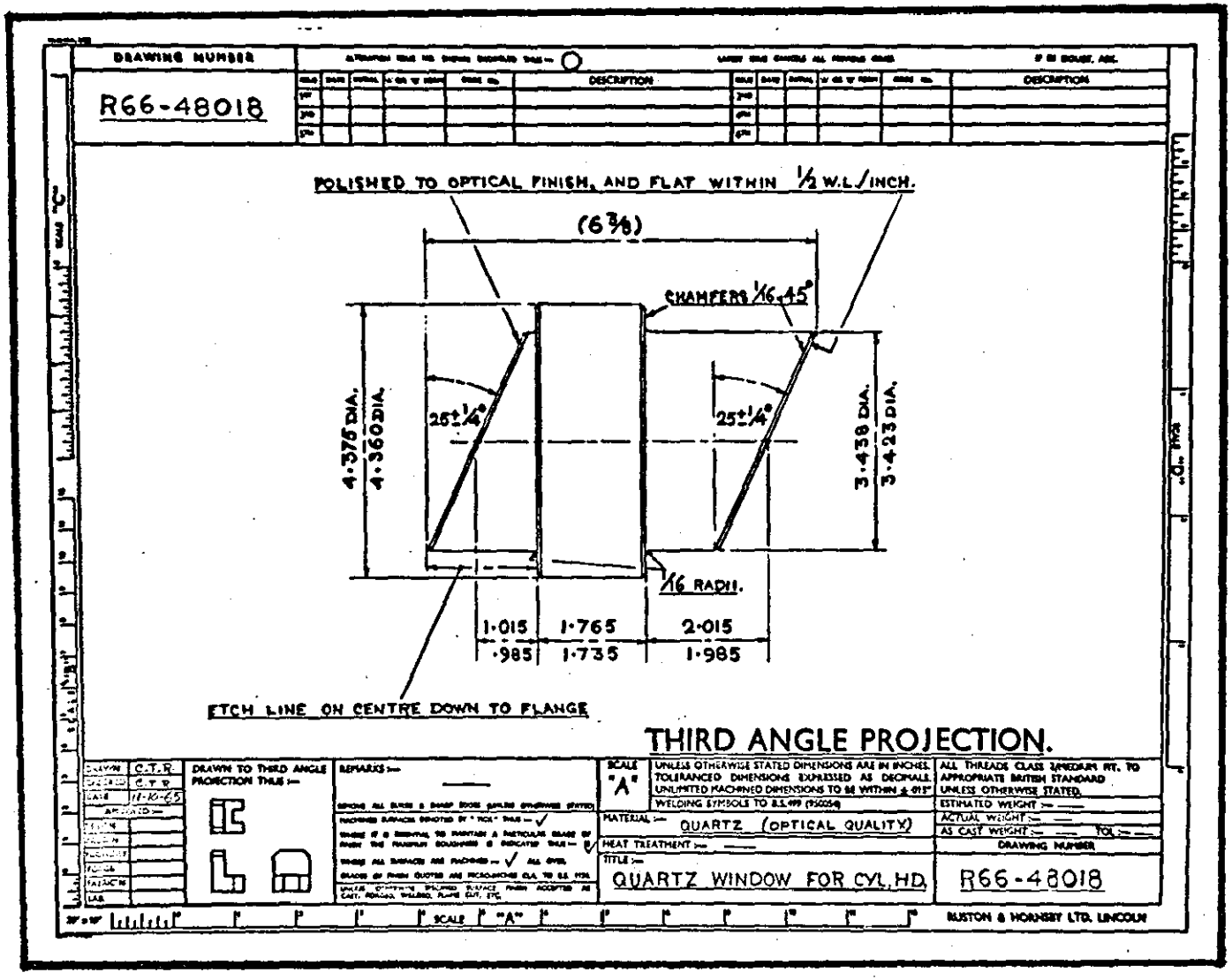

Appendix VIII 8. Final design of cylinder head.

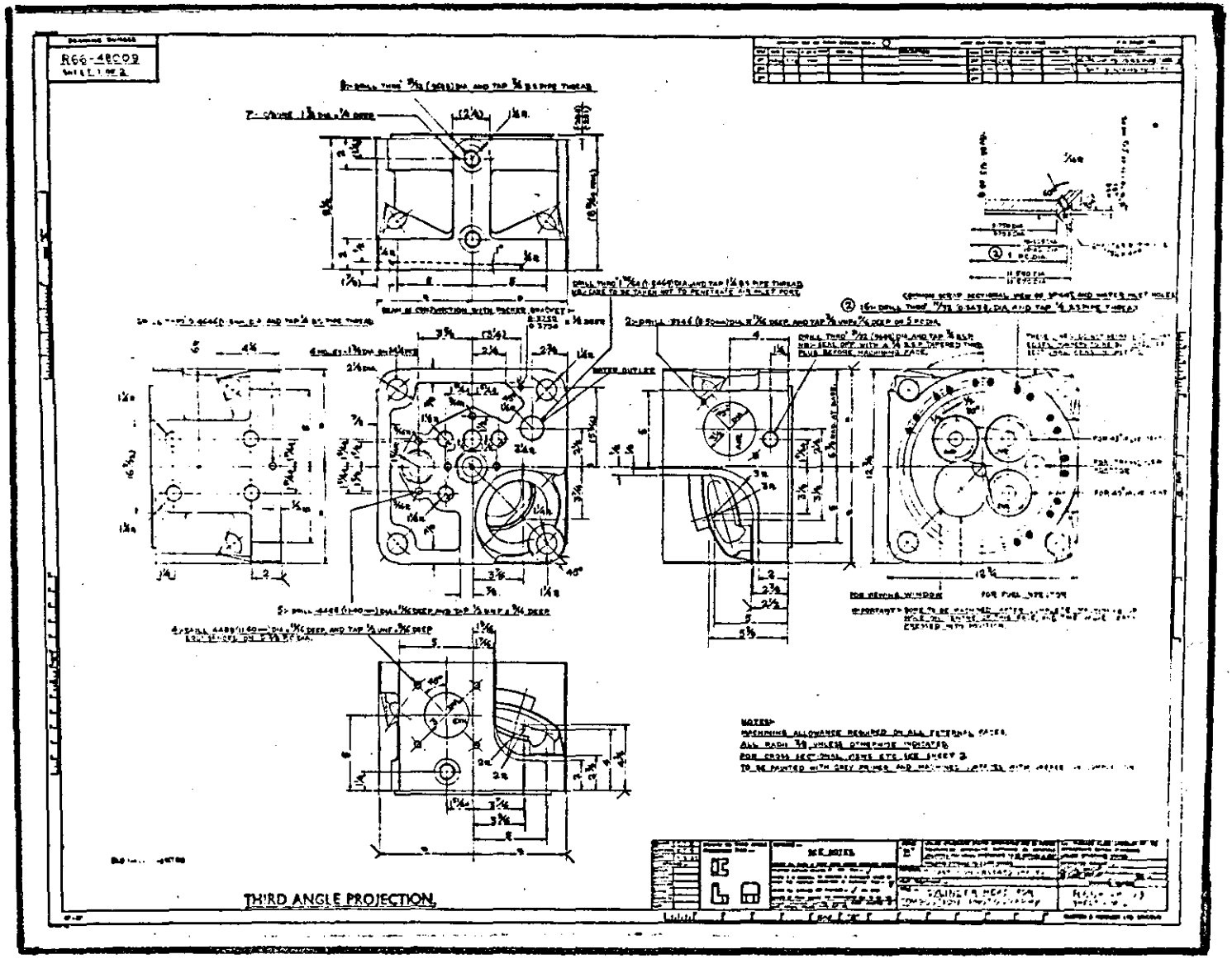

Appendix VIII h. Final design of cylinder head.

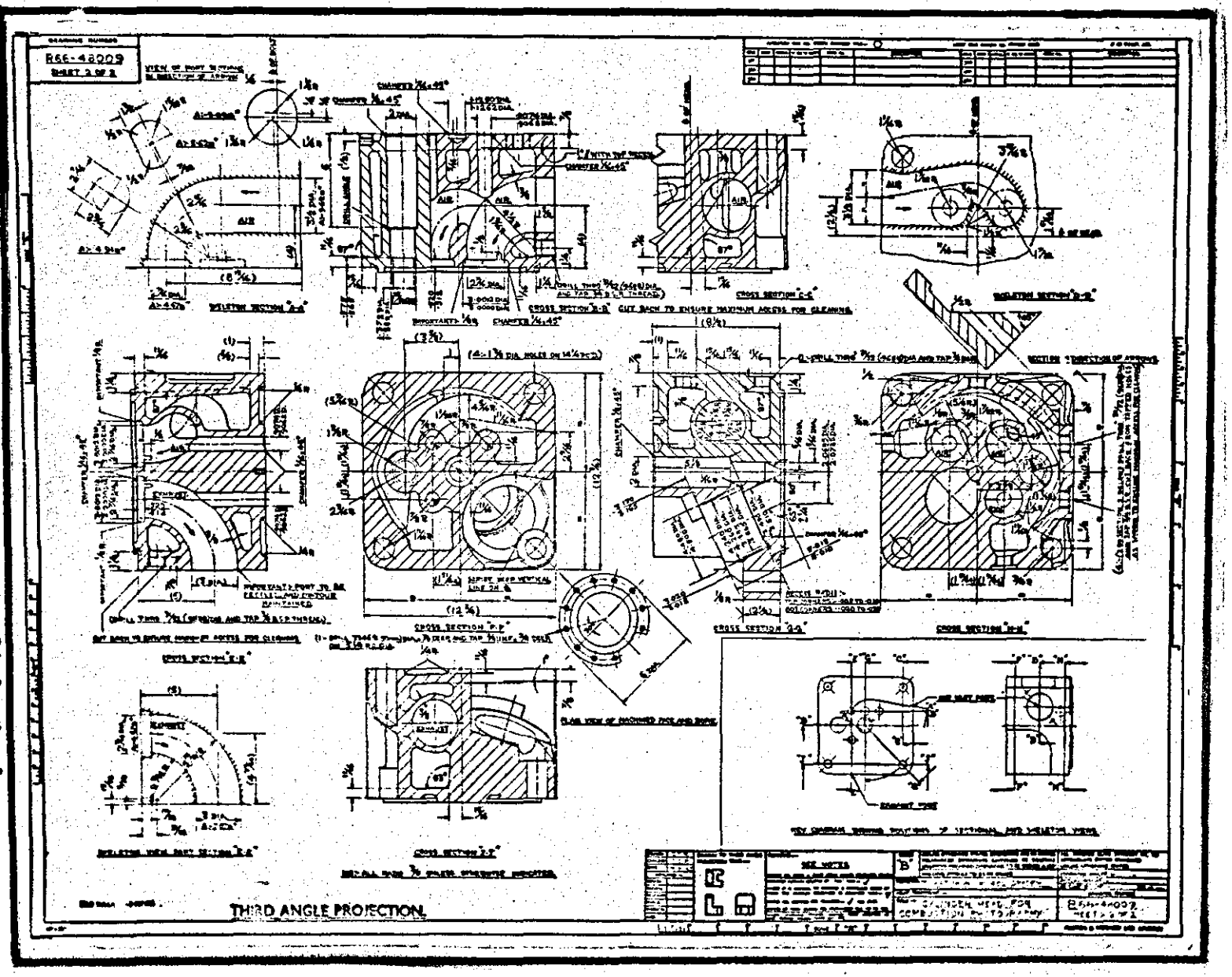

Appendix VIII 1. Design of injector.

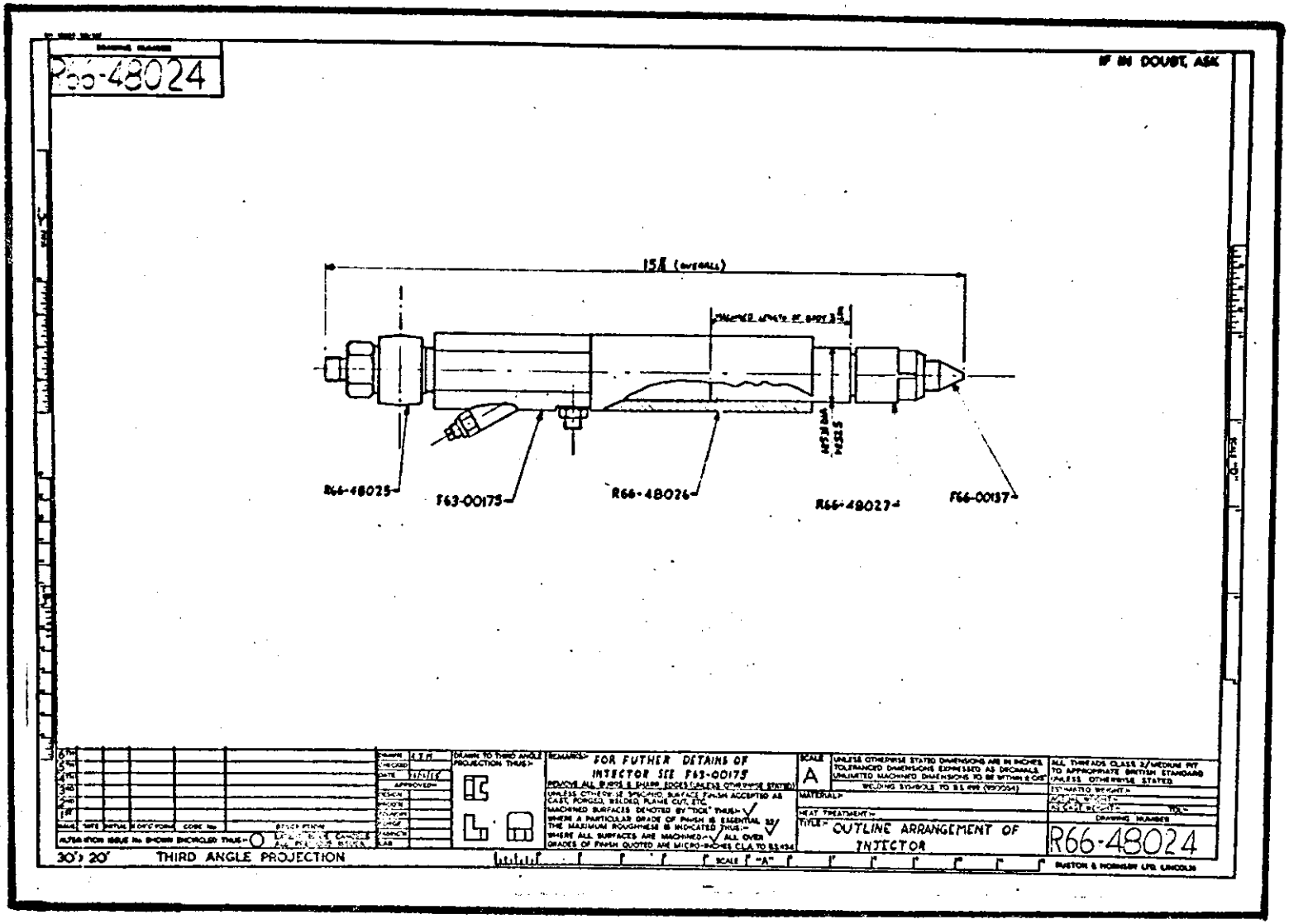

APPENDIX IX

Basis for calculations on air fuel ratios in fuel sprays by Wakuri [15].

$$\lambda = \frac{2\,\delta \tan\theta}{L_{th}\sqrt{c\,\sigma}} = \frac{2\tan\theta}{\lambda_{th}\sqrt{C}}\sqrt{\frac{\rho_a}{\rho_f}}\;\frac{x}{d}$$

Where $\delta = \frac{x}{d}$

x = distance of penetration

d = orifice diameter

2θ = Spray angle

C = Coefficient of discharge

$\sigma = \frac{\rho_f}{\rho_a}$

ρ_f = Density of fuel

ρ_a = Density of air

L_{th} = Theoretical Air quality

λ = Excess air coefficient